e-ISSN 2667-9973
p-ISSN 1512-1127

საქართველოს გეოფიზიკური საზოგადოების ჟურნალი

მყარი დედამიწის, ატმოსფეროს, ოკეანისა და კოსმოსური პლაზმის ფიზიკა

ტომი 27 , № 2

JOURNAL
OF THE GEORGIAN GEOPHYSICAL SOCIETY

Physics of Solid Earth, Atmosphere, Ocean and Space Plasma

Vol. 27 , № 2

Tbilisi
2024

e-ISSN 2667-9973
p-ISSN 1512-1127

საქართველოს გეოფიზიკური საზოგადოების ჟურნალი

მყარი დედამიწის, ატმოსფეროს, ოკეანისა და კოსმოსური პლაზმის ფიზიკა

ტომი 27 , № 2

JOURNAL
OF THE GEORGIAN GEOPHYSICAL SOCIETY

Physics of Solid Earth, Atmosphere, Ocean and Space Plasma

Vol. 27 , № 2

Tbilisi
2024

საქართველოს გეოფიზიკური საზოგადოების ჟურნალი
მყარი დედამიწის, ატმოსფეროს, ოკეანისა და კოსმოსური პლაზმის ფიზიკა
მთავარი რედაქტორი: თ. ჭელიძე

სარედაქციო კოლეგია

ა. ამირანაშვილი (მდივანი), თ. ბიბილაშვილი (აშშ), ე. ბოლოპოულოსი (საბერძნეთი), გ. ჩაგელიშვილი, თ. ჭელიძე, ლ. დარახველიძე, დ. დემეტრაშვილი, კ. ეფტაქსიასი (საბერძნეთი), ვ. ერემეევი (უკრაინა), ნ. ღლონტი, ა. გოგიჩაიშვილი (მექსიკა), ი. გეგენი (საფრანგეთი), თ. გვენცაძე, ზ. კერესელიძე, ო. ხარშილაძე, ზ. ხვედელიძე, ჯ. ქირია (მთ. რედაქტორის მოადგილე), თ. ქირია, გ. კოროტაევი (უკრაინა), თ. მაჭარაშვილი, გ. მეტრეველი, ვ. სტაროსტენკო (უკრაინა), კ. თავართქილაძე, ნ. ვარამაშვილი, ვ. ზაალიშვილი (რესპუბლიკა ჩრდილოეთ ოსეთი-ალანია, რუსეთი), ვ. ზალესნი (რუსეთი), ი. ჩშაუ (გერმანია).

ჟურნალის შინაარსი:

ჟურნალი მოიცავს მყარი დედამიწის, ატმოსფეროს, ოკეანისა და კოსმოსური პლაზმის ფიზიკის ყველა მიმართულებას. ჟურნალში ქვეყნდება: კვლევითი წერილები, მიმოხილვები, მოკლე ინფორმაციები, დისკუსიები, წიგნების მიმოხილვები, განცხადებები, კონფერენციების მოხსენებები.

JOURNAL OF THE GEORGIAN GEOPHYSICAL SOCIETY

Physics of Solid Earth, Atmosphere, Ocean and Space Plasma

Editor-in-chief: T. Chelidze

Editorial board:

A. Amiranashvili (secretary), T. Bibilashvili (USA), E. Bolopoulos (Greece), G. Chagelishvili, T. Chelidze, L. Darakhvelidze, D. Demetrashvili, K. Eftaxias (Greece), V. N. Eremeev (Ukraine), N. Ghlonti, A. Gogichaishvili (Mexica), Y. Gueguen (France), T. Gventsadze, Z. Kereselidze, O. Kharshiladze, Z. Khvedelidze, J. Kiria (Vice-Editor), T. Kiria, G. K. Korotaev (Ukraine), T. Matcharashvili, G. Metreveli, V. Starostenko (Ukraine), K. Tavartkiladze, N. Varamashvili, V.B. Zaalishvili (Republic of North Ossetia-Alania, Russia), V. B. Zalesny (Russia), J. Zschau (Germany).

Scope of the Journal:

The Journal is devoted to all branches of the Physics of Solid Earth, Atmosphere, Ocean and Space Plasma. Types of contributions are: research papers, reviews, short communications, discussions, book reviews, announcements, conference reports.

ЖУРНАЛ ГРУЗИНСКОГО ГЕОФИЗИЧЕСКОГО ОБЩЕСТВА

Физика Твердой Земли, Атмосферы, Океана и Космической Плазмы

Главный редактор: Т. Челидзе

Редакционная коллегия:

А. Амиранашвили (секретарь), Т. Бибилашвили (США), Е. Болополоус (Греция), Г. Чагелишвили, Т.Л. Челидзе, Л. Дарахвелидзе, Д. Деметрашвили, К. Эфтаксиас (Греция), В. Н. Еремеев (Украина), Н. Глонти, А.Гогичайшвили (Мексика), И. Геген (Франция), Т. Гвенцадзе, З. Кереселидзе, О. Харшиладзе, З. Хведелидзе, Дж. Кирия (зам. гл. редактора), Т. Кирия, Г. К. Коротаев (Украина), Т. Мачарашвили, Г. Метревели, В. Старостенко (Украина), К. Таварткиладзе, Н. Варамашвили, В.Б. Заалишвили (Республика Северная Осетия-Алания, Россия), В. Б. Залесный (Россия), И. Чшау (Германия).

Содержание журнала:

Журнал Грузинского геофизического общества охватывает все направления физики твердой Земли, Атмосферы, Океана и Космической Плазмы. В журнале публикуются научные статьи, обзоры, краткие информации, дискуссии, обозрения книг, объявления, доклады конференций.

მისამართი:

საქართველო, 0160, თბილისი, ალექსიძის ქ. 1, მ. ნოდიას სახ. გეოფიზიკის ინსტიტუტი
ტელ.: 233-28-67; ფაქსი; (995 32 2332867); ელ. ფოეტა: tamaz.chelidze@gmail.com; avtandilamiranashvili@gmail.com;
geophysics.journal@tsu.ge

გამოქვეყნების განრიგი და ხელმოწერა:

გამოიცემა წელიწადში ორჯერ. მყარი ვერსიის წლიური ხელმოწერის ფასია: უცხოელი ხელმომწერისათვის - 30 დოლარი, საქართველოში - 10 ლარი. ხელმოწერის მოთხოვნა უნდა გაიგზავნოს რედაქციის მისამართით. შესაძლებელია უფასო ონლაინ წვდომა:
http://openjournals.gela.org.ge/index.php/GGS

ჟურნალი ინდექსირებულა Google Scholar-ში:
https://scholar.google.com/citations?hl=en&user=pdG-bMAAAAAJ

Address:

M. Nodia Institute of Geophysics, 1 Alexidze Str., 0160 Tbilisi, Georgia
Tel.: 233-28-67; Fax: (99532) 2332867; e-mail: tamaz.chelidze@gmail.com; avtandilamiranashvili@gmail.com;
geophysics.journal@tsu.ge

Publication schedule and subscription information:

The journal is issued twice a year. The subscription price for print version is 30 $ in year.
Subscription orders should be sent to editor's address. Free online access is possible:
http://openjournals.gela.org.ge/index.php/GGS

The journal is indexed in the Google Scholar:
https://scholar.google.com/citations?hl=en&user=pdG-bMAAAAAJ

Адрес:

Грузия, 0160, Тбилиси, ул. Алексидзе, 1. Институт геофизики им. М. З. Нодиа
Тел: 233-28-67; 294-35-91; Fax: (99532)2332867; e-mail: tamaz.chelidze@gmail.com; avtandilamiranashvili@gmail.com;
geophysics.journal@tsu.ge

Порядок издания и условия подписки:

Журнал издается дважды в год. Годовая подписная цена для печатной версии - 30 долларов США. Заявка о подписке высылается в адрес редакции. Имеется бесплатный онлайн доступ
http://openjournals.gela.org.ge/index.php/GGS

Журнал индексирован в Google Scholar:
https://scholar.google.com/citations?hl=en&user=pdG-bMAAAAAJ

This journal uses Open Journal Systems 2.4.8.3, which is open source journal management and publishing software developed, supported, and freely distributed by the Public Knowledge Project under the GNU General Public License.

(http://openjournals.gela.org.ge/index.php?journal=GGS&page=about&op=aboutThisPublishingSystem)

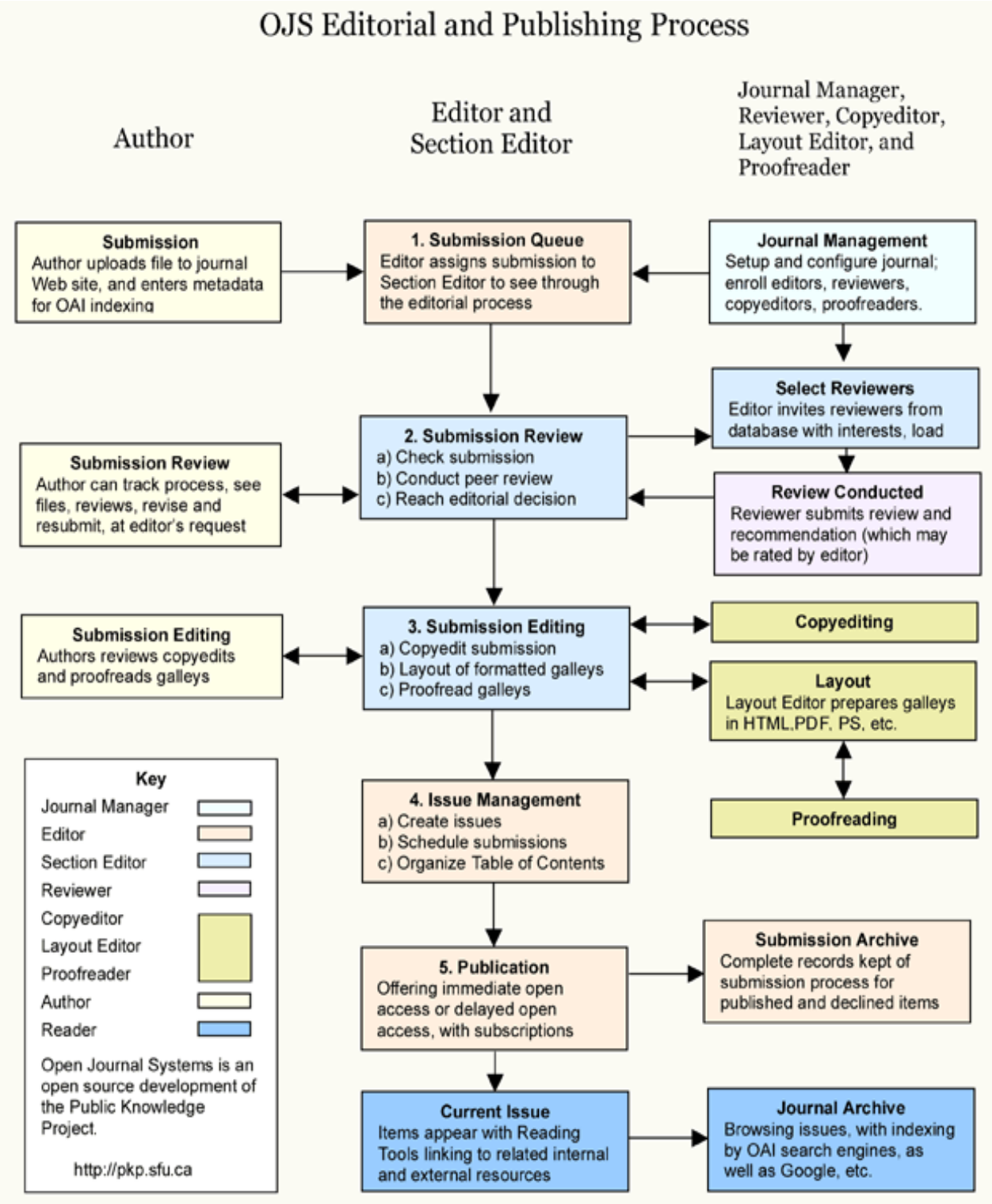

Journal of the Georgian Geophysical Society, e-ISSN: 2667-9973, p-ISSN: 1512-1127
Physics of Solid Earth, Atmosphere, Ocean and Space Plasma, v. 27(2), 2024, pp. 5 – 7

The Impact of the Earthquake in Racha on the Enguri Arch Dam and the Adjacent Area

[1]Jemal K. Kiria, [1]Temur A. Tsaguria, [2]Evgeni A. Sakvarelidze, [1]Nadezhda D. Dovgali, [1]Lali A. Davitashvili, [2]Guram A. Kutelia

[1]M. Nodia Institute of Geophysics of I. Javakhishvili Tbilisi State University, Georgia
[2]I. Javakhishvili Tbilisi State University, Georgia

ABSTRACT

As is well known, the Enguri Arch Dam, 271.5 meters high, was constructed on the Enguri River in the 1970s. It is built in a seismically active region with a complex geological structure.
The Enguri Dam's foundation crosses a branch of the Ingirishi fault, on which geophysical monitoring (using a deformograph) is conducted. The fault's edges move with the variation of the water level in the dam reservoir. Strong earthquakes can also cause displacement of the fault's edges.
This was the basis for conducting parallel geological, geophysical, geodetic, and other types of monitoring during the design and construction of the dam, some of which continue to this day
Key words: *Enguri Dam, deformograph, geophysical monitoring.*

Introduction

Tilt-metric and deformographic observations in the lower reach of the dam began in 1970 and are still ongoing. Since 1998, tilt-metric observations have also been conducted on the body of the dam. Currently, observations are conducted at seven different points on the dam (Fig. 1).

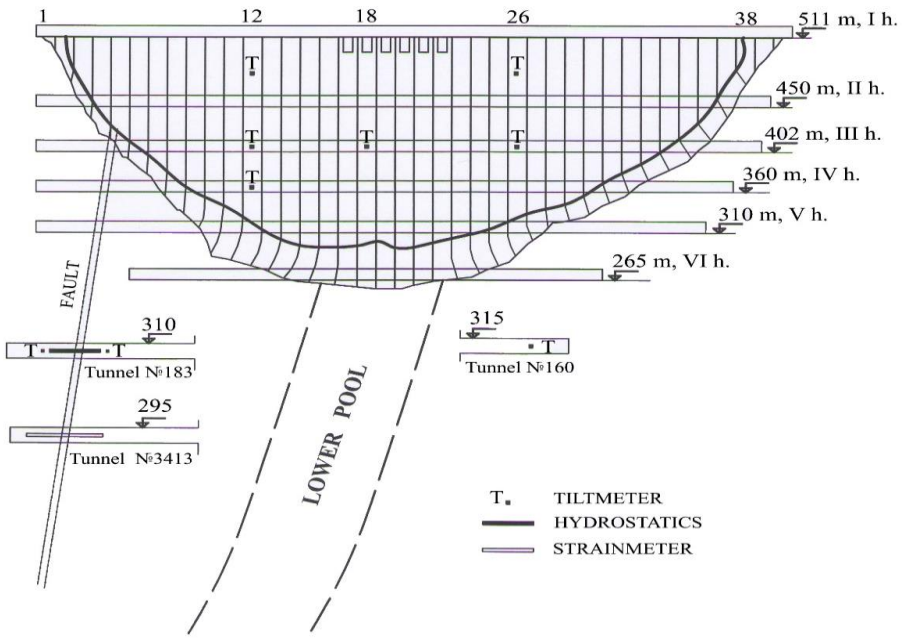

Fig. 1. The layout of the geophysical stations installed on the body and foundation of the Enguri Arch Dam.

As shown in the Fig. 1, the observation points are located at elevations of 360 m, 402 m, and 475 m in the 12th and 26th sections, as well as at the 402 m elevation in the central 18th section. At each point,

high-precision electrolitical tiltmeters of model 701-2A from an American company are installed. On August 20, 2024, a 4-magnitude earthquake occurred in Racha, causing deformation both on the fault and on the dam.

A branch of the Ingirishi fault crosses the foundation of the Enguri Dam, where geophysical observations are made using laser instruments with an accuracy of ± 1 micron. The fault edges experience deformation with changes in the water level of the dam. Earthquakes also cause deformation of the fault edges.

As shown in Fig. 2, the deformation caused by the earthquake on the fault reaches approximately 80 microns, which is a significant deformation (annual deformation = 120 microns). However, the edges quickly return to their original state, meaning that no residual deformation remains. Thus, the earthquake-induced wave caused the fault to shift.

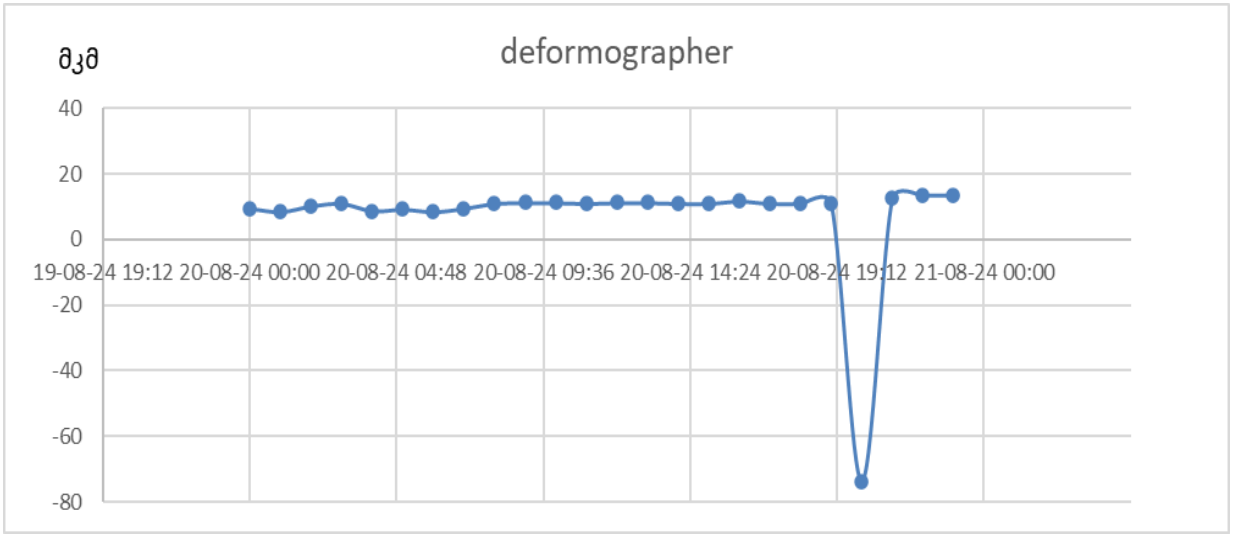

Fig. 2.

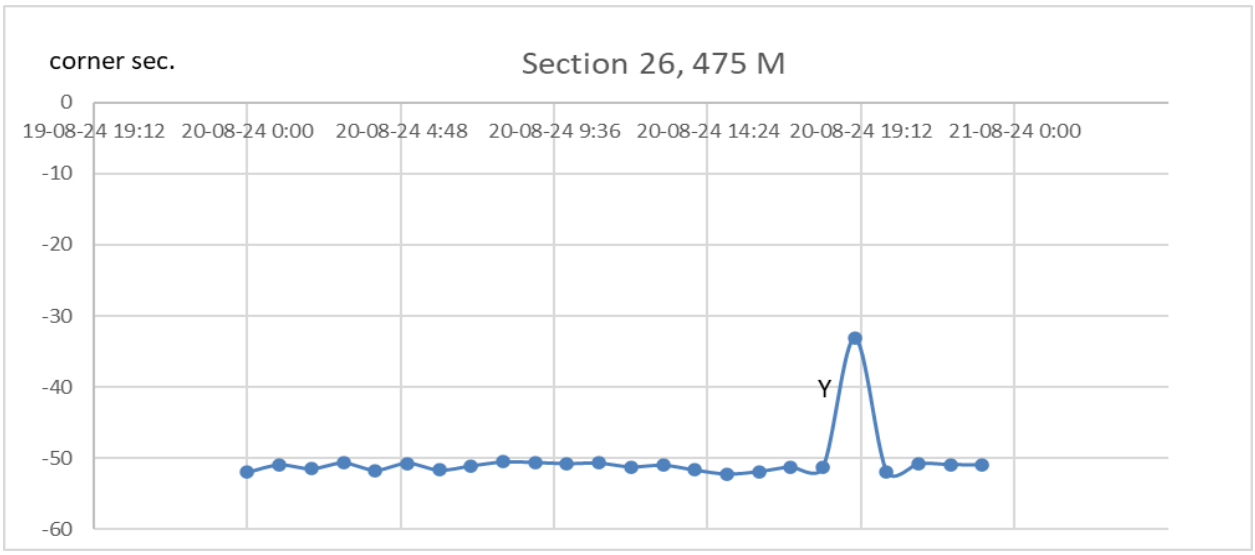

Fig. 3

Fig. 3 shows the deformation caused by the earthquake on the dam, specifically at the 475 m elevation in section 26. The value of the deformation does not exceed 18 arc-seconds. Similarly to the fault, the observation point returned to its original state after some time, indicating no residual deformation here either

In conclusion, we can state that the earthquake in Racha did not cause any significant changes to the dam or the fault.

References

[1] Abashidze V., Chelidze T., Tsaguria T., Sakvarelidze E., Dovgali N., Davitashvili L., Kutelia G. Results of tilt-metric observations conducted at the gravimetric laboratory of the Geophysics Department of the Faculty of Physics, Tbilisi State University. Works of the M. Nodia Institute of Geophysics, Vol. LXVII, 2017, pp. 96-104.
[2] Abashidze V., Chelidze T., Dovgali N., Davitashvili L. Dynamics of fault blocks passing through the Enguri Arch Dam's body and foundation based on stationary geophysical observation data. Works of the M. Nodia Institute of Geophysics, Vol. LXIX, 2018.

რაჭის მიწისძვრის გავლენა ენგურჰესის თაღოვან კაშხალსა და მის მიმდებარე ტერიტორიაზე

ჯ. ქირია, თ. ცაგურია, ე. საყვარელიძე, ნ. დოვგალი,
ლ. დავითაშვილი, გ. ქუთელია

რეზიუმე

როგორც ცნობილია, მდ. ენგურზე გასული საუკუნის 70- იან წლებში აშენდა მაღლივი 271.5 მ. სიმაღლის თაღოვანი კაშხალი. იგი აშენებულია რთული გეოლოგიური აგებულების და სეისმურად აქტიურ რეგიონში.
ენგურჰესის კაშხლის ფუძეში გადის ინგირიშის ნაპრალის განშტოება, რომელზეც წარმოებს გეოფიზიკური დაკვირვება (დეფორმოგრაფი). ნაპრალის ბორტები მოძრაობენ ჰესში წყლის დონის ცვალებადობის დროს. ბორტების ამოძრავება ასევე შეუძლია ძლიერ მიწისძვრასაც.
სწორედ ეს გახდა საფუძველი იმისა, რომ ამ ობიექტის პროექტირებისა და მშენებლობის პერიოდში პარალელურად მიმდინარეობდა გეოლოგიური, გეოფიზიკური, გეოდეზიური და სხვა სახის დაკვირვებები, რომელთა გარკვეული ნაწილი დღესაც გრძელდება.
საკვანძო სიტყვები: ენგურგესის კაშხალი, დეფორმოგრაფი,გეოფიზიკური მონიტორინგი.

Влияние землетрясения в Раче на арочную плотину и прилегающую территорию в районе Ингури ГЭС

**Дж. Кириа, Т. Цагурия, Е. Сакварелидзе, Н. Довгали,
Л. Давиташвили, Г. Кутелиа**

Резюме

Как известно, в 70-х годах прошлого века на реке Ингури была построена арочная плотина высотой 271,5 м. Она расположена в геологически сложном и сейсмически активном регионе
Основание плотины Ингурской ГЭС пересекает разлом Ингири, на котором проводится геофизическое наблюдение (деформограф). Берега разлома движутся в зависимости от изменения уровня воды в ГЭС. Также движения берегов могут быть вызваны сильными землетрясениями.
Это стало основанием для того, чтобы в процессе проектирования и строительства данного объекта одновременно проводились геологические, геофизические, геодезические и другие виды наблюдений, часть которых продолжается и по сей день.

Ключевые слова: плотина Ингурской ГЭС, деформограф, геофизический мониторинг.

Journal of the Georgian Geophysical Society, e-ISSN: 2667-9973, p-ISSN: 1512-1127
Physics of Solid Earth, Atmosphere, Ocean and Space Plasma, v. 27(2), 2024, pp. 8 - 14

Confidence Interval of Parameters for Gaussian Statistical Structures Z-Criteria's Application

[1]Zurab S. Zerakidze , [2]Jemal K. Kiria, [2]Tengiz V. Kiria

[1]Gori State University, Gori, Georgia
[2]M. Nodia Institute of Geophysics of I. Javakhishvili Tbilisi State University, Georgia

ABSTRACT

In this paper is proven 100% confidence interval of parameters for Gaussian statistical structures in Banach space of measures.
Key words: *Gaussian statistical structure, consistent estimators of parameters, Z-criteria, orthogonal structure, strongly separable structure, confidence interval of parameters.*

Introduction

Recall that a statistical criterion is any measurable mapping from the set all possible samples values to the set of hypothesis. It is said that an error of h-th kind of the δ criterion occurs, if the criterion ejects the main hypothesis of H_h. The following $\alpha_h(\delta) = \mu_h(\{x: \delta(x) \neq h\})$ is called the probability of an error of the h-th kind for a given criterion δ.

The notion and corresponding construction of Z-criteria (same "Generalization criterion of Neiman-Pearson, consistent criterion") for hypothesis testing were introduced and studied by Z. Zerakidze (see [2-13]).

We recall some definitions from the works [1-14].

Let (E,S) be a measurable space. The density of Gaussian law is determined by the equality

$$f(x) = \frac{1}{\sqrt{2\pi}\sigma} e^{-\frac{(x-a)^2}{2\sigma^2}}$$

Let μ be the probability measure given on $([-\infty,+\infty), L[-\infty,+\infty))$ by the formula $\mu(A) = \int_A f(x)dx, A \in L[-\infty;+\infty)$, where $L([-\infty,+\infty))$ is Lebesgue σ-algebra. Let $\{\mu, i \in I\}$ be Gaussian measures.

Definition 1. An object $\{E,S,\mu,i \in I\}$ is called an Gaussian statistical structure. Definition 2. An Gaussian statistical structure $\{E,S,\mu_,i \in I\}$ is called orthogonal if μ_i and μ_j are orthogonal for each $\forall i \neq j, i \in I, j \in I$.

Definition 3. An Gaussian statistical structure $\{E,S,\mu,i \in I\}$ is called weakly separable if there exists a family of S-measurable sets $\{X,i \in I\}$ such that the relations are fulfilled:

$$(\forall i)(\forall j)(i \in I \& j \in I) \Rightarrow \mu_i(X_) = \begin{cases} 1, & \text{if } i = j \\ 0, & \text{if } i \neq j \end{cases}$$

Let $\{\mu_,i \in I\}$ be Gaussian measures defined on the measurable space (E,S). For each $i \in I$ we denote by $\bar{\mu}_i$ the completion of the measure μ_i, and by $\mathrm{dom}\,(\bar{\mu}_i) -$ the $\sigma -$ algebra of all $\mu_i -$ measurable subsets of E . We denote $S_1 = \bigcap_{i\in I}\mathrm{dom}\,(\bar{\mu}_i)$.

Definition 4. The Gaussian statistical structure $\{E,S,\mu_l,i \in I\}$ is called strongly separable Gaussian statistical structure if there exists a family of S-measurable sets $\{Z_i,i \in I\}$ such that the relations are fulfilled

1 $\mu_i(Z_i) = 1, \forall i \in I;$

2 $Z_i \cap Z_j = \emptyset \forall i \neq j; i,j \in I$

3 $\bigcup_{i\in I} Z_i = E.$

Let I be set of parameters and $\mathrm{B(I)}$ be σ-algebra if subsets of I which contains all finite subsets of I.

Definition 5 . We will say that the Gaussian statistical structure $\{E,S_1,\bar{\mu}_i,i \in I\}$ admits a consistent estimators of parameters if there exists at least one measurable mapping $f\colon (E,S_1) \to (I,B(I))$, such that $\bar{\mu}_i(\{x\colon f(x) = i\}) = 1, \forall i \in I.$

Let H be set of hypotheses and $B(H)$ be σ-algebra of subsets of H which contains alle finite subsets of H .

Definition 6. We will say that the Gaussian statistical structure $\{E,S_1,\bar{\mu}_h,h \in H\}$ admits Z-criterion (same "Generalization Neimana-Pearson,consistent criterion") for hypothesis testing if there exists at least one measurable mapping $\delta\colon (E,S_1) \to (H,B(H))$, such that

$\bar{\mu}_h(\{x\colon \delta(x) = h\}) = 1, \forall h \in H.$

Definition 7. The probability $\alpha_h(\delta) = \bar{\mu}_h(\{x\colon \delta(x) \neq h\})$ is called the probability of error of hth kind for the given criterion δ.

Theorem 1. The Gaussian statistical structure $\{E,S_1,\bar{\mu}_h h \in H\}$ admits a Z-criterion (same "Generalization Neimana-Pearson, consistent criterion") for hypothesis testing if and only if this probability of error of kind is equal to zero for the criterion δ.

Proof. Necessity. Since the statistical structure $\{E,S_1,\bar{\mu}_h h \in H\}$ admits a Z-criterion countable Gaussian statistical structure $\{E,S,\mu_h,h \in H\}$ admits a Z-criterion for hypothesis testing, there exists a measurable mapping $\delta\colon (E,S_1) \to (H,B(H),$ such that $\bar{\mu}_h(\{x\colon \delta(x) = \ h\}) = 1, \forall h \in H.$ Therefore, $\alpha_h(\delta) = \bar{\mu}_h(\{x\colon \delta(x) \neq h\}) = 0, \forall h \in H.$

Sufficiency. Since the probability of any kind is equal to zero, have $\alpha_h(\delta) = \bar{\mu}_h(\{x\colon \delta(x) \neq h\}) = 0, \forall h \in H.$

On other hand, $\mu\{x\colon [(\delta(x) = h) \cup (\delta(x) \neq h)]\} = \bar{\mu}_h(\{x\colon \delta(x) = h\}) = 1, \forall h \in H.$

2. Confidence interval for of parameters Gaussian statistical structures in Banach space of measures

Let M^σ be a real linear space of all alternating finite measures on S.

Definition 8. A linear subset $M_B \subset M^\sigma$ is called a Banach space of measures if:

1 The norm on M_B can be defined so that M_B it is Banach space with respect to this norm, and the inequality $\| \mu + \lambda v \| \geq \| \mu \|$ holds for any orthogonal measures $\mu, v \in M_B$ and real number $\lambda \neq 0$;

2 If $\mu \in M_B$ and $|f(x)| \leq 1$, then $v_f(A) = \int_A f(x)\mu(dx) \in B_B$ and $\|v_f\| \leq \| \mu \|$;

3 If $v_n \in M_B, v_n > 0, v_n(E) < \infty, n = 1,2,\ldots$ and $v_n \downarrow 0$, then for any linear functional $l^* \in M_B^*: \lim_{n\to\infty} l^*(v_n) = 0$, where M_B^* conjugate to linear space M_B.

Remark 1. The definition and construction of a Banach space of measures were given by Z . Zerakidze (see [14]).

Definition 8. Let I be a set of indexes and M_{B_i} is a Banach space for all $i \in I$. The Banach space $M_B = \{X_i\}_{i\in l}: X_i \in M_{B_i}, \forall i \in I, \sum_{i\in I} \|X_i\| \leq 0\}$ with the norm $\|X_i\|_{i\in I} = \sum_{i\in I} \|X_i\|_{M_{B_i}}$ is called the direct sum of Banach space M_{B_i} and is denoted by $M_B = \bigoplus M_{B_i}$.

Remark 2. Obviously, any Banach space of measures is a Banach space the elements of which are alternating measures, but not vice versa. The following theorem was proved in [14].

Theorem 2. Let M_B be a Banach space of measures, then there exists the funnily of pairwise orthogonal probability measures $\{\mu_{h_i}, i \in I\}$, Card $I = 2^{2^c}$, such that $M_B = \bigoplus M_{B_i}(\mu_{h_i})$ is Banach space of elements v of the from

$v(B) = \int f(x)\mu_{h_i}(dx), B \in S, \int |f(x)|\mu_{h_i}(dx) < +\infty$, with the norm

$$\| v \|_{M_{B_l}(\mu_{B_i})} = \int |f(x)|\mu_{h_i}(dx).$$

We define by $\mathrm{F} = \mathrm{F}(M_B)$ the set of real function f such that $\int f(x)\bar{\mu}_h dx$ is defined all $\bar{\mu}_h = M_B$. Theorem 3. Let $M_B = \bigoplus M_{B_i}(\bar{\mu}_h)$, Card $H \leq c$ be the Banach space of measures, E be a complete separable metric space, $S_1 = \bigcap_{h\in H} \mathrm{dom}\,(\bar{\mu}_h)$ is a Borel σ-algebra on E. In order for the Borel orthogonal Gaussian statistical structure $\{E, S_1, \bar{\mu}_h h \in H\}$, Card $H = c$ to admit Z-criterion (same "Generalization Neimana; Pearson consistent criterion") for hypothesis testing in the theory (ZFC)&(MA) it is necessary and sufficient the correspondence $f \leftrightarrow h_f$ defined by the

equality $\int f(x)\bar{\mu}_h(dx) = l_f(\bar{\mu}_h)$, $\bar{\mu}_h \in M_B$ was one-to-one (here l_f is a linear continuous functional on $M_B, f \in F(M_B)$.

Proof. Necessity. The existence of Z-criterion for hypothesis testing $\delta: (E, S_1) \to (H, B(H))$, implies that $\bar{\mu}_h(\{x: \delta(x) = h\}) = 1, \forall h \in H$. Setting $X_h = (\{x: \delta(x) = h\}) = 1, \forall h \in H$ we get:

1 $\bar{\mu}_h(X_h) = 1, \forall h \in H$;

2 $X_{h'} \cap X_{h''} = \emptyset$ for all different h' and h'' from H;

3 $\cup_{n\in H} X_h = \{x: \delta(x) \in H\} = E$.

Therefore the Gaussian statistical structure $\{E, S_1, \bar{\mu}_h h \in H\}$ is strongly separable, hence, there exists S_1 - measurable sets $\{X_h, h \in H\}$ such that $\bar{\mu}_h(X_{h'}) = \begin{cases} 1, & \text{if } h = h' \\ 0, & \text{if } h \neq h' \end{cases}$

We put the linear continuous functional l_{c_h} into correspondence to function by the formula $\int l_{c_h}(x)\bar{\mu}_h(dx) = l_{c_h}(\bar{\mu}_h) = \|\bar{\mu}_h\|_{M_B(\bar{\mu}_h)}$.

Let l_{X_h} be a linear continuous functional that correspondence to the function $\bar{f_1}(x) = f_1(x)I_{X_h}(x)$. Then for any $\bar{\mu}_{h_1} \in M_B(\bar{\mu}_h)$ we have

$$\int \bar{f_1}(x)\bar{\mu}_{h_1}(dx) = \int f_1(x)f(x)I_{X_h}(x)\bar{\mu}_h(dx) = l_{\bar{f_1}}(\bar{\mu}_{h_1}) = \|\bar{\mu}_{h_1}\|_{M_B(\bar{\mu}_h)}.$$

Let $\sum$ be the set of extensions of a functional that satisfy the condition $l_f \le p(x)$ in those subspace where they are defined. Lets introduce a partial ordering into, assuming $l_{f_1} < l_{f_1}$ if f_2 is defined on a large set than l_{f_1} and $l_{f_1} = l_{f_2}$ where both of them are defined.

Let $\{l_{f_h}\}_{h\in H}$ be a linear ordered subsid in $\sum, M_B(\bar{\mu}_h)$ the subspace on which l_{f_h} is defined. We define $l_f \in \cup M_B(\bar{\mu}_h)$ setting $l_f(\mu) = l_{f_h}(\mu)$ if $\mu \in M_B(\bar{\mu}_h)$. It is obvious that $l_{f_h} < l_f$. Since any lineally ordered subset in $\sum$ has an upper bound due to the Chorn lemma $\sum$ contains the maximal element λ defined on some set X' satisfying the condition $\lambda \le \mathrm{p(x)}$ for $x \in X'$. But X' must coincide with the entire space M_B because otherwise we could extended λ to a wider space by adding as above one more dimension. This contradicts the maximality of λ and, hence $X' = M_B$. Therefore, the extension of the functional is defined everywhere.

Let l_f be a linear functional that corresponds to the function $f(x) = \sum g_h(x)I_{X_h}(x) \in F(M_B)$. Then we have $\int f(x)\mu(dx) = \| \mu \| = \sum \|\bar{\mu}_h\|_{M_B(\bar{\mu}_h)}, M_B(\bar{\mu}_h)$ where

$$\mu(B) = \sum \int g_h(x)\bar{\mu}_h(dx),\ B \in S_1$$

Sufficiency. If for each $f \in F(M_B)$ the integral $\int f(x)\bar{\mu}_h(dx), \forall\bar{\mu}_h \in M_B$, is defined them there exist a countable subsets I_f in H for which $\int f(x)\bar{\mu}_h(dx) = 0$, if $h\bar{\in} I_f$, $\sum\int |f(x)|\bar{\mu}_h(dx) < \infty$ and for any countable subset $\bar{I} \subset H$ and for the measure

$v(c) = \int_{h\in i}\int_c g_h(x)\bar{\mu}_h(dx)$ we have $\int_E f(x)v(dx) = \sum_{h\in I_f\cap\bar{I}}\int_E f(x)g_h(x)\bar{\mu}_h(dx)$.

Let the correspondence $f \to l_f$ be calefied the equality $\int_E f(x)\bar{\mu}_h(dx) = l_f(\bar{\mu}_h)$, then for $\bar{\mu}_{h_1}$, $\bar{\mu}_{h_2} \in M_B(\bar{\mu}_h)$ we have $\int_E f_{h_1}(x)\bar{\mu}_{h_2}(dx) = l_{f_{h_1}}(\bar{\mu}_{h_2}) = \int_E f_1(x)f_2(x)\bar{\mu}_{h_1}(dx) = \int_E f_{h_1}(x)f_{h_2}(x)\bar{\mu}_{h_1}(dx)$.

Therefore $f_{h_1}(x) = f_1(x)$ almost everywhere with respect to the measure $\bar{\mu}_{h_1}$. Let $f_{\bar{\mu}_{h_1}}(x) > 0$ almost everywhere with respect to $\bar{\mu}_{h_i}$ and $\int_E f_{\bar{\mu}_h}(x)\bar{\mu}_h(dx) < \infty$. If we denoyte now $\bar{\mu}_h(c) = \int_c f_{\bar{\mu}_h}(\mathrm{x})\bar{\mu}_h(dx)$, the we obtain $\int_E f_{\bar{\mu}_h}(x)\bar{\mu}_{h'}(dx) = l_{f_{\bar{\mu}_h}}(\bar{\mu}_{h'}) = 0, \forall h \ne h'\ \forall\bar{\mu}_h \in M_B(\bar{\mu}_h)$.

Denote by $C_h = \{x: f_{\bar{\mu}_h}(x) > 0\}$. Then $\mu_{h'}(C_h) = 0 \forall h \ne h'$. Therefore, there exist S_1 − measurable sets $(h \in H)$ such that that $\mu_h(X_{h'}) = \begin{cases}1, & \text{if } h = h'\\ 0, & \text{if } h \ne h'\end{cases}$ and hence the Gaussian statistical structure

$\{E, S_1, \bar{\mu}_h h \in H, \text{card}H = c\}$ is weakly separable. We represent as an inductive sequence $\{\bar{\mu}_h < w_1\}$ where w_1 denotes the first ordinal number of the power of the set H .

We define w_1 sequence Z_h of parts of the E such that the following relations hold: 1) Z_i is Borel subset of E, $\forall h < w_1$; 2) $Z_h \subset X_h, \forall h < w_1$; 3) $Z_h \cap Z_{h'} = \emptyset$ for all $h' < w_1, h = h'$; 4) $\bar{\mu}_h(Z_h) = 1, \forall h < w_1$.

Suppose that $Z_{h_0} = X_{h_0'}$. Suppose that the partial sequence $\{Z_{h'}\}_{h'<h}$ is already defined for $h < w_1$. It is clear that $\mu^*(\cup_{h'<h} Z_{h'}) = 0$. Thus there exists a Borel subset y_h of the space E such that the following relations are valid $\cup_{h'<n} y_h$ and $\mu^*(y_h) = 0$. Assuming that $Z_h = X_h\ y_h$, we construct the w_1 sequence $\{Z_h\}_{h<w_1}$ of disjunctive measurable subsets of the space E. Therefore, $\mu_h(Z_h) = 1, \forall h < w_1$ and the Gaussian statistical structure $\{E, S_1, \bar{\mu}_h h \in H, \text{card}H = c\}$ is strongly separable because that exists a family of elements of the σ-algebra $S_1 = \cap_{h\in H} \text{dom}\,(\bar{\mu}_h)$ such that 1) $\bar{\mu}_h(Z_h) = 1, \forall h \in H; 2) Z_{h'} \cap Z_h = \emptyset, \forall h' \neq h; 3) \cup_{h\in H} Z_h =$ E.

For $x \in E$, we put $\delta(x) = h$, where h is the unique hypothesis from the set H for which $x \in Z_h$. The existence of such a unique hipotez from H can be proved using conditions 2), 3).

Let now $y \in B(H)$. Then $\{x: \delta(x) \in y\} = U_{h\in H} Z_h$.

It $h_0 \in H$, then $\{x: \delta(x) \in y\} = U_{h\in H} Z_h = Z_{h_0} \cup (U_{h\in H} Z_h)$. On the other hand the validity of the condition $\cup_{h\in H} Z_h \subseteq E - Z_{h_0}$ implies that $\bar{\mu}_{h_0}(\cup_{h\in y-h_0} Z_h) = 0$. The last equality yields $\cup_{h\in y-h_0} Z_h \in \text{dom}\,(\bar{\mu}_{h_0})$. Since $\text{dom}\,(\bar{\mu}_{h_0})$ is a σ-algebra, we deduce that $\{x: \delta(x) \in y\} \in \text{dom}\,(\bar{\mu}_h)$.

If $h_0 \notin y$, then $\{x: \delta(x) \in y\} = U_{h\in H} Z_h \leq (E - Z_{h_0})$ and we conclude that $\bar{\mu}_{h_0}(\{x: \delta(x) \in y\}) = 0$. The last relation implies that $\{x: \delta(x) \in y\} \in \text{dom}\,(\bar{\mu}_{h_0})$.

We have shown that the map $\delta: (E, S_1) \to (H, B(H)$ is a measurable map. Since B(H) contains all singletons of H we as certain that $\bar{\mu}_h(\{x: \delta(x) = h\}) = \bar{\mu}_h(Z_h) = 1, \forall h \in H$.

The following Theorem is proven to Theorem 2.

Theorem 3. Let $M_B = \oplus M_B(\bar{\mu}_i)$, Card $I \leq c$ be the Banach space of measures, E be a complete metric space, $S_1 = \bigcap_{i\in I} \text{dom}\,(\bar{\mu}_i)$ is a Borel σ-algebra on E. In order for the Borel orthogonal Gaussian statistical structure $\{E, S_1, \bar{\mu}_i, i \in I\}$, Card $I \leq c$ to admit consistent estimator of parameters it is necessary and sufficient that correspondence $f \leftrightarrow l_f$ defined by the equality $\int f(x)\bar{\mu}_i(dx) = l_f(\bar{\mu}_i), \bar{\mu}_i \in M_B$ was one-to-one (have l_f is a linear continuous functional on $M_B, f \in F(M_B)$.

The following Theorems 1,2,3,4 follows that exponentials Gaussian structures existence consistent estimator of parameters Z-criterion for hypothesis testing and 100% confidence interval of parameters.

References

[1] Ibramhalilov I., Skorokhod A. Consistent estimates of parameters of random processes. Naukova Dumka. Naukova Dumka. Kiev, 1980.

[2] Zerakidze Z. Banach space of measures. Probability Theory and Mathematical Statistics. Proceeding of the fifth Vilnius Conference. VSP, Moksha's, V.1, 1990.

[3] Zerakidze Z. Generalization of Neimann-Pearson criterion. Collection of Scientific works of Gori University, 2005.

[4] Zerakidze Z. Generalization of Neimann-Pearson criterion. Proceeding of international Scientific conference: "Internation technologies. Tbilisi. Georgian Technical University, 2008.

[5] Aleksidze L., Eliauri L., Mumladze M., Zerakidze Z. Consistent criteria in metric Space. Proceedings of IV International conference "Problems of cybernetics and informatics", Baku, 2012.

[6] Eliauri L., Mumladze M., Zerakidze Z. Consistent criteria for checking Hypotheses. Journal of Mathematics and System Science, V.3, № 10, October 2013.

[7] Aleksidze L., Mumladze M., Zerakidze Z. Consistent criteria for checking hypotheses Modern Stochastics. Theory and Applications, V. 1, №1, 2014.

[8] Zerakidze Z., Purtukhia O. Extreme Points and Consistent criteria for hypothesis Testing in Banach space of measures. Bulletin of the Georgian National Academy of Sciences, V. 12, № 4, 2014.

[9] Zerakidze Z., Mumladze M. Statistical structures and consistent criteria for checking hypotheses. Lambert Academic Publishing Saarbrucken, 2015.

[10] Purtukhia O., Zerakidze Z. The Consistent criteria for hypotheses testing. Math. 1. 71, № 4, 2019.

[11] Purtukhia O., Zerakidze Z. On consistent criteria of hypotheses testing for non-separable complete metric space. Bulletin of TICMI, V. 23, № 2, 2019.

[12] Aleksidze L., Mumladze M., Zerakidze Z. The Z-criteria of hypothesis testing in Hilbert space of measures. Report of Enlarged Sessions of the seminar of I. Vekua institute of Applied Mathematics, 2024.

[13] Zerakidze Z., Tsotniashvili S. The consistent criterion for hypothesizing testing. Bulletin of TICMI, V. 28, №1, 2024.

[14] Chkonia T., Tkeburava M. The Z-criteria of hypothesis testing for exponential statistical structure in Banach space of measures. Report of Enlarged sessions of the Seminar of I. Vekua Institute of Applied Mathematics, 2024.

პარამეტრების ნდობის ინტერვალი გაუსის სტატისტიკური სტრუქტურებისათვის Z - კრიტერიუმის გამოყენებით

ზ. ზერაკიძე, ჯ. ქირია, თ. ქირია

რეზიუმე

ნაშრომში განმარტებულია გაუსის ორთოგონალური, სუსტად განცალებადი, განცალებადი და ძლიერად განცალებადი სტატისტიკური სტრუქტურები. ასევე განმარტებულია პარამეტრების ძალდებული შეფასებები და პარამეტრების ჰიპოთეზათა შემოწმების სტრუქტურებისათვის Z - კრიტერიუმი (იგივეა, რაც „განზოგადოებული ნეიმან-პირსონის კრიტერიუმი“, „ძალდებული კრიტერიუმი“).

აგებულია გაუსის ალბათობების ზომების მიხედვით ბანახის ზომათა სივრცე და დამტკიცებულია ამ სივრცეში აუცილებელი და საკმარისი პირობები პარამეტრების ძალდებული შეფასებების და Z - კრიტერიუმის არსებობის შესახებ.

აგებულია გაუსის სტატისტიკური სტრუქტურების პარამეტრებისათვის 100%-იანი ნდობის ინტერვალი.

საკვანძო სიტყვები: გაუსის სტატისტიკური სტრუქტურა, თანმიმდევრული პარამეტრების შეფასებები, Z-ტესტი, ორთოგონალური სტრუქტურა, მკაცრად განცალკევებული სტრუქტურა, პარამეტრების ნდობის ინტერვალი.

Доверительный интервал параметров для статистических структур Гаусса с использованием Z-критерия

З. Зеракидзе, Дж. Кирия, Т. Кирия

Аннотация

В статье объясняются ортогональные, слабо разделимые, разделимые и сильно разделимые статистические структуры Гаусса. Также даются пояснения о вынужденных оценках параметров и Z-критерии для проверки гипотез о параметрах статистических структур (аналогичен «обобщённому критерию Неймана-Пирсона», «вынужденному критерию»). На основе вероятностных мер Гаусса построено пространство размерностей выборки и доказаны необходимые и достаточные условия существования вынужденных оценок параметров и Z-критерия в этом пространстве.

Для параметров статистических структур Гаусса построен 100%-й доверительный интервал.

Ключевые слова: гауссовская статистическая структура, состоятельные оценки параметров, Z-критерий, ортогональная структура, сильно разделимая структура, доверительный интервал параметров.

Journal of the Georgian Geophysical Society, e-ISSN: 2667-9973, p-ISSN: 1512-1127
Physics of Solid Earth, Atmosphere, Ocean and Space Plasma, v. 27(2), 2024, pp. 15 - 28

The Radio Image of an Object with an Elongated, Face-Fragmented, Dielectrically Complex Structure was Studied Using the Method of Georadar Physical Modeling

David T. Odilavadze, Tamaz L. Chelidze, Olga V. Yavolovskaya

Mikheil Nodia Institute of Geophysics of Ivane Javakhishvili Tbilisi State University, Tbilisi, Georgia
odildavit@gmail.com

ABSTRACT

Georadiolocation method has been widely used in many fields with geological content. Important results are obtained in the solution of many problematic issues of urban engineering, the solution of many tasks has become possible in archaeogeoradiolocation.
For archaeological work, it is important to fix and decipher the radio image of the object as a result of the mutual distance between the target objects and the georadar antenna. During archaeological work, the distance of the target object is unknown, which distorts or even makes it impossible to fix the radio image of the object. Important information may not be received.
A radio view of the object is allocated, which embeds the location of the object and exceeds its geometric dimensions spatially by approximately three times. At the same time, the lower part of the object is connected to the radio image in general with the so-called feature of antennas. With the content of the diagram of the direction of the electromagnetic field, that is, it clearly defines and separates the location of the object considered as a secondary radiation antenna.
Thus, it is possible to determine the physical model of the foundation and, therefore, the radio image of the field object based on the theory of the similarity of geolocation electromagnetic fields. The depth of the model object is clearly defined by the location of the last horizontal synch axis recorded on the radio face on the radargram, both during horizontal and vertical georadiolocation exposure.
***Keywords**: Archaeogeoradiolocation method, radio image, physical modeling, Zond 12-e.*

Introduction

The Radio Image of an Object with an Elongated, Face-Fragmented, Dielectrically Complex Structure was Studied Using the Method of Georadar Physical Modeling

The method of georadiolocation has found wide application in many areas of geological content. Important results have been obtained in solving many problematic issues of urban development, the solution of many problems has become possible in archeogeoradiolocation [1-9].

Problem

For archaeological work, it is important to record and decipher the radio image of an object as a result of the mutual arrangement between the target objects and the ground penetrating radar antenna, i.e., to solve the inverse problem of electrodynamics. In order for the radio image of an object to be fully recognized, the GPS antenna must be located in the far zone of the target object, i.e. the distance between the antenna and the object must exceed the wavelength of the radiation. In archaeological work, the distance to the target object is unknown, so the object can be located both in the near zone and in the middle and far zones relative to the antenna, which distorts or even makes it impossible to record and recognize the radio image of the object. As a result, important information may not be obtained during archaeological GPR work [10,11,12,13].

Methods and tools

In the sector of applied and experimental geophysics of the Institute of Geophysics, using a device for georadar physical modeling, studies were conducted to determine the radio features of objects located in the middle zone. Based on the theory of similarity using three-dimensional scaling coefficients, it is possible to

calculate the frequency and geometric dimensions for detecting natural target objects and recording their radio images [2,3,4,5,11,12,13,14,15].

Model

For archaeological research we have chosen such an important object as a model of a fragment of the foundation of the wall. The model is made of basalt parallel-faced blocks of irregular shape with a thickness of about 0.05-0.06m, the average length varies within 0.25-0.35m, the gaps between the blocks are filled with the material that makes up the model environment - sand. The model itself is presented in the form similar to a parallelepiped with curvature. Its uneven dimensions are on average 0.7x0.3x0.2 m, and the curvature of the surface varies by 0.05-0.10m.[2,4,14]

Ground penetrating radar from the day surface.

For the sand-covered object, seven parallel profiles were drawn across the foundation-object/wall. Below is a diagram of the relative position of the longitudinal model object and the ground penetrating radar profiles.

The ground penetrating radar profiles were drawn using the Zond 12-e ground penetrating radar, a 2GHz receiving and transmitting standard antenna, data search, processing and interpretation were carried out using the Prizm-2.70 software.[.]

Georadar physical model of a parallelepiped of complex dielectric and fragmentary composition (Scheme 1).

.

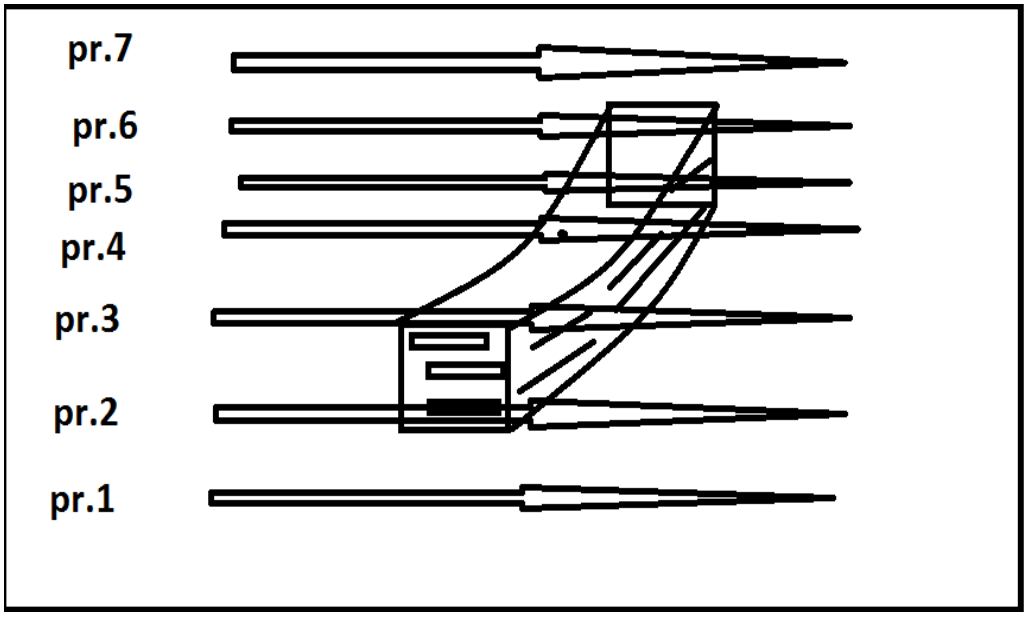

Scheme 1.

An object composed of basalt blocks with uneven boundaries, having the shape of a curved parallelepiped with parallel edges, the spaces between which are filled with sand, which constitutes the modeling environment, was chosen as a model. The dimensions of the object are approximately 0.7x0.3x0.16m. The object is located 0.05-0.10m below the air-sand horizontal surface.

The model is placed inside the model area of the sand-containing environment measuring 2.4x1.4x1.4m. With horizontal ground penetrating radar exposure, the profiles are parallel and are spaced from each other at a distance of 0.12m.

When exposed from a vertical wall, the profiles pass through the surface of the submerged model, covering only the air-containing space, the second profile covers the part containing the object, and the third passes through the lower part, where the radio image of the object should be located.

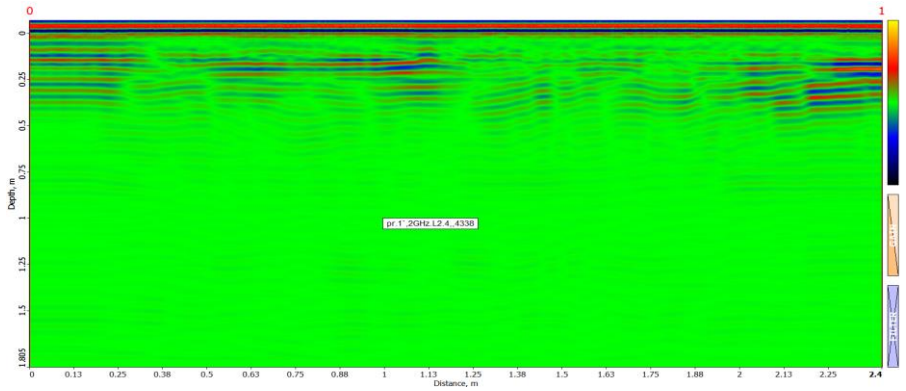

Fig. 1. Shows the corresponding radargram Prof-1, obtained with the transmitting-receiving antenna of the ground penetrating radar "Zond 12-e", 2 GHz.

The location of the object of study on the course of profile-1 (Fig. 1) is not marked, therefore its influence on the radargram is not visible. The radio image of the model object against the background of the existing lateral anomalies is not clearly readable, but the part of the radio image caused by the “bow-tai” type of “hole” /model space, wall-wall model/ is poorly distinguishable but easy to read.

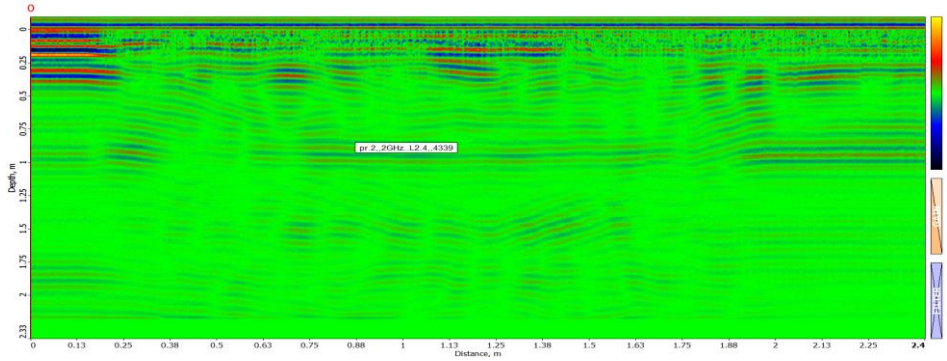

Fig. 2. Shows the corresponding radargram of profile-2, obtained using the receiving and transmitting antenna of the Zond 12e georadar, 2 GHz.

The location of the object of study along profile-2 is poorly marked (Fig. 2), so its influence on the radargram is partially visible. The radio image of the model object is not clearly read against the background of the existing lateral anomalies.

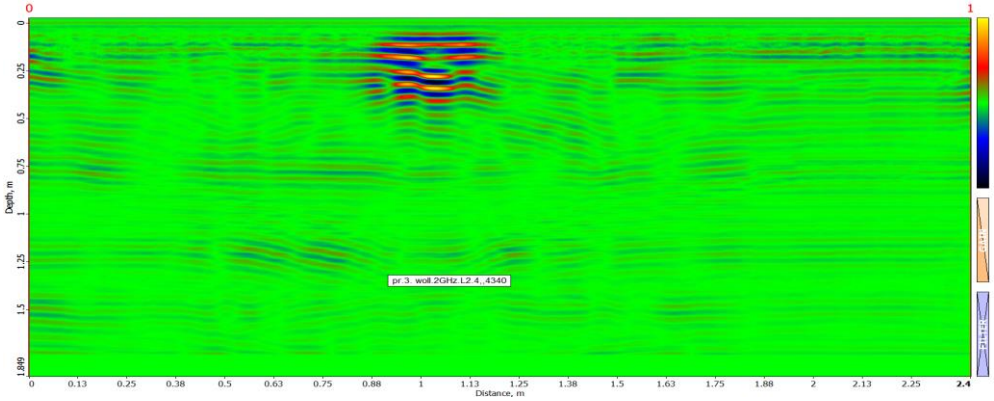

Fig. 3. Shows the corresponding Prof-3 radargram obtained using the Zond 12e 2 GHz range ground penetrating radar transceiver antenna.

The location of the object under study is clearly marked on the Profile-3 course (Fig. 3), so its influence on the radargram is visible. The radio image of the model object is well readable against the

background of minimal lateral anomalies. The location of the object is limited from below by the last clear continuous section of the in-phase axis at distances of 0.9-1.25m and a depth of 0.2m. The object is made of uneven slabs and is unevenly located, which often happens when working in field conditions with archaeological sites. Directly under the object, on the radio image, at a distance of 1.05-1.13m, a spatial area is observed, decompressed from the in-phase axes, with the center at a depth of 0.25m.

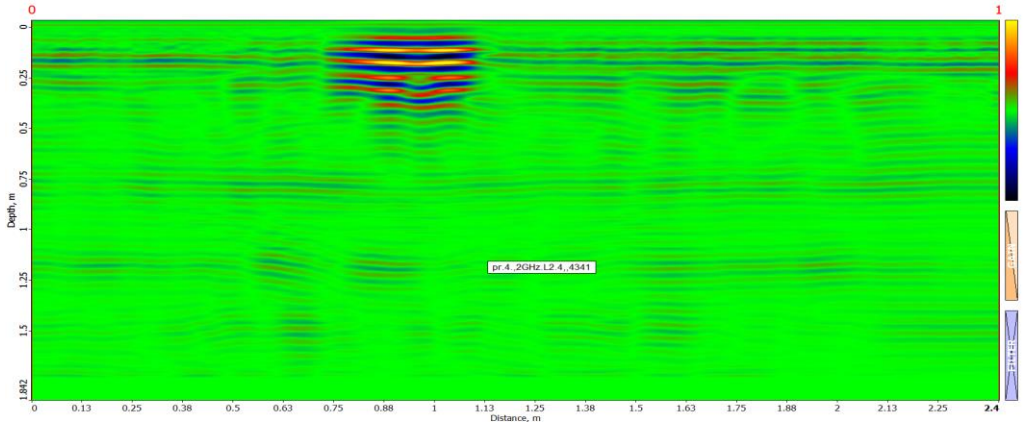

Fig. 4. Shows a radargram corresponding to Profile-4, made with a receiving and transmitting antenna of the Zond 12e 2 GHz georadar.

The location of the object of study is clearly marked on the Profile-4 course (Fig. 4), so its influence on the radargram is visible. The radio image of the model object is well readable against the background of minimal lateral anomalies. The location of the object is limited from below by a section of the last clear continuous in-phase axis at distances of 0.9-1.13m and a depth of 0.2m. The object is made of uneven slabs and is unevenly located, which often happens when working in field conditions with archaeological sites. The increase in the depth of the object's radio surface is caused by its curvature. Directly under the object, on the radio image, a spatial area is visible, decompression from the in-phase axes at a distance of 0.9-1.1m, with a depth center of 0.27m.

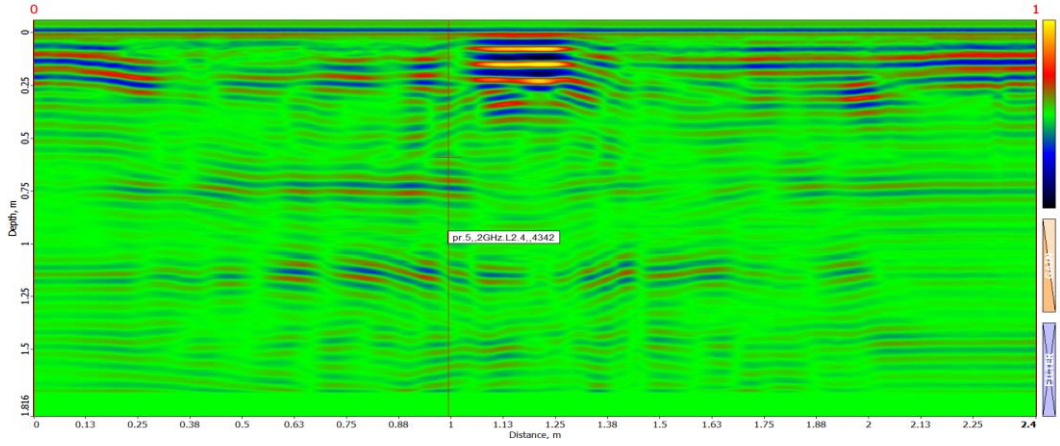

Fig.5. The location of the object under study is clearly marked on the profile-5 course, so its influence on the radargram is visible.

The radio image of the model object (Fig.5) is well readable against the background of minimal lateral anomalies. The location of the object is limited from below by the last clear continuous section of the in-phase axis at distances of 1.08-1.25m and a depth of 0.22m. The object is made of uneven slabs and is unevenly located, which often happens when working in the field with archaeological sites. The increase in the depth of the object's radio image is caused by its curvature. Directly under the object, on the radio image, a spatial region is visible, decompressed and separated from the in-phase axes at distances of 1.15-1.25.1m, with the center at a depth of 0.29 m.

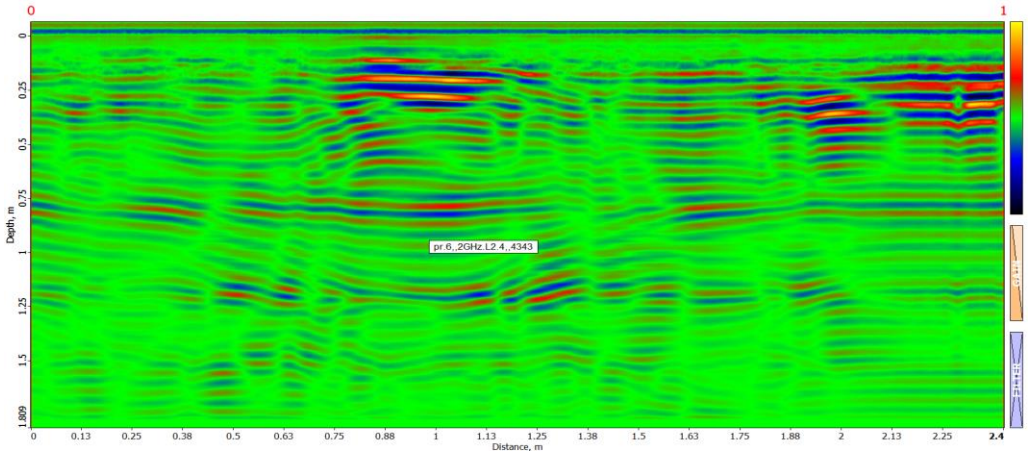

Fig. 6. Shows a radargram corresponding to Profile-6, made with a receiving and transmitting antenna of the Zond 12e 2 GHz georadar.

The location of the research object is weakly manifested during Profile-6 (Fig. 6), so the distorted radio image partially shows its influence on the radargram. The radio image of the model object is still well readable against the background of lateral anomalies.

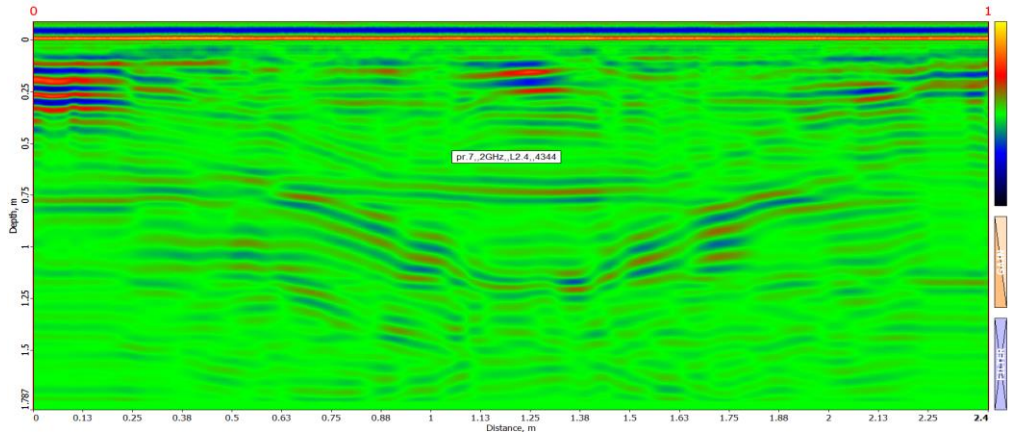

Fig. 7. Shows a radargram corresponding to profile-7, made with a Zond 12e, 2 GHz georadar receiving and transmitting antenna.

Along profile-7 (Fig. 7), the location of the research object is less noticeable, so its influence on the radargram is minimal. The radio image of the model object is weak and less legible against the background of existing lateral anomalies.

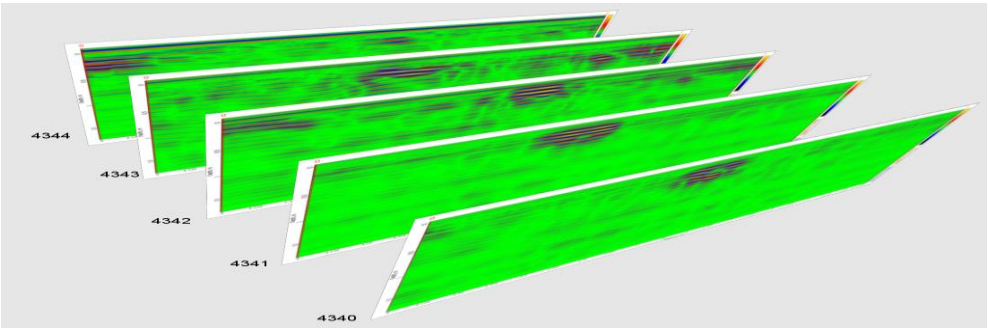

Fig. 8. Shows five profiles (profiles 3-7), constructed by Voxler 4.

Fig. 8 shows five profiles (profiles 3-7), constructed by Voxler 4, which sequentially depict the spatial arrangement of the radio image and their feature in the form of separation of the in-phase axes. Which is presented in the form of obliquely located in-phase axes, after parallel horizontal in-phase lines, determining the depth of the object, in accordance with the unevenness of the image of the object.

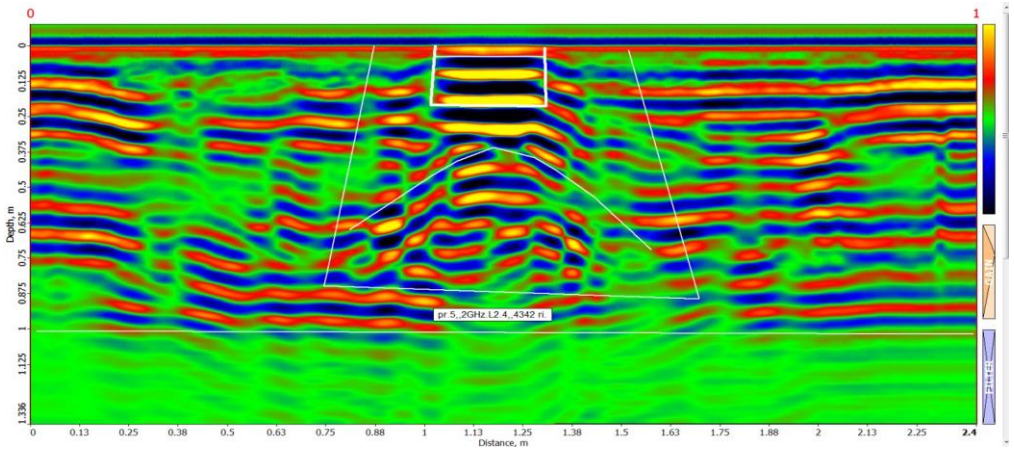

Fig. 9. Shows the depth-encompassing radio image of the object on the prof-5, outlined with a white line.

The radio image of the object (Fig. 9) is distinguished, which imprints the location of the object and exceeds its geometric dimensions in space by about three times. In this case, the lower part of the object is connected with the radio image as a whole by the content of the so-called electromagnetic field pattern, characteristic of antennas, that is, it clearly defines and separates the location of the object, which is considered as a secondary radiation antenna. Thus, based on the theory of similarity, the foundation model and, consequently, georadar electromagnetic fields, it is possible to clearly and unambiguously record the radio image of a field object in accordance with the numerical calculation using the model coefficients.

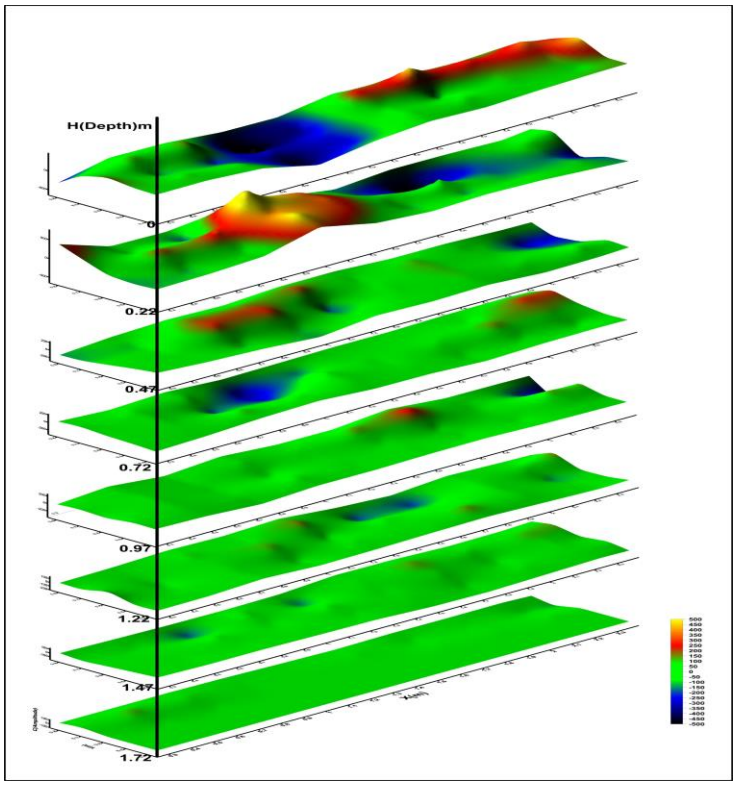

Fig. 10. Shows a spatial 3D radio image constructed using profiles Prof.3-7 (by Surfer 9 software), depending on the depth of the object relative to the ground penetrating radar antenna in the near and middle zones.

The presented 3D radio image corresponds to the geometric dimensions of the object location, composed of fragmentary elements of the "wall foundation" for depths of 0.22-0.25m. The boundaries of the model location are clearly outlined, and the vertices correspond to the uneven ridges of the object fragments. The longitudinal size of the minimum area of the object, from which the reflected wave is proportional to the order of a quarter of the incident wave, was recorded.

The depth of the model object is clearly defined by the position of the last horizontal synphase axis, recorded at the radio boundary on the radargram. Reflected and refracted electromagnetic rays are recorded by the radar and the Prizm 2.7 software. The radio image is clearly distinguished on the radargram by three intensity levels of the electromagnetic wave synphase axes: the first is the upper part of the physical position of the object itself, the second is a clearly horizontal axis of the last synphase, limiting the location of the lower part of the object, after which the presence of the upper part of the radio image appears, i.e. the radio image itself, exceeding the width and depth of the object by about three times. From the lateral side, it is an isosceles trapezoidal shape.

Composite physical model

Let's consider the same object - a fragmentary model of a foundation, with a clearly defined metal insert in the surrounding medium of a disk-insert, located 0.3-0.7m away from the foundation model.

The physical model of the study consists of a parallelepiped of uneven curvature (Scheme 2) and a metal disk with a diameter of 0.4m at a distance of 0.7m from it with a concave cavity of 0.04m. In field conditions, the model corresponds to the reality of objects similar to a metal hatch near archaeological or urban development works.

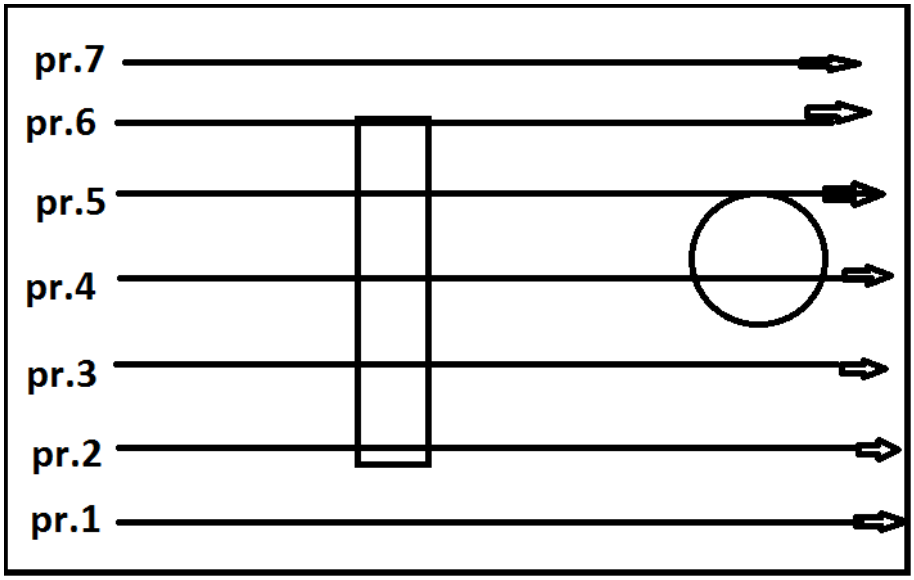

Scheme 2. Representation of the layout of a composite model of a dielectric parallelepiped and a metal disk.

Fig. 11 shows Prof-1 F+D. The corresponding radargram obtained using the antenna of the Zond 12e 2GHz ground penetrating radar transceiver for the physical model of the foundation+disk. The radargram corresponds to the ground penetrating radar section with background effects, the presence of model objects is not recorded by the radio image.

Fig. 12 shows prof-2 F+D. The corresponding radargram made with the help of the antenna of the Zond 12e 2GHz ground penetrating radar transceiver for the physical model of the foundation+disk and spaced from prof.1 at a distance of 0.12m.

The radargram corresponds to the ground penetrating radar section with a partial influence of the effect of the presence of the model.

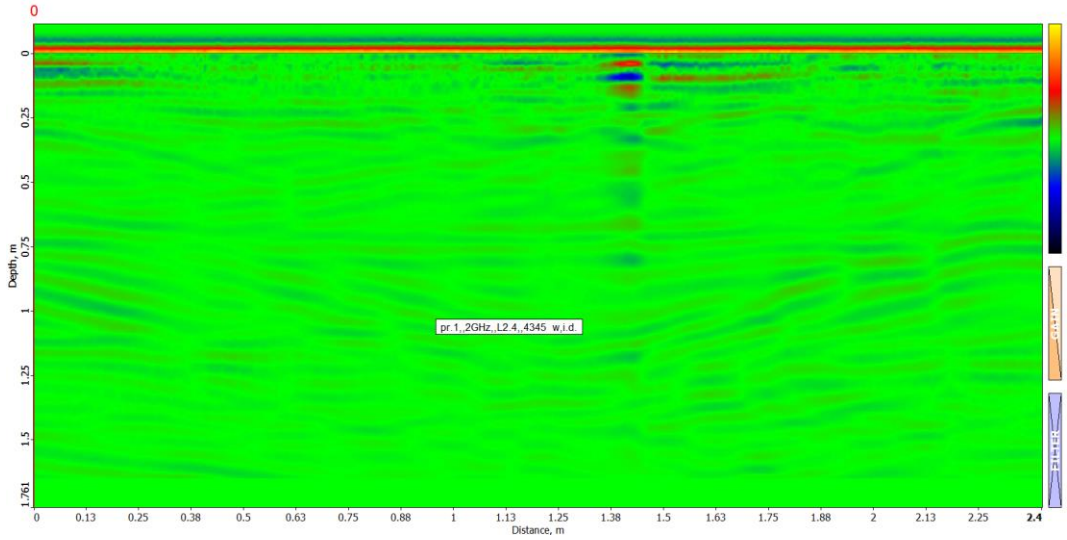

Fig. 11. Prof.1 F+D.

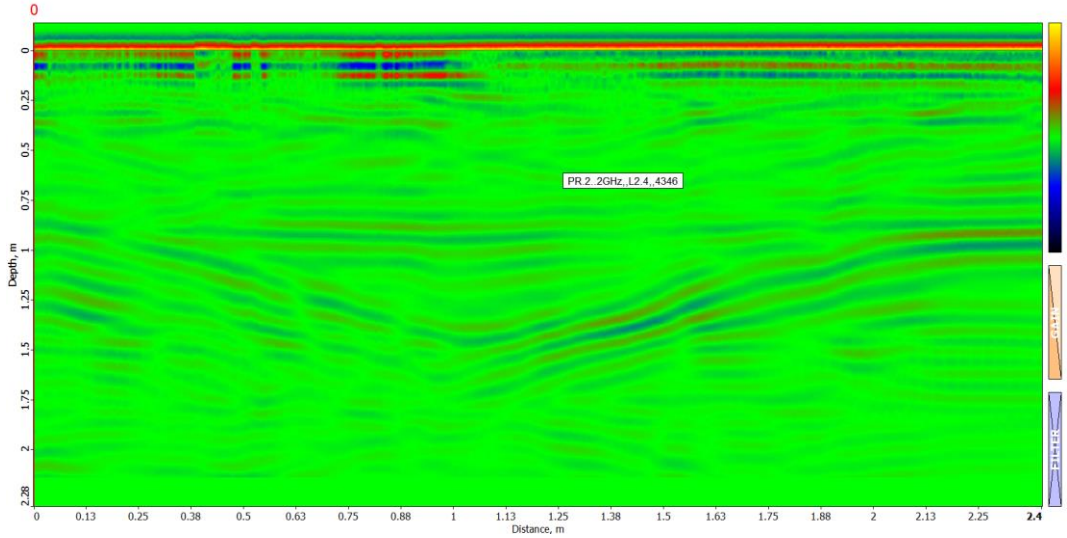

Fig. 12. Prof.2 F+D

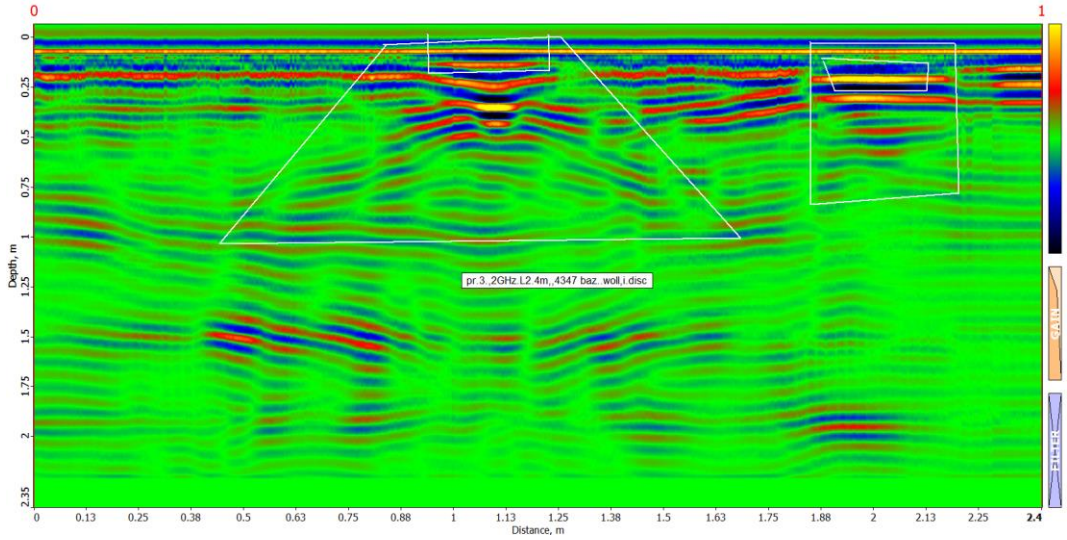

Fig. 13. Prof.3 F+D presented.

The corresponding radargram (Fig. 13) made with the help of the antenna of the Zond 12e 2GHz ground penetrating radar transceiver for the physical model of the foundation+disk and spaced from prof.1 at a distance of 0.24m.

The radargram corresponds to the ground penetrating radar section with the radio image of the foundation model and the influence of the disk.

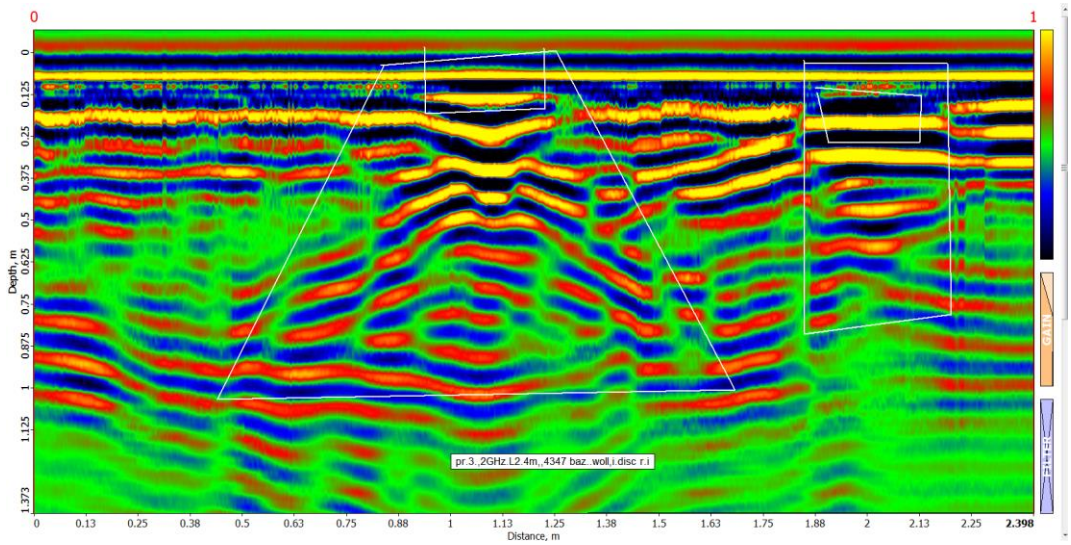

Fig. 14. Shows prof.3-F+D.

The corresponding radargram (Fig. 14) obtained using the antenna of the Zond 12e 2GHz ground penetrating radar transceiver for the physical model of foundation + disk and spaced from prof.1 at a distance of 0.24m. The digital gain option is used when processing the lower side of the radio image on the radargram. The radargram corresponds to the ground penetrating radar section with the representation of foundation + disk as a single radio image consisting of a model radio image and a disk radio image. The constituent radio images are highlighted with white lines. The influence of the void under the disk on its radio image is revealed.

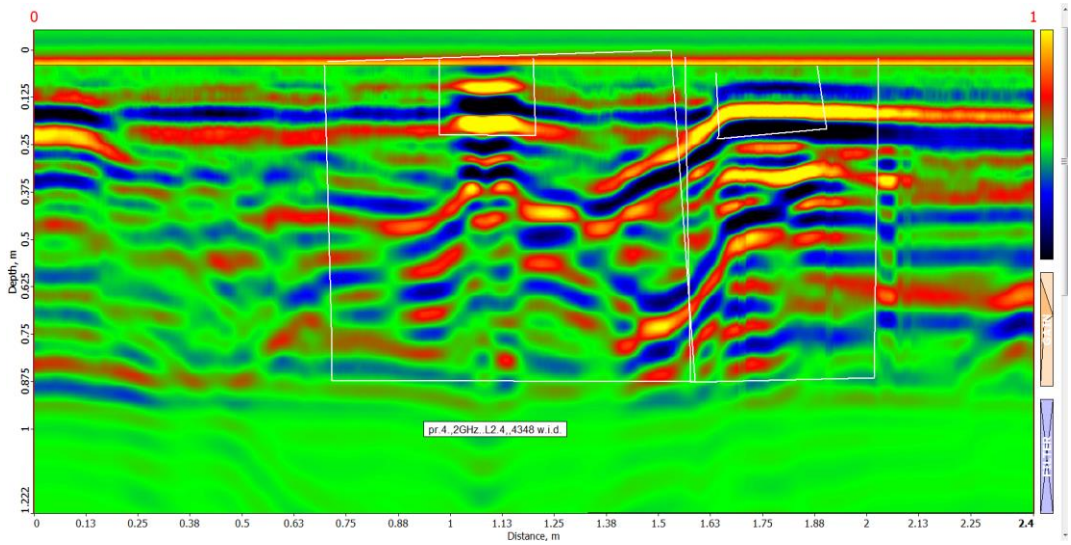

Fig. 15. Shows prof.4 F+D.

The corresponding radargram (Fig. 15) obtained using the Zond 12e ground penetrating radar transceiver antenna, 2 GHz for the physical model of foundation + disk and spaced from pr-1 at a distance of 0.48m.

The radargram corresponds to the ground penetrating radar section with strong foundation + disk influences on the in-phase axes of a single radioimage consisting of the model radioimage of the foundation and the disk radioimages. The constituent radioimages are highlighted with white lines. The influence of the void under the disk on its radioimage and the radioimage of the foundation model is clearly visible. The in-phase axes are sharply curved at distances of 1.13-1.75m. Despite the strong influence in the form of

curvature, the in-phase axes clearly show the location of both the base of the dielectric wall and the metal/iron disk on the radargram.

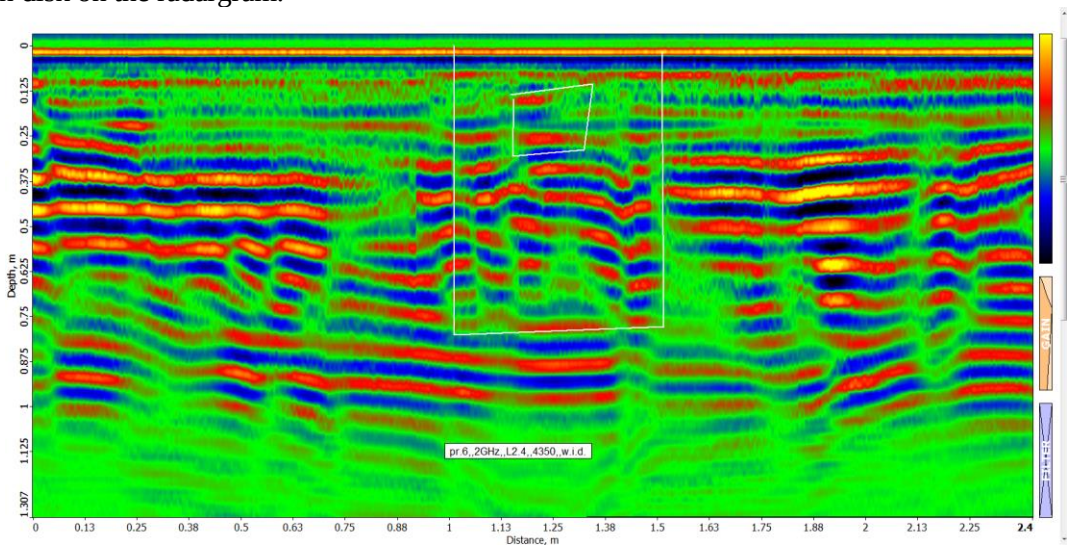

Fig. 16. Shows prof- 6 F+D. The corresponding radargram obtained using the antenna of the Zond 12e 2 GHz ground penetrating radar transceiver for the physical model of foundation+disk.

Prof-6 is less informative (Fig. 16), although it accurately reflects the dimensions of the foundation model.

Based on the above, the radio image of the disk contains additional information about the presence of a disk cavity and fragmentation of the foundation base.

We can propose “Borrowing” from antenna theory the term “antenna directivity patterns” for the secondary radiation objects observed on the radargram, which, like the receiving and transmitting ground penetrating radar antennas, will depend on the exposure of the ground penetrating radar antennas.

The radargrams obtained during vertical exposure of the ground penetrating radar section.

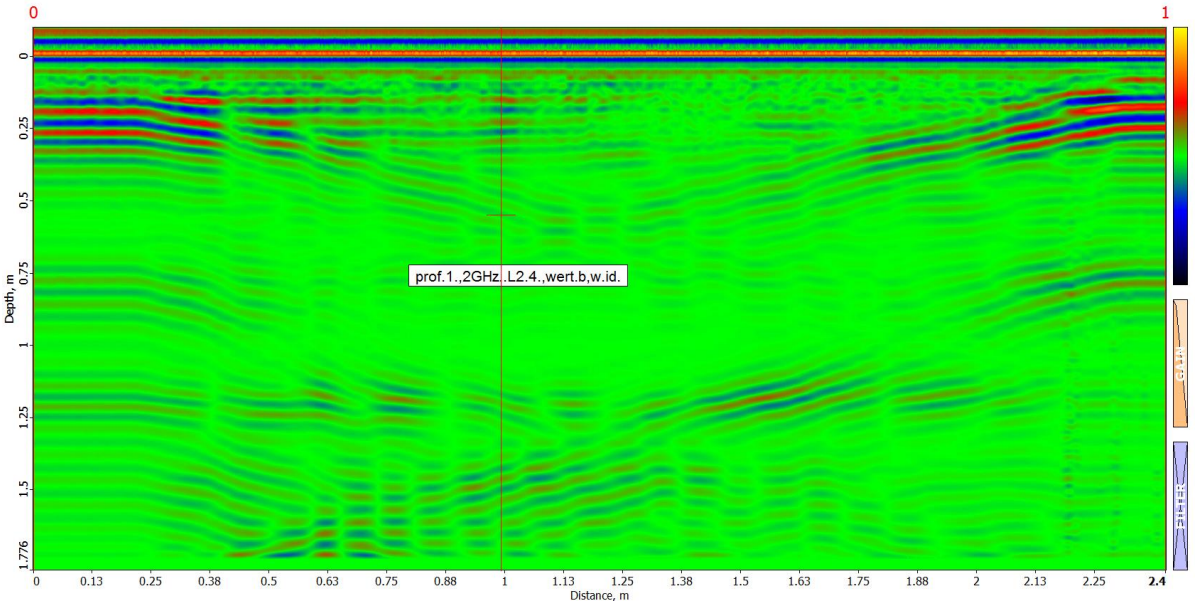

Fig. 17. Prof-1 F+D shows a georadar section of vertical exposure with a foundation model and a metal disk insert.

The profile (Fig. 17) did not reflect the anomaly, since the receiving and transmitting antenna passed above the daylight surface.

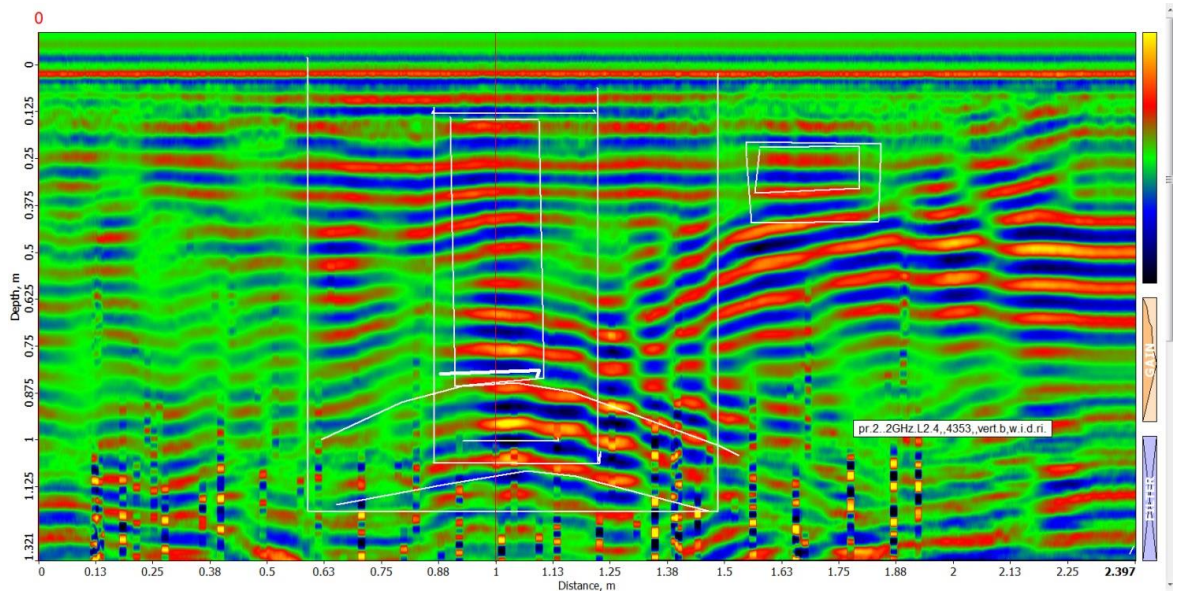

Fig. 18. Shows a georadar section, prof.-2 vert., made in vertical exposure with a foundation model and a metal disk insert.

A georadar section (Fig. 18) obtained by shooting from a vertical plane for a complex physical model of a foundation + an iron hollow disk is presented.

The radio image presented for the model (Fig. 18) shows a hyperbolic arc of the electromagnetic field observed in the vertical exposure of the foundation, marked with white lines.

The profile showed an anomaly, since the receiving and transmitting antenna passed below the day surface, although close to the surface.

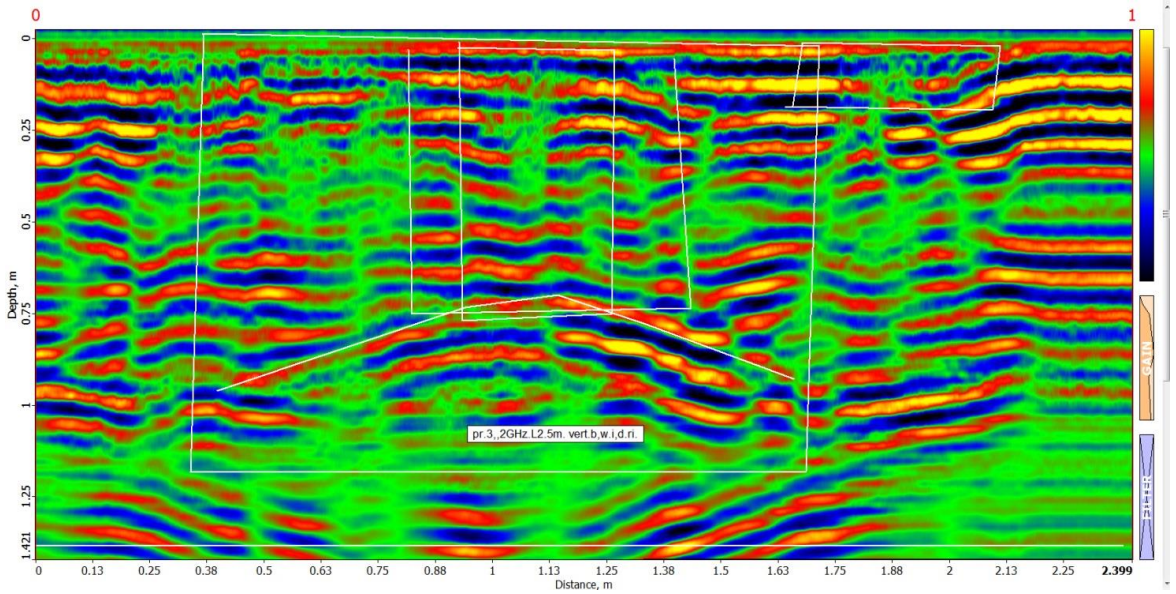

Fig. 19. Shows a ground penetrating radar section of profile 3 vert, in vertical exposure with a foundation model and a metal disk insert.

The anomaly was reflected in the profile (Fig. 19) when the receiving and transmitting antenna passed below the day surface, at a depth of 0.1m.

The radio image obtained for the physical model of a foundation + a hollow iron disk of complex heterogeneous composition, obtained during irradiation from a vertical plane, is clearly visible at a depth with the beginning of the object 0.25-0.3m away from the wall containing the host medium and below the day surface.

An arc in the form of a hyperbola separating the end of the object was clearly reflected. The dimensions of the object/foundation/body are recorded in the exposure.

We can offer a three-dimensional representation of the field distribution, made at a phenomenological level for ground penetrating radar irradiation of an ideal parallelepiped type. We can call this type of field representation a secondary radiation diagram of an object inserted into the environment, which is an additional characteristic of the radio image of the object and will give us an idea of the type of object.

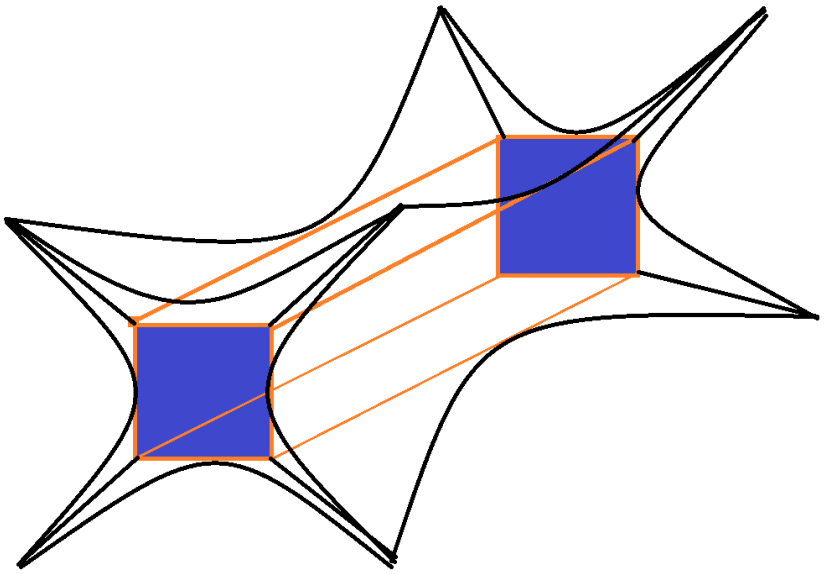

.

Scheme 3.

The illustration (Scheme 3) shows a schematic representation of the electromagnetic field diagram of the direction of a stylized parallelepiped in the GPR (georadar) field in the in-phase axes of the radio image, with the exposure of georadar profile in all directions, this time without taking into account lateral effects.

It is interesting to note that with a geometric length of the characteristic scale of 1 m and a model frequency of 2 GHz, the natural scale at 500 MHz will be 4m. Consequently, in field conditions, the size of the field parallelepiped will be 0.7x4 = 2.8m, 0.3x4= 1.2m, 0.2x4m = 0.8m, respectively, with an unchanged permittivity of the environment. We discussed the calculation of scale factors for GPR physical modeling in the articles.

Conclusion

The depth of the model object is clearly defined by the position of the last horizontal axis of the in-phase line, recorded on the radio image located on the radargram, both for horizontal and vertical ground penetrating radar exposure.

The radio image of the parallelepiped in the electromagnetic radiation field of the ground penetrating radar, recorded by the ground penetrating radar and software, is clearly distinguished on the radargram by three levels of in-phase axes intensity.

The first is the upper part of the physical location of the object itself;

The second is a clear horizontal axis of the final in-phase, delimiting the location of the lower part of the object, above which the presence of the upper part of the object is manifested;

The third intensity level is the full radio image, exceeding the dimensions of the object several times both in depth and horizontally and having a shape close to an isosceles trapezoid. Based on the analysis of the radio images, in the case of 3D ground penetrating radar exposure, we will obtain truncated stylized cones.

In general, the radio image of a parallelepiped with a 6-sided georadar exposure corresponds to and contains the content of the antenna directivity diagram and expresses the directions of the predominant increase in the electric field intensity, which is presented in the form of an illustrated figure.

References

[1] Lezhava Z., Tsikarishvili K., Asanidze L., Chikhradze N., Karalashvili1 T., Odilavadze D., Tarkhnishvili A. The results of a complex study of the Turchu limestone hollow (polje). Western Georgia, Caucasus. European Journal of Geography, BeISSN 1792-1341, DOI: https: //doi.org: 10.48088/ejg.z.lez.12.3.006.020. Volume 12, Issue 3, 03-Nov-2021, pp. 6 –20.

[2] Odilavadze D.T., Chelidze T.L. Physical simulation of georadiolocation field in direct and inverse problems of electrodynamics. Geophysical Journal, Kiev, V.35, №4, 2013, pp. 154-160, (in Russian).

[3] Odilavadze D.T., Chelidze, T.L. Physical Modeling of Lava Tubes in the GPR. Transactions of Mikheil Nodia Institute of Geophysics, Publishing house of the Tbilisi State University, ISSN 1512-1135, vol. LXVII, 2017, pp. 129-142.

[4] Odilavadze D., Chelidze T., Tskhvediashvili G. Georadiolocation Physical Modeling for Disk-Shaped Voids. Journal of the Georgian Geophysical Society, Physics of Solid Earth, Tbilisi, vol. 18, 2015, pp. 26-39

[5] Odilavadze D., Chelidze T., Ghlonti N., Kiria J., Tarkhnishvili A. Physical modelling of a layered wedge type model in direct and inverse tasks of georadiolocation. Mikheil Nodia Institute of Geophysics Transactions, ISSN 1512-1135, vol. LXIX, Publishing house of the Tbilisi State University, Tbilisi, 2018, pp. 44-61.

[6] Odilavadze D., Kiria J., Ghlonti N., Yavolovskaya O. The Results of Archaeogeoradiolocation Investigations of the Territory Inside the Rampart of St. Sophia Church of Khobi. „Moambe" Bulletin of the Georgian National Academy of Sciences, V.14, n.4, 2020, pp. 51-56.

[7] Bigman D. GPR Basics. Bigman Geophysicsl, LCC, Suwanee, USA, 2018.

[8] Chelidze T., Odilavadze D., Pitskhelauri K. Archaeogeophysics in Georgia-New Results, New Prospects. Proceedings of the Georgian National Academy of Sciences, Series of History, Archeology, Ethnology and Art History, N1, 2012.

[9] Odilavadze D.T., Chelidze T.L. A Preliminary GPR investigation of Metekhi Cathedral and the surrounding area. Journal of the Georgian Geophysical Society, № 14, 2011.

[10] Neal A. Ground-penetrating radar and its use in sedimentology: principles, problems and progress. Earth-Sci. Rev. 2004, pp.66, 261—330.

[11] Negi J. G., Gupta C. P. Models in applied geoelectromagnetics. Earth Sci. Rev. 1968, pp 219—241.

[12] Sena D'Anna A. R. Modeling and imaging of ground penetrating radar data. Texas: The University of Texas at Austin, Repositories. Lib.Utexas.edu, 2004, 251 p.

[13] Sharma P.V. Environmental and engineering geophysics. Cambridge: Cambridge University Press, 1997.

[14] Kofman L., Ronen A., Frydman S. Detection of model voids by identifying reverberation phenomena in GPR records. Journal of Applied Geophysics, (59), 2006, pp.284-299.

[15] Odilavadze D., Chelidze T., Yavolovskaya O. Some georadiolocation images of cylindrical bodies built with different dielectric fillers, placed in a dielectric environment. Mikheil Nodia Institute of Geophysics of Ivane Javakhishvili Tbilisi State University, International Scientific Conference "Geophysical Processes in the Earth and its Envelopes". Proceedings, ISBN 978-9941-36-147-0, Tbilisi, Georgia, November 16-17, 2023, pp.217-220.

გეორადიოლოკაციაური ფიზიკური მოდელირების მეთოდით გამოკვლეული განგრძობითი, წახნაგოვან-ფრაგმენტული, დიელექტრიკულად რთული აგებულების ობიექტის რადიოსახე

დ. ოდილავაძე, თ. ჭელიძე, ო. იავოლოვსკაია

რეზიუმე

გეორადიოლოკაციური მეთოდის გამოყენება ფართოდ გავრცელდა გეოლოგიური შინაარსის მქონე მრავალ დარგში. მნიშვნელოვანი შედეგები მიიღება ურბანული ტექნიკის მრავალი პრობლემური საკითხის გადაწყვეტაში, მრავალი ამოცანის გადაწყვეტა გახდა შესაძლებელი არქეოგეორადიოლოკაციაში.

გამოყოფილია ობიექტის რადიოსახე რომელიც ჩასდევს ობიექტის განთავსების ადგილს და აღემატება მის გეომეტრიულ ზომებს სივრცულად დაახლოებით სამჯერ. ამასთან ობიექტის ქვედა ნაწილი რადიოსახესთან დაკავშირებულია ზოგადად ანტენების მახასიათებლის ე.წ. ელექტრომაგნიტური ველის მიმართულების დიაგრამის შინაარსით, ანუ მკაფიოდ განსაზღვრავს და გამოყოფს მეორადი გამოსხივების ანტენად მიჩნეული ობიექტის ლოკაციას.

ამდენად, შესაძლებელია საძირკველის ფიზიკური მოდელის და მაშასადამე გეორადიოლოკაციური ელექტრომაგნიტური ველების მსგავსობის თეორიიდან გამომდინარე საველე ობიექტის რადიოსახის დაფიქსირება.

სამოდელო ობიექტის დაღრმავება მკაფიოდ განისაზღვრება რადიოსახეზე დაფიქსირებული ბოლო ჰორიზონტალური სინფაზურობის ღერძის მდებარეობით რადაროგრამაზე, როგორც ჰორიზონტალურ ისე ვერტიკალური გეორადიოლოკაციური ექსპოზიციის დროს.

საკვანძო სიტყვები: აექეოგეორადარიოლოკაცია, რადიოსახე, ფიზიკური მოდელირება, Zond 12-e.

Исследование методом георадиолокационного физического моделирования радиообраза объекта сплошной, гранёно-фрагментарной, диэлектрически сложной структуры

Д. Одилавадзе, Т. Челидзе, О. Яволовская

Резюме

Для археологических работ важна фиксация и расшифровка радиообраза объекта в результате взаимного расположения между целевыми объектами и антенной георадара, т.е. решение обратной задачи электродинамики. Для того, чтобы радиообраз объекта был полностью распознан, антенна GPS должна располагаться в дальней зоне целевого объекта, то есть расстояние между антенной и объектом должно превышать длину волны излучения. При археологических работах расстояние до целевого объекта неизвестно, поэтому объект может находиться, как в ближней зоне, так и в средней и дальней зоне относительно антенны, что искажает или даже делает невозможным фиксацию и распознавание радиообраза объекта. В результате при археогеорадиолокационных работах важная информация может быть не получена.

Метод георадиолокации нашёл широкое применение во многих областях геологического содержания. Важные результаты получены в решении многих проблемных вопросов градостроительства, решение многих задач стало возможным в археогеорадиолокации.

Ключевые слова: археорадиолокация, радиообраз, физическое моделирование, Zond 12-e.

Journal of the Georgian Geophysical Society, e-ISSN: 2667-9973, p-ISSN: 1512-1127
Physics of Solid Earth, Atmosphere, Ocean and Space Plasma, v. 27(2), 2024, pp. 29 - 36

Reaction of the Geomagnetic Field on the Earthquakes Preparation Process in Georgia

Tamar T. Jimsheladze, George G. Melikadze, Genadi N. Kobzev, Aleksandre Sh. Tchankvetadze, Tamaz G. Matiashvili

M. Nodia Institute of Geophysics of the I. Javakhishvili Tbilisi State University, Georgia,
e-mail: melikadze@gmail.com

ABSTRACT

During the monitoring of earthquake precursors including extra information as the variations of electromagnetic fields analysis, it is possible to define earthquakes precursors is very actual and important problem. Connection between the variation of the geomagnetic field and seismic activities is an essential element of the fundamental problem of earthquake forecasting. In terms of geodynamic, Georgia is one of the most active regions. The macro structural factor here is represented by the contact with the Arabian and Eurasian tectonic plates, which in addition to the geological diversity of the area conditions the high seismicity of mentioned region. The article represents the observations of following seismic processes such as: geomagnetic field.

Key words: *Geomagnetic field, earthquakes precursors.*

Introduction

The article contain information about several geomagnetic anomalies were observed on the Dusheti Geomagnetic Observatory of M. Nodia institute of Geophysics.

Dusheti Geomagnetic Observatory is located in Dusheti town (Georgia, Lat 42.052N, Lon44.42E), Alt900m). It is equipped with modern precise Fluxgate Magnetometer Model LGI and it accomplishes non-stop registration of X, Y, Z elements. The data includes minute and second records of the field elements. It is measured with 0,1nT accuracy daily.

Materials and methods

There was analyzed earthquakes data in region with Lat42.052N and Long44.42E for January-November of 2024, reported in EMSC: Earthquake research results, magnitude range from 3.5 to 9.0; Minute data of Geomagnetic fields elements received from Dusheti Geomagnetic observatory or 60 samples per hour, with 0,1nT accuracy;

During a long period of observation there have been identified individual cases in which Dusheti station reacted to the earthquake preparation process [1-4].

During the mentioned period (January-November of 2024) several medium earthquakes occurred in our region (Mag<5).

Results

1. ***Earthquake in Ambrolauri area-02.01.2024, Mag-4.4.***

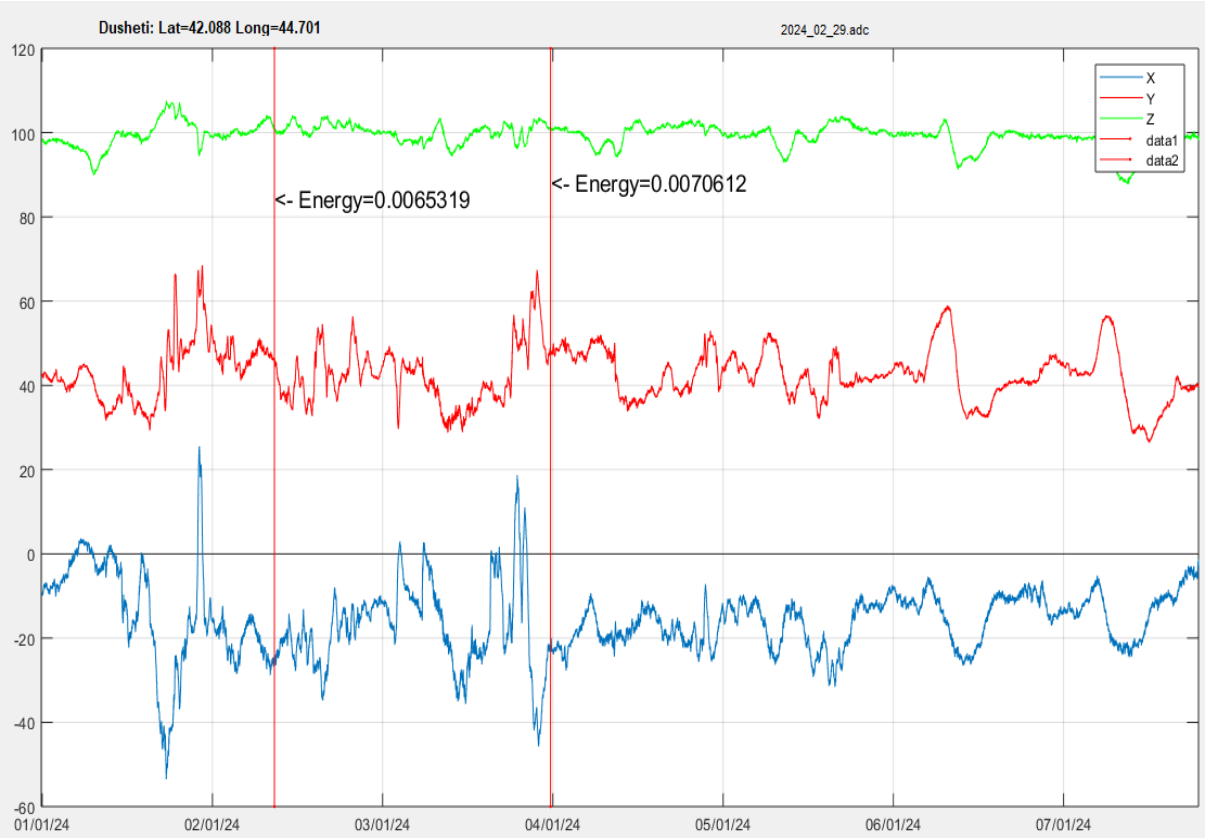

Fig.1. Variation of X, Y, Z components of the magnetic field, Dusheti.

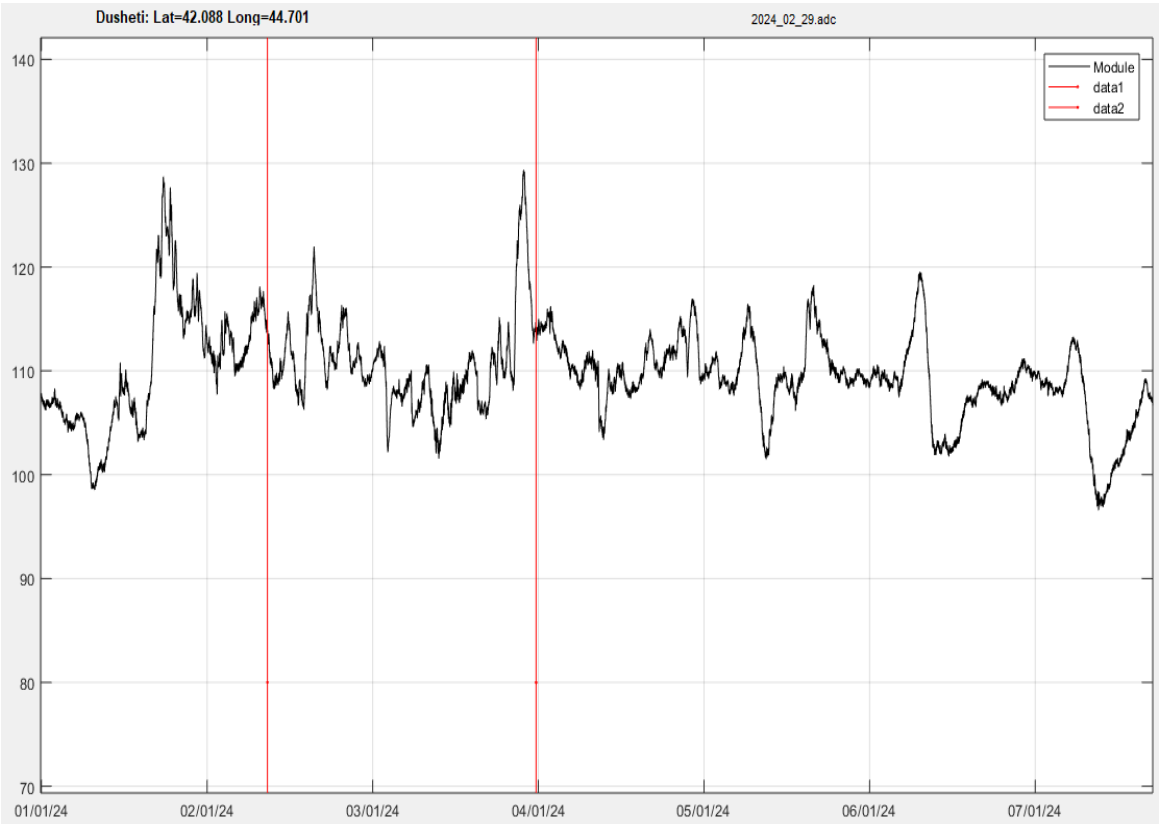

Fig. 2. Variation of the module value, Dusheti.

2. Earthquake in Oni area-30.03.2024, Mag-4.7

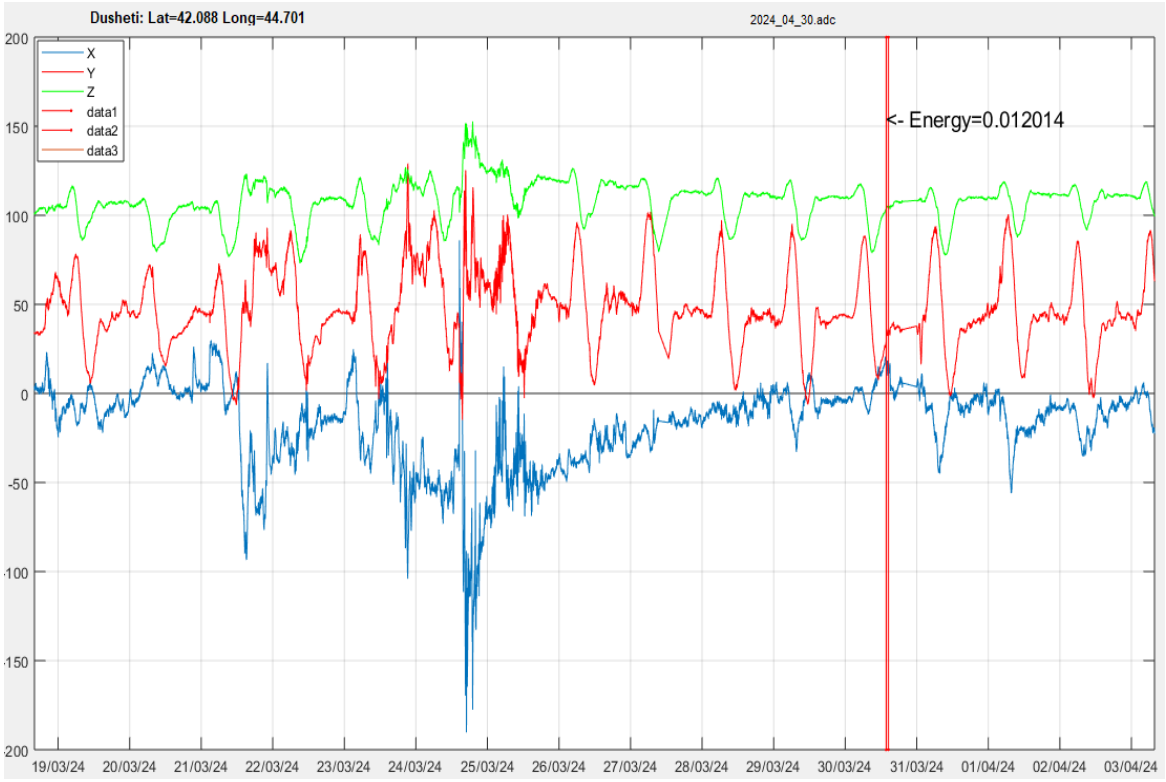

Fig.3. Variation of X, Y, Z components of the magnetic field, Dusheti.

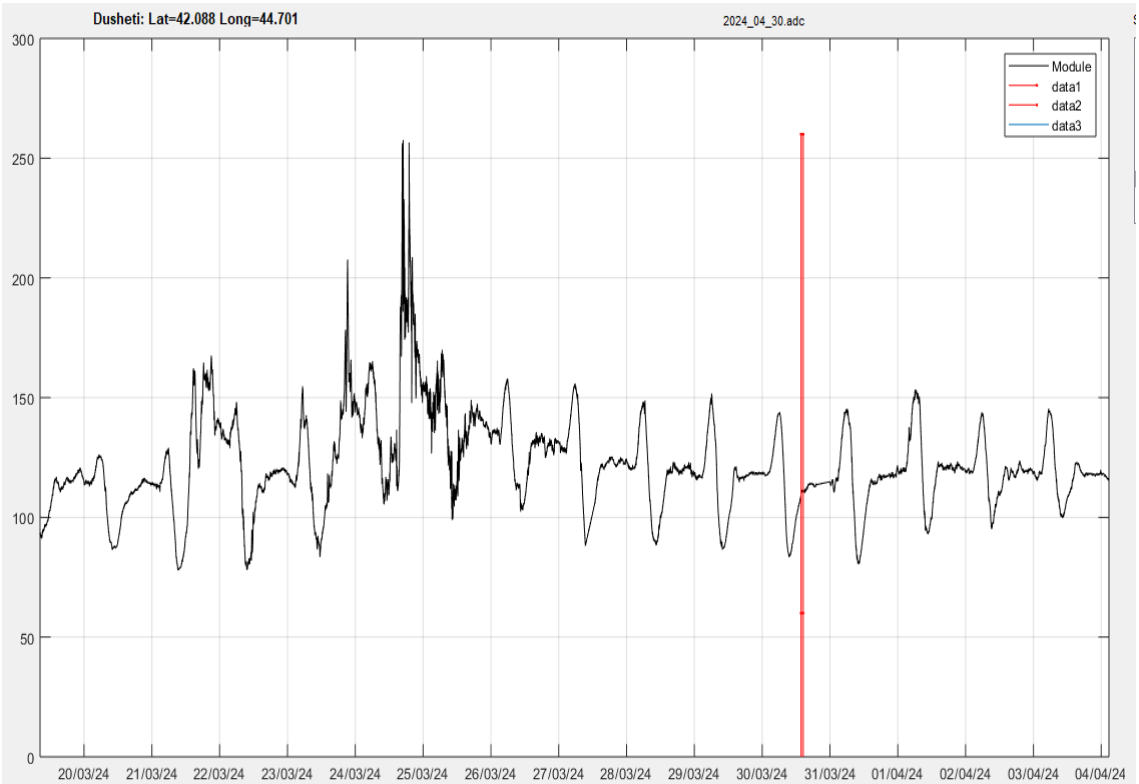

Fig. 4. Variation of the module value, Dusheti.

3. Earthquake in Chkhorotsku area-27.07.2024, Mag-4.0.

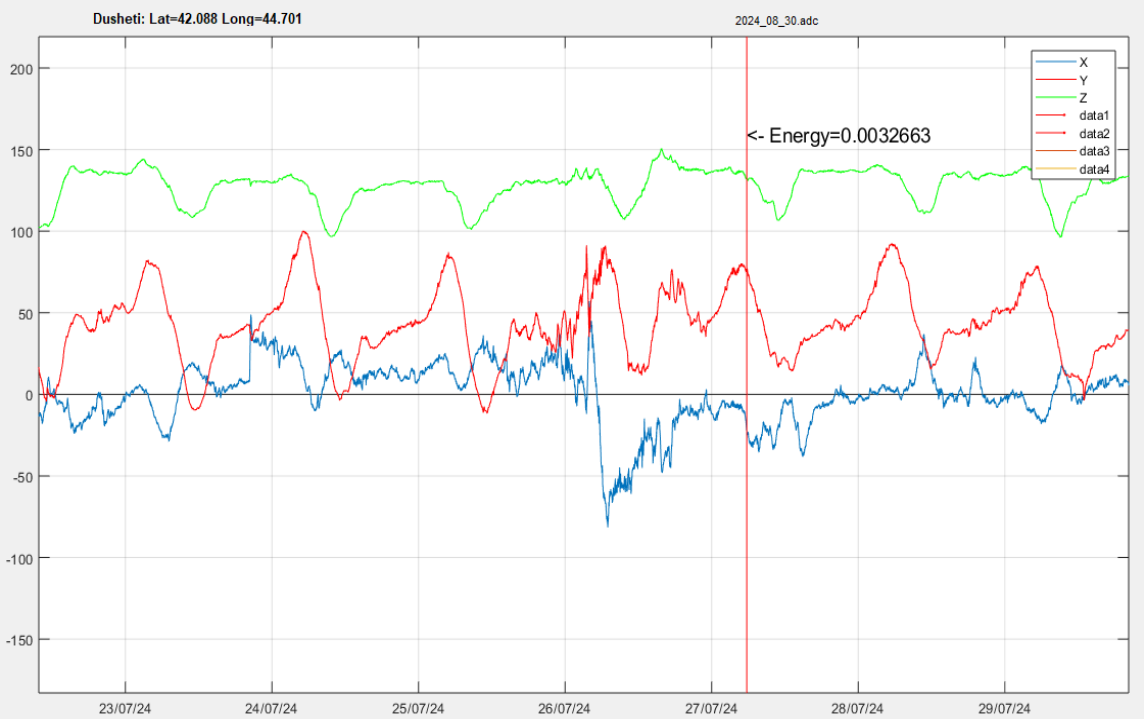

Fig.5. Variation of X, Y, Z components of the magnetic field, Dusheti.

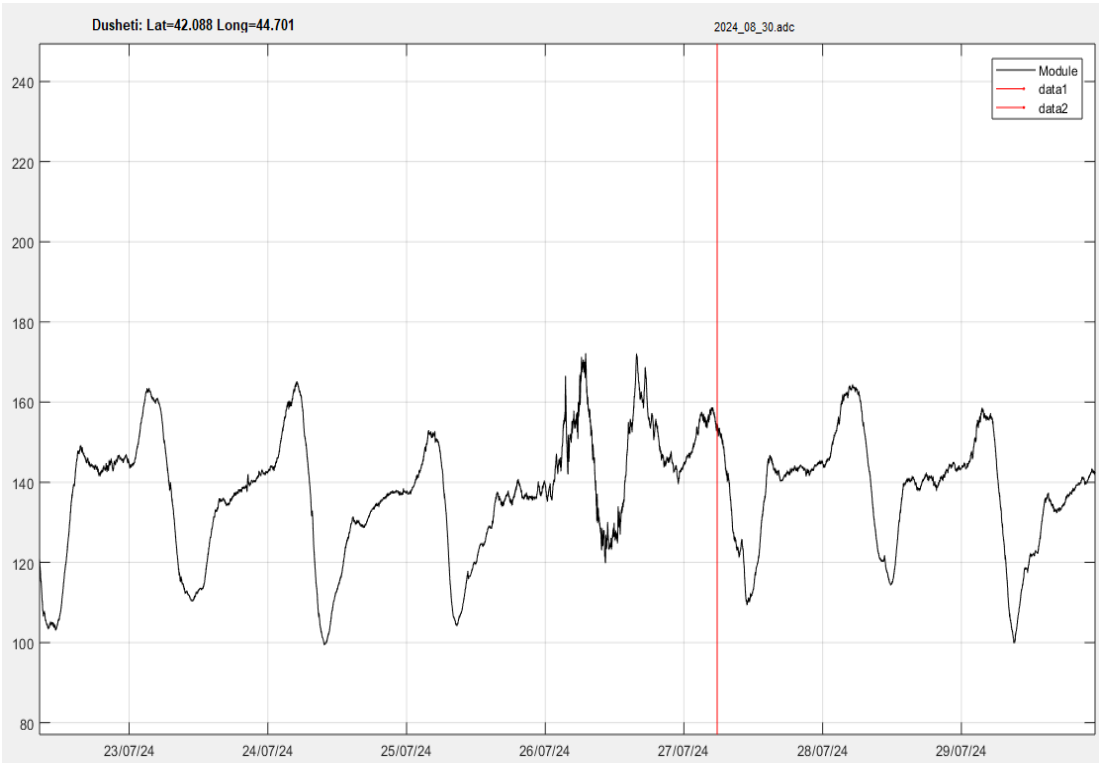

Fig. 6. Variation of the module value, Dusheti.

4. Earthquake in Tianeti area-14.10.2024, Mag-4.0.

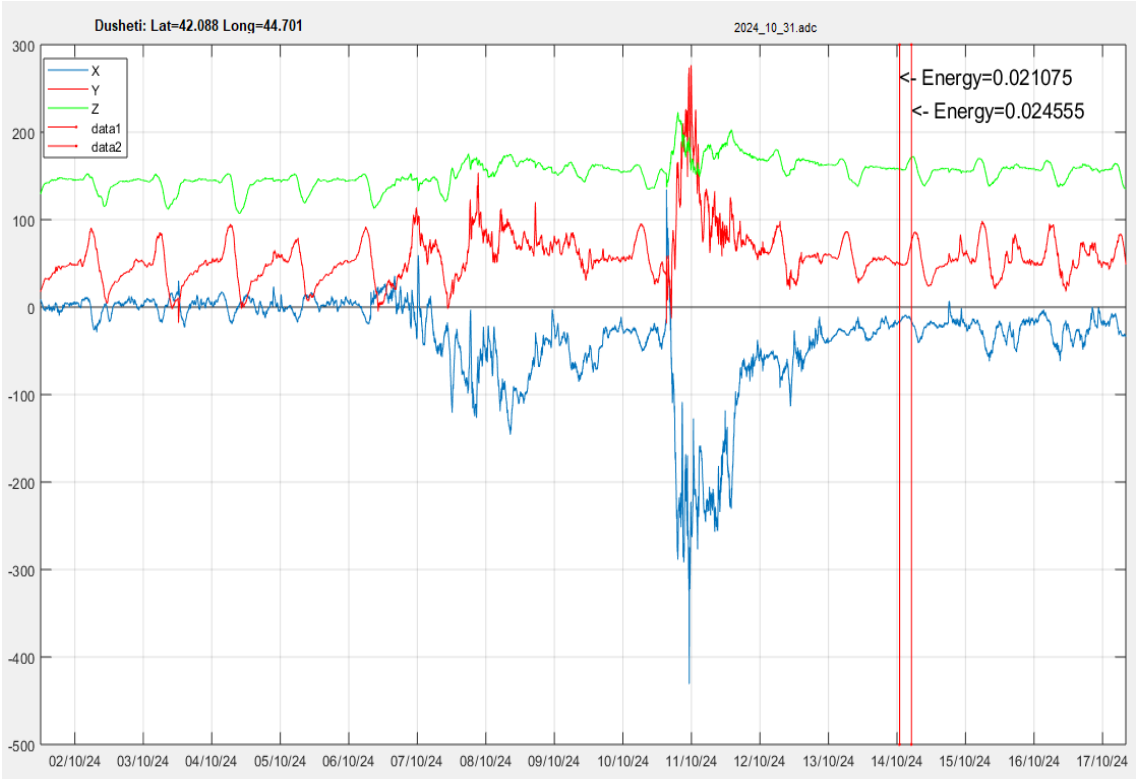

Fig.7. Variation of and X, Y, Z components of the magnetic field, Dusheti.

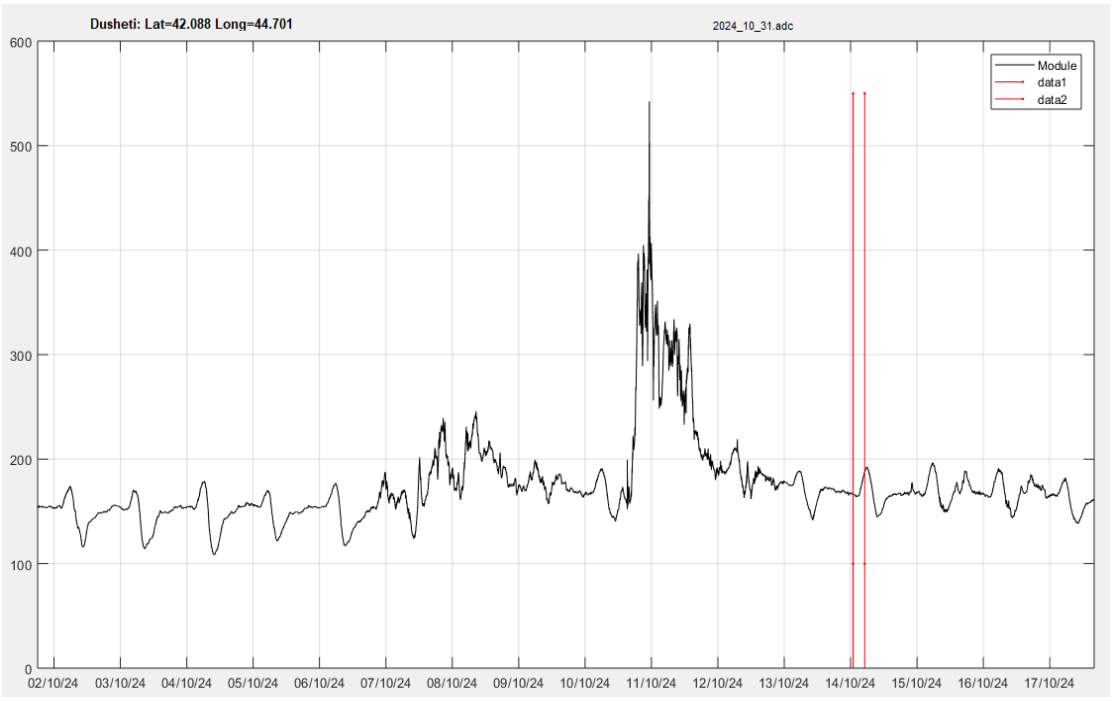

Fig. 8. Variation of the module value, Dusheti

5. Earthquake in Black Sea area-14.10.2024, Mag-4.5.

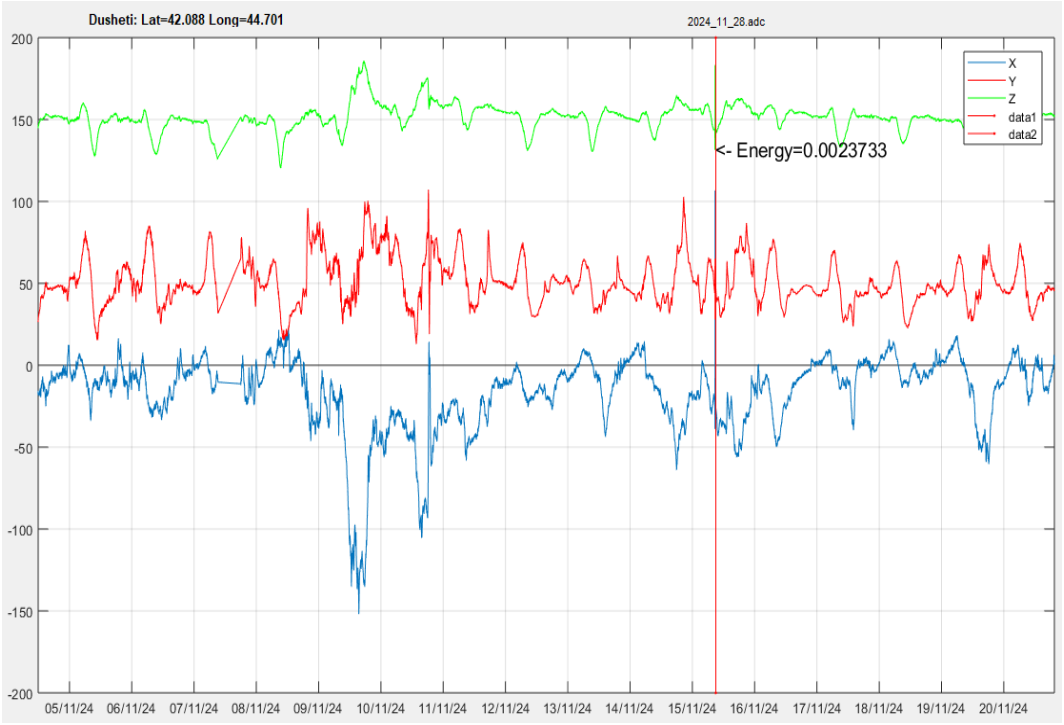

Fig.9. Variation of and X, Y, Z components of the magnetic field, Dusheti.

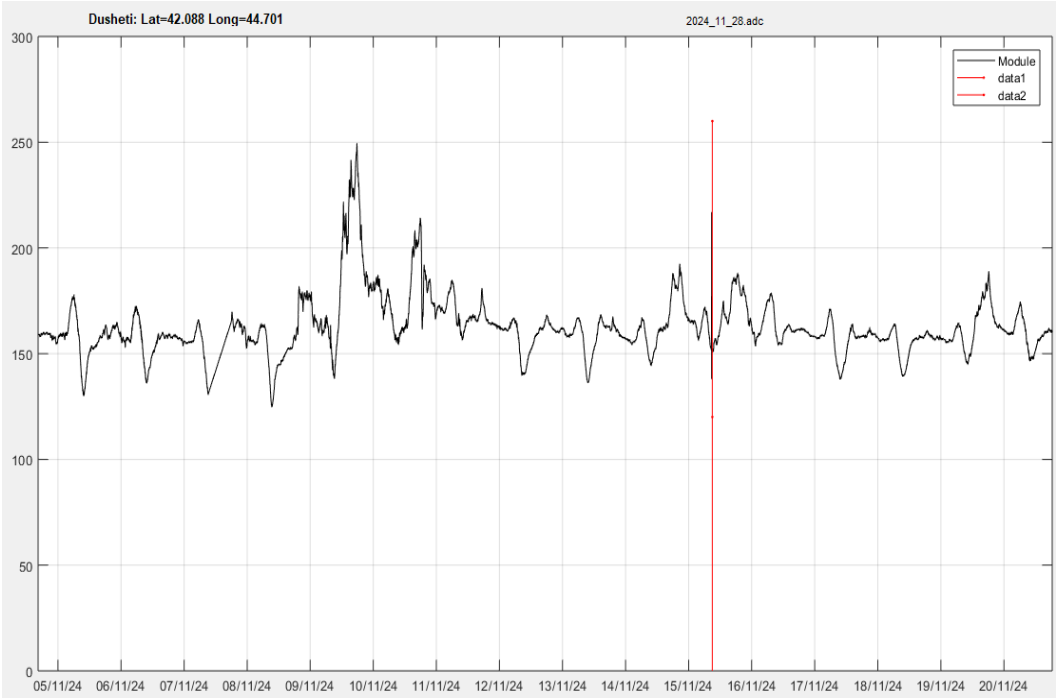

Fig. 10. Variation of the module value, Dusheti

Conclusion

Variations in geomagnetic parameters are caused by the earth stress. Fig. 1-8 shows, that before seismic event character of variation changed above “background” value, as indicator of tectonic activity. During the observed time period were fixed earthquakes with Magnitude 3.5-5 occurred on the territory of Georgia. Period of “anomalies” varied between 2-5 days. The recorded anomalies coincide with the preparation period for strong earthquakes. Characteristics of anomalies (amplitude, period, etc) are correlated with earthquake strength.

References

[1] Jimsheladze T., Melikadze G., Chankvetadze A., Gogua R., Matiashvili T. The Geomagnetic Variation in Dusheti Observatory Related with Earthquake Activity in East Georgia, Journal of the Georgian Geophysical Society, Issue A. Physics of Solid Earth, vol. 15A, 2012, pp.118-128.

[2] Melikadze G., Jimsheladze T., Kikuashvili G., Mavrodiev S., Pekevski L., Chkhitunidze M. Study of Geomagnetic Variations in Georgia and establishment the Anomaly Nature of Earthquake Precursors_BlackSeaHazNet Series, Volume 2, 2011, pp. 205-214.

[3] Jimsheladze T., Melikadze G., Chankvetadze A., Gogua R., Matiashvili T. The geomagnetic variations in Dusheti Observatori (January-June 2013). Journal of The Georgian Geophysical Society Issue (A). Physics of Solid Earth. vol.16A, 2013, pp.37-43.

[4] Mavrodiev S., Pekevski L., Jimsheladze T. Geomagnetic-Quake as Iminent Reliable Earthquake’s Preqursor: Starting point Future Complex Regional Network. Electromagnetic Phenomena related to earthquake s and volcanoes. Editor: Birbal Singh. Publ., Narosa Pub. House, New Delhi. 2008, pp. 116-134.

გეომაგნიტური ველის რეაქცია მიწისძვრების მომზადების პროცესზე საქართველოში

თ. ჯიმშელაძე, გ. მელიქაძე, გ. კობზევი, ა. ჭანკვეტაძე, თ. მათიაშვილი

რეზიუმე

მიწისძვრის წინამორბედების მონიტორინგის დროს, დამატებითი ინფორმაციის სახით ელექტრომაგნიტური ველების ანალიზის ვარიაციებით, შესაძლებელია მიწისძვრის წინამორბედების განსაზღვრა, რაც ძალიან აქტუალური და მნიშვნელოვანი პრობლემაა. გეომაგნიტური ველის ცვალებადობასა და სეისმურ აქტივობას შორის კავშირი მიწისძვრის პროგნოზირების ფუნდამენტური პრობლემის არსებითი ელემენტია. გეოდინამიკური პროცესების არაცალსახობის თვალსაზრისით საქართველო მიეკუთვნება ერთ-ერთ განსაკუთრებულად რთულ რეგიონს. მაკრო სტრუქტურული ფაქტორი აქ არის არაბეთისა და ევრაზიის ტექტონიკური ფილების კონტაქტი, რასაც ემატება ლოკალურ გეოლოგიური სტრუქტურული მრავალფეროვნება, თუმცა ყველა ეს ადგილი გამოირჩევა მღალი სეისმურობით. სტატიაში წარმოდგენილია სეისმური პროცესების მომდინარეობის ისეთ ინდიკატორებზე დაკვირვება როგორიცაა: გეომაგნიტური ველი.

საკვანძო სიტყვები: გეომაგნიტური ველი, მიწისძვრის წინამორბედები.

Реакция геомагнитного поля на процесс подготовки землетрясений в Грузии

**Т. Джимшеладзе, Г. Меликадзе, Г. Кобзев,
А. Чанкветадзе, Т. Матиашвили**

Резюме

При мониторинге предвестников землетрясений, включая информацию в виде анализа вариаций электромагнитных полей, определение наиболее надежных предвестников землетрясений является весьма актуальной и важной проблемой. Связь между вариациями геомагнитного поля и сейсмической активностью является существенным элементом фундаментальной проблемы прогнозирования землетрясений. С точки зрения геодинамики Грузия является одним из наиболее активных регионов. Макроструктурным фактором здесь является контакт с Аравийской и Евразийской тектоническими плитами, что в дополнение к геологическому разнообразию территории обуславливает высокую сейсмичность указанного региона. В статье представлены наблюдения за геомагнитным полем, сопровождающим сейсмические процессы.

Ключевые слова: магнитное поле, предвестники землетрясений.

Journal of the Georgian Geophysical Society, e-ISSN: 2667-9973, p-ISSN: 1512-1127
Physics of Solid Earth, Atmosphere, Ocean and Space Plasma, v. 27(2), 2024, pp. 37 - 47

^{222}Rn Concentration Levels in Soil Gas and Water in Kvemo Kartli Region, Georgia - ^{222}Rn Mapping

[1]Nino A. Kapanadze, [1]George G. Melikadze, [1]Aleksandre Sh. Tchankvetadze, [1]Tamar T. Jimsheladze, [1]Zviad I. Magradze, [2]Shota D. Gogichaishvili, [1]Marina Sh. Todadze, [1]Elene V. Chikviladze, [2]Lia T. Chelidze

[1]M. Nodia Institute of Geophysics of the I. Javakhishvili Tbilisi State University, Georgia,
[2]E. Andronikashvili Institute of Physics, Ivane Javakhishvili Tbilisi State University, Tbilisi, Georgia

[1]e-mail: ninokapanadze@gmail.com

ABSTRACT

Within the framework of the SRNSFG FN-19-22022 project "^{222}Rn mapping and Radon risk assessment in Georgia", the authors carried out fieldwork to quantify the ^{222}Rn distribution in water and soil gas as well as to ascertain geological factors influencing the ^{222}Rn concentration levels in some geographical areas of Georgia. On-site ^{222}Rn concentration has been measured in soil gas (68 sampling points) and in various water sources (boreholes and springs, 75 water points, 66- springs, 9 boreholes) using AlphaGUARD PQ2000 PRO (Saphymo GmbH) Radon monitor. The ^{222}Rn concentration ranged from 0.12 to 73 Bq/L in water and up to 36.9 Bq m^{-3} in soil gas. All observation sites were marked by GPS position. The data underwent basic statistical analysis and were visualized using various plots. Subsequently, the field data were digitized and integrated into a GIS system, which highlighted the ^{222}Rn distribution in water and soil gas on the territory of Kvemo Kartli.

Key words: *Rn mapping, soil gas, water, GIS, Kvemo Kartli, Georgia*

Introduction

Following the aims and tasks of the SRNSFG FN-19-22022 project "Radon mapping and Radon risk assessment in Georgia", during 2020-2022, the authors carried out fieldwork in order to quantify the ^{222}Rn distribution, ascertain geological factors influencing the ^{222}Rn concentrations in indoor air, water and soil gas in different geographical areas of Georgia. With the project Georgia joined the countries that carry out systematic Radon (^{222}Rn) surveys in indoor air, soil gas and water. In Georgia, ^{222}Rn mapping in soil gas has included ten regions. ^{222}Rn concentrations obtained in the Kvemo Kartli region are presented and discussed in this paper. Of 143 locations, In soil gas, ^{222}Rn concentration was measured in 68 locations and in water in 75 locations with AlphaGUARD monitor. For all observation sites, the geochemical properties have been characterised, and their coordinates in GPS recorded.

The works [10-11, 13-14] present the results of our early studies of ^{222}Rn content in soil gas and water in various regions of the country.

Geological and lithological data of the study area

Kvemo Kartli, located in the southeastern part of Georgia, is a region distinguished by its diverse geology and lithology, shaped by tectonic, volcanic, and sedimentary processes. Situated within the tectonic framework of the Lesser Caucasus, the region exhibits complex geological characteristics [1-2].

The area is dominated by volcanic rocks, including basalts, andesites, and tuffs, which are remnants of ancient volcanic activity. Intrusive rocks such as granites and diorites are also present, formed through deep-seated magmatic processes. These rocks frequently contain elevated levels of uranium and thorium, whose

radioactive decay produces ^{222}Rn gas. As a result, areas with volcanic and intrusive rocks are potential ^{222}Rn hotspots.

Sedimentary formations in Kvemo Kartli include limestones, sandstones, shales, and marls. These rocks typically exhibit lower uranium content than igneous rocks, which reduces their ^{222}Rn -emission potential. The region also features conglomerates, indicative of high-energy river activity during their deposition. Additionally, river valleys and plains in Kvemo Kartli are dominated by quaternary alluvial and fluvial deposits, consisting of clays, silts, sands, and gravels, reflecting dynamic sedimentary processes.
Soils derived from ^{222}Rn -rich parent rocks, such as volcanic or granitic materials, may contribute to higher ^{222}Rn emissions. Loose and porous soils, such as those from alluvial and fluvial deposits, can facilitate the upward migration of ^{222}Rn to the surface.

Kvemo Kartli's tectonic setting includes active faults and fractures, which serve as conduits for 222Rn gas. Areas near fault lines often exhibit elevated ^{222}Rn concentrations due to the migration of gas from deeper geological layers. Groundwater flow in aquifers can either trap ^{222}Rn or transport it to the surface. Volcanic rock aquifers may have higher ^{222}Rn levels due to dissolved ^{222}Rn in groundwater [3-4].
Homes and buildings located in ^{222}Rn -prone areas, particularly those with poor ventilation and direct contact with the ground, are at risk of experiencing elevated indoor ^{222}Rn concentrations.

Measurement methodology

Measurements in Water

The field study was carried out by the mobile groups of researchers using an AlphaGUARD PQ 2000 PRO (hereafter "AlphaGUARD monitor") portable ^{222}Rn monitor based on the measurement principle of the pulse ionization chamber [2]. The instrument measures ^{222}Rn concentrations in air, soil gas as well as in water. For water samples, the AquaKIT was used [3], consisting of the following components: AlphaGUARD monitor, degassing vessel, security vessel and AlphaPUMP [4] (Fig. 1). The components were connected in a closed circuit, and ^{222}Rn concentration was measured according to the manual's protocol [5-7]. First, the water sample was collected from the source in a plastic bottle, which was filled entirely and closed tightly in order to avoid ^{222}Rn escape from the sample. Second, the water sample was injected into the degassing vessel. The AlphaPUMP was turned on for 10 minutes with a flow rate of 0.3 L/min for degassing ^{222}Rn from water to air. After turning it off, the AlphaGUARD monitor remained on for 20 minutes to carry out the measurements. As a final value for determining ^{222}Rn concentration in the sample, the indicated mean value in Bq/m3 on the monitor screen was taken.

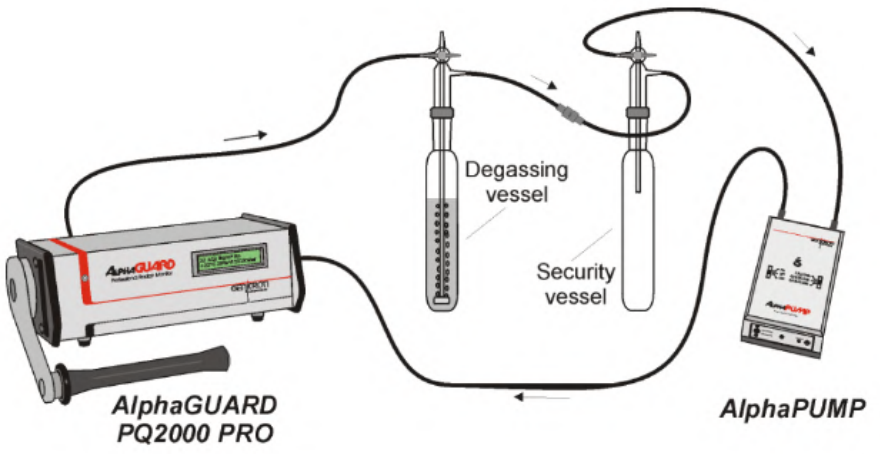

Fig. 1. AquaKIT measurement set-up [6].

The ^{222}Rn activity concentration in the water sample was calculated by equation (1), which considers the ^{222}Rn quantity diluted by the air within the measurement set-up as well as remains diluted in the watery phase [8]:

$$c_{Water} = \frac{c_{Air} \times \left(\frac{V_{System} - V_{Sample}}{V_{Sample}} + k\right) - c_0}{1000} \quad (1)$$

where:

c_Water = ^{222}Rn concentration in water sample [Bq/L],

c_Air = ^{222}Rn concentration [Bq/m3] in the air of the circuit,

c_0 = ^{222}Rn concentration before sampling (zero level) [Bq/m3],

V_System = interior volume of the circuit [in our case 1.102 L],

V_Sample = volume of the water sample [in our case 0.1 L],

k = ^{222}Rn distribution coefficient [0.26, since the measurements were performed in the temperature range 10-30 °C].

As a rule, the measurements followed the sampling with minimum delay. In case of delayed measurement, equation (2) was applied:

$$C_0 = C \times e \frac{ln2}{t_{1/2}} \Delta t \quad (2)$$

where, C_0 is the value at the moment of sampling, C is the measured value, t_(1/2) is a half-life of Czech Geological Survey. Praha, Rn, Δt is the time delay between sampling and measurement.

Measurements in Soil gas

The ^{222}Rn concentration measurements in soil gas were performed in the vicinity of every sampled water source and in the additional points without water sources to obtain dense coverage of the area. For the measurement, the soil gas exterior probe (STITZ-by Geophysik GCD Leipzig) was used. The closed circuit was set as follows: soil gas probe, AlphaPUMP, AlphaGUARD monitor and ^{222}Rn progeny filter (Fig. 2a), following the user manual [8]. The soil gas probe, locked at the rivet at the tip, was hammered into the ground approximately to the depth of 0.7-1.0 m. The AlphaGUARD monitor and AlphaPUMP were set to flow mode with a 1 min cycle and flow rate of 1 L/min, respectively. The quantity of gas and the filling time of the ionization chamber were assessed with the 1-litre balloon attached to the air outlet nozzle of the AlphaGUARD monitor (Fig. 2b). Only the soil gas samples, with an extraction duration of less than 3 min, were measured. After completing the waiting time of 10 minutes for the decaying of the thoron, the measurement process continued for 20 min. As a final result, the mean value of the ^{222}Rn concentration indicated on the monitor screen in Bq/m3 was considered.

a)

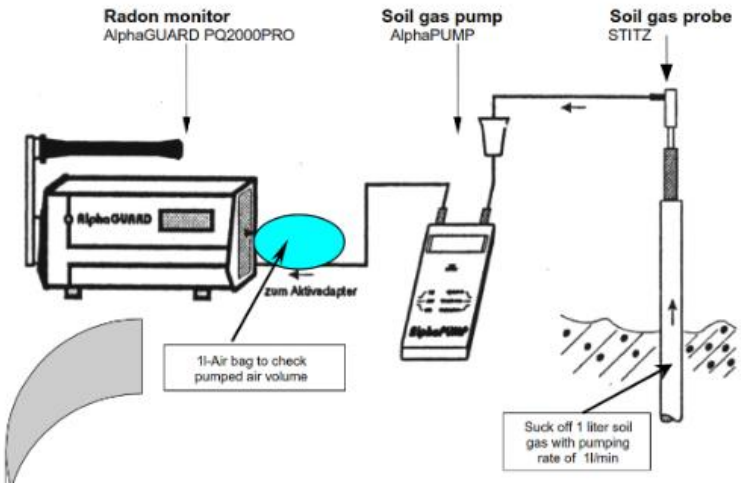

b)

Fig. 2. a) Schematic view of soil gas measurement setup [8]; b) Measurement by AlphaGUARD, AlphaPUMP and 1-L balloon attached to the air outlet nozzle of the AlphaGUARD

The ^{222}Rn survey was conducted during favorable environmental conditions, and the days with snow cover and precipitation were avoided.

All observation sites were marked by GPS position. Results of analyses on ^{222}Rn concentration were marked on topographic and geological maps. In order to figure out the connection of ^{222}Rn anomalies to geological and hydro-geological structures, the field data were digitized and transferred into the GIS system.

Data calculation and results

All 143 observation sites were marked by GPS position. Results of analyses on 222Rn concentration were marked on topographic and geological maps. In order to figure out the connection of 222Rn anomalies to geological and hydro-geological structures, the field data were digitized and transferred into the GIS system for further analysis (Fig. 3).

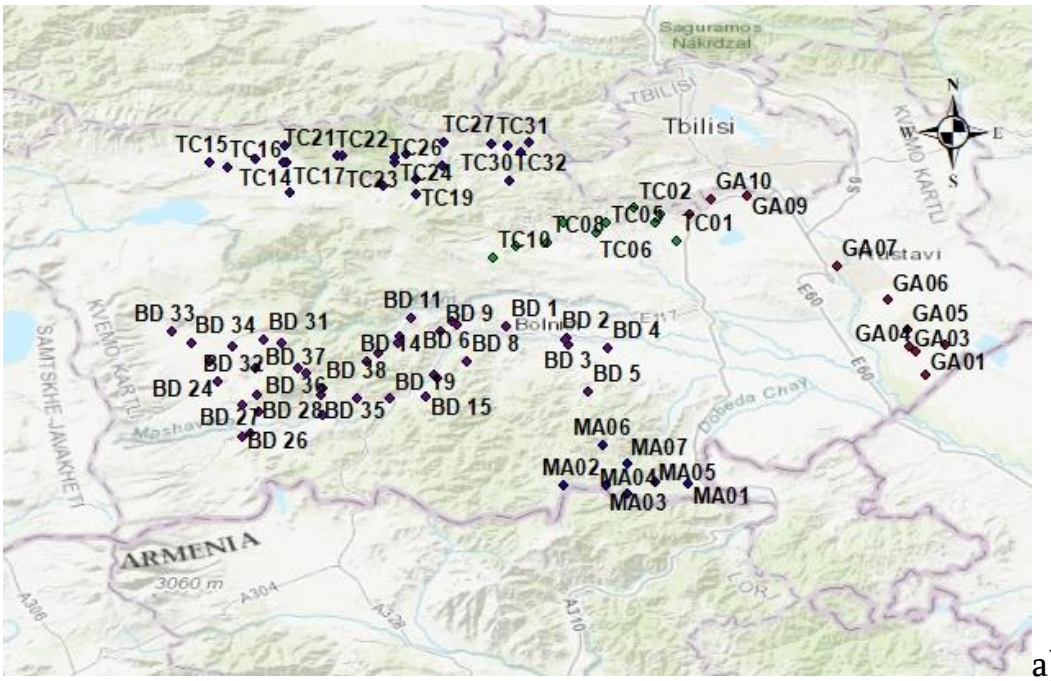

a)

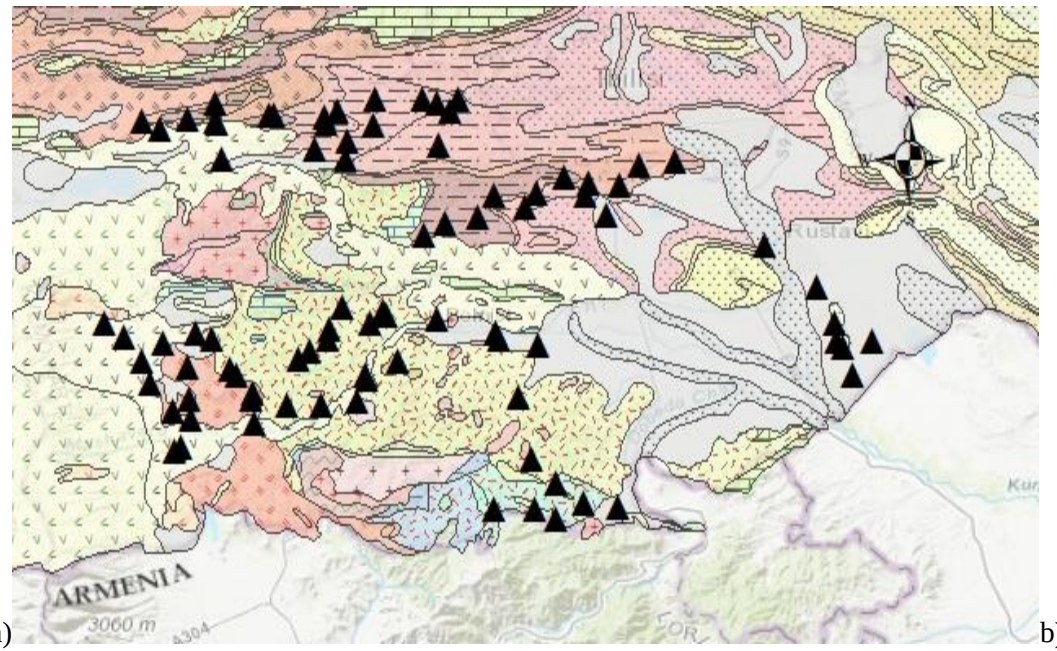

a) b)

Fig. 3. Location of sampled water and soil gas points on (a) a topographic map and (b) a geological map [9] of the Shida Kartli area.

Measured ^{222}Rn concentrations in water and soil gas are provided in Table 1.

Table 1. ^{222}Rn concentration values of samples water and soil gas points, Kvemo Kartli.

N	Water point Type	Water, Soil gas	Name of location	Rn(w) Bq/L	Rn(G) kBq/m3
Bd1		Rn_W/S	Ratevani	8.95	6.53
Bd2	mineral	Rn_W/S	Rachisubani	0.81	9.49
Bd3	well	Rn_W/S	Samtredo	0.37	20.6
Bd4	spring	Rn_W/S	Savaneti	15.57	12.1
Bd5	spring	Rn_W/S	Talavari	6.95	8.72
Bd6		Rn_W/S	Akaurta	7.01	13.2
Bd8	spring	Rn_W/S	MuSevani	33.76	23.9
Bd9	spring	Rn_W/S	Kvemo KveSi	15.10	9
Bd10	spring	Rn_W/S	Tandzia	20.51	11.8
Bd11	spring	Rn_W/S	Bertakari	5.30	16.2
Bd12	spring	Rn_W/S	Tsipori	12.01	3.1
Bd13	spring	Rn_W/S	Darbazi	20.20	5.83
Bd14	spring	Rn_W/S	Darbazi 2	0.47	22.1
Bd15	spring	Rn_W/S	Balicha	15.26	14.7
Bd18		Rn_S	Kazreti		14.3
Bd19	spring	Rn_W/S	Didi Dmanisi	42.60	0.276
Bd20	spring	Rn_W/S	Boslebi	34.54	27.1
Bd21	well	Rn_W/S	Gantiadi	2.24	6.02
Bd22		Rn_S	Iakublo		7.71
Bd24	spring	Rn_W/S	Karabulakhi	9.29	7.52

Bd28	spring	Rn_W/S	Dagarakhlo	9.98	12.8
Bd29	spring	Rn_W/S	Dagarakhlo 2	1.09	2.05
Bd30	spring	Rn_W/S	Saja	18.70	12.1
Bd32	spring	Rn_W/S	Kvemo Karabulakhi	8.71	19.7
Bd35	spring	Rn_W/S	Kizilqilisa	28.90	19.3
Bd36		Rn_W/S	Ormasheni	17.76	15.2
Tc1	spring	Rn_W/S	Koda	8.48	3.53
Tc2	spring	Rn_W/S	Goubani	13.19	27.1
Tc3	spring	Rn_W/S	Borbalo	9.48	7.46
Tc4	spring	Rn_W/S	Vashlovani	14.74	5.76
Tc5	well	Rn_W/S	AsureTi	8.38	22.3
Tc6		Rn_S	EnageTi		22
Tc7	spring	Rn_W/S	Ardisubani	1.56	2.28
Tc8	spring	Rn_W/S	Sagrasheni	14.63	8.86
Tc10		Rn_S	TeTritskaro		10.8
TC11	Spring	Rn W/S	Arjevani	0.15	3.86
TC12	spring	Rn W/S	Cholmani	21.52	4.43
TC13		RnW/S	Livadi	5.27	6.3
TC15	spring	Rn W/S	Tijisi	4.48	1.8
TC16	spring	Rn W/S	Sabechisi	6.60	1.87
TC17		Rn S	Tsalka		1.95
TC18	spring	Rn W/S	Akhalsofeli	3.19	32
TC19		Rn S	Sapudzvrebi		29.5
TC20	spring	Rn W/S	Algeti	13.19	11.2
TC21	spring	Rn W/S	Chinchriani	1.78	10.8
TC23	spring	Rn W/S	Shekhvetila	0.56	18.4
TC24	spring	Rn W/S	Manglisi	51.35	15.6
TC26	spring	Rn W/S	Didi Toneti	0.80	14.1
TC27	spring	Rn W/S	Mokhisi	10.71	1.23
Tc28	spring	Rn W/S	Tskluleti	0.95	5.41
TC30	spring	Rn W/S	Vanati	4.64	4.59
TC31	spring	Rn W/S	Shamta	8.30	11.1
Tc32	spring	Rn W/S	Orbeti	2.94	6.45
MA01	spring	Rn W/S	Sadakhlo	0.68	2.3
MA02	spring	Rn W/S	Chamchakhi	0.21	1.72
MA03	spring	Rn W/S	At Armenian border	0.12	34
MA04	spring	Rn W/S	Khojorni	33.13	20.5
MA05	spring	Rn W/S	Tsopi	24.07	13.4
MA06	spring	Rn W/S	Tseraqvi	3.36	10.7
MA07	spring	Rn W/S	Jankhoshi	8.39	30.1
GA01	well	Rn W/S	Vakhtangisi	1.16	11.6
GA02	soil	Rn S	Jandara		4.01
GA05	soil	Rn S	Gardabani		1.76
GA06	soil	Rn S	Gardabani 2		21.6
GA07	spring	Rn W/S	Akhali Rustavi	12.87	5.29
GA08	spring	Rn W/S	Kumisi	4.68	36.9

GA09	spring	Rn W/S	ქვემო თელეთი, წყარო	38.20	26.8
GA10	spring	Rn W/S	Zemo Teleti	1.10	17.9

^{222}Rn in Water

In the Kvemo Kartli Region, ^{222}Rn in water sources was monitored at 75 points (66 spring and 9 borehole) in the period of May-October 2022 using the AlphaGUARD monitor and the AquaKIT, consisting of the following components: AlphaGUARD monitor, degassing vessel, security vessel and AlphaPUMP [7] (Fig. 1). The components were connected in a closed circuit, and ^{222}Rn concentration was measured according to the manual's protocol [6].

The ^{222}Rn activity concentration in the water sample was calculated by equation (1), which considers the ^{222}Rn quantity diluted by the air within the measurement set-up as well as remains diluted in the watery phase [6]. As a rule, the measurements followed the sampling with minimum delay. In case of delayed measurement, equation (2) was applied.

Although the dataset for our ^{222}Rn concentration data in water is limited, the basic statistical analysis for the sampled points is presented in the table 2. As noticed, arithmetic mean (AM) and geometric mean (GM) ^{222}Rn concentrations are lower in boreholes than in natural springs. ^{222}Rn concentration for all water points ranges from 0.12 to 73.50 kBq m^{-3} with AM of 12.43 kBq m^{-3}, The values are in the ranges obtained in our previous study [10]. One of the main factors contributing to the variation in ^{222}Rn concentrations is the influence of anomalously high values, which are caused by specific lithological features and the presence of local radioactive elements along the flow path from recharge to discharge areas. In our case, the ^{222}Rn levels are indicative of the geological characteristics of the water sampling sites. Although ^{222}Rn concentration values in water are generally not ideal for detailed statistical analysis, they still offer valuable insights into the underlying geological and hydrogeological processes.

Table 2. Basic statistics of ^{222}Rn concentration in water, Kvemo Kartli

		222Rn concentration / Bq/L						
Type	No. points	Min	Max	Median	AM	ASD	GM	GSD
All	75	0.12	73.50	8.71	12.43	13.40	6.04	4.36
Spring	66	0.12	73.50	9.38	12.86	13.44	6.60	4.18
Borehole	9	0.37	32.72	2.24	9.24	13.40	3.15	4.58

Type: Type of water point; No: number of measuring points; AM: arithmetic mean; ASD: arithmetic standard deviation; GM: geometric mean; GSD: geometric standard deviation; Min: minimum; Max: maximum.

For better visualization of ^{222}Rn concentrations, the values were represented using box plot graphs (Fig. 4). These graphs reveal that natural springs exhibit higher 222Rn concentrations compared to boreholes.

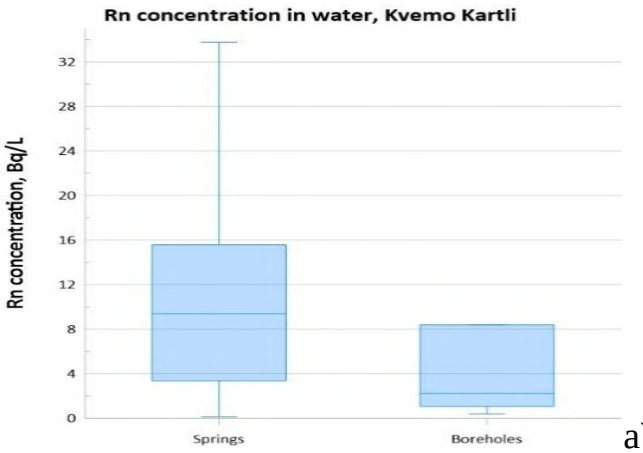

a)

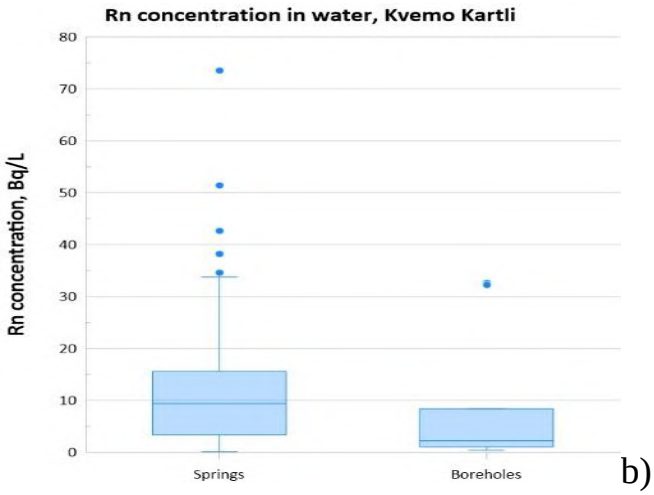

Fig. 4. The distribution of ^{222}Rn concentrations in sampled springs and boreholes is illustrated in two ways: a) Including "outliers" to show the full range of variability. b) Excluding "outliers" to highlight the central trend and reduce the influence of extreme values.

^{222}Rn in soil gas

In the Kvemo Kartli Region, ^{222}Rn in soil gas was monitored at 68 points in the period of May-October 2022 in the vicinity of every sampled water source and in the additional points without water sources to obtain dense coverage of the area, using the AlphaGUARD monitor [2]. The closed gas cycle was set as follows: probe-AlphaPUMP-AlphaGUARD, including ^{222}Rn progeny filter and water break in accordance with the user manual [5; 7-8]. The soil gas probe, locked at the rivet at the tip, was hammered into the ground to approximately a depth of 0.7–1.0 m. The AlphaGUARD and AlphaPUMP were set to flow mode at 1 min (cycle = 1 min F) and 1 L min^{-1}, respectively. The volume of gas and the filling time of the ionization chamber were assessed with the 1-L balloon attached to the air outlet nozzle of the AlphaGUARD. Only the soil gas samples with an extraction duration of less than 3 min were measured. After a waiting time of 10 minutes, for short-lived radionuclides (thoron) to decay, the activity was measured for 20 min, and the mean value read was taken as the representative ^{222}Rn concentration. The measuring setup is shown in Fig. 2.

In general, the data on ^{222}Rn concentration in soil gas is not rich because the measurements are more demanding and complex than those in water and especially in indoor air [12].

Although the database of our ^{222}Rn concentration in soil gas is modest, the summary statistic of ^{222}Rn concentration in soil gas is given in Table 3. As noticed, arithmetic mean (AM) and geometric mean (GM) ^{222}Rn concentrations are lower than it is expected in volcanic rocks. ^{222}Rn concentration ranges from 0.28 to 36.90 kBq/m^3 with AM of 13.49 kBq /m^3, The values are in the ranges obtained in the previous study [7; 9-10]. One of the main factors which may cause the difference is soil permeability. Although volcanic rocks may have high porosity due to the presence of vesicles, their permeability is often constrained by a lack of connectivity among them [15-16].

Table 3. Basic statistics of ^{222}Rn concentration in soil gas in volcanic rocks, Kvemo Kartli

	^{222}Rn concentration, kBq·m^{-3}						
No	Min	Max	Median	AM	ASD	GM	GSD
68	0.28	36.90	11.15	13.49	11.02	8.65	2.91

No: number of measuring points; AM: arithmetic mean; ASD: arithmetic standard deviation; GM: geometric mean; GSD: geometric standard deviation; Min: minimum; Max: maximum

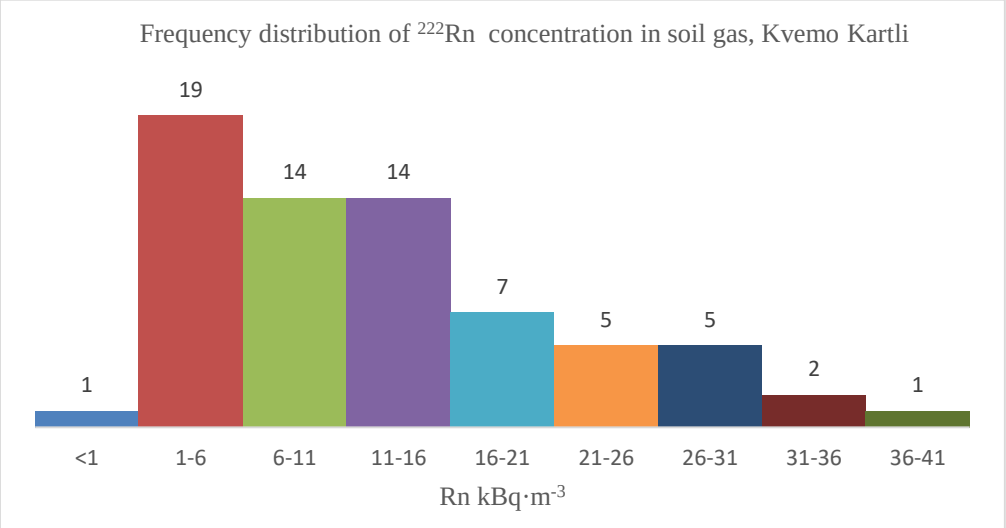

Fig. 5. Frequency distribution of ^{222}Rn concentration in soil gas, Kvemo Kartli.

Data, presented on the histogram plot (Fig. 5), show that the most of the measured concentrations, 19 values are 1-6 and 14-14 values are in the range of 6-11 and 16-21 kbq·m^{-3}.

Fig. 6 shows a cumulative frequency of ^{222}Rn concentrations.

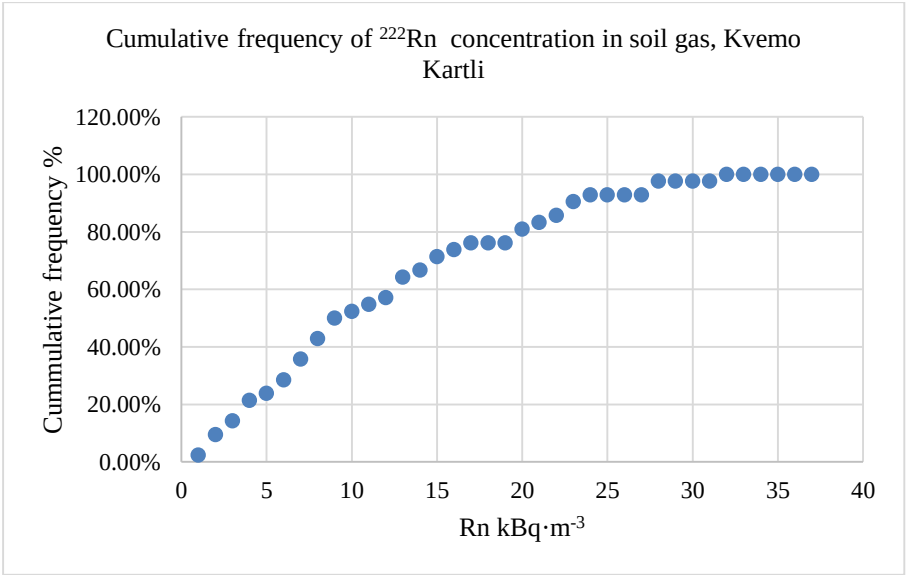

Fig. 6. Cumulative frequency of ^{222}Rn concentration

As seen from the figure, the values roughly fit a lognormal distribution. The values could be distinguished into 4 groups. The first group, in the region of >12 kBq m^{-3}, The 2nd group, in the region of 13-19 kBq·m^{-3}, the third, in the region of 20-27 kBq·m^{-3} and the 4th group 28-37 kBq·m^{-3}. Due to the wide range of permeability in volcanic and sedimentary rocks, such a result is expected [15-17], reflecting the area's geological structure.

Conclusion

From 143 ^{222}Rn measurements carried out and water points within the project *^{222}Rn mapping and ^{222}Rn risk assessment in Georgia*, in Kvemo Kartli region, 68 were in soil gas and 75 in water point. The arithmetic means of 13.49 ± 11.02 kBq·m^{-3} was obtained for ^{222}Rn concentration in soil gas and 12.43 ± 13.40 Bq/L, in

water (for springs 12.86 ± 13.44 Bq/L and for boreholes 9.24 ± 13.40 Bq/L). The values in soil gas roughly fit a lognormal distribution. The values could be distinguished into 4 groups. The first group, in the region of >12 kBq m^{-3}, The 2nd group, in the region of 13-19 kBq m^{-3}, the third, in the region of 20-27 kBq m^{-3} and the 4th group 28-37 kBq·m^{-3}. The dataset for ^{222}Rn concentrations in water and soil gas is limited and provides only a general overview of Rn levels in the region. Therefore, further exploration of this area is recommended. Analyzing the existing ^{222}Rn data in water and soil gas, along with indoor air measurements and an evaluation of site characteristics and geochemical data, will enable a more comprehensive assessment of 222Rn risk to the population.

Acknowledgements. The paper is a part of the research done within the SRNSFG FN-19-22022 project "^{222}Rn mapping and ^{222}Rn risk assessment in Georgia". As recipients of the Research State Grant, the authors thank the Shota Rustaveli National Science Foundation of Georgia.

References

[1] Adamia, S., Akhvlediani, K. T., Kilasonia, V. M., M. Nairn, A. E., Papava, D., Patton, D. K. Geology of the Republic of Georgia: A Review. International Geology Review, 34(5), 1992, pp. 447–476. https://doi.org/10.1080/00206819209465614

[2] Maisuradze G.M., Kuloshvili S.I. Nekotorye voprosy geologii molodogo vulkanizma Javakhetskogo nagoria. Trudy GIN AN Gruzii. Novaia seria, 1999, s. 220-228, (in Russian).

[3] Nunes L.J.R., Curado A., Lopes S.I. The relationship Between Radon and Geology: Sources, Transport and Indoor Accumulation. Applied Sciences, 13, 2023, 7460.

[4] Barnet I., Pacherová P., Neznal M., Neznal M. Radon in Geological Environment - Czech Experience, Special Papers No. 19, Czech Geological Survey, Praha, 2008, pp 16–19.

[5] AlphaGUARD PQ2000 PRO Portable Radon Monitor, Saphymo GmbH, Frankfurt / Main – Germany; User Manual 08/2012

[6] AlphaKIT Accessory for Radon in water measurement in combination with the Radon monitor AlphaGUARD. User Manual, Genitron Instruments, Frankfurt/Main, Germany, 09, 1997.

[7] AlphaPUMP, Technical Description, User manual, Genitron Instruments Germany, 2001.

[8] AlphaGUARD Soil Gas Measurements. Short instructions for the use of the Soil Gas Probe in combination with the Radon monitor, User Manual, Genitron Instruments, Frankfurt/Main, Germany, 2001.

[9] Gudjabidze G.E., Gamkrelidze I.P. Geological map of Georgia, 2003, 1: 500 000.

[10] Kapanadze N., Melikadze G., Vaupotič J., Tchankvetadze A., Todadze M., Jimsheladze T., Chikviladze E., Gogichaishvili Sh., Chelidze L. Radon-222 Concentration Levels in Soil and Water in Different Regions of Georgia – Radon Mapping, RAD Conf. Proc., vol. 6, 2022, pp. 60–64.

[11] Kapanadze N., Melikadze G., Tchankvetadze A., Todadze M., Jimsheladze T., Gogichaishvili Sh., Chikviladze E., Chelidze L., Vaupotič J. Radon in Soil Gas in Crystalline Shales and Volcanic Grounds in Selected Regions of Georgia. 16th Int. workshop GARM - Geological aspects of Radon risk mapping; September 19th – 21st, 2023, Prague, Czech Republic. A

[12] Cinelli G., De Cort M., Tollefsen T., et al. European Atlas of Natural Radiation. Cinelli, G., De Cort, M. and Tollefsen, T. editor(s), Publications Office of the European Union, Luxembourg, 2019, ISBN 978-92-76-08259-0, JRC116795.

[13] Vaupotič J., Bezek M., Kapanadze N., Melikadze G., Makharadze T., Machaidze Z., Todadze M. Radon and Thoron Measurements in West Georgia. Journal of Georgian Geophysical Society, Issue (A), Physics of Solid Earth, 15a, 2011–2012, pp. 128–137.

[14] Amiranashvili A., Chelidze T., Melikadze G., Trekov I., Todadze M., Chankvetadze A., Chelidze L. Preliminary Results of the Analysis of Radon Content in the Soil and Water in Different Regions of West Georgia. Institute of Geophysics ISSN 1512-1135, vol. 60, Tbilisi, 2008, pp. 213–218 (in Russian).

[15] Evans J.P., Forster C.B., Goddard J.V. Permeability of Fault-Related Rocks, and Implications for Hydraulic Structure of Fault Zones. Journal of Structural Geology, 19, 1997, pp. 1393–1404.

[16] Mitchell T., Faulkner D. Towards Quantifying the Matrix Permeability of Fault Damage Zones in Low Porosity Rocks. Earth and Planetary Science Letters, 339, 2012, pp. 24–31.

[17] Rashid F., Glover P., Lorinczi P., Collier R., Lawrence J. Porosity and Permeability of Tight Carbonate Reservoir Rocks in the North of Iraq. Journal of Petroleum Science and Engineering, 113, 2015, pp. 147–161.

^{222}Radon კონცენტრაციის დონეები ნიადაგსა და წყალში ქვემო ქართლის რეგიონში - ^{222}Rn-ის აგეგმვა

ნ. კაპანაძე, გ.მელიქაძე, ა.ჭანკვეტაძე, თ.ჯიმშელაძე,
ზ. მაღრაძე, შ. გოგიჩაიშვილი, მ. თოდაძე, ე.ჩიკვილაძე, ლ.ჭელიძე

რეზიუმე

SRNSFG FN-19-22022 პროექტის „რადონის აგეგმვა და რადონის რისკის შეფასება საქართველოში“ ფარგლებში, საქართველოს რიგ გეოგრაფიულ ზონებში ჩატარდა საველე სამუშაოები როგორც წყალსა და ნიადაგში რადონის (^{222}Rn) განაწილების რაოდენობრივად განსაზღვრის მიზნით, ასევე რადონის კონცენტრაციების განმსაზღვრელი გეოლოგიური ფაქტორების შესაფასებლად. ადგილზე რადონის კონცენტრაცია გაზომილი იქნა ნიადაგის აირში (68 სინჯის აღების წერტილი) და სხვადასხვა წყალპუნქტებში (ჭები და წყაროები, სულ 75 წყალპუნქტი, 66- წყარო, 9 ჭაბურღილი) AlphaGUARD PQ2000 PRO (Saphymo GmbH) რადონის მონიტორის გამოყენებით. რადონის კონცენტრაცია მერყეობდა 0,12-დან 73 Bq/L წყალში და 36,9 Bq·m^{-3}-მდე ნიადაგის აირში. ყველა სადამკვირვებლო ადგილი მონიშნული იყო GPS პოზიციით. მონაცემები დამუშავდა საბაზისო სტატისტიკური ანალიზით და წარმოდგენილი იქნა სხვადასხვა გრაფიკების მეშვეობით. შემდგომში, ქვემო ქართლის ტერიტორიაზე წყალსა და ნიადაგის გაზში რადონის განაწილების ვიზუალიზაციისათვის მოხდა საველე მონაცემების აციფვრა და ინტეგრირება GIS სისტემაში.

საკვანძო სიტყვები: Rn-ის აგეგვმა, ნიადაგის აირი, წყალი, GIS, ქვემო ქართლი, საქართველო.

Уровни концентрации ^{222}Rn в почве и воде в регионе Квемо Картли, Грузия - картирование ^{222}Rn

Н. Капанадзе, Г. Меликадзе, А. Чанкветадзе, Т. Джимшеладзе, З. Маградзе, Ш. Гогичаишвили, М. Тодадзе, Е. Чиквиладзе, Л. Челидзе

Резюме

В рамках проекта SRNSFG FN-19-22022 «Картирование ^{222}Rn и оценка риска радона в Грузии» авторы провели полевые работы по количественной оценке распределения ^{222}Rn в воде и почвенном газе, а также по установлению геологических факторов, влияющих на уровни концентрации ^{222}Rn в некоторых географических районах Грузии. На месте концентрация ^{222}Rn была измерена в почвенном газе (68 точек отбора проб) и в различных источниках воды (скважины и родники, 75 водозаборных точек, 66 родников, 9 скважин) с использованием радонового монитора AlphaGUARD PQ2000 PRO (Saphymo GmbH). Концентрация ^{222}Rn варьировалась от 0.12 до 73 Бк/л в воде и до 36.9 Бк·м$^{-3}$ в почвенном газе. Все места наблюдения были отмечены местоположением GPS. Данные прошли базовый статистический анализ и были визуализированы с помощью различных графиков. Впоследствии полевые данные были оцифрованы и интегрированы в ГИС-систему, которая выявила распределение ^{222}Rn в воде и почвенном газе на территории Квемо Картли.

Ключевые слова: картирование радона, почвенный газ, вода, ГИС, Квемо Картли, Грузия

Journal of the Georgian Geophysical Society, e-ISSN: 2667-9973, p-ISSN: 1512-1127
Physics of Solid Earth, Atmosphere, Ocean and Space Plasma, v. 27(2), 2024, pp. 48 - 62

On the Issue of Modelling the Dynamic Picture of the Spread of a Mudflow in the Shovi Gorge due to a Collapse on the Glacier Buba

Zurab A. Kereselidze, Nodar D. Varamashvili

M. Nodia Institute of Geophysics of I. Javakhishvili Tbilisi State University, Tbilisi, Georgia
Nodar.varamashvili@tsu.ge

ABSTRACT

Glaciers have always been a potential hazard in the Caucasus region, where mountain canyons are quite densely populated. The processes associated with global climate change occurring everywhere have greatly exacerbated the problem of preventing the population from glacial disasters. For example, there is a sad experience associated with the collapse of the Kolka glacier, which caused a giant ice mudflow in 2002. A similar disaster should include the glacial mudflow from the Buba glacier on 9/3/2023, which resulted in a tragedy with numerous victims at the Shovi resort. Determining the possible place and time of development of such catastrophic events (earthquakes, volcanic eruptions, large-scale floods) has a very low degree of reliability and is problematic, despite the modern level of scientific methods of ground and space monitoring. In particular, there is an obvious need for long-term monitoring and comprehensive diagnostics of the current state of the Caucasus glaciers, taking into account each new experience. It should be noted that there is a paucity of information that allows us to judge the processes that have occurred on the Buba glacier over the past decades. Therefore, hardly anyone could imagine a large-scale virtual picture of the spread of a glacial mudflow along the gorges of the Bubistskali and Dzhandzhakhi rivers, adequate to what it turned out to be in reality. At the same time, in the case of a sufficiently complete database of observation results and its correct analysis, based on the principle of hydrodynamic similarity, there is a possibility of theoretical modeling of probable parameters of a flood or glacial mudflow in any mountain gorge. For example, in the case of the Caucasus region, one can use some of the results obtained by numerical modeling of the Dzhankuat and Kolka glaciers. In particular, these models are quite useful not only for determining probable causes, but also for retrospective analysis of the consequences of destruction on the Buba glacier. First of all. This concerns the process of propagation of hydrodynamic waves in a heterogeneous mudflow. For this purpose, records of seismic equipment are also important, which contain information on the frequency spectrum of acoustic waves generated by the process of destruction on the Buba glacier. Hydrodynamic waves of various types could have existed in the gorges of the Bubistskali and Chanchakhi rivers. In the characteristic range of the Froude similarity number, the most probable is the generation of running rolling waves, the height of which could reach several meters. The appearance of solitary waves (solitons), as well as the so-called gravity waves, was unlikely, but one cannot exclude the possibility of their generation in those places for which local conditions were suitable. In the lower, widest section of the Shovi gorge, in the zone of the so-called cottages, the movement of the mudflow was similar to the movement of the ice mudflow in the Genaldon River gorge after the collapse of the Kolka glacier in 2002. Despite the huge difference in the initial volumes of mudflows that came down from the Buba and Kolka glaciers, the deposit of viscoplastic mass in the last sections of its distribution turned out to be comparable taking into account the spatial scale and the amplitude of the waves in both cases decreased to heights of 1-3 meters.
Key words: *natural disasters, glacier, debris-flow, acoustic waves, viscoplastic.*

Introduction

There is sufficiently comprehensive information on the dynamics of glaciers in the Central Caucasus, suitable for modeling glacial processes that lead to the formation of debris flows, which spread through the riverbeds of mountain rivers, canyons, and mountain valleys. These models are based on two sources: the analysis of results from field morphological studies of glaciers and the observed changes in the landscape that occurred after debris flow events on specific glaciers. In the latter case, particular attention is given to the movement of the rock-ice debris flow, for which hydrodynamic equations are used. Regardless of its location, such a scheme forms the basis for an analytical or numerical model of glacier dynamics. Therefore, to some extent, it is universal, though it may have specific elements in particular cases. Specifically, these are the simulation models for the Djankuat and Kolka glaciers [1,2]. These and similar models can serve as tools for the retrospective analysis of the causes and outcomes of large-scale destructive events associated with glaciers in various regions of the Earth. However, their ability to predict the time and

location of a potential disaster is not only limited but also unlikely. Nevertheless, the results of modeling the Djankuat glacier, as well as the disaster on the Kolka glacier, may be useful for analyzing the consequences of the destructive event on the Buba glacier, which caused a catastrophe in the Shovi Gorge. The first model generalizes data from long-term expeditions to the Djankuat glacier. The analytical basis for both models is the hydrodynamic equations. A quantitative assessment of the geophysical parameters of the Djankuat glacier was obtained, which, in terms of linear characteristics, is almost identical to the Buba glacier, located 100 km to the southwest. In the second model, a retrospective picture of the spread of a giant ice debris flow was reconstructed, virtually simulating the catastrophic process on the Kolka glacier in 2002. In particular, this model simulates the conditions for the generation of giant waves that actually spread through the Karmadon and Genaldon gorges. The obtained model parameters for the movement of the debris flow were in agreement with its destructive impact, as determined from satellite and ground-based observations.

The Event on the Buba Glacier

There are two fairly detailed reports on the disaster at the Buba glacier (Figure 1), caused by the collapse of a glacial debris flow at about 15:03 h on August 3, 2023. The first report was prepared by the National Environment Agency of Georgia [16], and the second was prepared by Swiss specialists [15]. These reports were published a few months after the disaster and have a clear structural similarity, as well as identical main conclusions: the disaster occurred due to the overlap of several natural factors, making it impossible to accurately predict the timing of the event. Given the practical full alignment of the methodology and input data used in both reports for the computer simulation of the disaster, the final part of this work will provide an analysis of the main conclusions from the report prepared by the Swiss specialists.

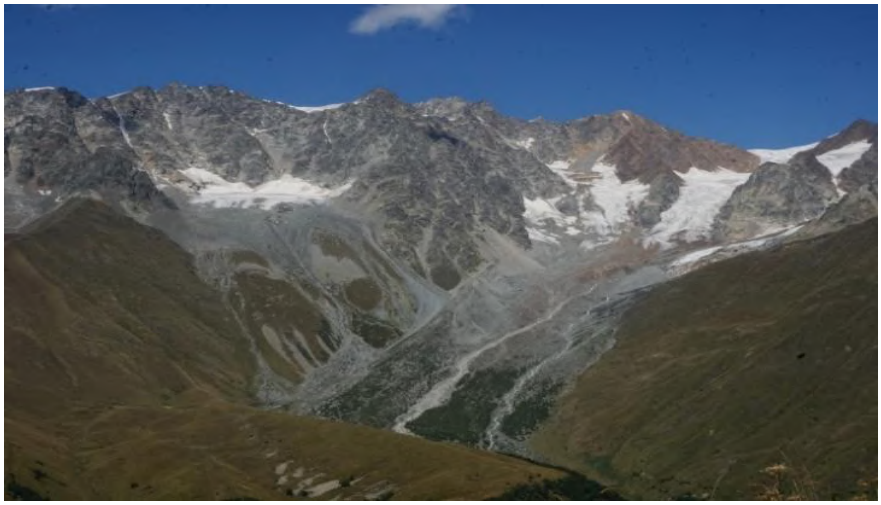

Fig.1. Buba Glacier (photo by D. Svanadze).

A particularly important element related to the discussed disaster is the recording of seismic oscillations generated by the collapse on the Buba Glacier. Along with the emission of acoustic waves, a powerful glacial debris flow spread through the gorges of the Bubistkali and Dzhandzhakhi rivers. We have records from the seismograph of the Seismic Monitoring Service of Georgia, located in the village of Gari ($42^0 35' 12.75'' N$, $43^0 27' 58.81'' E$) adjacent to the district center of Oni, as well as data from four stations located on the northern side of the Caucasus Range, kindly provided by the Seismic Monitoring Service of the North Caucasus (Figure 2c), where the waves, accompanying the destructive process on the Buba Glacier was particularly well recorded. Together, these records provide a clear understanding of the nature of the process that began at about 15:03 h on August 3, 2023 (Figure 2b,c). It is clear that the mechanism for generating and spreading seismic and acoustic waves in the Earth's medium is identical. The boundary between the frequencies of seismic and acoustic waves is somewhat conditional. Specifically, the generation of acoustic waves is always accompanied by the process of destruction of ice clusters of any size and shape. It is accepted that this boundary is near the lower frequencies audible to the human ear. It is believed that above this threshold, seismic wave packets represent the so-called high-frequency trace, the intensity of which decreases with distance according to a nonlinear law. Thus, higher-frequency acoustic waves are formally a continuation of seismic waves. They can be recorded by seismic equipment at distances of up to

several dozen kilometers from the epicenter of the earthquake [3]. Spectral analysis of the acoustic radiation from glacial processes is an effective tool for studying structural formations on glaciers. On glaciers in various regions, the method of acoustic emission in the frequency range of 15-20 kHz [4] has been used to diagnose ice movement and ice formation, as well as rockfalls. As a result of these studies, links between the acoustic radiation spectrum and the parameters of dynamic changes in glaciers were identified. Generalizing the results of acoustic studies obtained from several glaciers provided a quantitative estimate of the impact of potential mechanical obstacles on the parameters of ice displacement in the glacier bed, when acoustic effects characteristic of ice destruction were recorded [4,5]. These results demonstrate the effectiveness of diagnostics using acoustic waves not only in cases of smooth ongoing glacial processes but also in cases of spontaneously occurring phenomena, which most often lead to glacier destruction. For example, the recordings in Figure 2b,c, clearly indicate that on the Buba Glacier, with an interval of approximately 3-4 seconds, two destructive events occurred. According to popular opinion, and following the aforementioned reports, these events are more likely related to the fall of a rock mass rather than the breaking of ice from the glacier's tongue. According to eyewitnesses of the event in the Shovi Gorge, the sound wave was the first alarming signal. Additionally, according to eyewitnesses, the powerful effect that typically accompanies the propagation of a shock wave was not felt. Thus, it can be assumed that rockfall or icefall was one of trigger for the destruction process on the Buba Glacier [15,16]. A similar mechanism for a glacial mudflow has been discussed in connection with the Kolka glacier disaster [17]. The paper deals with an 11 m side ice cube, the so-called energetic reference. Was calculated the volume of a rock avalanche (approximately 40,000 m3), falling from a height of about 1 km, which is necessary to melt a 0^0C reference ice cube, which would give us about 1300 cubic meters of water [17]. In the case of Shovi, the height is likely much less, so it is almost certain that there was a theoretical possibility production about of a 10,000 m^3 water, if $(0.5 - 1)10^6$ m^3 of rock fall occurred simultaneously, which is not yet clear and maybe could be confirmed by an expedition to the disaster site. In that case, it can be hypothesized that the catastrophic event started, for example, due to the rupture of the integrity of the subglacial water reservoir(s) in a certain local area of the glacier. It is likely that the size of this area could have increased sharply within a very short time. This circumstance may be one of the arguments in favour of the hypothesis that, for some reason, whether due to the fall of rock debris or the break-off of ice from the glacier's tongue, the subglacial water reservoir(s) were emptied. Therefore, it may be justified to assume that information about the linear characteristics that define the volume of the reservoir is present in the acoustic wave frequency spectrum. In this regard, it is worth noting that the lowest frequencies in the infrasound range in the recordings, such as those from the ZEI seismic station, may reflect the natural mechanical vibrations of the Buba Glacier as a unified elastic body. It is known that the spectrum of natural vibrations is related to the linear characteristics of the body, i.e., its size. Typically, natural vibrations occur due to some external trigger. In the case of glaciers, vibrations can be caused by any mechanical reason, such as a seismic shock, a snow avalanche, the collapse of rocks, or the breaking of ice. It is known that in the spectrum of natural mechanical vibrations of an elastic body, the lowest frequency is dominant, and higher frequencies are overtones (harmonics). Usually, the spectrum of acoustic radiation from a vibrating body is discrete, but in the case of complete degeneration, it can become practically continuous. The filling of the spectrum with overtones occurs due to the complex structure and the presence of cavities or heterogeneous-density formations within the body. Such structural features are present in every glacier. Accordingly, each glacier should have a characteristic spectrum of its own acoustic radiation. In calm conditions, this spectrum should primarily reflect the mechanical vibrations of the glacier's internal structures. However, in the presence of a strong external trigger, the entire glacier may also vibrate. Therefore, it is clear that, in most cases, the spectrum of natural frequencies will be relatively high-frequency, as the linear dimensions of even the largest internal heterogeneities of glaciers are typically several times smaller than the size of the glacier. As confirmation of this reasoning, the study [6] provides a broad set of data that determined the characteristic acoustic radiation interval of the natural mechanical vibrations of glacial structures: f = 100-300 Hz. It is clear that the process of spontaneous outflow of water from internal glacier reservoirs must also be accompanied by the emission of acoustic waves in this range. The main frequency of such wave packets should also be linked to the characteristic linear size (volume) of the reservoir.

The lowest frequency in the spectrum of the glacier's natural vibrations should indicate either its slow movement or the oscillation of the glacier as a single body. This bears some resemblance to the emission of seismic waves from the elastic zone of an earthquake's epicenter. Similar to seismic waves, the emission of

acoustic waves from the hypocenter of an earthquake is a quite common phenomenon. Acoustic waves, in this case, propagate not only through the Earth's medium but also through the atmosphere. Therefore, the emission of acoustic radiation in the frequency range of 20-20,000 Hz is used as an indicator of the intensity of glacial processes during monitoring [4].

a)

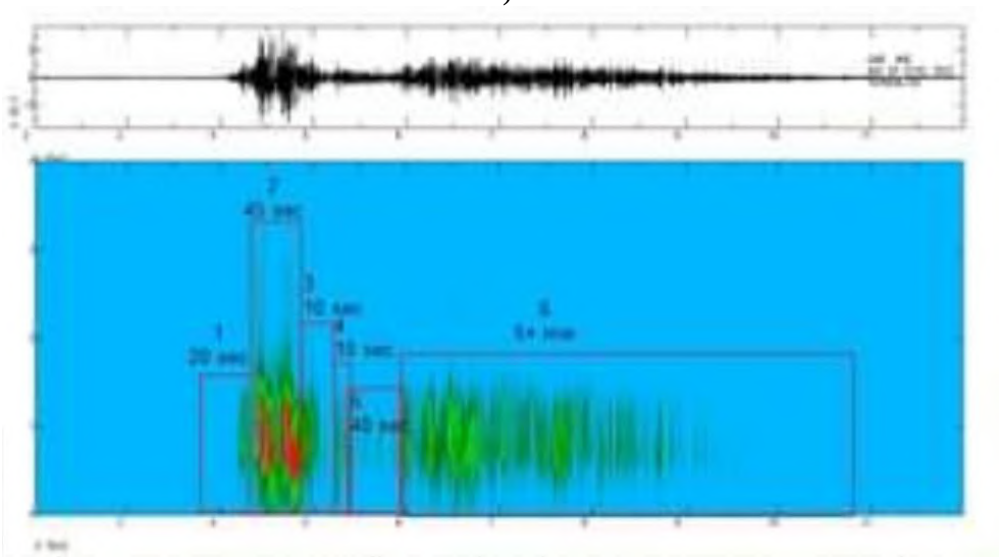

b)

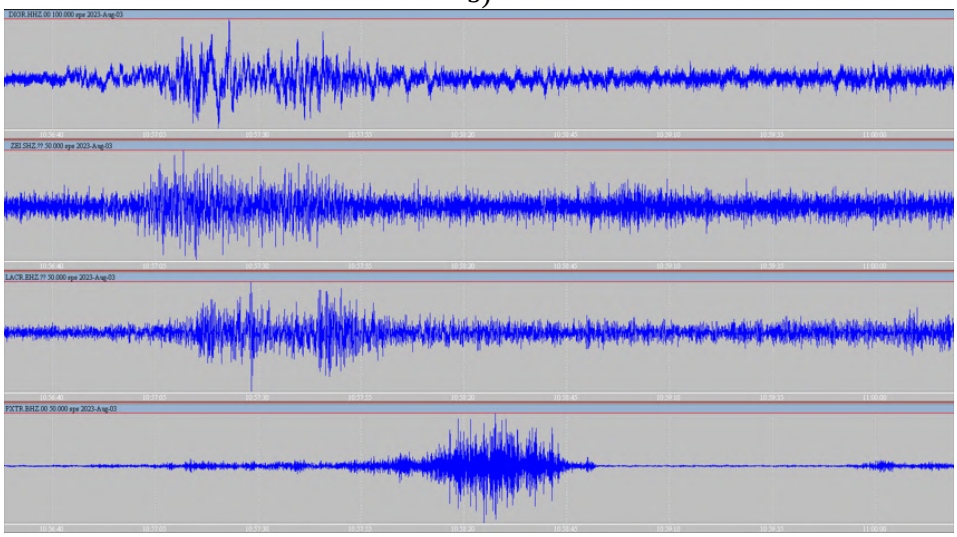

c)

Fig.2. a) Seismic station layout, b) Gari station (Georgia), c) Records of stations in North Ossetia (Russia) (courtesy of the North Caucasus Seismic Monitoring Survey).

It is evident that this type of noise effect, which emerged after the destruction on the Buba Glacier, reached the resort area in the Shovi Gorge. As mentioned earlier, there may have been water reservoirs under this glacier. Therefore, the delay between two bursts recorded on the seismograms may indicate that there was a rupture or collapse of two reservoirs, separated by ice partitions. Certainly, this assumption is not definitive. Indeed, if there was only one water reservoir, its ice wall could have collapsed first to a certain level. Then, after some delay, the remaining part could have collapsed. In any case, the existence of multiple subglacial water reservoirs is quite plausible. It is likely that clarity on this issue could be provided either by direct examination of the glacier or through satellite observation, i.e., if traces of geomorphological changes in solid structures are found in the area of the glacier tongue.

Thus, the spectrum of the glacier's natural mechanical vibrations can be quite rich. Typically, the texture of a glacier consists of numerous surface and subsurface formations, each with characteristic natural sizes. To generate vibrations corresponding to these formations, a mechanical trigger is needed. Such triggers include seismic shocks, rockfalls, and ice blocks breaking off from the glacier. Additionally, mechanical vibrations—and therefore the emission of acoustic waves—can be triggered by the slow movement of the entire glacier and small local shocks that sporadically occur in the ice field, similar to ice floe collisions during ice drift in rivers. These effects can lead to the development of parametric resonance at a certain natural frequency of the glacier, which would amplify the acoustic emission. As a result, the surface density of the ice and its plasticity may change in certain areas. Laboratory modeling has also shown that the periodicity of wave movements related to the glacier's natural vibrations and its structural components can manifest as periodic secondary textures in the form of bulges and nodes characteristic of standing waves. In the case of their formation, structures with changing ice density could negatively affect the stability of the glacier's surface layer, especially at its boundary, i.e., where the glacier contacts solid rock [7].

Formula (1) represents the simplest relationship between the parameters of the wave.

In the frequency spectrum range, the natural oscillation frequencies of the glacier may include frequencies corresponding to oscillations of subglacial water reservoirs. Their linear parameters, as well as the characteristic sizes of the glacier, are present in the simple expression for the phase velocity of acoustic waves:

$$f_0=v/d, \qquad (1)$$

where f_0 - is the fundamental frequency, v - is the speed of sound in the Earth's medium, and d - is the characteristic linear size of the glacier or its structure. Specifically, in the approximation of harmonic oscillations, all subsequent frequencies in the discrete spectrum of the glacier's natural oscillations can be considered harmonics of its fundamental frequency. However, the approximation of harmonic oscillations is an ideal abstraction for a heterogeneous, dispersive solid medium like a glacier. In reality, the complex form of any oscillating body leads to the emergence of overtones caused by frequency splitting in the harmonic series. In the case of a glacier, due to the superposition of multiple frequencies in the vibration spectrum, a noise background should form, accompanying any glacial process. However, through spectral analysis of peak frequencies, it is possible to judge the degree of disruption in the harmonic oscillation series. It is clear that in a heterogeneous solid medium, particles of rock and ice fragments of different sizes may be present. Therefore, chaotic scattering and degeneration of acoustic waves will occur, contributing to the saturation of the noise background accompanying glacier oscillations. A body of arbitrary geometric shape can have several linear scales. Nevertheless, it can be approximated by some symmetric body. For example, a glacier can be most simply represented as a rectangular parallelepiped. The natural (free) mechanical oscillations of a parallelepiped may be axisymmetric, i.e., the frequency spectrum of its oscillations may include two or three fundamental frequencies, depending on the shape of its cross-section. In reality, to determine the frequency spectrum of free oscillations of a body, formula (1) is too simple. In fact, any elastic homogeneous body, regardless of its shape, must have a dominant fundamental frequency of its natural mechanical oscillations. The specific spatial configuration of such a body, assuming small perturbations in its shape, reflects the nature of the spectrum of its natural oscillations. In this regard, the spectrum of spheroidal oscillations is the simplest, the generation of which occurs with small perturbations of the surface of a homogeneous elastic sphere, a body that has a single linear scale, its radius. Clearly, in a very rough approximation, a glacier can only be abstractly approximated as a sphere, for example, based on the condition of equal volumes. Sometimes, such an approximation can be useful for specific analysis. For example, one can use the analytical formula for the discrete spectrum of natural mechanical oscillations f_n of

an elastic spherical body [8]. It was derived using a physical analogy with the natural hydromechanical oscillations of a liquid spherical droplet, which occur due to the effect of surface tension of the droplet [9]. It should be noted that this formula has proven quite effective for modelling the frequency spectrum of natural mechanical oscillations in the elastic zone of moderate-strength earthquake foci. Along with seismic waves, acoustic waves are also generated there, whose frequency spectrum is an extension of the spectrum of lower-frequency acoustic waves:

$$f_n = \frac{V_p}{2\pi R}\left[(n-1)(n+2)n\right]^{1/2},\ n=2,3,4.....,\qquad (2)$$

where v - is the longitudinal seismic wave speed, and R is the radius of the sphere. The fundamental oscillation frequency corresponds to n=2.

In the presence of subglacial water reservoirs, as well as cavities and other heterogeneous formations of various sizes and densities, their natural oscillation frequencies will be present in the general spectrum of the glacier's acoustic radiation. The low-frequency part of this spectrum should be associated with the linear characteristics of the glacier as a unified body. Let us demonstrate this with a specific example and estimate the possible discrepancy in the change of the fundamental frequency of the glacier's natural oscillations using formulas (1) and (2). Suppose we have a parallelepiped with sides $a=2.\ 10^3$ m, $b=2.\ 10^2$ m and $c=10^2$ m. The volume of this parallelepiped is $Q=4.\ 10^7$ m^3. Consequently, the radius of the equivalent sphere with the same volume is $R \approx 2.1\ 10^2$m^3. A typical value for the longitudinal seismic wave speed in the Caucasus region is $V_p \approx 5.\ 10^3$m/sec. Therefore, for each side of the parallelepiped, the frequencies corresponding to formula (1) are: $f_{a0} = 2.5$ Hz, $f_{в0} = 25$ Hz, $f_{c0} = 100$ Hz. For the fundamental frequency of the sphere equivalent to the parallelepiped, from formula (2), we obtain: $f_2 \approx 11$ Hz. Thus, using formula (1), the fundamental frequency of the natural mechanical oscillations of the model glacier varies in the range /2.5−100/ Hz, which starts with infrasonic frequencies. This range also includes the fundamental frequency of the natural oscillations of the virtual equivalent sphere. In the absence of a mechanical trigger, oscillations of the glacier as a unified body are unlikely. Apparently, for this reason, infrasonic frequencies are outside the typical range of the glacier's oscillation frequency spectrum, which was determined through statistical analysis: f=/100—300/ Hz [6]. For this range, using formula (1) with $V_p \approx 5\ 10^3$m/sec, the average statistical range of linear scale variation is d=/17-50/m. If the reservoirs are approximated as spheres, i.e., the linear scale is equated with the radius, the limiting volumes of the virtual equivalent spherical water reservoirs are $Q_1 \approx 500000$ m^3 and $Q_2 \approx 15000$ m^3. In rough approximation, one can consider that the first of these values is in satisfactory quantitative agreement with the presumed water volume in the debris flow that reached the Shovi Gorge. According to unconfirmed estimates, the volume of the debris mass, in which water accounted for approximately ≈20-30 %,: Q≈ 1500000 m^3. Therefore, if the destruction on the Buba glacier began after the rupture of a subglacial water reservoir, the dominant frequency in the spectrum of acoustic waves generated at that time could have been f≈100 Hz.

Glaciers of the Central Caucasus are well studied

The Djankuat glacier has been the object of careful study for several decades. Therefore, it can be considered a reference for the purpose of identifying general patterns in the dynamic processes occurring on other glaciers of the Central Caucasus. Analysis of morphological changes occurring on glaciers is obviously a traditional tool necessary for identifying empirical relationships between glacier parameters and variable external factors. Undoubtedly, numerical models using observation data can provide a diagnostic picture of glacial processes. The long-term goal of such models, based on hydrodynamic equations, is such a qualitative and quantitative interpretation of observation results, which is necessary for real forecasting of catastrophic events associated with glaciers. Obviously, this is preceded by reliable confirmation of cause-and-effect relationships between various physical factors capable of causing a catastrophic result. An example is the numerical model of the ice mudflow that came down from the Kolka glacier and caused a gigantic catastrophe in the Karmadon Gorge and in the Geraldon River Canyon. In particular, this model, like other similar models, can be useful for analyzing the results of the catastrophic event on the Buba glacier. For this purpose, information on the dynamics of the Djankuat glacier, which has been the object of fairly detailed monitoring for a number of years, is also valuable. There is an obvious similarity in the geophysical characteristics of the Buba and Djankuat glaciers, which are in almost identical climatic

conditions. However, field observations have not been carried out on the Buba glacier since the Soviet era. First of all, there are no data on changes in ice thickness that occurred during climate change. At the same time, there is fairly complete information on the Djankuat glacier.

It is assumed that the trigger for the rupture of the subglacial water reservoir on the Buba glacier was a rockfall, There is a possibility that the cause of the destruction on the Buba glacier could be a decrease in the thickness of the ice in the manner noted in the upper part of the Djankuat glacier at altitudes of 3000-3100 m, occurring synchronously with an increase in the area of ice in the nearest area of the glacier bed. As a result of this effect, since this zone is an area of rapid transformation of the pressure field, the local threshold of glacier stability could decrease. A similar effect in sea and lake ice, as well as on rivers, leads to the formation of ice hummocks. Therefore, it cannot be ruled out that a similar phenomenon took place on the Buba glacier. In this regard, the following questions arise: how real is the possibility of the formation and subsequent detachment of a structure similar to an ice hummock from the glacier surface? Was this event impulsive or was it prepared for a certain time? It is impossible not to assume that something similar has already happened many times or will happen in the future on other glaciers, including the Buba Glacier. It seems quite reasonable that the effects of global climate change on glaciers should be especially active in their upper part, where the slope of the relief to the horizon is usually steeper than in the lower sections of the glacier.

Thus, there is a possibility of new destruction on the Buba glacier and a repeated mudflow in the Shovi gorge. Therefore, the most important task is to control the thickness of the Buba glacier, especially in its upper part, which can hardly be done only by satellite observations. For this purpose, the radio sounding method is especially convenient, which highlights the internal structures of the glacier. Accurate data on the thickness of the ice increases the effectiveness of the empirical formula that determines the magnitude of the shear stress in the glacier bed using the difference in height between the top and base of the glacier ΔH [1]

$$\tau = 0{,}005 + 1{,}598\Delta H - 0{,}435\Delta H^2. \quad (3)$$

$$h = \frac{\tau}{\beta\rho g \sin\alpha} c, \quad (4)$$

where h- is the thickness of the ice, β - is the coefficient of the cross-sectional shape of the glacier, ρ - is the density of the ice, g - is the acceleration of gravity, α - is the angle of inclination of the surface to the horizontal plane, c - is the coefficient of quantitative correction.

Obviously, the parameters τ and α are variable and depend on the specific parameters of the glacier. The coefficient β depends on the surface friction at the boundary and in the bed of the glacier, i.e. in the area of contact of the glacier with the enclosing medium. The angle α should be averaged over a segment, the length of which is approximately an order of magnitude greater than the ice thickness. It is believed that in this case, model (4) will be in agreement with the approximation of ideal plasticity, the condition of which is the minimization of shear stress. From formula (3) it follows that for large glaciers (ΔH> 1.6 km), the shear stress is on average $\tau \approx 150$ kPa with ± 30% error. For medium glaciers, such as Djankuat and Buba, $\tau \approx 110$ kPa. Formulas (3) and (4) are quite useful, although there is a significant error in quantitative estimates. In any case, they correspond to the general ideas about quasi-stationary processes of glacier parameter changes over a long period of time, comparable to several decades and centuries. A significant error will obviously affect the results of a comparative analysis between new and retrospective data. Probably, this shortcoming can be corrected within the framework of numerical models, the value of which seems undoubted in the process of transition from diagnosing the state of glaciers to predicting the time and place of destructive phenomena.

Glacial flow in the Shovi gorge

Glacial mudflow should be considered either as a heterogeneous liquid or as a water-containing plastic mass. In both cases, the movement of the medium in a canyon or in an open area is subject to the laws of hydrodynamics. It is known that, depending on its viscosity, a liquid medium can be classified as a Newtonian or so-called rheological liquid (for example, Bingham's liquid). Water is a Newtonian fluid, but the mudflow from the Buba glacier, which is a mixture of water with solid particles and ice fragments, is considered a suspension that belongs to the class of viscoplastic (pseudo plastic) Bingham fluid with a plastic viscosity coefficient of: $\eta \approx /10^9 - 10^{10}/$ Pa s. Such a liquid, unlike water, always has an initial shear stress

τ_0, which is in the functional dependence: $\tau = f(\beta)$ on the strain rate: $\beta = (\frac{\partial \xi}{\partial t})$, where ξ - is the linear strain. This dependence qualitatively changes from nonlinear to linear with an increase in the parameter β. During this process, pseudo plastic viscosity is transformed into dynamic viscosity, i.e. the Bingham fluid acquires the qualities of an ordinary Newtonian fluid. In this case, the following equation is valid for the shear stress:

$$\tau = \tau_0 + \eta\beta \qquad (5)$$

Among the special properties of Bingham fluid that distinguish it from Newtonian fluid, of particular importance is its ability to maintain its spatial structure after flow deceleration on a solid surface. This state continues up to a certain point and can be disrupted by the action of some factor, for example, due to an increase in the angle of inclination of the flow channel to the horizon α. In this case, the force required to shift the viscoplastic mass must exceed the force of surface friction. Such a medium belongs to the class of viscoplastic (pseudoplastic) Bingham fluid with a characteristic coefficient of plastic viscosity: $\eta \approx /10^9$ - 10^{10}/ Pa s.

According to information received from eyewitnesses of the event, as well as as a result of the analysis of numerous television programs, the mudflow in the lower part of the Shovi gorge acquired a viscoplastic character within approximately 20-25 minutes after the collapse on the Buba glacier. Interestingly, in fact, in the same time interval, a picture of the spread of an ice mudflow after the destruction of the Kolka glacier developed. This circumstance allows us to imagine the movement of the mudflow in the Shovi gorge in the image of the movement of the ice-rock mass in its last section in the Genaldon River gorge. According to the principle of hydrodynamic similarity, these two pictures of the mudflow propagation could differ only in the quantitative factor. It is known that in the numerical modeling of the movement of a liquid medium, a standard set of hydrodynamic parameters is used, among which the cornerstone is the coefficient of dynamic viscosity of the liquid. As indicated above, in the case of a viscoplastic suspension, the coefficient of dynamic viscosity is transformed into the coefficient of plastic viscosity. In a normal liquid, its value determines the degree of flow turbulence, i.e. the value of this parameter changes depending on the flow regime. Consequently, until a mudflow with suspended solid particles retains the qualities of a normal liquid, the distribution of the solid fraction along the bed of the liquid will largely depend on its dynamic viscosity. Due to the orographic similarity of the Shovi and Genaldon gorges, despite the huge difference in the volumes of mudflows, the degree of turbulence in both cases can be considered the same. Therefore, in these gorges, one can assume a similarity in the distribution of the solid fraction. This process may also have been influenced by stochastic changes in river beds [10]. Such changes were probably prepared by the active action of a number of geological, geophysical and climatic factors:

- activity of erosion formations in the river beds, in the gorges of which frequent floods are typical;
- increase in solid sediments incomings of rivers, depending on the geological structure of the gorge, geophysical properties of rocks and activity of the liquid component of the mudflow;
- change in turbulent characteristics of the mudflow due to surface and deep erosion of the slopes of the gorge;
- roughness of the river bed and slopes of the gorge, change in its angle of inclination;
- climate change.

Mudflow with variable rheology

The movement of a non-uniform liquid in a gravity field along an inclined channel approximating a river bed is a physical analogue of the propagation of a mudflow along a mountain gorge. The mathematical problem of studying various liquid flows is associated with solving the equations of hydrodynamics. One of the areas is turbulent flows and waves that occur in both ordinary and rheological liquids. The flow of liquid in channels at sufficiently large angles of inclination can become unstable, as a result of which waves of various types can arise in the liquid. An important parameter of the waves is their height, which can be analytically determined, for example, after solving the well-known Burgers equation. However, for a general idea of the process of propagation of waves that arose in the mudflow in the Shovi gorge, one can use only a simplified analysis, without using solutions to specific equations. In particular, after the standard transformation to the dimensionless form of the equation of fluid motion in the channel, two criteria of hydrodynamic similarity appear: the Reynolds number and the Froude number, which are associated with the parameters of the fluid flow and the linear characteristics of the channel [12]. The Reynolds number determines the flow regime, which in case of very strong flow will necessarily be turbulent. In this case, in a normal fluid, depending on the value of the Froude number, various waves can be generated. In a viscous-

plastic medium with Bingham rheology, wave motions can be less diverse than in a normal fluid. For example, in a mixing heterogeneous fluid, waves arise due to the development of instability due to a velocity shift in layers with different densities. Also, due to the restructuring of the flow structure, heterogeneous layers with large gradients of velocity and density arise in the rheological fluid. The appearance of such a texture in a liquid flow makes it possible to simplify the problem of mathematical modeling of waves by introducing a small parameter. It is the ratio of the channel depth to the wavelength and is the criterion for the approximation of the so-called shallow water. Although this model significantly simplifies the hydrodynamic equations, complications associated with the nonlinearity of the waves may arise for a rheological fluid. Therefore, such waves in a viscous-plastic fluid are not discussed below.

By means of retrospective analysis it is possible not only qualitatively, but also, to a certain extent, quantitatively to present a hydrodynamic picture of the propagation of a glacial mudflow along the gorges of the Bubiskali and Dzhandzhakhi rivers, which together form the Shovi gorge. For example, based on the tracks in the river beds it is possible to analyze the rheological properties of the water-saturated soil mass, which forms the basis of the mudflow, which allows estimating the probability of generating various types of hydrodynamic waves. This goal can also be achieved by estimating the ranges of dimensionless hydrodynamic numbers in different sections of river beds during the movement of the mudflow mass, which allows applying the principle of hydrodynamic similarity. In particular, in the case of approximating the mudflow bed with a rectangular channel, it is possible to use the results of those analytical solutions based on simplifying assumptions of the shallow water equations. They are valid within certain intervals of change in the Reynolds and Froude similarity numbers. For example, for large Reynolds numbers, when the fluid is highly turbulent, the Froude parameter quite simply characterizes the process of changing the flow regime due to the generation of hydrodynamic waves, the specifics of which are associated with negative effects that often arise as a result of the propagation of wave disturbances. For example, during the propagation of the mudflow in the Shovi gorge, so-called rolling hydrodynamic waves could be generated, which could well have been one of the reasons that determined the catastrophic scale of the glacial mudflow.

In the one-dimensional approximation, at sufficiently large Reynolds numbers, the unsteady shallow water equations, with turbulent fluid friction at the bottom of an inclined channel, have the form [12,13]

$$\frac{\partial}{\partial t} h + \frac{\partial}{\partial x}(hu) = 0, \qquad (6)$$

$$\frac{\partial}{\partial t}(hu) + \frac{\partial}{\partial \times}\left(hu^2 + \frac{gh^2}{2}\cos\varphi\right) = gh\sin\varphi - C_w\ u^2, \qquad (7)$$

where h, u - are the average depth and velocity of the fluid; g - is the acceleration of gravity; φ - is the angle of inclination of the channel; C_w - is the friction coefficient, which is assumed to be constant for simplicity. The first equation (1) denotes the continuity of the medium, (2) determines the movement of the fluid in an inclined channel.

After the standard transition to dimensionless variables and parameters, the form of the continuity equation (6) does not change, but equation (7) takes the form

$$\frac{\partial}{\partial t}(hu) + \frac{\partial}{\partial \times}\left(hu^2 + \frac{h^2}{2}\right) = \alpha h - u^2, \qquad (8)$$

where $\alpha = tg\varphi/C_w$ - is the only dimensionless parameter that determines the flow. If there is a uniform fluid flow in a channel with a normal depth h_0, then the Froude number of such a flow will be determined by the parameter α, related to the Froude number: $Fr = \sqrt{\alpha}$. In the shallow water approximation, the Froude number allows us to classify hydrodynamic waves that can be generated at sufficiently large Reynolds numbers, when the flow is highly turbulent. In particular, in the case of approximating the channel of a mudflow with a rectangular channel, we can use the results of known analytical and numerical solutions obtained for some types of hydrodynamic waves.

Let us estimate the characteristic intervals of change of the hydrodynamic similarity numbers. Reynolds number $Re = \frac{u_0\, d}{\eta}$, where u_0 is the characteristic velocity value, d is the channel width, η is the kinematic viscosity coefficient. Froude number $Fr = \frac{u_0}{\sqrt{gh_0 \cos\varphi}}$, where h_0 is the normal (characteristic) channel depth. It has been proven that the flow in the channel becomes unstable when *Fr>2 (α>4)*. For example, the characteristic velocity of the mudflow and the parameters of the Shovi gorge: u_0= */10-20/m/sec,* d= /40-60/m,

h_0 =/8-10/m, $\alpha=5^0$. For water containing solid particles, $\eta\approx$/1-10/$10^{-6}m^2$/sec. Therefore, we will have the following characteristic intervals of change of the indicated dimensionless parameters of hydrodynamic similarity: Re≈/4-12/ 10^7 and Fr≈/1-2.2/. The large value of the Reynolds number means that the degree of flow turbulence in the main part of the Shovi gorge was critically high. Such an effect could probably be noticeable in the last, widest section of the gorge, where the viscoplastic nature of the mudflow could be fully revealed. In this place, the movement of the mudflow mass had a complete similarity with the movement of a viscoplastic medium with a small (≈20%) water content. In this regard, the question of the nature of wave motions, the spectrum of which can be presented based on the results of some solutions of shallow water equations, as well as on the data of laboratory experiments, seems interesting [12].

Thus, in the shallow water approximation, the value of the Froude parameter allows us to classify the waves whose generation is most probable in the case of sufficiently large Reynolds numbers. This means that the degree of flow turbulence in the main part of the gorge was critically high. It is also likely that the value of the Froude number in some places of the gorge could go beyond the characteristic interval. For example, due to local changes in the depth of the flow or a decrease in its speed. Therefore, the question of the nature of those wave motions, the spectrum of which can be represented by the results of solving the shallow water equations and data from laboratory experiments, is of particular interest [12]. In this case, the Froude number is a determining parameter that can serve as a quantitative criterion distinguishing between different types of long hydrodynamic waves whose generation is possible in the shallow water approximation [13,14]. Thus, the probability of generating waves of different types depends on the value of the Froude number:

1) $0.3\leq Fr\leq 0.5$. Such an interval of the Froude number for the case of a mudflow in the Shovi gorge is unlikely. It is more typical for a channel of finite depth, along the bottom of which a liquid with a higher density flows than in the surface layer. It is known that with such a flow structure in an inhomogeneous liquid, so-called gravity (density) waves can be generated;

2) $0.9<Fr<1.1$. According to the Kadomtsev-Petviashvili equation, for such Froude numbers, with a balance of the influence of linear dispersion, nonlinearity and spatial effects, the generation of solitons (solitary waves) is possible. The probability of such a balance, as well as the conditions necessary for the generation of gravity waves, is quite low. Nevertheless, despite the rigidity of the mathematical criteria, the probability of soliton propagation in the Shovi gorge cannot be completely excluded;

3) $Fr\leq 2$. In this case, according to the shallow water equations, as a result of the effect of turbulent friction on the channel bottom, so-called linear rolling waves can be generated. For these waves, the critical value is Fr=2, which determines the threshold for the development of linear instability and a noticeable increase in amplitude;

4) $Fr>2$. At a sufficiently large Re, a nonlinear stage of increasing flow instability develops. This case corresponds to a certain critical channel depth, in which a picture of a turbulent flow arises. So-called depression waves appear in the liquid, as well as rolling waves with hydraulic jumps, which facilitate a change in the flow regime from subcritical to supercritical. A feature of such wave solutions is the presence of a smooth section of the wave trajectory, indicating the transition from subcritical to supercritical flow [12] (sections 2, 1 in Fig. 3,a,b).

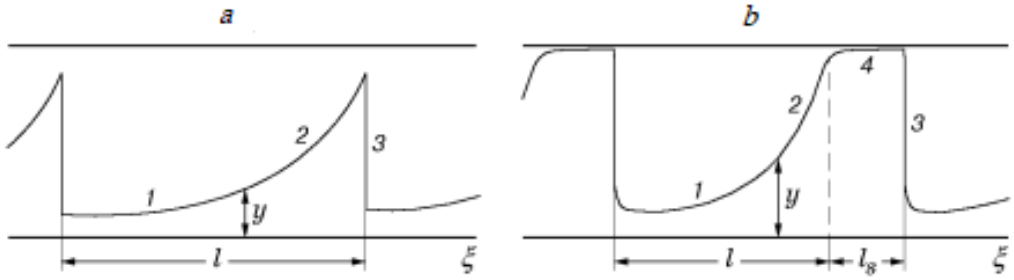

Fig. 3. Rolling waves (V.Yu., Lyapidevsky, V.M. Teshukov. Mathematical models of the propagation of long waves in an inhomogeneous liquid. Novosibirsk, Publishing House SB RAS, 2000, 420 p (in Russian).

5) $2<Fr<6$. In a turbulent flow, the effect of modulation of running packets of nonlinear rolling waves, averaged within certain spatial and temporal scales, may occur. Such a specific wave effect in the Shovi Gorge could occur in places where there was a sharp increase in the local Froude number.

As an example of what can happen to a wave packet with an increase in the Froude number, we can use the result of numerical modeling when Fr=5. Fig. 4 corresponds to the theoretical picture of the evolution of a

packet of modulated rolling waves. They were generated in a flow of inhomogeneous fluid as a result of a nonlinear increase in small disturbances, the initial amplitude of which was ≈1% of the normal channel depth h_0 [12]. The maximum amplitudes that were recorded in the corresponding laboratory experiment turned out to be significantly less than the theoretical ones. Nevertheless, the qualitative nature of the growth of the amplitude of the wave packet, which initially had an exponential nature, was confirmed. However, after the traveling wave has passed a certain distance, the amplitude stops growing. It turned out that for a developed turbulent flow, the average values of the minimum depths satisfy the inequality: $\frac{xC_w}{h_0} \leq 10$, where C_w, is the friction coefficient. It is believed that small disturbances grow exponentially along the channel until the wave reaches the boundary of the hyperbolicity region of the shallow water equation system, after which the wave amplitude stops growing and the flow becomes quasi-periodic. The bold lines show the distribution of the average values of the maximum and minimum wave depths along the channel over many periods. Note that the average values of the minimum wave depth in a developed flow, determined in a laboratory experiment and as a result of non-stationary numerical calculations, agree well. At the same time, the corresponding experimental values of the maximum amplitude turned out to be significantly less than the analytically determined theoretical amplitudes.

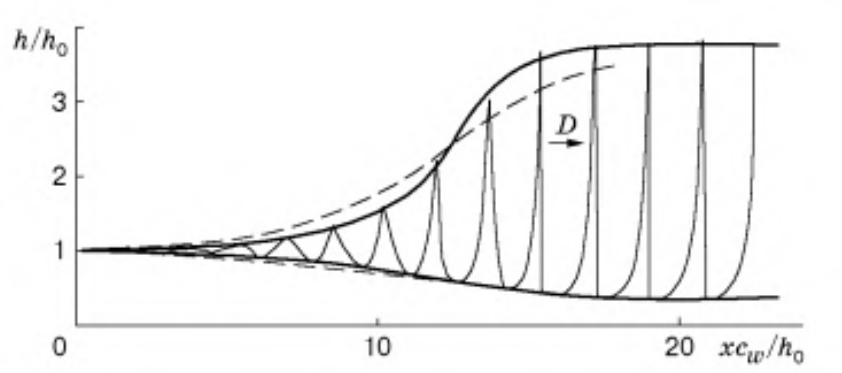

Fig. 4. results of numerical calculations on the evolution of a rolling wave packet (V.Yu., Lyapidevsky, V.M. Teshukov. Mathematical models of the propagation of long waves in an inhomogeneous liquid. Novosibirsk, Publishing House SB RAS, 2000, 420 p (in Russian))

Georgia, Shovi Disaster, Event Analysis. Report №14230941, Zolikofen, November 28, 2023, 42 p.

It was noted above that the reports [15,16] use an almost identical structure, with the exception that the report of the Georgian Nature Agency devotes a lot of space to the general geology and hydrology of the Caucasus Range, which is hardly not directly related to the disaster in the Shovi Gorge. In these reports, the Swiss RAMSS simulation program is used to model the hydrodynamic parameters of the glacial mudflow. Therefore, we consider it sufficient to cite some data and conclusions from [15], which are actually repeated in [16]. It can only be briefly noted that these initial data, as well as the results of modeling the parameters of ice mudflow movement, are to some extent universal, since they also characterize other glaciers and viscous-plastic mudflows. It can be considered that the obvious similarity of the hydrodynamic picture in such cases is the result of the actual identity of the computer programs, which are based on the equations of hydrodynamics and the input initial conditions and boundary conditions, which is obviously a consequence of the general similarity of the orography of mountain canyons and their physical parameters in the Caucasus and in other mountain systems.

Thus, we consider it convenient to present those extracts from [15] that seem especially important:

Estimation of the event volume from August 2023. *"Debris Source Volume, estimation [m^3] Rockfall (release area) ca. 10^6 m^3 Upper channel (periglacial area) ca. (0.5 – 1) 10^6 m^3 ; Middle flat part (above tree line) ca. (0.1 - 0.2) 10^6 m^3 ; Middle and lower channel (below tree line) ca. (0.5 – 0.8) 10^6 m^3 . Total (2 – 3) 10^6 m^3 ."*

Input parameters for RAMMS simulation (August 2023 event). *"The volume that reached the valley is an important input parameter for the debris flow simulation. The parameters for the simulation of the debris flow due to the slope failure on 3rd August 2023 are described in Table 2: Table 2: Applied simulation parameters RAMMS for the reconstruction of the August 2023 event. Dry friction coefficient (Mu) μ [-] 0.05* ***Turbulent friction coefficient (Xi) ξ [m/s^2] 1000; Volume [m^3] (1.5 - 2.5) 10^6 . Density: 1,8 10^3 kg/m^3 ."***

The estimated volume that reached the valley is about 2 Mio. m^3 - max. 3 Mio. m^3 *, which corresponds to the volume estimation of NEA. *".The trigger of the event can only be assumed – there are many uncertainties. But, we assume that the rock mass was "ready to fail" due to the severe weakening of the previous years. With the high temperatures in summer and the maximum melting rate of fissure ice (permafrost), the fissures and cavities in the rock were probably filled with water at this time. It is conceivable that the precipitation on the days before August 3rd, 2023 could have produced a brief overpressure of water in the right place in the rock, causing the rock mass to collapse".*

**** According to our (Z. Kereselidze, N. Varamashvili) assessments, the maximum volume that reached valley is overestimated by about ≈ 50%.***

Causality of the Process. *"The causality lies in the interplay of the geological disposition (large-scale tectonic structures, fracturing, strong loosening), the local geomorphology (steep glacier and glacier fore field with large debris deposits), the long-lasting, recurring high summer temperatures (climate change with ever higher zero-degree limit in summer and associated strong degradation of permafrost and glacier melt) and the weather on the day of the event (local and strong precipitation intensity). In the following sections, the individual influencing factors are explained, and their interplay explored".*

We therefore strongly recommend carrying out a disposition analysis to localize the hotspots for such processes*. "Existing methods (e.g. Swiss methodology) can be used for this purpose. For such an analysis, the evaluation of satellite data is a must. Only with satellite data localities with active movements can be evaluated over large areas in an efficient way. Combined with the disposition analysis, the hotspots in the Georgian Caucasus can be evaluated*. Such an analysis should definitely be carried out in a multi-stage process. Then, not all localities with a high risk of collapse are critical for the settlement area. Only with a multi-stage process the areas that are really critical for the settlements can be determined. It has to be discussed to test the methodology and adapted to Georgian circumstances in a small test area with high damage potential".*

Conclusion

The analysis of the causes of the collapse of the Buba glacier on 3/9/2023 is an ambiguous task. The tragic event that took place in the Shovi gorge was prepared by a number of natural phenomena, probably associated with global climate change. Characteristic signs of this process were noted on the Djankuat glacier, a supporting glacier for the Central Caucasus, which has a certain similarity with the Buba glacier. Therefore, it can be assumed that the dynamic changes on these two glaciers occurred, to some extent, according to a similar pattern. This assumption allows us to use information on the change in ice thickness in the upper part of the Djankuat glacier for extrapolation to the Buba glacier. It cannot be ruled out that this phenomenon caused the formation of ice hummocks on the surface of the glacier, the shift of which was facilitated by the intensive melting process. Along with a possible rockfall, the collapse of ice hummocks in the glacier bed could have triggered the destruction of the intraglacial water reservoir, after which a mudflow spread in the river beds flowing in the Shovi Gorge. The available information about the collapse on the Buba Glacier and monitoring of the changes that occurred in the Shovi Gorge require filling with new data from ground and space observations; In particular, we consider it necessary to check whether the rockfall process was a one-off event or consisted of separate, spaced out in time events. A ground expedition to the Buba Glacier can clarify this.

During the propagation of the mudflow in the gorges of the Bubiskali and Chanchakhi rivers, which make up the Shovi gorge, hydrodynamic waves of various types could have existed. In particular, for the characteristic range of the Froude hydrodynamic similarity number, the most probable is the generation of running rolling waves, the height of which could reach several meters. The appearance of solitary waves (solitons), as well as the so-called gravity waves, was unlikely, but one cannot exclude the possibility of their generation in those places where local conditions were suitable. In the lower, widest section of the Shovi gorge, in the zone of the so-called cottages, the movement of the mudflow mass was similar to the movement of the ice mudflow in the Genaldon River gorge that came down after the collapse of the Kolka glacier in 2002. Despite the huge difference in the initial volumes of glacial mudflows that came down from the Buba and Kolka glaciers, the thickness of viscoplastic deposits in the last flat areas of their distribution turned out to be comparable, taking into account the difference in covered areas. Obviously, this is due to the same nature of the braking of the viscous-plastic mudflow at the stage of its final stop, which is also indicated by a decrease in wave amplitudes within /1-3/ m.

References

[1] Lavrentiev I.I., Kutuzov S.S., Petrakov D.A., Popov G.A. Thickness, subglacial relief and ice volume of the Djankuat glacier. Ice and Snow, No. 4, 2014, pp. 26–342 (in Russian)

[2] Kotlyako V.M., Rototaeva O.V., Nosenko G.V. The September 2002 Kolka Glacier Catastrophe in North Ossetia, Russian Federation: Evidence and Analysis. Mountain Research and Development, т. 24, вып. 1, 2004/02, с. 78–83. ISSN 1994-7151 0276-4741, 1994-7151. doi:10.1659/0276.4741(2004)024[0078:TSKGCI]2.0.CO;2.

[3] Surkov V. V., Pilipenko A. Estimate of ULF electromagnetic noise caused by a fluid flow during seismic or volcano activity. Annals of Geophysics, vol. 58, No. 6, 2015. S0655, doi:10.4401/ag-6767.

[4] Epifanov V.P., Glazovsky A.F., Osokin N.I. Physical modeling of the glacier contact with the bed. Ice and Snow, No. 1 (121), 2013, pp. 43–52 (in Russian)

[5] Yepifanov V.P. Fizicheskoye modelirovaniye rezhimov dvizheniya lednikov. Lod i Sneg, t. 56, № 3, 216, s. 333-34, .doi:10.15356/2076-6734-2016-3-333-344.

[6] Roux P.-F., Marsan D., Metaxian J.-P., O'Brien G., Moreau L. Microseismic activity within a serac zone in an alpine glacier (Glacier d'Argentiere, Mont Blanc, France). Journ. of Glaciology, V. 54. № 184, 2008, p. 157–168.

[7] Epifanov V.P., Sazonov K.E. Wave structures in an ice field and their influence on the strength of salt ice. Ice and Snow, v. 60, no. 4, 2020, pp.624-636, doi: 10.31857/S2076673420040066 (in Russian).

[8] Kereselidze Z., Gegechkori T., Tsereteli N., Kirtskhalia V. Modeling of Elastic Waves Generatedby a Point Explosion. Georgian International Journal of Science and Technology, v. 2, Iss. 2, 2010, p. 155-166, NovaPublishers, https://www.novapublishers.com/catalog/product_info.php?products_id=14264 (in Russian)

[9] Landau L.D., Lifshits E.I. Continuum Mechanics. Moscow, Publishing House of Technical Literature, 1954, 795 p. (in Russian)

[10] Petrakov D.A., Drobyshev D.N., Aleinikov A.A., Aristov K.A., Tutubalina O.V., Chernomorets S.S. Changes in the zone of the Genaldon glacial catastrophe in the period 2002-2010. Earth's Cryosphere, v.17, no.1, 20013, pp.35-46 (in Russian)

[11] Popovin V.V., Petrakov D.A., Tutubalina O.V., Chernomorets S.S. Glacial catastrophe of 2002 in North Ossetia. Earth's Cryosphere, v.7, no.1, 2003, pp. 3-17 (in Russian)

[12] Lyapidevsky V.Yu., Teshukov V.M. Mathematical models of long wave propagation in an inhomogeneous liquid. Novosibirsk, SB RAS Press, 2000, 420 p (in Russian)

[13] Kereselidze Z. A. Varamashvili N. D. Regarding the Spontaneous Mechanism of Atmospheric Whirlwind Generation in Narrow Mountain Canyons. Journal of the Georgian Geophysical Society, e-ISSN: 2667-9973, ISSN: 1512-1127, Physics of Solid Earth, Atmosphere, Ocean and Space Plasma, v. 26(2), 2023, pp. 13 – 21.

[14] Melnikova O. N., Dynamics of channel flow, Moscow: Max Press, Physics Department of Moscow State University, 2006, p. 136 (in Russian)

[15] Georgia, Shovi Disaster, Event Analysis. Report №14230941, Zolikofen, November 28, 2023, 42

[16] Report on the assessment of natural disasters in the Bubistskali River Gorge on August 3, 2023. LEPL National Environmental Agency. Tbilisi 2024, 69 p (in Georgian)

[17] Poznanin V.L., Gevorkyan S.G. The impact mechanism of the preparation of the Kolka glacier to the mudflow accident: the physical processes during the large landslides. Earth's Cryosphere, Vol. XI, No. 2, 2007, pp. 84–91, (in Russian)

ბუბას მყინვარზე ნგრევის გამო შოვის ხეობაში ღვარცოფის ნაკადის გავრცელების დინამიკის მოდელირების საკითხი

ზ. კერესელიძე, ნ. ვარამაშვილი

რეზიუმე

მყინვარები ყოველთვის პოტენციურ საფრთხეს წარმოადგენდნენ კავკასიის რეგიონში, სადაც მთის კანიონები საკმაოდ მჭიდროდ არის დასახლებული. გლობალურ კლიმატის

ცვლილებასთან დაკავშირებულმა პროცესებმა, რომლებიც ყველგან ხდება, უკიდურესად გაამწვავა მყინვარული კატასტროფებისგან მოსახლეობის პრევენციის პრობლემა. მაგალითად, არსებობს სამწუხარო გამოცდილება, რომელიც დაკავშირებულია კოლკას მყინვარის ნგრევასთან, რამაც გამოიწვია გიგანტური გლაციალური ღვარცოფი 2002 წელს. ასეთი კატასტროფის კატეგორიაში უნდა შედიოდეს გლაციალური ღვარცოფის გენერირება ბუბას მყინვარიდან 9/3/2023, რამაც გამოიწვია ტრაგედია უამრავი მსხვერპლით კურორტ შოვში. ასეთი კატასტროფული მოვლენების განვითარების შესაძლო ადგილისა და დროის განსაზღვრას (მიწისძვრები, ვულკანური ამოფრქვევები, ფართომასშტაბიანი წყალდიდობები) აქვს საიმედოობის ძალიან დაბალი ხარისხი და პრობლემატურია, მიუხედავად სახმელეთო და კოსმოსური მონიტორინგის სამეცნიერო მეთოდების თანამედროვე დონისა. კერძოდ, აშკარაა საჭიროება კავკასიის მყინვარების ამჟამინდელი მდგომარეობის გრძელვადიანი მონიტორინგისა და ყოვლისმომცველი დიაგნოსტიკის, ყოველი ახალი გამოცდილების გათვალისწინებით. უნდა აღინიშნოს ინფორმაციის სიმცირე, რომელიც საშუალებას არ გვაძლევს ვიმსჯელოთ ბოლო ათწლეულების განმავლობაში ბუბას მყინვარზე მიმდინარე პროცესებზე. ამიტომ, ნაკლებად სავარაუდოა, რომ ვინმეს წარმოედგინა მდინარეების ბუბისწყლისა და ჯაანჯახის ხევებზე მყინვარული ღვარცოფის გავრცელების ფართომასშტაბიანი ვირტუალური სურათი, ადექვატური იმისა, რაც სინამდვილეში აღმოჩნდა. ამავდროულად, თუ არსებობს დაკვირვების შედეგების საკმარისად სრული მონაცემთა ბაზა და მისი სწორი ანალიზი, ჰიდროდინამიკური მსგავსების პრინციპზე დაფუძნებული, შესაძლებელია, მაგალითად, მთის ნებისმიერ ხეობაში წყალდიდობის ან მყინვარული ნაკადის სავარაუდო პარამეტრების მოდელირება. კავკასიის რეგიონის შემთხვევაში, შეგიძლიათ გამოიყენოთ ზოგიერთი შედეგი, მიღებული ჯანკუათის და კოლკას მყინვარების რიცხვითი მოდელირების გამოყენებით. კერძოდ, ეს მოდელები საკმაოდ გამოსადეგია არა მხოლოდ სავარაუდო მიზეზების დასადგენად, არამედ ბუბას მყინვარზე ნგრევის შედეგების რეტროსპექტულ ანალიზისათვის. პირველ რიგში. ეს ეხება ჰეტეროგენულ ღვარცოფში ჰიდროდინამიკური ტალღების გავრცელების პროცესს. ამ მიზნით ასევე მნიშვნელოვანია სეისმური ხელსაწყოების ჩანაწერები, რომლებიც შეიცავს ინფორმაციას ბუბას მყინვარზე ნგრევის პროცესის შედეგად წარმოქმნილი აკუსტიკური ტალღების სიხშირის სპექტრის შესახებ. ბუბისწყლისა და ჭანჭახის ხეობებში შეიძლება არსებობდეს სხვადასხვა ტიპის ჰიდროდინამიკური ტალღები. ფრუდის მსგავსების რიცხვის მნიშვნელობების დამახასიათებელ დიაპაზონში ყველაზე სავარაუდო უნდა ჩაითვალოს მორბენალი მგორავი ტალღების წარმოქმნა, რომელთა სიმაღლემ შეიძლება მიაღწიოს რამდენიმე მეტრს. მარტოხელა ტალღების (სოლიტონების) გამოჩენა, ასევე ე.წ. გრავიტაციული ტალღები ნაკლებად სავარაუდო იყო, თუმცა მათი წარმოშობის შესაძლებლობა იმ ადგილებში, სადაც ადგილობრივი პირობები იყო შესაფერისი, არ არის გამორიცხული. შოვის ხეობის ქვედა, ყველაზე ფართო მონაკვეთში, ე.წ. კოტეჯების ზონაში, ღვარცოფის მასის მოძრაობა მსგავსი იყო 2002 წელს მდინარე გენალდონის ხეობაში კოლკას მყინვარზე ჩამონგრევის შედეგად აღძრული მყინვარული ღვარცოფის მოძრაობისა. მიუხედავად დიდი განსხვავებისა ბუბას და კოლკას მყინვარებიდან ჩამოსული ღვარცოფების საწყის მოცულობებში, ბლანტპლასტიკური მასის გამონატანი, ტალღების სივრცითი მასშტაბისა და ამპლიტუდის გათვალისწინებით, მისი განაწილების ბოლო უბნებში შედარებითი აღმოჩნდა და ორივე შემთხვევაში 1-3 მეტრის სიმაღლემდე შემცირდა.

საკვანძო სიტყვები: ბუნებრივი კატასტროფები, მყინვარი, ღვარცოფი, აკუსტიკური ტალღები, ვისკოპლასტიკური.

К вопросу моделирования динамичекой картины распространения селевого потока в ущелье Шови вследствие обрушения на леднике Буба

З. Кереселидзе, Н. Варамашвили

Резюме

Ледники всегда представляли потенциальную опасность в регионе Кавказа, где горные каньоны являются достаточно густо населенными. Процессы, связанные с глобальными климатическими изменениями, происходящими повсеместно, крайне обострили проблему превенций населения от гляциальных катастроф. Например, имеется печальный опыт, связанный с обрушением ледника Колка, ставшего причиной возникновения гигантской по объему ледовой сели в 2002 году. К разряду подобной катастрофы следует отнести сход гляциальной сели с ледника Буба 9/3/2023 г, в результате которого произошла трагедия с многочисленными жертвами на курорте Шови. Определение возможного места и времени развития подобных катастрофических событии (землетрясения, извержения вулканов, масштабные наводнения) имеет весьма низкую степень достоверности и является проблемным, несмотря на современный уровень научных методов наземного и космического мониторинга. В частности, является очевидной необходимость долгосрочного мониторинга и всестороннего диагностирования текущего состояния ледников Кавказа, с учетом каждого нового опыта. Следует отметить скудность информаций, позволяющий судить о процессах, протекавших на леднике Буба за последние десятилетия. Поэтому, вряд ли кто мог представить масштабную виртуальную картину распространения гляциальной сели по ушельям рек Бубисцкали и Джанджахи, адекватную той, какой она оказалась в реальности. В то же время, в случае наличия достаточно полной базы результатов наблюдений и ее корректного анализа, на основе принципа гидродинамического подобия, существует возможность теоретического моделирования вероятных параметров наводнения или гляциальной сели в любом горном ущелье. Например, в случае Кавказского региона можно воспользоваться некоторыми результатами, полученными при помощи численного моделирования ледников Джанкуат и Колка. В частности, эти модели являются достаточно полезными не только определения вероятных причин, а также ретроспективного анализа, последствий разрушения на леднике Буба. В первую очередь. Это касается процесса распространения гидродинамических волн в неоднородном селевом потоке. Для этой цели также важными являются записи сейсмической аппаратуры, которые содержат информацию о спектре частот акустических волн, генерированных процессом разрушения на леднике Буба. В ущельях рек Бубисцкали и Чанчахи могли существовать гидродинамические волны различного типа. В характерном диапазоне величин числа подобия Фруда наиболее вероятными следует считать генерацию бегущих катящихся волн, высота которых могла достигать нескольких метров. Появление уединенных волн (солитонов), а также т.н. гравитационных волн, было маловероятным, однако нельзя исключить возможность их генерации в тех местах, для которых локальные условия были подходящими. На нижнем, наиболее широком участке ущелья Шови, в зоне т.н. коттеджей, движение селевой массы было подобным движению ледового селя в ущелье реки Геналдон после обрушения на леднике Колка в 2002 г. Несмотря на огромную разницу первоначальных объемов селей, сошедших с ледников Буба и Колки, выносы вязкопластической массы, на последних участках ее распространения, оказались соизмеримы с учетом пространственных масштабов и амплитуды волн в обоих случаях уменьшилась до высот 1-3 метра.

Ключевые слова: природные катастрофы, ледник, селевые потоки, акустические волны, вязкопластика.

Journal of the Georgian Geophysical Society, e-ISSN: 2667-9973, p-ISSN: 1512-1127
Physics of Solid Earth, Atmosphere, Ocean and Space Plasma, v. 27(2), 2024, pp. 63 - 73

Conical Model of Non-Uniform Rotation and Interaction of Elements of the Atmospheric Rotation Chain in a Linear Approximation

[1]Zurab A. Kereselidze, [1]Avtandil G. Amiranashvili, [1]Victor A. Chikhladze, [1]Marina S. Chkhitunidze, [2] George J. Lominadze, [2] Eleonora B. Tchania

[1]M. Nodia Institute of Geophysics of I. Javakhishvili Tbilisi State University, Georgia
[2]Vakhushti Bagrationi Institute of Geography of I. Javakhishvili Tbilisi State University, Georgia,
[1]e-mail: z_kereselidze@yahoo.com; marina_chxitunidze@yahoo.com

ABSTRACT

The global atmosphere can be considered as an open thermodynamic system within which various disturbing factors act. For example, even in calm atmospheric conditions, orography can cause a violation of the stationary thermal balance between the Earth and the atmosphere. In general, the formation of vortex structures in any gaseous or liquid medium is stochastically determined. This means that the process of vortex formation is to a certain extent probabilistic. Therefore, in mathematical modeling of the field of atmospheric gyres, it is rational to exclude random factors by identifying specific contributing conditions. For example, a strong division of the earth's relief contributes to turbulence of air flows on a regional and local scale. In particular, the process of formation of low-intensity atmospheric vortices in mountain valleys can always be considered as a violation of local stability, the cause of which is the unevenness of the temperature field created at the boundary of different orography and landscapes. Also, the generation of vortices and the process of their dissipation in the atmosphere can always be considered as a violation of the stability of the environment on certain spatial scales, which is expressed in the violation of its thermodynamic parameters.

Keywords: *atmospheric vortices, thermodynamic parameters, relief, mathematical modeling.*

The class of atmospheric vortices with spatial scales that differ sharply from weak atmospheric vortices includes two phenomena of seemingly similar thermodynamic nature: vortices and tornadoes. A vortex is an atmospheric process caused locally by air currents rising from the extremely hot surface of the Earth, the intensity of whose circulation increases sharply from the periphery of the vortex to its center. The speed of its rotational motion is quite high, in some cases destructive, reaching several tens of meters per second. Traces of dust particles carried away by the vortex from the surface of the Earth show that the movement of the mass inside it is upward and has the character of a large-scale screw rotation. Such a process usually retains a regular form and is more or less amenable to mathematical modeling, unlike another type of atmospheric phenomena called a tornado. The origin of this gigantic atmospheric phenomenon in scale, unlike an ordinary vortex, occurs in the so-called "Mother" in the cloud, from where the tornado body descends to the ground in the form of a long "tornado". Inside a tornado, the air rotates at a particularly high speed, which can be even an order of magnitude higher than the linear rotation speed characteristic of a normal vortex. A tornado has a so-called "Eye", a stagnation zone, i.e. a zone of immobility (rest) of the air mass. Unlike a tornado, the "parent" cloud is the source of a small storm, which has a spiral structure in space, directed from the cloud towards the Earth. From an energy point of view, a vortex can be explained as the result of a local disturbance of the thermodynamic system of the atmosphere. In this sense, a tornado is incomparably more powerful and larger than a vortex. In this case, we are dealing not with a local disturbance of the atmosphere, but with the formation of a large-scale open thermodynamic system. Perhaps this is why there is no systematic theory of a tornado as a catastrophic natural phenomenon. For example, it is possible to explain why a group of vortices of much smaller scales will be observed in the vicinity of the "eye" of a tornado. A qualitative

explanation of this phenomenon is probably possible through laboratory modeling if the phase portrait method is also used to interpret the experimental data.

Modeling atmospheric vorticity in a kinematic approximation. It is known that in the atmosphere, which is a dissipative medium, the dynamics of vortices is described by the Navier-Stokes equation, the exact solution of which is usually associated with special difficulties [1]. In cases where the coefficient of air viscosity can be neglected, it is permissible to use the Euler equation, which is simpler than the Navier-Stokes equation, valid for an ideal medium. However, in some cases, due to mathematical complexities, an exact analytical solution to the Euler equation is also impossible. For example, mathematical modeling of the interaction of vortices of different sizes, due to the nonlinear nature of this process, is possible only with the use of certain simplifying assumptions. In particular, in an ideal gas medium, this problem can be reduced to such a simplified scheme of vortex interaction that it gives a qualitative picture of the time development of the dissipation process in the atmosphere in a linear approximation. This goal can be achieved using any kinematic model of a vortex. Such a model, at a minimum, must satisfy the continuity equation of the medium, which is one of the conditions for the dynamic possibility of motion. There are various kinematic models, including a non-uniform rotating flat stationary model, which was used in the problem of the magnetohydrodynamic effect of rotation of the ionospheric medium in the Earth's polar cusp [2]. Using this model, a solenoidal solution was obtained, which, in addition to the continuity equation, also satisfies the Euler equation.

Inhomogeneous rotation, in addition to the curvilinear movement of liquid or gaseous medium, also implies the possibility of developing certain types of hydrodynamic instability. This factor is a particularly important point in terms of the problem of the generation of atmospheric whirlwinds and their dissipation. Therefore, we believe that the flat model mentioned above will be useful, especially since there is a possibility of its correct transformation into a spatial model, taking into account the effect of the compressibility of the environment. However, in order to satisfy the dynamic criterion of the possibility of movement, it is necessary to introduce additional simplifying restrictions, which, in our opinion, cannot have a qualitative impact on the content of the transformed model. According to the first constraint, the density of the atmospheric medium is only a function of time. The second limitation concerns the vertical component of the spatial atmospheric vorticity velocity, which, according to the assumption, depends only on the coordinate of the corresponding direction. Taking into account these additional conditions, the equation of continuity in cylindrical coordinates will have the form

$$\frac{\partial \rho}{\partial t} + \rho\left(\frac{1}{r}\frac{\partial (rV_r)}{\partial r} + \frac{1}{r}\frac{\partial V_\varphi}{\partial \varphi} + \frac{\partial V_z}{\partial z}\right) = 0\ , \qquad (1)$$

where ρ- the density, V_r , V_φ , V_z - velocity components.

Thus, the spatial transformation of a plane kinematic model of inhomogeneous rotation has the form

$$V_r = \frac{1}{2}u_0\left(\frac{r}{R_0}\right)(cos\varphi + sin\varphi), \quad V_\varphi = u_0\left(\frac{r}{R_0}\right)(cos\varphi - sin\varphi),$$

$$V_z = u_0\left(\frac{z}{h_0}\right), \quad \rho = \rho_0 e^{-\frac{u_0}{h0}t} \quad , \qquad (2)$$

where u_0 - is the characteristic linear velocity of the vortex, R_0 - is the characteristic radius of the vortex, h_0 - is the characteristic height of the vortex. z- momentary direction of rotation axis.

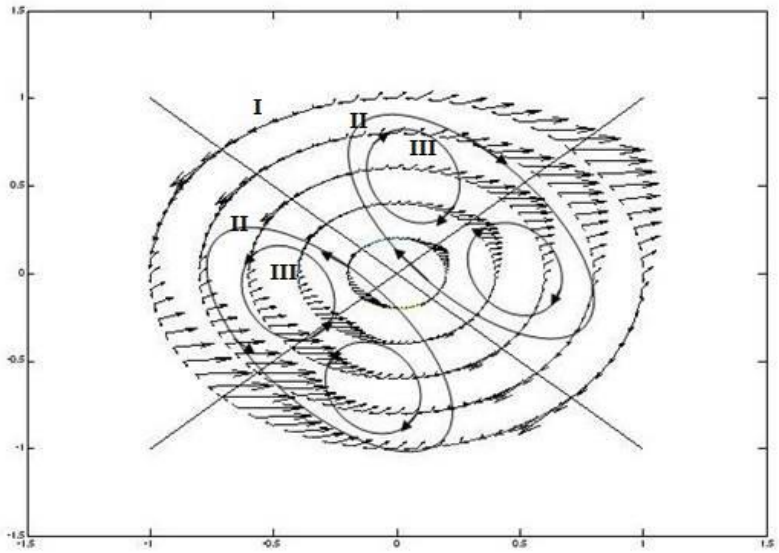

Fig. 1. Scheme of flat vortex decomposition normalized to u_0

The first two members of the model (2) : $V_r = \frac{1}{2}u_0\left(\frac{r}{R_0}\right)(cos\varphi + sin\varphi)$ and $V_\varphi = u_0\left(\frac{r}{R_0}\right)(cos\varphi - sin\varphi)$, Determine the non-uniform nature of rotation. A flat vortex is unstable, which means that its decay gives rise to a chain of vortices [3]. Based on the principle of hydrodynamic similarity, the chain links obtained through the decomposition of the initial vortex are schematically easy to imagine. In the static approach, the gyral chain forms an abstract cone in space, the axis of which can be directed anywhere (Fig. 2). In dynamics, as a result of the interaction of secondary eddies with different linear scales, generated due to the inevitable bifurcation of multiple eddies constituting the turbulent field, a permanent change of the turbulent field should take place in the atmosphere. Therefore, the physical task requires that the model (2) is only linearly approximated and qualitatively corresponds to the hydrodynamic picture of the transformation of the gyre field in time. Nevertheless, such a scheme of atmospheric vortex breakdown, which is visualized in Fig. 2, is quite useful. Such a process corresponds to a sequence of unstable and short-lived but equilibrium states. At the same time, it qualitatively quite convincingly presents the mechanism causing local disturbance of the temperature field and other thermodynamic parameters of the atmosphere as a result of the dissipation of eddies.

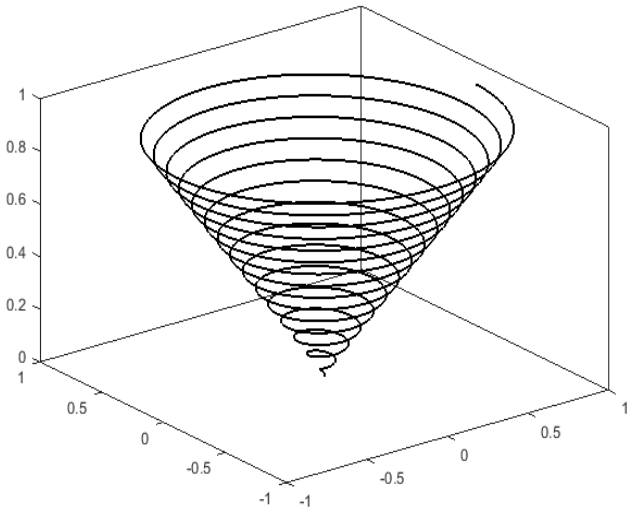

Fig. 2. Visualization of the spatial model of non-uniform rotation.

Atmospheric eddies transport mass and energy. Therefore, in the process of their disintegration and mixing, the level of heterogeneity of the environment changes, which becomes the reason for the creation of new eddies. We do not touch on the details of this process, we consider it necessary to note that the stability of the air mass, that is, the threshold of the turbulization process is considered to be the criterion: - $\frac{\partial P}{\partial z} < \frac{g}{c_p}$, where P is atmospheric pressure, c_p is the specific heat capacity of air. According to this criterion, in the case of a 100 m high mountain, a temperature drop < 1^0 is enough to maintain the stability of the atmosphere. Otherwise, convection begins, which usually occurs during strong heating of the earth's surface by the sun. It is natural that the final result of the convective movement should be such mixing of the air mass as to eliminate the temperature gradient.

The presence of free atmospheric vortices in a turbulent medium is excluded. Naturally, in most cases their interaction takes place, which, generally speaking, will be a nonlinear process that cannot be characterized by simple merging. The interaction between vortices, relatively nonlinear, is easier to imagine in a linear approximation, when the combination of vortices in space creates such structures, the shape of which is similar to a ring. For example, such an idea was formulated by V. Artsukovsky, a well-known adherent of the theory of physical ether, according to whose hypothesis vortex rings can be considered as moving formations in a viscous compressible gas, which is given an impulse by an air stream. Although the concept of ether is considered erroneous, since it essentially contradicts quantum mechanics, we believe that within the framework of Artsukovsky's idea it is possible to consider the interaction of simple vortex rings, when there is only toroidal rotation, when a vortex ring in the form of a tube rotates around its axis of symmetry. Under the conditions of such an assumption, the interaction between vortex rings is possible only in the following cases [4]:

1. Rings rotating in the opposite direction are close to each other and have a common imaginary axis;

2. One ring pulls the other, i.e. the speed of the first exceeds the speed of the second;

3. The rings move in opposite directions along the imaginary axis;

4. Rings move parallel, or their trajectories of movement cross close.

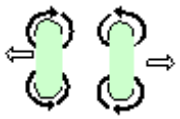

Fig. 3. Vortex rings moving in the forward direction.

In the first case, if the rings rotating in the opposite direction are very close, the loading forces will act between them (Fig. 3). At fairly large distances, the same displacement effect occurs, but in this case the reason is the rings' own rotation. In the second case, when one ring touches another, or rings with a common imaginary axis moving in the same direction come into contact, mutual penetration is possible between them, when the rear ring passes the front. . Then this process is repeated, that is, it is possible to change the sequence of rings multiple times (Fig. 4).

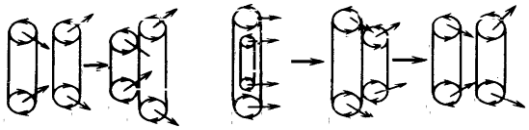

Fig. 4. Alternation of gyral rings.

In the third case, which refers to the gyro rings moving in the opposite direction, the following options are possible: 1. The rings are not calibrated (arbitrary size), general case; 2. Rings are not calibrated, private case; 3. The rings are calibrated.

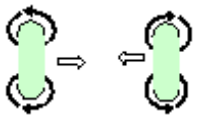

Fig. 5. Interaction of converging gyral rings.

In general, if the rings are not calibrated, a smaller ring passes into a larger one, or one ring expands, as in the case of one ring passing into another. In this case, the ring whose rotation speed is less expands once. After passing through each other, the rings move in different directions. In the special case, when the rings are not calibrated, then in the case of a certain balance of forces, it is possible to establish an equilibrium state in the vortex field, at this time, the small ring remains stationary inside the large one, and the air jet formed in the free space between the rings may act like a jet engine, which drives the pair of vortex rings about the axis of symmetry. along. The result of the collision of rings with the same size depends on the speed of their convergence. If the rings have gathered enough speed, it is possible to deform them (flatten or expand in the plane of contact), or multiple disintegration into small-sized whirling rings. If the counter-rotating calibrated rings with a single axis accidentally come into contact slowly, a thrust force associated with the toroidal rotation of the vortex elements can be induced. This effect will cause the rings to move apart. Such a situation is unstable, because any external influence will disturb the equilibrium picture between the initial gyral rings. Naturally, if the rings move in parallel or cross each other in any way, it is possible to rotate them so that one of the above cases is realized. Also, it should be noted that it is permissible to have gyratory rings which, in addition to being toroidal, can also rotate with respect to the diameter of the ring. In such a case, their interaction with other rings will be non-linear and will no longer be subject to simple determinism.

Thus, the linear approximation provides a sufficient representation of the dynamic process taking place in the turbulent field, the main element of which is the breakup of eddies and the interaction between them. In particular, such a process should take place in the atmosphere of a narrow mountain valley during its spontaneous disturbance, which is likely to accompany the inversion of the direction of the horizontal velocity in the atmosphere in the valley or above it. The question is: How realistic is the formation of gyral rings, for example, during an inversion event in a narrow mountain valley? It is impossible to give an unequivocal answer to this question, however, formally, model (2) allows such a possibility. Imagine a turbulent field in which a vortex rotating in any direction and oriented in any direction moves. It should be noted that the kinetic model of non-uniform rotation does not rule out that in the process of disintegration of the main vortex, such vortices will be formed, which will not have hydrodynamic similarity with the initial vortex. This means that such vortices can have a constant direction of rotation, which will facilitate their unification in a closed ring. The characteristic radius of these vortices will be smaller than the radius of the original vortex. In the process of forming a vortex ring, it is completely permissible to connect the vortexes rotating in the same direction in such a way that each of them maintains the orientation of its axis of rotation. In this way, a gyratory chain with a truly curvilinear axis of symmetry can be formed, which can be locked and take the form of a ring. Presumably, such rings, in contrast to whirligigs with non-uniform rotation, will be quite stable. Therefore, eddies with a constant direction of rotation can be considered as the final stage of the transformation of the turbulent field, followed by the complete dissipation of stochastic disturbance energy. The existence of such an effect can be assumed at the qualitative level, which can become the reason for a sharp change in the local meteorological regime as a result of the development of an inversion event in the atmosphere.

In any place on Earth, during calm weather, the atmosphere regularly circulates under the influence of convection. In mountainous terrain, the dynamics of the atmosphere are particularly affected by changes in the meteorological regime and the vertical convection currents associated with them. However, this picture may change due to a sharp change in the meteorological regime as a result of the generation of vortex structures in the air. However, it is known that in narrow mountain valleys, even in calm atmospheric conditions, such a spontaneous disturbance of the atmospheric circulation may occur, the occurrence of which is associated with impulsive changes in the gradient of atmospheric temperature. The existence of such a factor is determined by the unevenness of solar radiation on the slopes of a narrow valley, which, together with the geographical position of the valley, may be associated with seasonal and orographic factors, as well as with the mobility of the valley slopes. In some cases, the cause of a spontaneous violation of the hydrodynamic pattern of atmospheric mass movement may be instability caused by the inversion of the direction of the

horizontal component of the air velocity in the valley, which is associated with the spontaneous generation of atmospheric vortices. The interaction of these vortices in the atmosphere leads to the dissipation of hydrodynamic energy, which causes nonlinear phenomena to develop, the analysis of which is a complex physical problem. However, it is permissible to consider the process of vortex interaction in a linear approximation, which gives a qualitatively correct idea, for example, of the event of spontaneous disruption of the local atmospheric regime of a narrow mountain valley. It is here that an irregular thermal mechanism can be stochastically activated, the action of which will lead to the convective movement of air masses surrounding the ridge that surrounds the valley. This phenomenon has the nature of an atmospheric disturbance, since the convective velocity vector changes its direction at a certain height (inversion phenomenon). Prandtl's theoretical model is known, which analytically determines the vertical profile of the horizontal convection velocity coefficient [5] in the approximation of a hydrodynamic boundary layer, which is unstable, since it has a maximum at a certain height, i.e., it has a critical point. Physically, this means that hydrodynamic instability of Rayleigh-Jones or Kelvin-Helmholtz may develop in this place. Therefore, there is a high probability of the formation of atmospheric vortices in this area. Their decay will lead to the transformation of the energy of hydrodynamic disturbances into disturbance of the atmospheric temperature field, which will entail an impulsive change in the local meteorological regime in the canyon. For example, this phenomenon may be dangerous for those who like to fly in narrow mountain valleys on individual aircraft (hang gliders, paragliders).

By means of ingenious mathematical transformations, in the approximation of a weakly turbulent atmosphere, where the coefficients of temperature transfer and kinematic viscosity can be considered equal to each other, Prandtl connected the boundary layer formed on a valley slope with the perturbation of the temperature field. In particular, he showed that the temperature θ in the free atmosphere increases linearly with the height, and the surface of the ridge slope introduces a small θ perturbation into the temperature field, after which the keystone equation of the Prandtl model was obtained

$$\frac{\partial^4 \theta'(n)}{\partial n^4} + \frac{g\beta B \sin^2 \propto}{\nu^2} \theta'(n) = 0, \qquad (3)$$

where *n* is the height calculated from the canyon slope, β is the air temperature expansion coefficient, *B* = *const* is the vertical temperature gradient, ν is the air kinematic viscosity coefficient.
Based on physical considerations, Prandtl used only one of the four possible solutions of equation (3)

$$\theta' = \theta'_0 \exp\left(-\frac{n}{L}\right)\cos\frac{n}{L}, \qquad (4)$$

which met the following boundary conditions [4. Khrigian]

$$\theta' = \theta'_0, \quad \text{when } n = 0; \quad \theta' = 0, \quad \text{when } n = \infty, \qquad (5)$$

The image (4) includes a characteristic vertical scale, the height corresponding to the maximum of the convection speed, which depends on the environmental parameters

$$L = \sqrt[4]{\frac{4\nu^2}{g\beta B \sin^2 \propto}} \quad . \qquad (6)$$

Disturbance of the temperature field along the slope of the canyon leads to the convective movement of the air mass, the speed of which is determined by the formula

$$V_1 = \theta'_0 \sqrt{\frac{g\beta}{B}} \exp\left(-\frac{n}{L}\right)\sin\frac{n}{L} \; . \qquad (7)$$

The image (7) gives a vertical profile of the convective movement speed, which has an inversion point (level) in which the speed changes direction (Fig. 6). This place can be imagined as an abstraction of a tangential discontinuity surface, on which there is such a speed shift, which in a liquid (gas) environment is a prerequisite for the development of Kelvin-Helmholtz or Rayleigh-Taylor hydrodynamic instability. Figure 6 shows the vertical profile of the convection speed for a typical set of atmospheric parameters. In addition to

the inversion point, the profile also contains the inflection point (Vmax), in which the development of hydrodynamic instability and the generation of atmospheric vortices are also possible. Thus, in the Prandtl model, the height of the velocity maximum (n_(m)=Lπ/4) and the height of the inversion level corresponding to the first minimum of the trigonometric function (n_(m)= πL) are clearly defined.

In the paper [6] it was shown that the use of only one private solution of equation (3) limits the possibility of the Prandtl model. The operation of the principle of synergy is generally characteristic of atmospheric processes. Therefore, it would be fair to consider the time-varying effect of the boundaryconditions in the physical picture of the generation of turbulence-inducing eddies in the valley atmosphere. Often, such an approach is used to solve long-term prognostic meteorological problems. Variation of boundary conditions is expected to be useful for quantitative correction as well. During modeling of short-term local atmospheric processes. Therefore, within the framework of the Prandtl model, it is permissible to use another pair of boundary conditions, different from (4)

$$\theta' = \theta'_0 \ , \quad \text{when } n = 0 \ ; \quad \theta' = \infty, \quad \text{when } n = \infty. \qquad (8)$$

These boundary conditions are satisfied by the particular solution of the equation (3), which also includes the inversion effect and (4) differs from the image only by the sign of the power of the exponential multiplier

$$\theta' = \theta'_0 \exp\left(\frac{n}{L}\right)\cos\frac{n}{L} \ , \qquad (9)$$

which also corresponds to the velocity image, which was obtained by using a different model of the temperature field change, which formally allows for an unlimited increase in temperature with height [5].

$$V_2 = -\theta'_0\sqrt{\frac{g\beta}{B}}\exp\left(\frac{n}{L}\right)\sin\frac{n}{L} \ . \qquad (10)$$

In this case, the velocity inversion event will occur at altitude $n_m = \frac{3L\pi}{4}$.

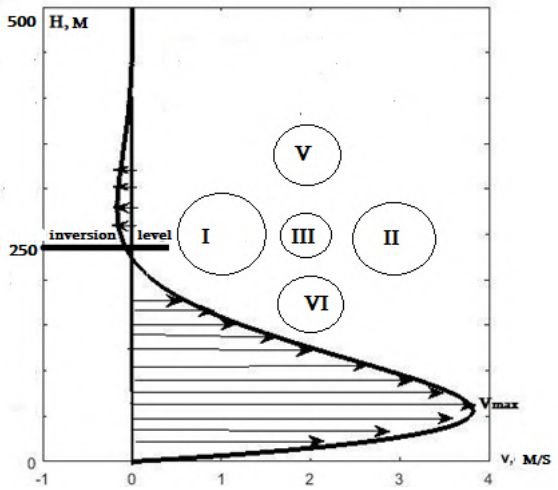

Fig. 6. Convection speed profile and atmospheric eddies

Thus, the vertical profile of the convection velocity in the atmosphere of the valley may have a critical point (points), where the probability of the development of Kelvin-Helmholtz hydrodynamic instability is high. At this time, the generation of atmospheric eddies will take place, which can be broken up and interacted in a linear approximation according to the scheme presented in the first part of this paper. This leads to the transformation of mechanical energy into thermal energy and disturbance of the atmospheric temperature field. This factor may contribute to the disturbance of the locally balanced, but unstable, thermodynamic state and the change of the meteorological regime in the valley. The characteristic time duration of this event will depend on the intensity of the temperature field disturbance. In case of strong turbulence, this process can be strongly non-linear. In particular, it is possible that disturbance of the temperature field in the area of velocity inversion causes the so-called "dynamo-effect", i.e. impulsive strengthening of turbulence. Since the generation of a chain of eddies in a limited space in a certain direction is possible, the structure of the temperature field in the

area of velocity inversion should probably be non-uniform and asymmetric. There is a solution to a similar mathematical problem, but for an object of a different spatial scale. In this work, which deals with the asymmetry of the temperature field in the polar cusp region of the Earth, the kinetic model of inhomogeneous rotation was also used [7].

There are many examples in nature of the transition from ordered motion to chaotic motion, the spatial scale of which varies from molecular to gigantic. Abstractly speaking, almost all of them have the same initial scenario, the ideological source of which is the Landau model and its further development, the so-called Ruel-Taken Model. According to these scenarios, the transition from the phase of laminar hydrodynamic motion to the turbulent (chaotic) phase occurs through the so-called infinite cascade of Hofi bifurcations. For example, in the case of an atmospheric vortex (blizzard, tornado), this process means that the intensity of turbulent pulsations generated in the vortex region, i.e. the power of the discrete frequency spectrum generated by the infinite sequence of Hof bifurcations, as a result of cascade doubling, expands, gradually becomes continuous and approaches a certain limit. At the initial stage of this process, the power of the frequency spectrum, growing like an avalanche, gradually decreases, which in some specific case, for example, for an atmospheric vortex, means the end of the process of its scattering. Unlike the Landau model, in the Ruelle-Tanken model the transition from the initial regular (laminar) motion to chaos occurs much faster due to a special factor, the so-called "strange attractor". In the problem of flow around smooth surfaces by a laminarly moving liquid, the presence of this factor is associated with the peculiarity of the analytical solution of the Navier-Stokes equation in the region of the critical point. The phase space provides an adequate representation of the specifics of the flow at the critical point and the mathematical complexities arising from it, with the help of which the behavior of the circles of the laminar flow in the region of the critical point is visualized. It is here that the integral surface is formed, onto which various topological variants of the special behavior (aspirations) of the circles of the laminar flow are projected. The physical reason for such diversity is the formation of reverse flows in the region of the critical point and their mixing with the main flow. Accordingly, in the laminar approximation of flow near the critical point, the topological diversity of the pattern of boundary current circles is due to the mixing of two currents of different causes. The main flow is due to the pressure gradient, and the reverse flow is due to the orography of the surrounding surface in the region of the critical point. Naturally, such an effect occurs only with laminar turbulence, although it is worth noting that this phenomenon can develop both in an ideal and in a viscous liquid (gas) near the critical point of any vortex structure, including tornadoes and whirlwinds [8,9].

Tornado and waterspout as topologically similar catastrophic events. To date, there are no known works that formulate a unified theory of large-scale atmospheric vortices. Existing publications mainly present a morphological interpretation of the results of meteorological observations. For example, it is known that the source of a tornado's energy is an ascending flow of warm air rotating unevenly. Its central, toroidal body-like part, the "trunk", rises sharply above the Earth's surface and extends quite high horizontally. However, in fact, the vortex is reflected in the atmosphere, not on the Earth's surface. Its main cause, unlike a tornado, is a thermodynamic process in a cloud. Over time, the air sucked into the vortex cools down and descends as a result of condensation of the steam mixed with it, but, despite the increase in density, continues to rotate around an imaginary vertical axis. A tornado, like a tornado, is distinguished by a certain stability and retains a funnel-shaped structure when moving significant distances along the earth's surface. At this time, the linear speed of rotation of the absorbed mass from the periphery of the tornado in the direction of its "mouth" (the throat of the funnel) can increase by an order of magnitude or even more than the typical value of 10 m / s. In terms of energy, a stochastic storm of a gigantic nature, a tornado, which is disproportionately stronger than a hurricane, usually occurs in the World Ocean, rarely in the area of large water bodies. A tornado, like a tornado, as a catastrophic natural phenomenon, has been well studied from a morphological point of view, the consequences of its destructive action are analyzed in detail [10-14]. However, a full-fledged theoretical modeling of this atmospheric phenomenon is associated with insurmountable physical and mathematical problems [1, 15]. The reasons for this situation are associated, first of all, with a multitude of factors, the joint action of which forms

the environmental conditions that contribute to the emergence of a tornado. In particular, the cornerstone of theoretical modeling of a tornado is associated with solving a system of three-dimensional equations of thermogasdynamic motion with adequate initial and boundary conditions of the dynamic characteristics of the real environment. Therefore, at this stage, the solution to this problem exceeds the capabilities of modern analytical methods and computer technology [15].

Conclusion.

The process of transition from laminar to turbulent atmospheric motion can have different stages. Therefore, this process can be presented as very diverse depending on how much certain deterministic characteristics change, determining it during the formation of vortices in the medium. Their presence at specific spatial scales determines the similarity of the elements of the environment. From this point of view, the transition from ordered motion to chaotic motion is nothing more than a sign that the turbulent medium loses its homogeneous quantitative characteristics at smaller and smaller scales. At this time, the main characteristic of the elements of the environment becomes chaotic rotation, creating a chaotic background. Naturally, the linear approximation gives only a simplified mechanical representation of such a process. In this sense, the kinematic model of non-uniform rotation is generally consistent with the deterministic scheme of chaos generation. In particular, with its help, at the initial stage of chaos development, it is quite easy to construct a qualitative picture of the process of vortex energy dissipation.

The Prandtl model and its modifications physically allow the possibility of formation of atmospheric vortices. In combination with this, using the kinematic model of non-uniform rotation, it is possible to simulate the interaction of atmospheric vortices in a linear approximation. This approach gives a fairly complete picture of the development of spontaneous crystalline disturbances in the atmosphere of a narrow mountain valley. The interaction of primary vortices formed due to the inversion of the convection velocity into simple vortices and rings formed during their subsequent connection, within the framework of the Artsukovsky hypothesis, determines the scale of turbulence and causes a change in the temperature field of the atmosphere. Accordingly, the level of its disturbance depends on the time scales and intensity of the generation of storm formations, as well as on the thermodynamic regime of the environment. Thus, the kinematic model of non-uniform rotation gives a qualitative idea of the mechanism of the process of generation and decay of atmospheric vortices. In addition, with its help, the disturbance of the temperature field of the atmosphere can be modeled using one of the particular solutions of the temperature conductivity equation.

References

[1] Kochin N.Ye, Kibel I.A., Roze N.V. Teoreticheskaya gidromekhanika. Moskva, gos. izd. fiz.-mat. lit.,1963, 366 s.

[2] Khantadze A.G., Aburdzhaniya G.D. O probleme sverkhvrashcheniya verkhney atmosfery v polyarnoy oblasti. Izvestiya RAN , Fizika atmosfery i okeana. T. 40, № 3, 2004, c.418-32.

[3] Khvedelidze N. I., Chkhitunidze M., Zhonzholadze N. Model of Local Atmospheric Disturbance of Lower Part of Gorge of River Vere. Transactions of Mikheil Nodia Institute of Geophysics, ISSN 1512-1135, vol. LXX, 2019 pp. 101-112.

[4] Atsyukovskiy V.A. Obshchaya efirodinamika. Moskva, Energoatomizdat, 2003, 584 s.

[5] Khrgian A.KH. Fizika atmosfery, t. 2. Leningrad, Gidrometeoizdat, 1978, 237 s.

[6] Kereselidze Z. A., Lominadze G. J., Salukvadze E.D., Tchania E.B. Regarding the Spontaneous Mechanism of Atmospheric Whirlwind Generation in Narrow Mountain Canyons. Journal of the Georgian Geophysical Society, e-ISSN: 2667-9973, ISSN: 1512-1127, Physics of Solid Earth, Atmosphere, Ocean and Space Plasma, v. 26(2), 2023, pp. 13 – 21.

[7] Kirtskalia V., Kereselidze Z., Dzonzoladze N., Chkhitunidze M. An Analytical Model of an Asymmetrical Temperature Field in the Polar and Auroral Ionosphere. Georgian International Journal of Science and Technology, Vol. 3, Iss. 4, 2012, pp. 381-390. https://www.novapublishers.com/catalog/product_info.php?products_id=32804

[8] Gonchenko S.V., Gonchenko A.S., Kazakov A.O., Kozlov A.D., Bakhanova YU.V. Matematicheskaya teoriya dinamicheskogo khaosa i yeye prilozheniya. Obzor. Chast' 2. Spiral'nyy khaos trekhmernykh potokov. Izv. Vuzov, PND, t. 27, № 1, 2019, 45 s. https://doi.org/10.18500/0869-6632-2019-27-1-xx-xx.

[9] Shuster, G. Determinirovannyy khaos . Moskva., Mir, 1988. - 450 s.

[10] Chikhladze V., Jamrishvili N., Tavidashvili Kh. Tornadoes in Georgia. Int. Sc. Conf. „Natural Disasters in the 21st Century: Monitoring, Prevention, Mitigation“, Proceedings, ISBN 978-9941-491-52-8, Tbilisi, Georgia, December 20-22, 2021, pp. 23-26.
[11] Chikhladze V., Amiranashvili A., Gelovani G., Tavidashvili Kh., Laghidze L., Jamrishvili N. Assessment of the Destructive Power of a Tornado on the Territory of the Poti Terminal on September 25, 2021. II International Scientific Conference “Landscape Dimensions of Sustainable Development Science – Carto/GIS – Planning – Governance”, Dedicated to the 75th Anniversary of Professor Nikoloz (Niko) Beruchashvili, Proceedings, 12-16 September 2022, Tbilisi, Georgia, Ivane Javakhishvili Tbilisi State University Press, 2022, ISBN 978-9941-36-030-5, pp. 275-281, (in Georgian). http://www.dspace.gela.org.ge/handle/123456789/10120
[13] Amiranashvili A., Chikhladze V., Pipia M., Varamashvili N. Some Results of an Expeditionary Study of the Tornado Distribution Area in Kakheti on June 25, 2024. Journal of the Georgian Geophysical Society, e-ISSN: 2667-9973, p-ISSN: 1512-1127, Physics of Solid Earth, Atmosphere, Ocean and Space Plasma, v. 27(1), 2024, pp. 57–76. https://ggs.openjournals.ge/index.php/GGS/article/view/7985
[14] Amiranashvili A., Chikhladze V., Kekenadze E., Pipia M., Samkharadze I., Telia Sh., Varamashvili N. Meteorological Conditions for the Tornado Formation in Kakheti (Georgia) on June 25, 2024. Int. Sc. Conf. “Complex Geophysical Monitoring in Georgia: History, Modern Problems, Promoting Sustainable Development of the Country”, Proceedings, ISBN 978-9941-36-272-9, Publish House of Iv. Javakhishvili Tbilisi State University, Tbilisi, Georgia, October 17-19, 2024, pp. 168 – 171.
[15] Aliyev I. N., Lyatifov R. E. Prostaya model' mekhanizma zarozhdeniya vozdushnykh vikhrey v atmosfere. Vestnik Moskovskogo gos. Oblastnogo universiteta, №2, 2023, s. 6-19, DOI: 10.18384/2310-7251-2023-2-6-19.

არაერთგვაროვანი ბრუნვის კონუსისებური მოდელი და ატმოსფერული გრიგალური ჯაჭვის ელემენტების ურთიერთქმედება წრფივ მიახლოებაში

ზ.კერესელიძე, ა. ამირანაშვილი, ვ. ჩიხლაძე, მ. ჩხიტუნიძე, გ.ლომინაძე, ე. ჭანია

რეზიუმე

გლობალური ატმოსფერო შეიძლება განვიხილოთ, როგორც ღია თერმოდინამიკური სისტემა, რომლის შიგნით მოქმედებენ სხვადასხვა შემაშფოთებელი ფაქტორები. მაგალითად, წყნარ ატმოსფერულ პირობებშიც კი ოროგრაფია შეიძლება გახდეს დედამიწასა და ატმოსფეროს შორის სტაციონარული სითბური ბალანსის დარღვევის მიზეზი. საზოგადოდ, გრიგალური სტრუქტურების წარმოქმნა ნებისმიერ გაზობრივ თუ თხევად გარემოში სტოქასტიკურად დეტერმინირებულია. ეს ნიშნავს, რომ გრიგალის წარმოქმნის პროცესი, მნივნელოვან წილად, ალბათურია. ამიტომ, ატმოსფერული გრიგალური ველის მათემატიკური მოდელირების დროს რაციონალურია შემთხვევითი ფაქტორების გამორიცხვა კონკრეტული ხელისშემწყობი პირობების გამოკვეთის გზით. მაგალითად, დედამიწის რელიეფის ძლიერი დანაწევრება ხელს უწყობს რეგიონალურ და ლოკალურ მასშტაბებში ჰაერის დინების ტურბულიზაციას. კერძოთ, სუსტი ინტენსივობის ატმოსფერული გრიგალების წარმოქმნის პროცესი მთიან ხეობებში

ყოველთვის შეიძლება განვიხილოთ, როგორც ლოკალური სტაბილურობის დარღვევა, რომლის მიზეზია განსხვავებული ოროგრაფიისა და ლანდშაფტების საზღვარზე შექმნილი ტემპერატურული ველის არაერთგვაროვნება. ასევე გრიგალების გენერაცია და მათი დისიპაციის პროცესი ატმოსფეროში ყოველთვის შეიძლება განვიხილოთ, როგორც გარკვეულ სივრცულ მასშტაბებში გარემოს სტაბილურობის დარღვევა, რაც გამოიხატება მისი თერმოდინამიკური პარამეტრების შეშფოთებაში.

საკვანძო სიტყვები: ატმოსფერული გრიგალები, თერმოდინამიკური პარამეტრები, რელიეფი, მათემატიკური მოდელირება.

Коническая модель неоднородного вращения и взаимодействие элементов вращательной цепи атмосферы в линейном приближении

З. Кереселидзе, А. Амиранашвили, В. Чихладзе, М. Чхитунидзе, Г. Ломинадзе, Э. Чания

Резюме

Глобальную атмосферу можно рассматривать как открытую термодинамическую систему, внутри которой действуют различные возмущающие факторы. Например, даже в спокойных атмосферных условиях орография может стать причиной нарушения стационарного теплового баланса между Землей и атмосферой. В целом, формирование вихревых структур в любой газообразной или жидкой среде является стохастически детерминированным. Это означает, что процесс образования вихря в определенной степени вероятностный. Поэтому, при математическом моделировании поля атмосферных круговоротов рационально исключить случайные факторы, выявив конкретные способствующие условия. Например, сильное разделение земного рельефа способствует турбулентности воздушных потоков регионального и локального масштаба. В частности, процесс формирования атмосферных вихрей слабой интенсивности в горных долинах всегда можно рассматривать как нарушение локальной устойчивости, причиной которого является неравномерность температурного поля, создаваемого на границе различной орографии и ландшафтов. Также генерацию вихрей и процесс их рассеяния в атмосфере всегда можно рассматривать как нарушение устойчивости среды в определенных пространственных масштабах, что выражается в нарушении ее термодинамических параметров.

Ключевые слова: атмосферные вихри, термодинамические параметры, рельеф, математическое моделирование.

Journal of the Georgian Geophysical Society, e-ISSN: 2667-9973, p-ISSN: 1512-1127
Physics of Solid Earth, Atmosphere, Ocean and Space Plasma, v. 27(2), 2024, pp.74 - 80

Coherent Analysis of Intense Geomagnetic Disturbances Using Dusheti Observatory Data and the DST Index

[1]Luka K. Tsulukidze, [1]Oleg A. Kharshiladze, [1]Alexandre P. Ghurchumelia, [2,3]Luca Sorriso-Valvo, [1,4]Khatuna Z. Elbakidze, [1]Tamaz G. Matiashvili

[1]Mikheil Nodia Institute of Geophysics of Ivane Javakhishvili Tbilisi State University, Tbilisi, Georgia
[2] CNR - Istituto per la Scienza e la Tecnologia dei Plasmi, Bari, Italy
[3] KTH - Space and Plasma Physics, Stockholm, Sweden
[4] Business and Technology University, Tbilisi, Georgia
luka.tsulukidze617@ens.tsu.edu.ge

ABSTRACT

Geomagnetic storms are intense disturbances in Earth's magnetosphere that can disrupt technological systems and impact human health. This study investigates the dynamics of solar-terrestrial interactions using data from the Dusheti Observatory and global geomagnetic indices. We examined the relationships between the interplanetary magnetic field (IMF), sunspot numbers, and the H-component of the geomagnetic field during the period from 2023 to 2024, focusing on the unprecedented geomagnetic storm of May 11, 2024. Through wavelet coherence and cross-correlation analyses, we identified significant interactions between solar and geomagnetic activity, with coherence patterns emerging well before the storm onset. The analysis of six solar cycles (1964–2024) revealed correlation at lag of 5 days, highlighting the potential predictive utility of sunspot numbers. This study also validated the reliability of local geomagnetic data, emphasizing its importance for understanding the regional manifestations of global geomagnetic events in Georgia. The findings contribute to the development of improved predictive models for geomagnetic disturbances and underscore the need for localized studies to better mitigate the risks associated with space weather.
Key words: *Geomagnetic storms, Dusheti observatory, Interplanetary magnetic field, DST index, Wavelet coherence, cross-correlation, Space weather prediction*

Introduction

Geomagnetic storms cause significant disruptions and sharp drops in Earth's magnetic field, they are primarily driven by the interaction between solar wind, the interplanetary magnetic field (IMF) and Earth's magnetic field. Geomagnetic storm of 11 may 2024 was the most powerful storm of 21st century and captured global attention [1].

The dynamics of these storms stem from nonlinear interactions between the Sun's plasma outflows and Earth's magnetic field, which underscores the need to study their evolution and coupling with external drivers such as the IMF and solar activity. To better understand these processes, this study examines geomagnetic data from the Dusheti Observatory and Disturbance Storm Time (DST) index, a global measure of geomagnetic storm intensity. The DST index quantifies magnetic field variations due to ring currents formed during storms [2]. Comparing them validated the accuracy of Dusheti's H component data, providing a foundation for further analysis of geomagnetic perturbations. We also explore relationships between geomagnetic field variations, IMF, and solar activity (sunspot numbers). Wavelet coherence and cross-correlation methods were used to analyze these connections, with a focus on identifying patterns that might serve as predictors for geomagnetic storms. Understanding these relationships is critical, as intense geomagnetic storms have significant implications for technology, infrastructure, and human health, Our primary interest lies in understanding how these storms impact Georgia, using Dusheti Observatory's data to gain insights into local manifestations of global geomagnetic events [3, 4].

This work aims to study quantifiable patterns and correlations between the geomagnetic field, the IMF, and solar activity during periods of intense geomagnetic activity. By doing so, we hope to enhance predictive capabilities for geomagnetic disturbances, which could mitigate the risks posed by space weather and

contribute to a better understanding of geomagnetic storm dynamics in both global and regional contexts [4, 5].

Data and methods

The study focuses on data collected from August 2023 to July 2024, analyzing different time periods to uncover relationships between geomagnetic field variations, sunspot numbers, and the interplanetary magnetic field (IMF). A key focus is the geomagnetic storm on May 11, 2024 (Fig. 1 and 2), one of the largest recorded during this period (Figure 2). The data used includes the DST index and sunspot numbers obtained from NASA's OMNIWeb service [7], alongside the H-component of the geomagnetic field recorded at the Dusheti observatory (station code: TBS, Geographic coordinates: 42.08°N, 44.7°E. Geomagnetic coordinates: 37.96°N, 117.16°E. Altitude: 982 m) in Georgia. All of the datasets have a resolution of one hour, enabling high-precision temporal analysis. Missing data points were addressed using linear interpolation to ensure continuity.

To investigate correlations between these datasets, we employed wavelet coherence analysis and cross-correlation techniques. Wavelet coherence is particularly suited for identifying and quantifying relationships between nonstationary signals across time and frequency domains. This method allows for a detailed exploration of how the phase and amplitude relationships between signals evolve over time, even in regions where individual wavelet coefficients are weak. By revealing periods and frequencies where the signals are coherent, wavelet coherence enhances our ability to identify and interpret significant patterns.

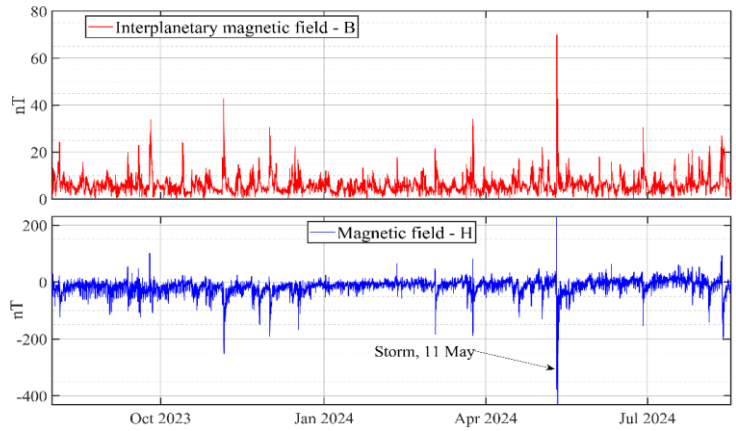

Fig. 1. B - Interplanetary magnetic field and H component of geomagnetic field.

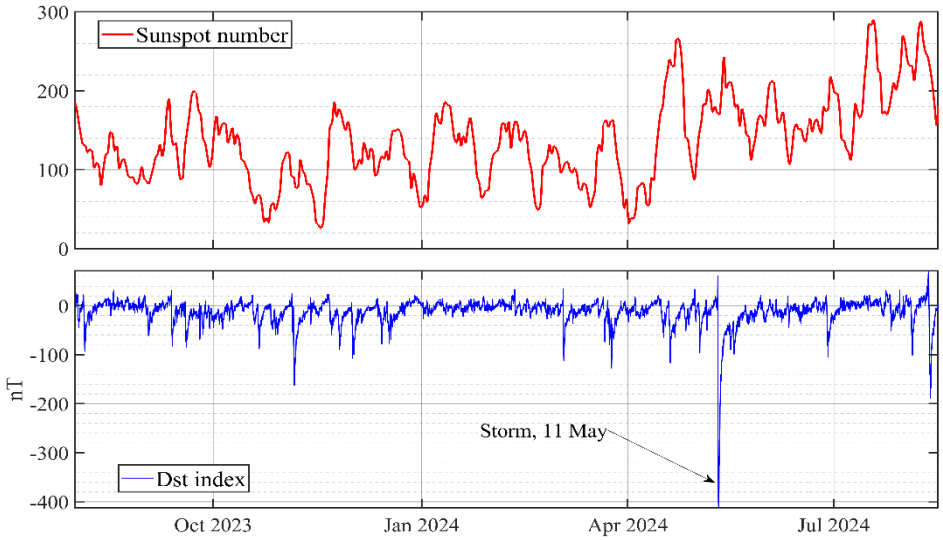

Fig. 2. Sunspot numbers and Dst index.

In addition to wavelet coherence, we divided the sunspot and DST data into six sections corresponding to solar cycles. This segmentation enabled a detailed cross-correlation analysis for each cycle. The cross-correlation function was calculated for detrended datasets, where trends were removed using moving averages, with windows of 365 days. This detrending process ensured that only fluctuations relevant to the study's objectives were analyzed. Than for the cross-correlation analysis: Each solar cycle segment was independently analyzed to compute the cross-correlation function over a maximum lag of 90 days. Correlation coefficients (ρ) and corresponding lags were calculated for each segment to determine the temporal relationship between the detrended sunspot and DST datasets. The results from all six segments were combined using a mathematical approach to aggregate the correlation results: The datasets were analyzed for their common signs at each lag to determine a consensus sign. The combined correlation was computed as the geometric mean of the absolute values of the segment correlations, weighted by the common sign.

This method provides a comprehensive view of the relationships between sunspot numbers and geomagnetic field variations across solar cycles, highlighting both consistent and cycle-specific patterns. The results have implications for understanding how solar activity influences Earth's geomagnetic environment and for identifying potential predictors of geomagnetic disturbances.

Results and discussion

Wavelet-Coherence analysis. The wavelet coherence analysis of the interplanetary magnetic field (IMF) and the H-component of the geomagnetic field at different time periods reveal interesting relationships between the two signals. In Figure 3, we see that from february to August 2024, the IMF and geomagnetic field exhibit coherence at the lowest frequencies. However, during geomagnetic storms, coherence becomes visible at higher frequencies, even before the storms begin. During intense geomagnetic storms, the coherence spans a broader spectrum of frequencies, extending to even lower periodicities. This suggests that geomagnetic storms influence the dynamics of the IMF and geomagnetic field across a wide range of frequencies, enhancing coherence between the two signals.

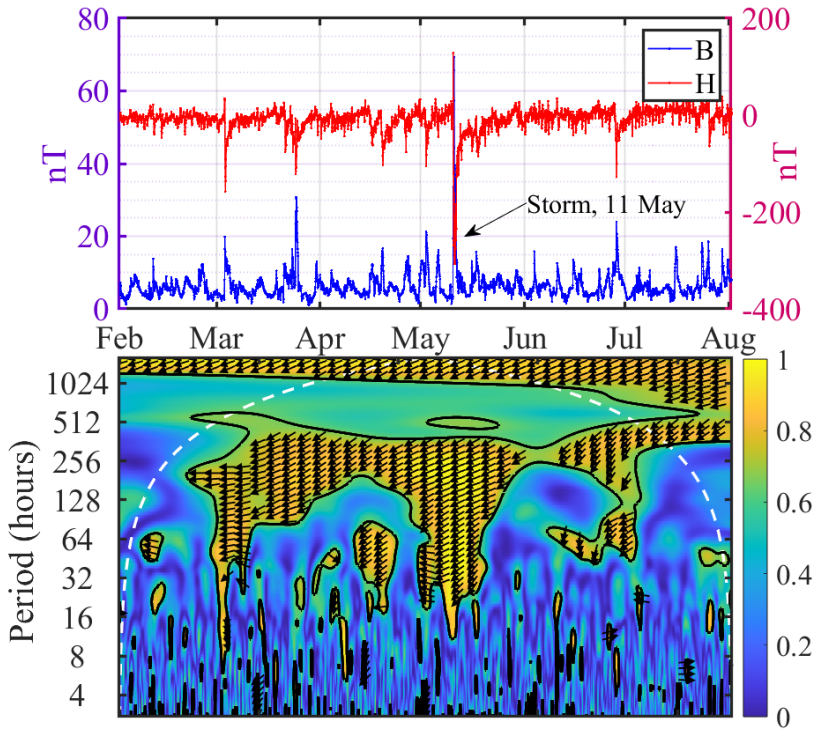

Fig. 3. Wavelet coherence between IMF and H component of geomagnetic field.

We applied the same method to analyze the coherence between sunspot numbers and both the H-component of the geomagnetic field and the DST index. Fig. 4 and 5 reveal coherence in both cases well before the geomagnetic storm occurs. This is indicated by the yellow regions on the plots, which appear as early as mid-March, approximately two months prior to the storm. These findings are particularly intriguing as they highlight the potential for using the relationship between sunspot numbers, geomagnetic data, and the DST

index as an early indicator of strong geomagnetic storms. However, further investigation is required to fully understand and validate this predictive capability.

Cross-correlation. In this study, we utilized the cross-correlation method to analyze the relationship between sunspot numbers and the Dst index on a larger scale. The data, spanning from 1964 to 2024, was segmented according to six solar cycles (the last cycle being incomplete). For each solar cycle, we measured the cross-correlation between these datasets and aggregated the results.

Our findings, presented in Fig. 6, indicate a cross-correlation of 8% with a 5-day lag. These results suggest the potential utility of sunspot numbers as a predictive indicator for geomagnetic activities.

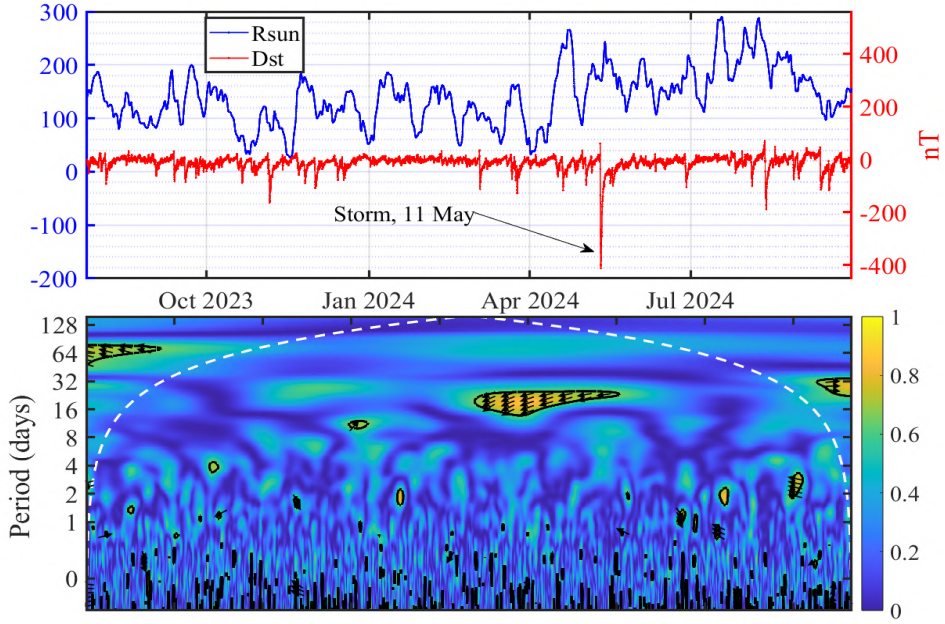

Fig. 4. Wavelet Coherence of sunspot number and DST index.

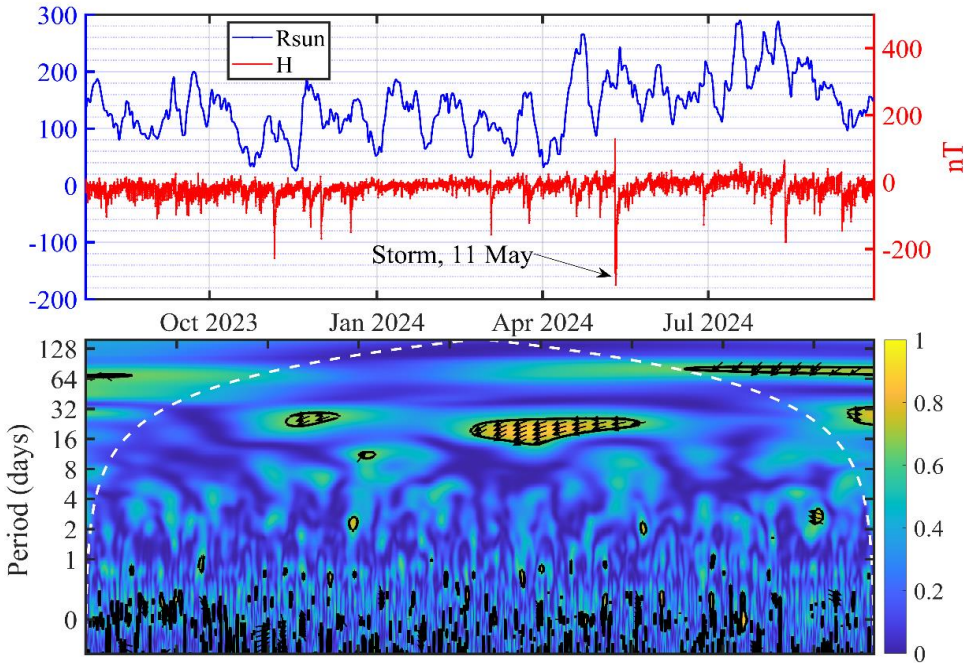

Fig. 5. Wavelet Coherence of sunspot number and H component of magnetic field.

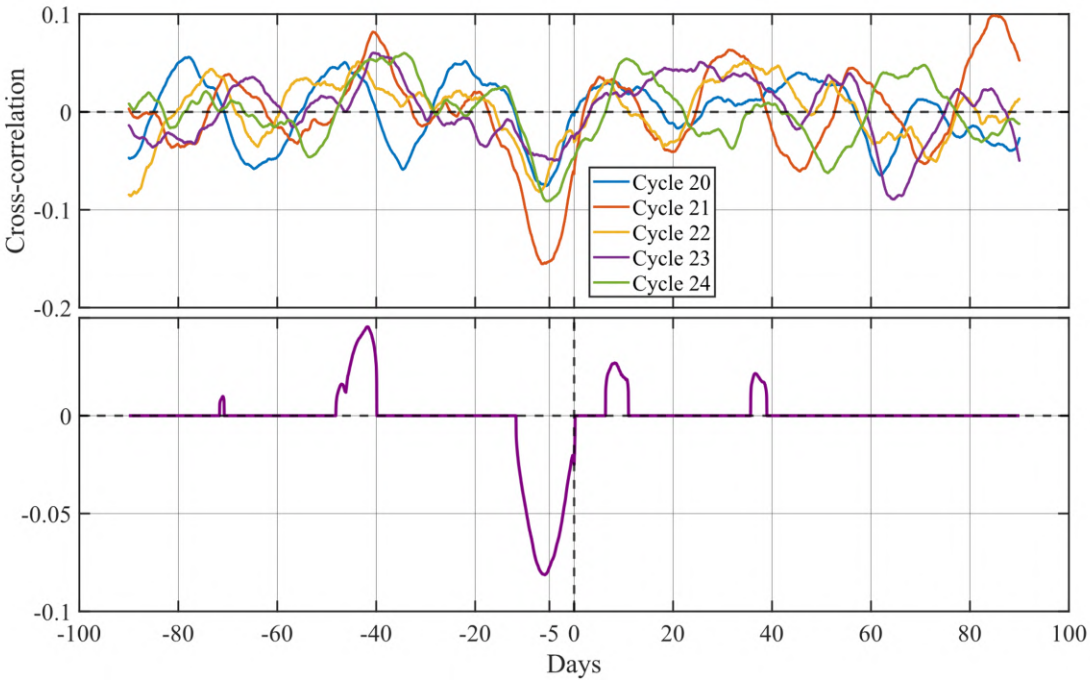

Fig. 6. Cross-Correlations of sunspot number and DST index.

Conclusion

This study provides a comprehensive analysis of the relationships between solar activity, the interplanetary magnetic field (IMF), and geomagnetic variations, with a particular focus on the geomagnetic storm of May 11, 2024. By utilizing high-resolution data from the Dusheti Observatory and global indices such as the Dst index, we validated the accuracy of local geomagnetic field measurements and explored their connections to solar drivers.

The wavelet coherence analysis revealed significant patterns of interaction between solar and geomagnetic datasets, particularly the ability to detect coherence at higher frequencies preceding geomagnetic storms. This underscores the potential for using sunspot numbers and IMF data as early indicators of geomagnetic disturbances. Cross-correlation analysis further supported this potential, demonstrating a measurable lagged relationship between sunspot activity and geomagnetic indices across multiple solar cycles.

These findings enhance our understanding of the dynamics of geomagnetic storms and their coupling with solar activity. They also highlight the potential for predictive modeling, which could mitigate the impacts of space weather events on infrastructure, technology, and human health. Future studies should focus on refining these methods and incorporating additional datasets to improve the robustness and accuracy of predictions.

References

[1] Diaz Jordi. Monitoring May 2024 solar and geomagnetic storm using broadband seismometers. Scientific Reports 14.1, 2024, pp. 1-13.
[2] Sugiura M, Poros D.J. Hourly values of equatorial Dst for the years 1957 to 1970. NASA, Goddard Space Flight Center; 1971 Jul.
[3] Breus T. K., Halberg F., Cornelissen G. Biological effects of solar activity. Biofizika, 40, 1995, pp. 737—749
[4] Chernogor L.F. Physics of geospace storms. Space Science and Technology, 27(1), 2021.
[5] Cliver E.W., Schrijver C.J., Shibata K., Usoskin I.G. Extreme solar events. Living Reviews in Solar Physics, 19(1):2, 2022 Dec.
[6] Akasofu S.I., Chapman S. Solar-terrestrial physics, 1972.
[7] https://omniweb.gsfc.nasa.gov/form/omni_min_def.html

[8] Torrence C., Compo G.P. A practical guide to wavelet analysis. Bulletin of the American Meteorological Society, vol. 79, no. 1, 1998, pp. 61–78
[9] Grinsted A., Moore J.C., Jevrejeva S. Application of the cross wavelet transform and wavelet coherence to geophysical time series. Nonlinear processes in geophysics, 11(5/6):561-6, 2004 Nov 18.
[10] Giri A., Adhikari B., Baral R, Idosa Uga C., Calabia A. Wavelet Coherence Analysis of Plasma Beta, Alfven Mach Number, and Magnetosonic Mach Number during Different Geomagnetic Storms. The Scientific World Journal, 2024; 2024(1):1335844.

მძლავრი გეომაგნიტური შეშფოთებების კოჰერენტული ანალიზი დუშეთის ობსერვატორიის მონაცემებისა და DST ინდექსის მაგალითზე

ლ. წულუკიძე, ო. ხარშილაძე, ა. ღურჭუმელია, ლ. სორისო-ვალვო,
ხ. ელბაქიძე, თ. მათიაშვილი

რეზიუმე

გეომაგნიტურმა ქარიშხალებს შეუძლიათ წყობიდან გამოიყვანონ ტექნოლოგიური სისტემები და გავლენა მოახდინონ ადამიანის ჯანმრთელობაზე. ამ კვლევაში განვიხილეთ მზე-დედამიწის ურთიერთქმედების დინამიკა დუშეთის ობსერვატორიის და გლობალური გეომაგნიტური ინდექსების გამოყენებით. ჩვენ გამოვიკვლიეთ ურთიერთობა პლანეტათაშორის მაგნიტურ ველს (IMF), მზის ლაქების რიცხვებსა და გეომაგნიტური ველის H - კომპონენტს შორის 2023 წლის აგვისტოდან 2024 წლის ივლისამდე პერიოდში, განსაკუთრებული ყურადღება გამახვილდა 2024 წლის 11 მაისის გეომაგნიტურ ქარიშხალზე. ვეივლეტ კოჰერენტული ანალიზით, ჩვენ გამოვავლინეთ მნიშვნელოვანი ურთიერთქმედებები მზის და გეომაგნიტურ მონაცემებს შორის, თანმიმდევრული პატერნებით რომლებიც ჩნდება ქარიშხლის დაწყებამდე. მზის ციკლების მიხედვით კორელაციურმა ანალიზმა (1964–2024) გამოავლინა 15 პროცენტიანი კორელაცია 5 დღის ჩამორჩენაზე, რაც ხაზს უსვამს მზის ლაქების რიცხვების პოტენციალს მაგნიტური ქარიშხლების წინასწარმეტყველებაში. ამ კვლევამ ასევე დაადასტურა ადგილობრივი გეომაგნიტური მონაცემების სანდოობა, ხაზი გაუსვა მის მნიშვნელობას საქართველოში გლობალური გეომაგნიტური მოვლენების რეგიონული გამოვლინებების გასაანიზებლად შედეგები ხელს უწყობს გეომაგნიტური ქარიშხლების გაუმჯობესებული პროგნოზირების მოდელების შემუშავებას და ხაზს უსვამს ლოკალიზებული კვლევების საჭიროებას კოსმოსურ ამინდთან დაკავშირებული რისკების უკეთ გასანალიზებლად.

საკვანძო სიტყვები: გეომაგნიტური შტორმები, დუშეთის ობსერვატორია, პლანეტათშორისი მაგნიტური ველი, DST ინდექსი, ვეივლეტ კოჰერენტობა, კორელაციური ანალიზი, კოსმოსური ამინდი.

Когерентный анализ мощных геомагнитных возмущений на примере данных обсерватории Душети и индекса DST

**Л. Цулукидзе, О. Харшиладзе, А. Гурчумелия, Л. Соррисо-Вальво,
Х. Элбакидзе, Т. Матиашвили**

Резюме

Геомагнитные бури — это интенсивные возмущения в магнитосфере Земли, способные нарушать работу технологических систем и оказывать влияние на здоровье человека. В данном исследовании анализируется динамика солнечно-земных взаимодействий с использованием данных обсерватории

Душети и глобальных геомагнитных индексов. Мы изучили взаимосвязи между межпланетным магнитным полем (IMF), числом солнечных пятен, индексом DST и H-компонентой геомагнитного поля в период с 2023 по 2024 год, сосредоточив внимание на геомагнитной буре 11 мая 2024 года. С помощью анализа вейвлет-когерентности и кросс-корреляции были выявлены значимые взаимодействия между солнечными и геомагнитными сигналами, при этом когерентность проявляется задолго до начала бури. Анализ шести солнечных циклов (1964–2024) показал наличие корреляции с задержкой в 5 дней, что подчеркивает потенциальную прогностическую полезность числа солнечных пятен. В исследовании также была подтверждена надежность локальных геомагнитных данных, что подчеркивает их важность для понимания региональных проявлений глобальных геомагнитных событий в Грузии. Полученные результаты способствуют разработке усовершенствованных прогностических моделей геомагнитных возмущений и подчеркивают необходимость проведения локальных исследований для эффективного снижения рисков, связанных с космической погодой.
Ключевые слова: Геомагнитные бури, Душетская обсерватория, Межпланетное магнитное поле, DST-индекс, Вейвлет-когерентность, кросс-корреляция, Прогноз космической погоды.

Journal of the Georgian Geophysical Society, e-ISSN: 2667-9973, p-ISSN: 1512-1127
Physics of Solid Earth, Atmosphere, Ocean and Space Plasma, v. 27(2), 2024, pp. 81 – 95

Some Results of the Joint Research of the M. Nodia Institute of Geophysics, TSU and Institute of Hydrometeorology, GTU from 2019 to 2023 and Prospects for their Further Development

[1]Nodar D. Varamashvili, [2]Mikheil G. Pipia

[1]M. Nodia Institute of Geophysics of the I. Javakhishvili Tbilisi State University, Georgia
[2]Institute of Hydrometeorology of the Georgian Technical University, Georgia

[1]e-mail: nodar.varamashvili@tsu.ge
[2]e-mail: m.pipia@gtu.ge

ABSTRACT

A brief information on joint research of the M. Nodia Institute of Geophysics, TSU and the Institute of Hydrometeorology, GTU, conducted in 2019–2023 and the prospects for their further development are presented.
Key words: *Hydrometeorology, climate, experimental modeling of atmospheric processes, bioclimate, ecology.*

Introduction

Over the past decades, the institutes of geophysics and hydrometeorology have conducted and are conducting important joint research on a wide range of atmospheric physics issues, in particular such as natural radioactive tracers in the atmosphere; air pollution; atmospheric electricity, thunderstorm-hail processes; climate change in Georgia; assessment of bioclimatic resources of Georgia; assessment of the risk of hydrometeorological disasters; radar meteorology; weather modification, etc. In addition to scientific work, attention was also paid to the popularization of atmospheric research [1].

The results of joint research have been published in both domestic and international journals and collections, and presented at conferences of various levels. Thus, in 2008, at the initiative of the institutes of geophysics and hydrometeorology, a major international conference, "Climate, Natural Resources, and Natural Disasters in the South Caucasus", was held within the framework of the International Year of Planet Earth [1].

The one of most important results were obtained in large-scale studies of modern climate change in Georgia, which were launched in 1996 jointly with the Vakhushti Bagrationi Institute of Geography and continue to this day. First of all, an inventory of greenhouse gases was conducted in Georgia, spatial and temporal variations in the fields of air temperature, precipitation, cloudiness, aerosol air pollution, equivalent-effective air temperature, surface cover and other climate-forming parameters were studied, and an assessment was made of expected changes in air temperature in Tbilisi for the next few decades and the effects of these changes on human health [2-8]. It is noteworthy that in 2009, a group of leading scientists (K. Tavartkiladze, Institute of Geography; N. Begalishvili, Institute of Hydrometeorology and A. Amiranashvili, Institute of Geophysics) were awarded the Georgian National Prize for a series of works in the field of climate change in Georgia.

The second most important result was achieved in 2015, when, as a result of extensive preparatory work, the anti-hail service, which had ceased to exist in 1989, was restored in Kakheti over the area of approximately 650 thousand hectares [9-12].

The restored anti-hail system includes: contemporary meteorological radar Meteor 735CDP10 of firm Selex ES; central remote-control station with the change personnel; the automated system of the fire control; 85 rocket launching sites; the autonomous automated rocket guns; anti-hail rockets; scientific group; the group of the maintenance of radar and rocket guns. The test probation of system showed the prospect of its further use for dealing with the hail. The physical and economic effectiveness of anti-hail works in 2015 year, in spite of the limited quantity of means of action (rockets), it was not worse than it is earlier in the years with the action. It is significant that if in the past in Kakheti personnel of anti-hail service comprised

more than 800 people, at present this work it ensures only 30 people. Subsequently is assumed an increase in the shielded from the hail areas, and also, besides the anti-hail works, the use of radar for monitoring of dangerous hydrometeorological processes in eastern Georgia and adjacent to its territories of Armenia and Azerbaijan [12].

A brief information on joint research of the M. Nodia Institute of Geophysics, TSU and the Institute of Hydrometeorology, GTU, conducted in 2019–2023 is presented below.

Materials and methods

The data of the ground based hydrometeorological network of the National Environment Agency of Georgia, radar Meteor 735CDP10 of firm Selex ES of the anti-hail service in Kakheti and satellite observations of the Earth Observation Mission are used. Various data on environmental pollution were obtained through direct instrumental measurements and the use of chemical analysis.

Data analysis was carried out with the use of the standard statistical analysis methods of random events and methods of mathematical statistics for the non-accidental time-series of observations. Numerical modeling methods were used to simulate the spread of impurities in the atmosphere. GIS technologies were used to create the maps.

Results

During 2019-2023, a total of 53 scientific papers were published [13-66], including four monographs [14,35,36,46] and one book [34]. Joint research was conducted in such areas as weather modification [13,21,45], climate change [17,25,30,33,44,46,48,55,56,59], natural disasters [18,23,24,26,41,42,47,49-54,57,65], adverse meteorological phenomena [16,19,20,22,32,43,58,60,64], environmental pollution [34-40], bioclimate [14,15,27-29,31,61-63].

A brief overview of some of the works are presented below.

The works [13,21,45] present an analysis of scientific and practical work on the artificial impact of weather on Georgia in the past and present (fighting against snow, regulating the activity of lightning in clouds, dissipating fog, artificial regulation of precipitation, etc.). The prospects for the further development of these works are discussed [13].

Fig. 1. Scheme for the development of works on weather modification in Georgia and related activities for active and passive prevention of some types natural disasters [13].

The next expansion the works in Georgia on weather modification is planned (Fig. 1).

Acting polygon - Kakheti (black points - rocket launchers). An increase in the number of missile points; installation of an additional radar covering the territory of Kakheti; creation of an expanded network of meteorological stations for ground monitoring of the results of active impacts on hail processes and precipitation, etc.

Planned polygons.

Kvemo Kartli (yellow points - rocket launchers). In this region in the past century was polygon on the territories of municipalities Tetritskaro, etc. In the environments of the territory of municipality Ninotsminda the work on an increase in the atmospheric precipitation was conducted.

Shida Kartli (blue points - rocket launchers). Polygon on the territory of municipalities Gori, etc.

Samtskhe-Javakheti (green points - rocket launchers). Polygon on the territory municipalities Aspindza, Adigeni, Akhalkalaki etc.

Mtskheta-Mtianeti (red points - rocket launchers). Polygon on the territory of municipalities Mtskheta, Tianeti, etc. In the environments of the territory of municipality Tianeti previously the work on an increase in the atmospheric precipitation was conducted.

Territory of the capital of Georgia - Tbilisi. Work on active actions on atmospheric processes with the use of rocket technology for purposes of safety of population here are forbidden. It is possible the use of aircraft technology for the hail suppression and to the atmospheric precipitation regulation. It is also possibly the arrangement of rocket points on the boundaries of city for the action on the hail processes out of its territory.

Ajara. It is planned to organize work to reduce excess rainfall using ground (rocket, aerosol generators, etc.) and aircraft technologies.

To improve the efficiency of weather modification works in Kakheti and their implementation in other regions of Georgia, it is planned to purchase several new meteorological radars. In particular, on the territory of eastern Georgia, it is planned to install 1-3 additional radars, which will be interfaced with the existing radar to Chotori.

Is assumed the expansion of scientific studies on the development of new and the improvement of the existing active and passive methods of the prevention of natural catastrophes (hail, thunderstorm, shower precipitation, flood, the dust storms, fogs, landslides, avalanche, frosts, drought, forest fires, etc.). Renewal of the tests of different existing, improved and newly created ice-forming and hygroscopic reagents, and also other artificial aerosol formations for the active actions on the clouds and the fogs, fight with the frosts, the smog (pollution of atmospheric air), etc. The production of anti-hail rockets with the improved ballistic characteristics is planned (increase in the effective radius of action, etc.).

In particular, in order to increase the efficiency of passive prevention of natural disasters, it is planned to build a regional model for the relationship of radar parameters with the above-mentioned dangerous hydrometeorological phenomena. This will allow for an early (several tens of minutes) warning of the population and relevant authorities about the upcoming dangerous hydrometeorological situation.

Examples of radar monitoring of hail processes, rainfall, and dust formation migration in eastern Georgia and its neighboring countries (Azerbaijan, Armenia) are presented in [12,51]. In the case of relevant interstate agreements, it is possible to organize an international service for short-term warning of the population and emergency structures about the possibility of dangerous meteorological phenomena.

In conclusion, it is noted that in connection with global changes (climate warming, an increase in the number of natural disasters), works on the weather modification is of particular relevance. In the last century, Georgia was one of the flagships of these works. After the restoration of the activities of the anti-hail service in Kakheti, which proved to be effective with minimal maintenance, there appeared prospects for further development of work on weather modification also in other regions of Georgia.

In the foreseeable future, it is planned to elaboration both active and passive methods of natural disasters preventing [13].

A number of works are devoted to the problems of climate change in Georgia (precipitation, cloudiness, wind, air temperature, etc.)[17,25,30,33,44,46,48,55,56,59].

In the monograph [46] the natural factors causing the formation and variability of weather, as well as one of the important problems of modernity, climate change and causing reasons are studied in the complex manner using modern technologies. The data of the ground based hydrometeorological network and satellite observations of the Earth Observation Mission are used. The impact of climate change on the number of sectors of the country's economy (construction industry, tourism, healthcare, education and others) has been evaluated. The monograph has both scientific and practical value. The monograph is intended for specialists working in this field and the wide society. It can be used as the supplementary handbook for students of the Faculty of Natural Sciences of higher education institutions.

Statistical data on meteorological parameters associated with the Holiday Climate Index (mean monthly maximum air temperature, mean monthly relative air humidity, cloud cover, monthly precipitation, wind speed) in thirteen mountainous regions of Georgia (Bakhmaro, Bakuriani, Borjomi, Goderdzi, Gudauri, Khaishi, Khulo, Lentekhi, Mestia, Pasanauri, Shovi, Stepantsminda, Tianeti) from 1956 to 2015 are presented in [30]. In particular, the changeability of the indicated meteorological parameters into 1986÷2015 in comparison with 1956÷1985 for above enumerated points is studied.

The results of a statistical analysis of the monthly, semiannual and annual values of total cloudiness G in Tbilisi in 1956-2015 are represented in [33]. In particular, it was found that in the period from 1986 to 2015 compared to the period 1956-1985 in Tbilisi for all months and periods of the year (with the exception of August and December - no change of G values, and October - increase of cloudiness), there is a decrease of the values of total cloudiness. The linear trends of total cloudiness were studied for the period from 1956 to 2015. It is shown that the largest decrease of G values in 2015 compared to 1956 relative to the average value of total cloud cover in 1956-2015 was observed in June: -20.3%, the smallest - in April: -6.4%.

Predictive estimates of the number of hail days (HD) and their moving averages (for 3, 5, 7, 9 and 11 years – HD_3…HD_11) per warm period of year to 2050 and 2085 an example of Tbilisi was performed in [48]. Forecasting was carried out using the AAA version of the exponential smoothing (ETS) algorithm taking into account the periodicity in the pre-forecast time series. In particular, the following results were obtained. For the time series of the measured number of days with hail and HD_11 years, no pronounced peak in periodicity is observed. For time series HD_3, the periodicity is 14 years, HD_5 – 32 years, HD_7 and HD_9 – 31 years. In the period from 2022 to 2050, the range of variability of the average values of the central points of the forecast for the number of days with hail and the values of their 95% upper level is as follows: HD - from 0.9 to 3.8, HD_3 - from 1.0 to 3.0, HD_11 – from 1.0 to 1.6. In the period from 2022 to 2085, the range of variability of the average values of the central points of the forecast for the number of days with hail and the values of their 95% upper level is as follows: HD_5 - from 0.4 to 3.0, HD_7 - from 0.7 to 1.8, HD_9 - from 0.5 to 3.

The research results of the variability of the mean max annual air temperature at 39 locations in Georgia against the background of global climate change in 1956-2015 are presented in [55]. The statistical characteristics of the mean max annual air temperature in the period 1956-2015 (T), 1956-1985 (T_1) and 1986-2015 (T_2) for each point were studied.

It has been established that in the second period compared to the first, there is a significant increase in the average max air temperature at the 29 stations from 0.3˚C (Stepantsminda) to 1.2˚C (Bakuriani); for Shovi this difference is 1.1˚C. It is shown that between the T_1, T_2 values and the terrain height there has been observed the high inverse linear correlation and regression relationship there. At the same time, the lines of the regression equations are parallel with the increasing in the second period compared to the first by 0.6 ˚C.

It is shown, that a significant value of $(T_2- T_1)/T$ changes from 2.0 % (Chokhatauri) to 11.0% (Bakuriani); for Shovi this indicator is 8.4 %. The significant value $(T_2- T_1)/T$ increases with terrain height in accordance with a second power polynomial

Some results of comparative analysis of the average maximum annual, seasonal and monthly air temperature variability in Tbilisi and Shovi during 1956-2022 against the background of global warming in [56] are presented. The statistical characteristics of the mean max annual, seasonal and monthly air temperature in the period 1956-2022 (T), 1956-1985 (T_1) and 1993-2022 (T_2) for each point were studied.

It is shown that compared to Tbilisi, climate warming in Shovi is much more significant. For example, the increase in the mean annual max air temperature in Tbilisi in 1993-2022 compared to 1956-1885 was 0.8 ˚C, while in Shovi it was 1.9 ˚C. The situation is similar for the warm and cold half of the year.

The maximum increase in the mean max monthly air temperature at both points was observed in August. At the same time, in Tbilisi - 1.9 ˚C, and in Shovi - 3.7 ˚C.

It is shown that the trend of the mean max annual and seasonal air temperature in 1956-2022 in Tbilisi is described by the second power polynomial, and in Shovi - by the third power polynomial (Fig. 2). Using these equations, the average annual rate of increase in air temperature at both points was calculated. In particular, it was found that in 2011-2020 this speed in Shovi is three times higher than in Tbilisi [56].

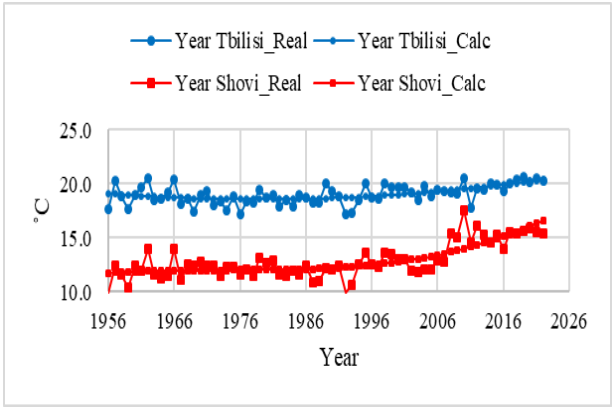

Trend of mean max annual air temperature in Tbilisi and Shovi in 1956-2022.

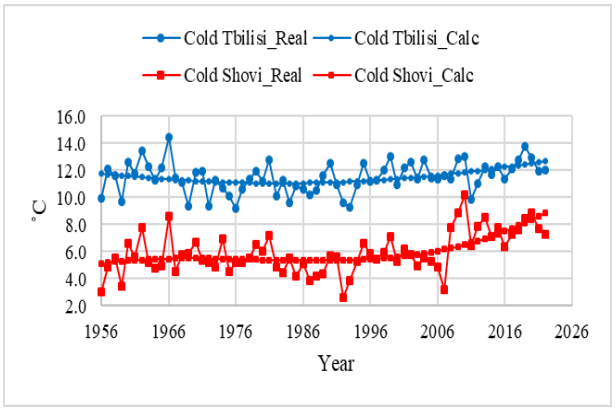

Trend of mean max air temperature in Tbilisi and Shovi in cold period in 1956-2022.

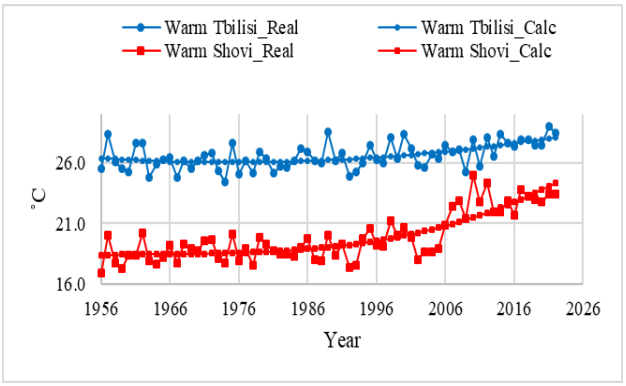

Trend of mean max air temperature in Tbilisi and Shovi in warm period in 1956-2022.

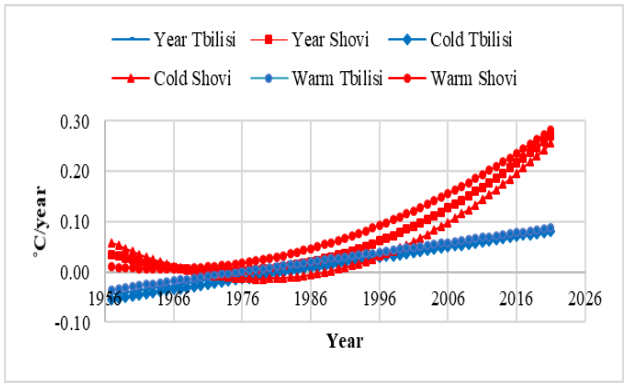

The mean max air temperature change rate in Tbilisi and Shovi in three periods of the year from 1956 to 2022.

Fig. 2. Average annual and seasonal variations of air temperature in Tbilisi and Shovi in 1956-2022 [56].

Some results statistical analysis of the daily mean (W_{mean}) and max (W_{max}) wind speed for Tbilisi from January 1, 1971 to December 31, 2020 are presented in [59]. In 1971-2020 annual mean of W_{mean} was 1.5 m/sec, and W_{max} - 9.1 m/sec. In 1996-2020 compared with 1971-1995 annual mean of W_{mean} increased by 0.8 m/sec, and W_{max} - by 0.3 m/sec. Intra annual distribution of monthly average of daily mean and max wind speed Tbilisi in 1971-2020 has the form of a sixth power polynomial. Regression equations were obtained for the relationship between the repetition of mean daily and maximum wind speed in Tbilisi with the central points of wind speed on the Beaufort Wind Scale.

A significant number of works are devoted to the study of natural disasters [18,23,24,26,41,42,47,49-54,57,65] and adverse meteorological phenomena [16,19,20,22,32,43,58,60,64] in Georgia (blizzards, forest fires, hail, heavy precipitation, floods, heavy snow and avalanches, storms, hurricanes, landslides, etc.). Some of the works [42,50,51-53,57,60] were carried out using data from the first natural disaster catalog created in Georgia [41,47,49,54,65].

In particular, according to data from 2014 to 2018 the distribution in Kakheti region of Georgia of hail storms (Fig. 3), heavy rainfall, floods and floodings (Fig. 4) was study [23,24].

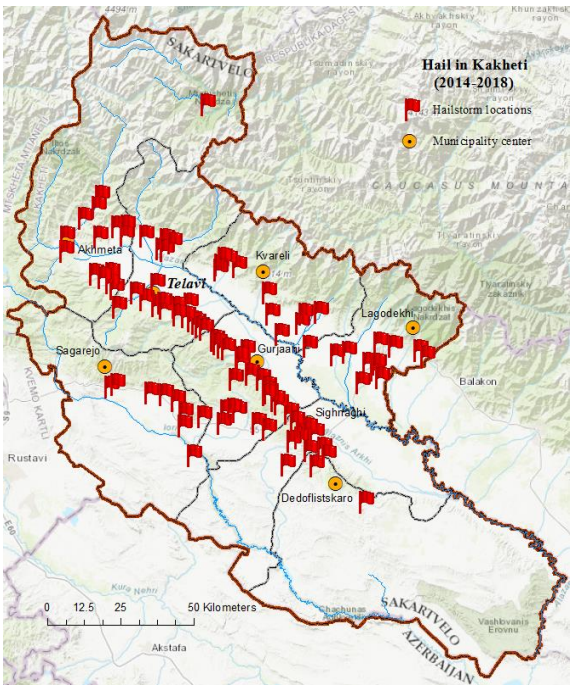

Fig. 3. Hail in Kakheti in 2014-2018 [23].

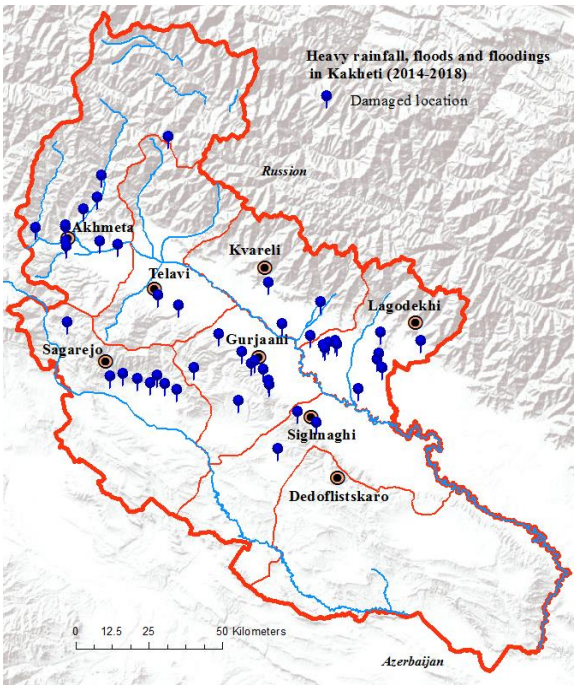

Fig. 4. Distribution of heavy rainfall, floods and floodings in Kakheti 2014-2018 [24].

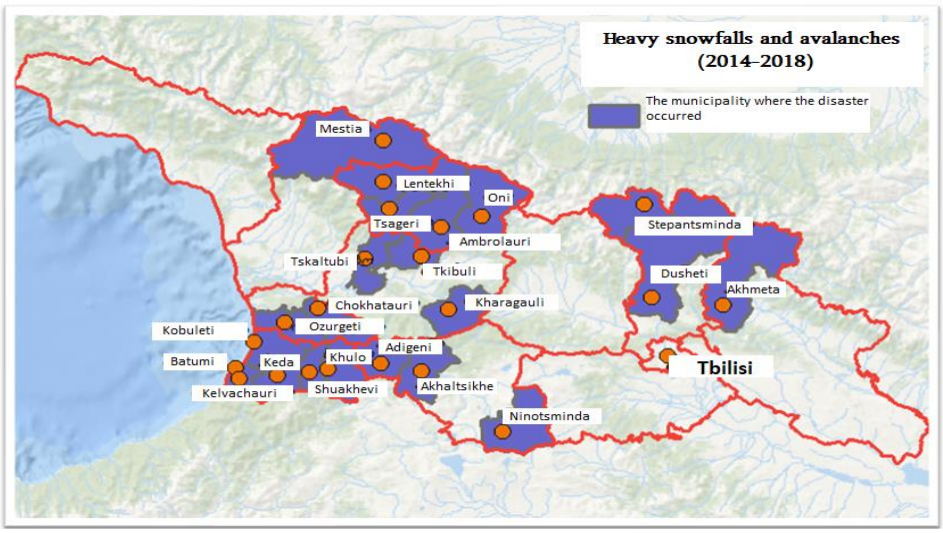

Fig. 5. Distribution of heavy snowfalls and avalanches in Georgia in 2014-2018 [43].

The results of the study of distribution on the territory of Georgia of heavy snowfalls and avalanches in 2014-2018 (Fig. 5) are presented in the work [43].

In [41,47,49,54,65] are present a new natural hazard database for the Republic of Georgia (GeNHs). This database includes a parametric catalogs of five types of natural hazard events (landslide, debris flow, flash flood, windstorm, and hail) causing significant economic loss and casualties in Georgia over the last decades and centuries, respectively. The compilation of these events is innovative as the entire country is covered, and it is timely and may be used by civil protection, risk managers, and other stakeholders in order to provide information for natural hazard and risk management as well as decision-making with respect to effective and efficient mitigation measures. The data included in the database was collected based on the

minimum requirements of data quality. Data quality included information on the order of magnitude for each hazard type and the related frequencies, a magnitude classification and harmonization of the corresponding data was carried out to obtain magnitude classifications. For each natural hazard type and event, the most reliable values of the main parameters were collected and determined from the set of available information. These included date of occurrence (year, month, day), time of occurrence (hour), location of occurrence (geographical coordinates), magnitude and intensity where appropriate, affected area, and associated loss (number of fatalities; losses in terms of economic values). The database contains the following information. Landslides were collected for the period between 1900 and 2022, with 1635 events. The magnitude of landslides (MLL) was taken as the logarithm of its volume (in m^3), with a resulting range between 3.0 and 9.0. Debris flows were collected for the period between 1776 and 2022, with 880 events. Debris flow magnitudes (MDF) were taken as the logarithm of the maximum volume (in m^3) of debris material discharged during a single event, with a resulting range between 3.5 and 7.5. Flash floods were collected for the period between 735 and 2022, with 1098 events. Flash flood magnitudes (MFF) were taken as the logarithm of the water peak discharge (in m^3/sec), with a range between 1.5 and 4.0. Windstorms were collected for the period between 1946 and 2022, with 1563 events. Windstorm magnitudes (MHR) were taken as wind speed (in m/s) divided by ten, with a range between 3.0 and 6.0. Hail storms were collected for the period between 1891 and 2022, with 2186 events. Hail storm magnitudes (MHL) were taken as the hail grain size (in mm) divided by ten, with a range between 0.4 and 11.0. This database will provide key input for further improvements of hazard and risk assessment, for the assessment of human and economic losses resulting from such hazards, for assessing possible effects of climate change as well as for evaluating new forecasting and early-warning efforts. The GeNHs database is accessible online [65] and will be kept updated in the future.

Some of the works [42,50,51-53,57,60] were carried out using data from the catalog [65].

For example, in [42] statistical analysis of the number of days with hail in Georgia in 2006-2021 was carried out. Long-term variations of the number of days with hail during the warm season in Tbilisi in 1891-2021 was study in [50].

The results of the analysis of radar studies of hail processes over the territories of Georgia and Azerbaijan on May 28 and July 13, 2019 in [51] are presented. Based on the values of the maximum size of hailstones in clouds, using the Zimenkov-Ivanov model, the expected sizes of hailstones falling on the earth's surface are calculated. The degree of damage to vineyards, wheat and corn, depending on the size of the hail, was determined by summarizing the known data on damage to these crops at different kinetic energy of hail and data on the average kinetic energy of hail of different magnitudes. Based on this compilation, regression equations were obtained for the relationship between the degree of damage to these crops and the size of hailstones, which have the form of a sixth degree of a polynomial. According to this equation, calculations were made of the degree of maximum damage to vineyards, wheat and corn along the trajectories of hail clouds over the territories of Georgia and Azerbaijan. In Fig. 6 example of maximum vineyards damage locations in Georgia and Azerbaijan is presented.

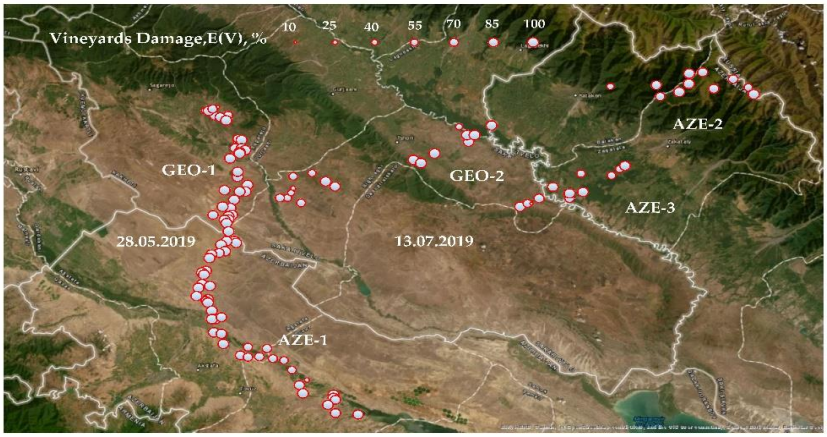

Fig. 6. Maximum vineyards damage locations in Georgia and Azerbaijan during the study period [51].

Analysis data on catastrophic floods in the vicinity of Tbilisi was conducted in [52]. Results of statistical characteristics of hurricane winds over Georgia for the period 1961–2022 in [53] was presented. In [57] statistical analysis of the number of days with hail and damage to agricultural crops from it in Kvemo Kartli (Georgia) was carried out.

A number of works are devoted to the study of environmental pollution [34-40].

The monograph [36] examines the assessment of the ecological state, conditions of placement of industrial arsenic waste in the industrial regions of Racha and Kvemo Svaneti, and also defines the main and possible directions of spread of arsenic toxic waste pollution. Based on the results of expeditionary and ecochemical studies, a numerical model of distribution of arsenic concentrations in water and bottom sediments of the Lukhuni and Tskhenistskali rivers by stationary sources is presented.

As for air pollution, very important and labor-intensive environmental studies have been carried out [34,35,37-40]. The studies used portable mobile devices Aeroqual Series 500 and TROTEC PC220 for measuring PM2.5, PM10 microparticles and some meteorological fields (wind speed, temperature, relative humidity), owned by the Institute of Hydrometeorology. With the help of these instruments, the data obtained as a result of special expeditionary measurements were used in the numerical implementation of the model of atmospheric processes on the scales α and β and the equations of pollution transfer-diffusion in a continuous medium, developed at the Institute of Geophysics.

As a result, the spread of dust, PM2.5 and PM10 microparticles in the cities of Tbilisi, Rustavi and Kutaisi and their environs was studied.

The main features characterizing the process of microparticle spread in complex terrain conditions were studied. The zones of increased dustiness of cities were identified, differences in the spatial distribution of atmospheric air pollution in the winter and summer seasons were revealed. The time intervals when areas of increased concentrations are formed or the air self-purification process occurs were determined. The temporal and spatial changes in dust concentration in the lower part of the atmospheric boundary layer were studied. The distribution of PM2.5 and PM10 concentrations in the atmosphere of Tbilisi during the COVID-19 pandemic (2020-2021) was investigated [34,35,37-40].

The book [34] is devoted to the problems of numerical modeling of dust dispersion in the atmosphere of Georgia. It provides a mathematical model of dust transport-diffusion in the atmosphere, a system of corresponding equations is obtained, an algorithm for numerical integration of equations is given, and the results of the model implementation are analyzed. In particular, the features of transboundary, regional and local dust dispersion are studied, the influence of relief of various scales on the dust transport-diffusion process. The model can be successfully used for theoretical study of the dispersion of atmospheric pollutants in areas with complex relief.

The monograph [35] is dedicated to the problems of numerical modeling of the propagation of microaerosols PM2.5 and PM10 (Particulate Matter) in the atmosphere of Tbilisi. It includes a mathematical model of the transfer-diffusion of a passive ingredient into the atmosphere, an algorithm for the numerical integration of equations, and an analysis of the results of the model implementation. The propagation of PM2.5 and PM10 in the atmosphere of Tbilisi during a background light air was studied. The model can be successfully used for the theoretical study of the distribution of air pollutants in a complex terrain.

The works [15,27-29,31,61-63] and monographs [14,46] discuss the bioclimatic features of Georgia and the related modern problems of development of the resort and tourism industry. A methodology for assessing tourism and recreational resources taking into account the dynamics of climate change has been developed in detail. The potential of tourism and recreational resources of different regions of Georgia and the patterns of its distribution in time and space have been determined.

The monograph [14] is devoted to modern problems of tourism industry. The method of evaluation of tourism-recreational resources is taken into consideration in detail in terms of climate change dynamics. The potential of tourism-recreational resources are estimated of two different regions of Georgia. The work uses the results of the project of the European Union “Tourism development prospects in Guria”.

In [27] a comparative analysis of data on the monthly values of Tourism Climate Index (TCI) and Holiday Climate Index (HCI) in Tbilisi is presented. Period of observation – 1956-2015. Average monthly values of HCI for the entire observation period varied from 62.0 ("Good", January) to 83.8 ("Excellent", May). As in the case with the TCI, according to the HCI, the bioclimatic conditions in Tbilisi are favorable for resort and tourist purposes all year round. Comparison of the values and categories of the Tourism Climate Index and Holiday Climate Index shows that the intraannual variation of both indices is similar and has a bimodal form. However, given that the TCI is calculated for the socalled "average tourist" (regardless of gender, age, physical condition), the values and categories of this index is lower than the HCI values and categories.

In [28] the detailed information on the variability of the monthly values of the Holiday Climate Index (HCI) in Tbilisi in 1956-2015 are presented. It also presents data on the interval forecast of variability of HCI values in Tbilisi for the next few decades.

Data about long-term monthly average values of Holiday Climate Index (HCI) for 12 locations of Kakheti (Akhmeta, Dedoplistskaro, Gombori, Gurjaani, Kvareli, Lagodekhi, Omalo, Sagarejo, Shiraki, Telavi, Tsnori and Udabno) are presented in [29]. For 6 stations of this region (Dedoplistskaro, Gurjaani, Kvareli, Lagodekhi, Sagarejo and Telavi) detailed analysis of the monthly, seasonally and annually HCIs values over a 60-year period (1956-2015) are carried out. Comparison of monthly values of HCI and Tourism Climate Index (TCI) for four points of Kakheti (Dedoplistskaro, Kvareli, Sagarejo and Telavi) based on data from 1961 to 2010 are carried out.

The long-term monthly average values of Holiday Climate Index (HCI) for 13 mountainous locations of Georgia (Bakhmaro, Bakuriani, Borjomi, Goderdzi, Gudauri, Khaishi, Khulo, Lentekhi, Mestia, Pasanauri, Shovi, Stepantsminda, Tianeti) are presented in [31,46,63]. Detailed analysis of the monthly, seasonal and annual HCIs values over the 60-year period (1956-2015) are carried out. Comparison of HCI and Tourism Climate Index (TCI) monthly values for three locations (Goderdzi, Khulo and Mestia) based on data from 1961 to 2010 are carried out. The variability of the HCI in 1986-2015 compared to 1956-1985 was studied, and the trends of the HCI in 1956-2015 were also investigated. Using Mestia as an example, the expected changes in monthly, seasonal and annual HCI values for 2041-2070 and 2071-2100 year periods has been assested.

In article [61] discusses the impact of climate and its changes on the development of the tourism sector in Georgia. To evaluate tourism-recreational resources in Georgia for the first time several the Tourism Climatic Indexes were used, based on the combination of different meteorological elements (air temperature, atmospheric precipitation, relative humidity, average duration of sunshine). On the basis of the obtained data, correct decisions should be made when designing tours in different climatic zones against negative climatic events.

It is noted that the World Meteorological Organization (WMO) has organized a number of events to support tourism. It provides World Tourism Organization (WTO) members with early warnings about natural disasters, glacier recession, water resources and climate change. WTO closely cooperates with WMO. Forecasts of climate and extreme hydro meteorological events provided by the National Hydro meteorological Services are particularly important in today's world, as regional climate variations have emerged in the wake of global climate change.

Conclusion

In the future, it is planned to continue the above-mentioned joint research, as well as to combine efforts to solve new scientific and applied problems (experimental modeling of atmospheric processes, development of recommendations for adaptation to expected climate changes, improvement of existing methods of active influence on atmospheric processes and creation of new ones, assessment of the vulnerability of biological systems to air pollution, development of proposals for the prevention of natural disasters, intensification of work on the creation of a bioclimatic passport of resort and tourist zones of Georgia, intensification of educational activities for a wide range of people, etc.).

Particular attention is planned to be paid to issues of experimental modeling of atmospheric processes in a large cloud chamber of the Institute of Geophysics. In particular, the following experiments are planned [67]:

- Modeling of soil erosion processes;
- Modeling of slanting rains on buildings and structures [the work has begun, 68];
- Development of new and improvement of existing methods for creating various aerodisperse systems (neutral and charged fogs, aerosol formations, etc.);
- Modeling the influence of a complex of various meteorological and geophysical parameters (electromagnetic fields and radiation, ozone, meteorological elements, etc.) on living organisms and plants;
- Development of new and improvement of existing methods of influencing harmful characteristics of the atmosphere (dispersion of warm fogs; purification of air from aerosol and gas impurities; protection of living organisms and plants from high concentrations of ozone and levels of electromagnetic fields and radiation, including ultraviolet, etc.);
- Improvement of precipitation control methods.

It is also planned to train specialists in the field of experimental atmospheric physics and applied meteorology, as well as to improve the qualifications of interested persons in this field of science.

It is also planned to use the resources of this facility to conduct various educational and cognitive activities.

Considering the importance of the above studies, under appropriate conditions of state support, the possibility of participating in international projects and obtaining the status of an international laboratory is not excluded.

References

[1] Ghlonti N., Tsintsadze T. Analysis of Contemporary State and Prospect for the Development of the Joint Operations of the Institutes of Geophysics and Hydrometeorology in the field of Atmospheric Research in Georgia. Transactions of the Institute of Hydrometeorology, Georgian Tekhnical University, vol. 119, 2013, 159-163, (in Russian)

[2] Budagashvili T., Karchava J., Gunia G., Intskirveli L., Kuchava T., Gurgenidze M., Amiranashvili A., Chikhladze T. Inventory of Greenhouze Gas Emissions and Sinks, Georgia's Initial National Communication on Under the United Nations Framework Convection on Climate Change, Project GEO/96/G31, Tbilisi, 1999,33-45.

[3] Tavartkiladze K., Begalishvili N., Kharchilava J., Mumladze D., Amiranashvili A., Vachnadze J., Shengelia I., Amiranashvili V. Contemporary Climate Change in Georgia. Regime of Some Climate Parameters and their Variability. Georgian Acad. of Sc., Inst. of Geography, Geophysics and Hidrometeorology, Monograph, Tbilisi, ISBN 99928-885-4.7, 2006, pp. 1-177, (in Georgian).

[4] Amiranashvili A., Chikhladze V., Kartvelishvili L. Expected Change of Average Semi-Annual and Annual Values of Air Temperature and Precipitation in Tbilisi. Journal of the Georgian Geophysical Society, Issue B. Physics of Atmosphere, Ocean and Space Plasma, ISSN 1512-1127, vol. 13B, Tbilisi, 2009, pp. 50 – 54.

[5] Amiranashvili A., Kartvelishvili L., Khurodze T. Application of Some Statistic Methods for the Prognostication of Long-Term Air Temperature Changes (Tbilisi Case), Transactions of the International Scientific Conference Dedicated to the 90th Anniversary of Georgian Technical University "Basic Paradigms in Science and Technology Development for the 21th Century", Tbilisi, Georgia, September 19-21, 2012, Part 2, ISBN 978-9941-20-098-4, Publishing House "Technical University", 2012, pp. 331-338, (in Russian).

[6] Amiranashvili A, Kartvelishvili L. Long – Term Variations of Air Effective Temperature in Tbilisi. Papers of the Int. Conference International Year of the Planet Earth "Climate, Natural Resources, Disasters in tne South Caucasus", Trans. of the Institute of Hydrometeorology, vol. No 115, ISSN 1512-0902, Tbilisi, 18 – 19 November, 2008, pp. 214 – 219 (in Russian).

[7] Amiranashvili A.G., Kartvelishvili L.G., Saakashvili N.M., Chikhladze V.A. Long-Term Variations of Air Effective Temperature in Kutaisi, Modern Problems of Using of Health Resort Resources. Collection of Scientific Works of International Conference, Sairme, Georgia, June 10-13, 2010, ISBN 978-9941-0-2529-7, Tbilisi, 2010, pp. 152-157, (in Russian).

[8] Amiranashvili A., Chikhladze V., Kartvelishvili L., Khazaradze K. Expected Change of the Extremal Air Temperature and its Influence on the Mortality (Based on the Example to Tbilisi City), International Cooperation Network for East European and Central Asian Countries: EECA Conference - October 7-8, 2010, Yerevan, Armenia, http://be.sci.am/.

[9] Amiranashvili A., Bakhsoliani M., Begalishvili N., Beradze N., Beritashvili B., Rekhviashvili R., Tsintsadze T., Rukhadze N. On the Restoration of Precipitation Modification Activities in Eastern Georgia.Trans. of the Institute of Hydrometeorology of Acad. of. Sc. of Georgia, vol. 108, ISSN 1512-0902, Tbilisi, 2002, pp. 249-260, (in Russian).

[10] Amiranashvili A., Bakgsoliani B., Begalishvili N., Beritashvili B., Rekhviashvili R., Tsintsadze T., Chitanava R. On the Necessity of Resumption of Atmospheric Processes Modification Activities in Georgia. Trans. of the Institute of Hydrometeorology, Georgian Technical University, 2013, v. 119, pp.144-152, (in Russian).

[11] Elizbarashvili E. Sh., Amiranashvili A. G., Varazanashvili O. Sh., Tsereteli N. S., Elizbarashvili M. E., Elizbarashvili Sh. E., Pipia M. G. Hailstorms in the Territory of Georgia. European Geographical Studies, ISSN: 2312-0029, vol.2, № 2, 2014, pp. 55-69, DOI: 10.13187/egs.2014.2.55, www.ejournal9.com, (in Russian).

[12] Amiranashvili A.G., Chikhladze V.A., Dzodzuashvili U.V., Ghlonti N.Ya., Sauri I.P. Reconstruction of Anti-Hail System in Kakheti (Georgia). Journal of the Georgian Geophysical Society, Issue B. Physics of Atmosphere, Ocean and Space Plasma, v.18B, Tbilisi, 2015, pp. 92-106.

[13] Amiranashvili A., Chikhladze V., Dzodzuashvili U., Ghlonti N., Sauri I., Telia Sh., Tsintsadze T. Weather Modification in Georgia: Past, Present, Prospects for Development. Int. Sc. Conf. "Natural Disasters in Georgia: Monitoring, Prevention, Mitigation". Proceedings, ISBN 978-9941-13-899-7, Publish House of Iv. Javakhishvili Tbilisi State University, December 12-14, Tbilisi, 2019, pp. 216-222, http://dspace.gela.org.ge/bitstream/123456789/8675/1/51_Conf_NDG_2019.pdf

[14] Kartvelishvili L., Amiranashvili A., Megrelidze L., Kurdashvili L. Turistul Rekreaciuli Resursebis Shefaseba Klimatis Cvlilebebis Fonze. Publish Hous "Mtsignobari", ISBN 978-9941-485-01-5, Tbilisi, 2019, 161 p., (in Georgian) http://dspace.nplg.gov.ge/bitstream/1234/293074/1/turistulRekreaciuliResursebisShefasebaKlimatisCvlilebebisFonze.pdf

[15] Amiranashvili A., Kartvelishvili L. Statistical Characteristics of the Monthly Mean Values of Tourism Climate Index in Mestia (Georgia) in 1961-2010. Journal of the Georgian Geophysical Society, ISSN: 1512-1127, Physics of Solid Earth, Atmosphere, Ocean and Space Plasma, v. 22(2), 2019, pp. 68 – 79, http://openjournals.gela.org.ge/index.php/GGS/

[16] Pipia M., Elizbarashvili E., Amiranashvili A., Beglarashvili N. Dangerous Regions of Blizzard in Georgia. Annals of Agrarian Science, ISSN 1512-1887, vol. 17, No 4, 2019, pp. 403 – 408. https://www.researchgate.net/profile/Avtandil-Amiranashvili-2/publication/341992370_Annals_of_Agrarian_Science_A_B_S_T_R_A_C_T_Dangerous_regions_of_blizzard_in_georgia/links/5edd2ab7299bf1c67d4b92ab/Annals-of-Agrarian-Science-A-B-S-T-R-A-C-T-Dangerous-regions-of-blizzard-in-georgia.pdf

[17] Amiranashvili A., Bliadze T., Kartvelishvili L. Statistical Characteristics of Monthly Sums of Atmospheric Precipitations in Tianeti (Georgia) in 1956-2015. Trans. of Mikheil Nodia institute of Geophysics, ISSN 1512-1135, vol. 70, Tb., 2019, pp. 112-118, (in Russian), http://dspace.gela.org.ge/handle/123456789/254

[18] Janelidze I., Pipia M. Hail Storms in Georgia in 2016-2018. Int. Sc. Conf. "Natural Disasters in Georgia: Monitoring, Prevention, Mitigation". Proceedings, ISBN 978-9941-13-899-7, Publish House of Iv. Javakhishvili Tbilisi State University, December 12-14, Tbilisi, 2019, pp. 114-116.

[19] Bliadze T., Kirkitadze D., Samkharadze I., Tsiklauri Kh. Statistical Characteristics of Angstrom Fire Index for Tbilisi. Int. Sc. Conf. "Natural Disasters in Georgia: Monitoring, Prevention, Mitigation". Proceedings, ISBN 978-9941-13-899-7, Publish House of Iv. Javakhishvili Tbilisi State University, December 12-14, Tbilisi, 2019, pp. 191-194.

[20] Bliadze T., Kirkitadze D., Samkharadze I., Tsiklauri Kh. Statistical Characteristics of Angstrom Fire Index for Telavi (Georgia). Int. Sc. Conf. „Modern Problems of Ecology", Proc., ISSN 1512-1976, v. 7, Tbilisi-Telavi, Georgia, 26-28 September, 2020, pp. 64-67.

[21] Amiranashvili A., Kveselava N., Ghlonti N, Chikhladze V., Tsintsadze T. History of Active Actions on the Natural Phenomena in Georgia. Int. Sc. Conf. „Modern Problems of Ecology", Proceedings, ISSN 1512-1976, v. 7, Tbilisi-Telavi, Georgia, 26-28 September, 2020, pp. 147-152, (in Georgian).

[22] Javakhishvili N., Kekenadze E., Mitin M., Samkharadze I. Storm Wind in Tbilisi and Rustavi Cities on 21 September 2019. Analysis of Data of Radar, Aerological and Ground-Based Measurements. Int. Sc. Conf. „Modern Problems of Ecology", Proc., ISSN 1512-1976, v. 7, Tbilisi-Telavi, Georgia, 26-28 September, 2020, pp. 172-175.

[23] Beglarashvili N., Janelidze I., Pipia M., Varamashvili N. Hail Storms in Kakheti (Georgia) in 2014-2018. Int. Sc. Conf. „Modern Problems of Ecology“, Proc., ISSN 1512-1976, v. 7, Tbilisi-Telavi, Georgia, 26-28 September, 2020, pp. 176-179.
[24] Beglarashvili N., Janelidze I., Pipia M., Varamashvili N. Heavy Rainfall, Floods and Floodings in Kakheti (Georgia) in 2014-2018. Int. Sc. Conf. „Modern Problems of Ecology“, Proc., ISSN 1512-1976, v. 7, Tbilisi-Telavi, Georgia, 26-28 September, 2020, pp. 180-184.
[25] Bliadze T., Gvasalia G., Kartvelishvili L, Kirkitadze D., Mekoshkishvili N. Variability of the Annual Sum of Atmospheric Precipitations in Kakheti in 1956-2015. Int. Sc. Conf. „Modern Problems of Ecology“, Proc., ISSN 1512-1976, v. 7, Tbilisi-Telavi, Georgia, 26-28 September, 2020, pp. 193-196.
[26] Beglarashvili N., Varamashvili N., Pipia M., Chikhladze V., Janelidze I. Hail Storms in Georgia in 2014-2018.Transactions of Mikheil Nodia Institute of Geophysics, ISSN 1512-1135, vol. LXXII, 2020, pp. 115-122, (in Georgian).
[27] Amiranashvili A., Kartvelishvili L., Matzarakis A. Comparison of the Holiday Climate Index (HCI) and the Tourism Climate Index (TCI) in Tbilisi. Int. Sc. Conf. „Modern Problems of Ecology“, Proc., ISSN 1512-1976, v. 7, Tbilisi-Telavi, Georgia, 26-28 September, 2020, pp. 424-427.
[28] Amiranashvili A., Kartvelishvili L., Matzarakis A. Changeability of the Holiday Climate Index (HCI) in Tbilisi. Trans. of M. Nodia Institute of Geophisics, ISSN 1512-1135, vol. LXXII, Tbilisi, 2020, pp. 131-139.
[29] Amiranashvili A.G., Kartvelishvili L.G. Holiday Climate Index in Kakheti (Georgia). Journal of the Georgian Geophysical Society, e-ISSN: 2667-9973, p-ISSN: 1512-1127, Physics of Solid Earth, Atmosphere, Ocean and Space Plasma, v. 24(1), 2021, pp. 44-62. DOI: https://doi.org/10.48614/ggs2420212883
[30] Amiranashvili A.G., Kartvelishvili L.G., Kutaladze N.B., Megrelidze L.D., Tatishvili M.R. Changeability of the Meteorological Parameters Associated with Holiday Climate Index in Different Mountainous Regions of Georgia in 1956-2015. Journal of the Georgian Geophysical Society, e-ISSN: 2667-9973, p-ISSN: 1512-1127, Physics of Solid Earth, Atmosphere, Ocean and Space Plasma, v. 24(2), 2021, pp. 78-91. DOI: https://doi.org/10.48614/ggs2420213326
[31] Amiranashvili A.G., Kartvelishvili L.G., Kutaladze N.B., Megrelidze L.D., Tatishvili M.R. Holiday Climate Index in Some Mountainous Regions of Georgia. Journal of the Georgian Geophysical Society, e-ISSN: 2667-9973, p-ISSN: 1512-1127, Physics of Solid Earth, Atmosphere, Ocean and Space Plasma, v. 24(2), 2021, pp. 92 – 117. DOI: https://doi.org/10.48614/ggs2420213327
[32] Beglarashvili N., Chikhladze V., Janelidze I., Pipia M., Tsintsadze T. Strong Wind on the Territory of Georgia in 2014-2018. Int. Sc. Conf. „Natural Disasters in the 21st Century: Monitoring, Prevention, Mitigation“. Proceedings, ISBN 978-9941-491-52-8, Tbilisi, Georgia, December 20-22, 2021. Publish House of Iv. Javakhishvili Tbilisi State University, Tbilisi, 2021, pp. 19 - 22.
[33] Bliadze T., Kartvelishvili L. Kirkitadze D. Changeability of the Total Cloudiness in Tbilisi in 1956-2015. Int. Sc. Conf. „Natural Disasters in the 21st Century: Monitoring, Prevention, Mitigation“. Proceedings, ISBN 978-9941-491-52-8, Tbilisi, Georgia, December 20-22, 2021. Publish House of Iv. Javakhishvili Tbilisi State University, Tbilisi, 2021, pp. 31 - 34.
[34] Surmava A., Intskirveli L., Kukhalashvili V. Numerical Modeling of the Transborder, Regional and Local Diffusion of the Dust in Georgian Atmosphere. Monography, ISBN 978-9941-28-810-4, Tbilisi, 2021, 117 p., (in Georgian). http://dspace.gela.org.ge/handle/123456789/9597
[35] Surmava A., Intskirveli L., Gigauri N., Kukhalashvili V. PM2.5 and PM10 Particulate Matters in the Atmosphere of Tbilisi City. Monography, ISBN 978-9941-8-4028-9, Tbilisi, 2021, 92 p., (in Georgian). https://dspace.nplg.gov.ge/bitstream/1234/364657/1/PM2.5_Da_PM10_Mikroaerozolebo_Tbilisis_Atmosferoshi.pdf
[36] Bagrationi N., Gverdtsiteli L., Gvakharia V., Chirakadze Ar., Surmava Al. Darishkhanis samretsvelo narchenebis gantavsebisa da gavrtselebis arealis ekologiuri mdgomareobis shepaseba. Monograpia, ISBN 978-9941-28-809-8, Tbilisi, 2021, 120 gv. https://publishhouse.gtu.ge/en/post/1753
[37] Surmava A., Gigauri N.,Kukhalashvili V., Intskirveli L., Demetrashvili D. Numerical Investigation of the Dependence of a Atmospheric Pollution of City with a Complex Relief on the Direction of Background Wind. Annals of Agrarian Science, vol. 19, N 3, 2021, pp.191-198.
[38] Gigauri N., Surmava A., Intskirveli L.,Demetrashvili D.,Gverdtsiteli L., Pipia M. Numerical Modeling of PM2.5 Propagation in Tbilisi Atmosphere in Winter. I. A Case of Background South Light Wind. Int. Sc. Conf. „Natural Disasters in the 21st Century: Monitoring, Prevention, Mitigation“. Proceedings, ISBN 978-9941-491-52-8, Tbilisi, Georgia, December 20-22, 2021. Publish House of Iv. Javakhishvili Tbilisi State University, Tbilisi, 2021, pp. 74 - 78.

[39] Surmava A., Gverdtsiteli L., Intskirveli L., Gigauri N. Numerical Simulation of Dust Distribution in City Tbilisi Territory in the Winter Period. Journal of the Georgian Geophysical Society, Issue B, Physics of solid Earth, Atmosphere, Ocean and Space Plasma, Vol.24(1), 2021, pp. 37-43

[40] Kukhalashvili V., Pipia M., Gigauri N., Surmava A., Intskirveli L. Study of Tbilisi City Atmosphere Pollution with PM2.5 and PM10-Microparticles During COVID-19 Pandemic Period. Journal of the Georgian Geophysical Society, e-ISSN: 2667-9973, p-ISSN: 1512-1127, Physics of Solid Earth, Atmosphere, Ocean and Space Plasma, v. 25(2), 2022, pp. 29–37. DOI: https://doi.org/10.48614/ggs2520225958

[41] Varazanashvili O.Sh., Gaprindashvili G.M., Elizbarashvili E.Sh., Basilashvili Ts.Z., Amiranashvili A.G. Principles of Natural Hazards Catalogs Compiling and Magnitude Classification. Journal of the Georgian Geophysical Society, e-ISSN: 2667-9973, p-ISSN: 1512-1127, Physics of Solid Earth, Atmosphere, Ocean and Space Plasma, v. 25(1), 2022, pp. 5-11. https://doi.org/10.48614/ggs2520224794

[42] Amiranashvili A., Basilashvili Ts., Elizbarashvili E., Gaprindashvili G., Varazanashvili O. Statistical Analysis of the Number of Days with Hail in Georgia According to Meteorological Stations Data in 2006-2021. Int. Conf. of Young Scientists “Modern Problems of Earth Sciences”. Proceedings, ISBN 978-9941-36-044-2, Publish House of Iv. Javakhishvili Tbilisi State University, Tbilisi, November 21-22, 2022, pp. 164-168. http://openlibrary.ge/handle/123456789/10249

[43] Beglarashvili N., Gorgijanidze S., Kobakhidze N., Pipia M., Chikhladze V., Janelidze I., Jincharadze G. Heavy Snow and Avalanches on the Territory of Georgia in 2014-2018. Journal of the Georgian Geophysical Society, e-ISSN: 2667-9973, p-ISSN: 1512-1127, Physics of Solid Earth, Atmosphere, Ocean and Space Plasma, v. 25(2), 2022, pp. 24–28. DOI: https://doi.org/10.48614/ggs2520225957

[44] Amiranashvili A., Jamrishvili N., Janelidze I., Pipia M., Tavidashvili Kh. Statistical Analysis of the Daily Wind Speed in Tbilisi in 1971-2016. Int. Conf. of Young Scientists “Modern Problems of Earth Sciences”. Proceedings, ISBN 978-9941-36-044-2, Publish House of Iv. Javakhishvili Tbilisi State University, Tbilisi, November 21-22, 2022, pp. 159-163. http://openlibrary.ge/handle/123456789/10250

[45] Kapanadze N., Mkurnalidze I., Pipia M. Retrospective Analysis of Articifial Regulation of Precipitation. Transactions of Mikheil Nodia Institute of Geophysics, ISSN 1512-1135, vol. LXXV, 2022, pp. 76-92 , (in Georgian).http://openlibrary.ge/handle/123456789/10300

[46] Kartvelishvili L., Tatishvili M., Amiranashvili A., Megrelidze L., Kutaladze N. Weather, Climate and their Change Regularities for the Conditions of Georgia. Monograph, Publishing House “UNIVERSAL”, ISBN: 978-9941-33-465-8, Tbilisi 2023, 406 p., https://doi.org/10.52340/mng.9789941334658

[47] Gaprindashvili G., Varazanashvili O., Elizbarashvili E., Basilashvili Ts., Amiranashvili A., Fuchs S. GeNHs: the First Natural Hazard Event Database for the Republic of Georgia. EGU General Assembly 2023, EGU23-1614, https://doi.org/10.5194/egusphere-egu23-1614; https://meetingorganizer.copernicus.org/EGU23/EGU23-1614.html

[48] Amiranashvili A., Elizbarashvili E., Pipia M., Varazanashvili O. Expected Changes of the Number of Days with Hail in Tbilisi to 2085. Int. Sc. Conf. "Geophysical Processes in the Earth and its Envelopes". Proceedings, ISBN 978-9941-36-147-0, Publish House of Iv. Javakhishvili Tbilisi State University, November 16-17, 2023, pp. 138-142. http://www.openlibrary.ge/handle/123456789/10420

[49] Varazanashvili O., Gaprindashvili G., Elizbarashvili E., Amiranashvili A., Basilashvili Ts., Fuchs S. New Natural Hazard Event Database for the Republic of Georgia (GeNHs): Catalogs Compiling Principles and Results. Int. Sc. Conf. "Geophysical Processes in the Earth and its Envelopes". Proceedings, ISBN 978-9941-36-147-0, Publish House of Iv. Javakhishvili Tbilisi State University, November 16-17, 2023, pp. 185-187, (in Georgian). http://109.205.44.60/bitstream/123456789/10431/1/44_IG_90.pdf

[50] Amiranashvili A., Elizbarashvili E., Varazanashvili O., Pipia M. Statistical Analysis of the Number of Days with Hail During the warm Season in Tbilisi in 1891-2021. Transactions IHM, GTU, ISSN: 1512-0902ISSN: 1512-0902, vol.133, 2023, pp.74-77, (in Georgian), doi.org/10.36073/1512-0902-2023-133-74-77; http://openlibrary.ge/bitstream/123456789/10340/1/133-14.pdf

[51] Pipia M., Amiranashvili A., Beglarashvili N., Elizbarashvili E., Varazanashvili O. Analysis and Damage Assessment of Hail Processes in Georgia and Azerbaijan Using Radar Data (On the Example of May 28 and July 13, 2019). Reliability: Theory & Applications, ISSN: 1932-2321, vol. 18, iss. SI 5 (75), pp. 267-274, DOI: 10.24412/1932-2321-2023-575-267-274, https://cyberleninka.ru/article/n/analysis-and-damage-assessment-of-hail-processes-in-georgia-and-azerbaijan-using-radar-data-on-the-example-of-may-28-and-july-13

[52] Amiranashvili A., Basilashvili Ts., Elizbarashvili E., Varazanashvili O. Catastrophic Floods in the Vicinity of Tbilisi. Transactions IHM, GTU, ISSN: 1512-0902, vol.133, 2023, pp. 56-61, (in Georgian), doi.org/10.36073/1512-0902-2023-133-56-61; http://openlibrary.ge/bitstream/123456789/10337/1/133-11.pdf; doi.org/10.36073/1512-0902-2023-133-56-61

[53] Elizbarashvili E.Sh., Varazanashvili O.Sh., Amiranashvili A.G., Fuchs F., Basilashvili Ts.Z. Statistical Characteristics of Hurricane Winds over Georgia for the Period 1961–2022. European Geographical Studies, E-ISSN: 2413-7197, 10(1), 2023, pp. 8-18, DOI: 10.13187/egs.2023.1.8, https://egs.cherkasgu.press

[54] Varazanashvili O., Gaprindashvili G., Elizbarashvili E., Amiranashvili A., Basilashvili Ts., Fuchs S. New Parametric Catalogs of Natural Hazard Events for Georgia. Transactions of Mikheil Nodia Institute of Geophysics, ISSN 1512-1135, vol. LXXVI, 2023, pp. 168-177, (in Georgian).. http://dspace.gela.org.ge/handle/123456789/10483

[55] Amiranashvili A., Kartvelishvili L., Kutaladze N., Megrelidze L., Tatishvili M. Variability of the Mean Max Annual Air Temperature in 39 Locations of Georgia in 1956-2015. Int. Sc. Conf. "Geophysical Processes in the Earth and its Envelopes". Proceedings, ISBN 978-9941-36-147-0, Publish House of Iv. Javakhishvili Tbilisi State University, November 16-17, 2023, pp. 122-126. http://109.205.44.60/handle/123456789/10417

[56] Amiranashvili A., Kartvelishvili L., Kutaladze N., Megrelidze L., Tatishvili M. Comparison of the Mean Max Annual, Seasonal and Monthly Air Temperature Variability in Tbilisi and Shovi in 1956-2022. Int. Sc. Conf. "Geophysical Processes in the Earth and its Envelopes". Proceedings, ISBN 978-9941-36-147-0, Publish House of Iv. Javakhishvili Tbilisi State University, November 16-17, 2023, pp. 127-132. http://www.openlibrary.ge/bitstream/123456789/10418/1/32_IG_90.pdf

[57] Amiranashvili A., Bolashvili N., Elizbarashvili E., Liparteliani G., Suknidze N., Tsirgvava G., Varazanashvili O. Statistical Analysis of the Number of Days with Hail and Damage to Agricultural Crops from it in Kvemo Kartli (Georgia). Int. Sc. Conf. "Geophysical Processes in the Earth and its Envelopes". Proceedings, ISBN 978-9941-36-147-0, Publish House of Iv. Javakhishvili Tbilisi State University, November 16-17, 2023, pp. 133-137. http://www.openlibrary.ge/handle/123456789/10419

[58] Beglarashvili N., Jamrishvili N., Janelidze I., Pipia M., Tavidashvili Kh. Analysis of Strong Precipitation in Tbilisi on August 29, 2023. Int. Sc. Conf. "Geophysical Processes in the Earth and its Envelopes". Proceedings, ISBN 978-9941-36-147-0, Publish House of Iv. Javakhishvili Tbilisi State University, November 16-17, 2023, pp. 143-146. http://www.dspace.gela.org.ge/handle/123456789/10421

[59] Beglarashvili N., Jamrishvili N., Janelidze I., Pipia M., Tavidashvili Kh., Tsintsadze T. Some Results of Statistical Analysis of the Daily Wind Speed in Tbilisi in 1971-2020. Int. Sc. Conf. "Geophysical Processes in the Earth and its Envelopes". Proceedings, ISBN 978-9941-36-147-0, Publish House of Iv. Javakhishvili Tbilisi State University, November 16-17, 2023, pp. 151-155. http://www.openlibrary.ge/handle/123456789/10423

[60] Elizbarashvili E., Varazanashvili O., Lagidze L., Pipia M., Chikhladze V. About Strong Winds in Kakheti Region. Int. Sc. Conf. "Geophysical Processes in the Earth and its Envelopes". Proceedings, ISBN 978-9941-36-147-0, Publish House of Iv. Javakhishvili Tbilisi State University, November 16-17, 2023, pp. 156-160, (in Georgian). http://www.openlibrary.ge/handle/123456789/10424

[61] Kartvelishvili L., Amiranashvili A. Development of the Tourism Industry on the Base Climate Change in Georgia. Int. Sc. Conf. "Natural Resources and Resorts, as Sustainable Development Factors". From a Series of Monographs "Natural Resources and Resorts as Sustainable Development Factors", ISBN 978-9941-8-5964-9, Tbilisi, October 27-28, 2023, pp. 114-117, https://nrr.gtu.ge/upload/docs/კრებული.pdf

[62] Amiranashvili A., Kartvelishvili L., Kezevadze N. Development Trends of the Tourism Industry in the Context of Climate Change in Georgia. Int. Sc. Conf. „Modern Problems of Ecology“, Kutaisi, Georgia, November 23-25, 2023, pp. 137-142, (in Georgian). https://mpe.openjournals.ge/index.php/mpe/article/view/7303/7304

[63] Tsintsadze T., Ghlonti N. Research of the Bioclimatic Potential of Georgia in the Joint Works of the Institutes of Hydrometeorology and Geophysics. Transactions IHM, GTU, vol.133, 2023, pp.62-68, (in Georgian). http://dspace.gela.org.ge/bitstream/123456789/10338/1/133-12.pdf, doi.org/10.36073/1512-0902-2023-133-62-68

[64] Beglarashvili N., Pipia M., Jamrishvili N., Janelidze I. Some Results of the Analysis of Number of Days with Strong Wind in Various Regions of Georgia in 2019-2022. Georgian Geographical Journal, E-ISSN: 2667-9701, Vol.3 (2), 2023, 5 p. DOI: https://doi.org/10.52340/ggj.2023.03.02.05

[65] Varazanashvili O., Gaprindashvili G., Elizbarashvili E., Basilashvili Ts., Amiranashvili A., Fuchs S. The First Natural Hazard Event Database for the Republic of Georgia (GeNHs). Catalog, 2023, 270 p. http://dspace.gela.org.ge/handle/123456789/10369; DOI: 10.13140/RG.2.2.12474.57286
[66] Varamashvili N., Pipia M. A Brief Overview of the Joint Works of the M. Nodia Institute of Geophysics, TSU and Institute of Hydrometeorology, GTU in the Last Five Years. Int. Sc. Conf. "Complex Geophysical Monitoring in Georgia: History, Modern Problems, Promoting Sustainable Development of the Country", Proceedings, ISBN 978-9941-36-272-9, Publish House of Iv. Javakhishvili Tbilisi State University, Tbilisi, Georgia, October 17-19, 2024, pp. 141 – 144, (in Georgian).
[67] Amiranashvili A., Bliadze T., Chikhladze V. Experimental Modeling of Atmospheric Processes in the Large Cloud Chamber of the M. Nodia Institute of Geophysics, TSU. Past, Present, Development Prospects. Int. Sc. Conf. "Complex Geophysical Monitoring in Georgia: History, Modern Problems, Promoting Sustainable Development of the Country", Proceedings, ISBN 978-9941-36-272-9, Publish House of Iv. Javakhishvili Tbilisi State University, Tbilisi, Georgia, October 17-19, 2024, pp. 172 – 175.
[68] Chikhladze V., Kartvelishvili L. Testing the "Slanting Rain" Recorder in a Thermobaric Chamber. Int. Sc. Conf. "Complex Geophysical Monitoring in Georgia: History, Modern Problems, Promoting Sustainable Development of the Country", Proceedings, ISBN 978-9941-36-272-9, Publish House of Iv. Javakhishvili Tbilisi State University, Tbilisi, Georgia, October 17-19, 2024, pp. 176 – 178, (in Georgian).

თსუ, მ. ნოდიას სახ. გეოფიზიკის ინსტიტუტისა და სტუ, ჰიდრომეტეოროლოგიის ინსტიტუტის ერთობლივი კვლევების ზოგიერთი შედეგები 2019-2023 წწ. და მათი შემდგომი განვითარების პერსპექტივები

ნ. ვარამაშვილი, მ. ფიფია

რეზიუმე

წარმოდგენილია მოკლე ინფორმაცია თსუ, მ. ნოდიას სახ. გეოფიზიკის ინსტიტუტისა და სტუ, ჰიდრომეტეოროლოგიის ინსტიტუტის ერთობლივი კვლევების შესახებ ჩატარებული 2019-2023 წწ. და მათი შემდგომი განვითარების პერსპექტივებზე.
საკვანძო სიტყვები: ჰიდრომეტეოროლოგია, კლიმატი, ატმოსფერული პროცესების ექსპერიმენტული მოდელირება, ბიოკლიმატი, ეკოლოგია.

Некоторые результаты совместных исследований Института геофизики им. М. Нодиа, ТГУ и Института гидрометеорологии, ГТУ в 2019–2023 гг. и перспективы их дальнейшего развития

Н. Варамашвили, М. Пипия

Резюме

Представлена краткая информация о совместных исследованиях Института геофизики им. М. Нодиа, ТГУ и Института гидрометеорологии, ГТУ, проведенных в 2019–2023 гг. и перспективах их дальнейшего развития.
Ключевые слова: гидрометеорология, климат, экспериментальное моделирование атмосферных процессов, биоклимат, экология.

Journal of the Georgian Geophysical Society, e-ISSN: 2667-9973, p-ISSN: 1512-1127
Physics of Solid Earth, Atmosphere, Ocean and Space Plasma, v. 27(2), 2024, pp. 96 – 105

Chronicle

International Scientific Conference "Complex Geophysical Monitoring in Georgia: History, Modern Problems, Promoting Sustainable Development of the Country"

[1]Nodar D. Varamashvili, [2]Mikheil G. Pipia

[1]M. Nodia Institute of Geophysics of the I. Javakhishvili Tbilisi State University, Georgia
[2]Institute of Hydrometeorology of the Georgian Technical University, Georgia

[1]e-mail: nodar.varamashvili@tsu.ge
[2]e-mail: m.pipia@gtu.ge

ABSTRACT

Information about the international scientific conference "Complex Geophysical Monitoring in Georgia: History, Modern Problems, Promoting Sustainable Development of the Country" Dedicated to 180 Anniversary of the Organization in Georgia of Regular Magneto-Meteorological Observations , which was held on October 17-19, 2024 at Ivane Javakhishvili Tbilisi State University is presented.

Key words: *Earth and its envelopes, geophysical processes, complex geophysical monitoring, natural disasters, earth ecology, mitigation, promoting sustainable development.*

Introduction

On October 17-19, 2024, Ivane Javakhishvili Tbilisi State University hosted the International Scientific Conference "Complex Geophysical Monitoring in Georgia: History, Modern Problems, Promoting Sustainable Development of the Country" Dedicated to 180 Anniversary of the Organization in Georgia of Regular Magneto-Meteorological Observations.

The conference was attended by about 200 researchers from 37 organizations from 13 countries (Georgia, Armenia, Germany, Greece, Hungary, Italy, Poland, Russia (Chechen Republic), Slovenia, Spain, Sweden, USA, Uzbekistan).

The aim of the conference was to present the results of research in the field of complex geophysical monitoring in Georgia and other countries (history, modern problems, assistance to sustainable development of countries) at the plenary session (oral\poster\video). As well as presentation of reports selected by the scientific committee and their discussion at plenary, sectional sessions and in the form of poster reports.

The target group was Georgian and foreign scientific, educational, governmental and non-governmental organizations, which have direct contact with the theme of the conference (universities, research institutes, educational organizations, structures of emergency situations, etc.).

The conference participants were given certificates.

The collection of conference materials and all of its separate articles is available on the website of the National Scientific Library: http://dspace.gela.org.ge/handle/123456789/10609

Goal of the Conference

- Discovering the potential scientists in the field of complex geophysical monitoring;
- Establishing and strengthening connections of scientists;
- Defining the prospects for the development of scientific research;
- Identify opportunities for improving the scientific-educational field of secondary and higher

education institutions in relation to the issues of the conference;
- Strengthening international scientific cooperation on conference topics;
- To acquaint the world scientific community, governmental structures, other interested organizations and individuals with the current state of the problems related to the fields of complex geophysical monitoring.

Conference Organizers

The conference was organized by the Mikheil Nodia Institute of Geophysics of the Tbilisi State University, Institute of Hydrometeorology of Technical University Of Georgia and the Georgian Geophysical Association.

Scientific Committee and Editorial Board

Tamaz Chelidze: Academician, Chairman of the Scientific Committee, Editor-in-Chief; **Nodar Varamashvili, Jemal Kiria:** Co-Chairmans of the Scientific Committee - TSU, M. Nodia Institute of Geophysics, Georgia; **Nana Bolashvili**: Co-Chairman of the Scientific Committee – TSU, Vakhushti Bagrationi Institute of Geography, Georgia; **Mikheil Pipia:** Co-Chairman of the Scientific Committee – GTU, Institute of Hydrometeorology, Georgia; **Avtandil Amiranashvili** (Deputy Editor-in-Chief), **Nugzar Ghlonti, George Melikadze** - TSU, M. Nodia Institute of Geophysics, Georgia; **Liana Kartvelishvili** - National Environmental Agency, Georgia; **Marika Tatishvili** - GTU, Institute of Hydrometeorology, Georgia; **Ketevan Khazaradze** - Georgian State Teaching University of Physical Education and Sport, Georgia; **Nino Japaridze** - Tbilisi State Medical University, Georgia; **Laura Rustioni, Gianluca Pappaccogli** - University of Salento, Italy; **Janja Vaupotič –** Jožef Stefan Institute, Slovenia; **István Fórizs** - Institute for Geological and Geochemical Research, Hungary; **Sergey Nazaretyan** - Regional Survey for Seismic Protection, Ministry of Internal Affairs of the Republic of Armenia, Armenia.

Organizing Committee

Manana Nikolaishvili: Chairman of Organizing Committee; **Zamira Arziani –** Deputy Chairman of Organizing Committee; **Sophiko Matiashvili, Ekaterine Mepharidze, Dimitri Amilakhvari, Dimitri Tepnadze, Levan Laliashvili** – TSU, M. Nodia Institute of Geophysics, Georgia; **Nino Taniashvili** - Georgian Geophysical Association, Georgia; **Nazibrola Beglarashvili,** - GTU, Institute of Hydrometeorology, Georgia; **Inga Janelidze –** Georgian Technical University, Georgia.

Conference Themes – All problems of the complex geophysical monitoring in Georgia and other countries.

Expected Results

- Promoting historical and modern achievements in the field of complex geophysical monitoring;
- To acquaint the world community with the current state of the problems related to the complex geophysical monitoring;
- Enhance international cooperation for the scientific and practical application of modern achievements related to the conference topics;
- Assess the social and economic risks associated with the conference topics and identify opportunities for joint action to prevent these risks;
- Assess opportunities to expand the use of complex geophysical monitoring to support sustainable development of countries;
- Identify opportunities to improve the scientific-educational base of secondary and higher education institutions in the field of complex geophysical monitoring.

The conference was opened by the deputy rector of Ivane Javakhishvili Tbilisi State University Kakha Cheishvili, chairman of the scientific committee academician Tamaz Chelidze, co-chairman of the scientific committee, director of Mikheil Nodia Institute of Geophysics, TSU, Nodar Varamashvili and co-chairman of the scientific committee, director of Institute of Hydrometeorology, GTU, Mikheil Pipia.

Speakers made a general overview about the modern problems of the complex geophysical monitoring in Georgia and wished the conference participants fruitful work.

A total of 48 oral and poster presentations were considered at the conference. 46 reports published (see References). Two reports, at the request of the authors, will be published in another edition (Kharshiladze O., Amilakhvari D., Davitashvili T., Kobaidze D. - Non-Linear Theory of Thermal Conductivity in the Atmosphere; Elbakidze Kh., Sorriso-Valvo L., Kharshiladze O., Gurchumelia A., Tsulukidze L. - Fractal and Correlation Analysis of Geomagnetic Activity Data).

The proceedings of this conference as a whole, as well as its individual works, are published and posted on the portal of the Institute of Geophysics, which are included in the international electronic library data base DSpace, indexed in Google Scholar and Publish or Perish.

According to the results of the conference, a decision was made, in which the achievements and gaps in the directions of the complex geophysical monitoring in Georgia and other countries are discussed. Future meetings have been planned.

Photos from Conference

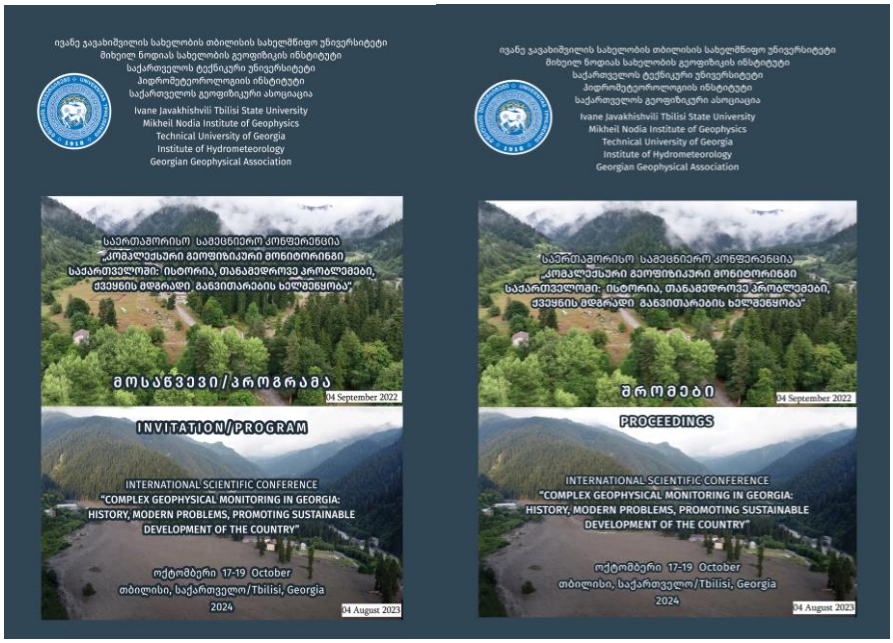


რიკოთის რკინაბეტონის კოშკი


UNIVERSITAS TPHILISIENSIS
1918


Our research concerns the radioecological issue of the soils of the automobile workshop located next to the residential areas of Tbilisi, the capital of Georgia. Specifically, soil pollution, which affects people's health.
We have done a lot of research on this issue and there is unmistakable
data based on research laboratory analysis


18.10.2024 12:05

References

[1] Gogua R. Dusheti (Tbilisi) Magnetic Observatory is One of the Oldest in the World. Int. Sc. Conf. "Complex Geophysical Monitoring in Georgia: History, Modern Problems, Promoting Sustainable Development of the Country", Proceedings, ISBN 978-9941-36-272-9, Publish House of Iv. Javakhishvili Tbilisi State University, Tbilisi, Georgia, October 17-19, 2024, pp. 3 – 6, (in Georgian).

[2] Varamashvili N., Darakhvelidze L. Academician Tamaz Chelidze – 90. Int. Sc. Conf. "Complex Geophysical Monitoring in Georgia: History, Modern Problems, Promoting Sustainable Development of the Country", Proceedings, ISBN 978-9941-36-272-9, Publish House of Iv. Javakhishvili Tbilisi State University, Tbilisi, Georgia, October 17-19, 2024, pp. 7 - 8.

[3] Chelidze T., Gogua R., Matiashvili T. The importance of the Dusheti (Tbilisi) Magnetic Observatory for the Georgian Scientific Environment. Int. Sc. Conf. "Complex Geophysical Monitoring in Georgia: History, Modern Problems, Promoting Sustainable Development of the Country", Proceedings, ISBN 978-9941-36-272-9, Publish House of Iv. Javakhishvili Tbilisi State University, Tbilisi, Georgia, October 17-19, 2024, pp. 9 – 12, (in Georgian).

[4] Kiria T., Nikolaishvili M., Chkhaidze T., Mebaghisvili N. Analysis of Geomagnetic Activity and Coronal Mass Ejections. Int. Sc. Conf. "Complex Geophysical Monitoring in Georgia: History, Modern Problems, Promoting Sustainable Development of the Country", Proceedings, ISBN 978-9941-36-272-9, Publish House of Iv. Javakhishvili Tbilisi State University, Tbilisi, Georgia, October 17-19, 2024, pp. 13 – 16.

[5] Nazaretyan S.N., Mirzoyan L.B., Nazaretyan S.S. – Basic Data for Compilation of a Special Macroseismic Scale for Assessing the Intensity of Historical Earthquakes in the Armenian Upland. Int. Sc. Conf. "Complex Geophysical Monitoring in Georgia: History, Modern Problems, Promoting Sustainable Development of the Country", Proceedings, ISBN 978-9941-36-272-9, Publish House of Iv. Javakhishvili Tbilisi State University, Tbilisi, Georgia, October 17-19, 2024, pp. 17 – 20.

[6] Nazaretyan S.N., Mirzoyan L.B. Important Features of the Methodology for Assessing the Maximum Seismic Risk of Large Territories (Based on the Example of Armenia). Int. Sc. Conf. "Complex Geophysical Monitoring in Georgia: History, Modern Problems, Promoting Sustainable Development of the Country", Proceedings, ISBN 978-9941-36-272-9, Publish House of Iv. Javakhishvili Tbilisi State University, Tbilisi, Georgia, October 17-19, 2024, pp. 21 – 25.

[7] Hovhannisyan S.R., Movsisyan A.D. Regularity of Periods of Tectonomagnetic Precursors. Int. Sc. Conf. "Complex Geophysical Monitoring in Georgia: History, Modern Problems, Promoting Sustainable Development of the Country", Proceedings, ISBN 978-9941-36-272-9, Publish House of Iv. Javakhishvili Tbilisi State University, Tbilisi, Georgia, October 17-19, 2024, pp. 26 – 28.

[8] Alania V., Enukidze O., Razmadze A. Tectonic Model of the Georgian Part of Lesser Caucasus Orogen Using Seismic Profile. Int. Sc. Conf. "Complex Geophysical Monitoring in Georgia: History, Modern Problems, Promoting Sustainable Development of the Country", Proceedings, ISBN 978-9941-36-272-9, Publish House of Iv. Javakhishvili Tbilisi State University, Tbilisi, Georgia, October 17-19, 2024, pp. 29 – 29.

[9] Arabidze V., Chkhikvadze K., Gigiberia M., Ghlonti N. Effect of Geological Faulting on Slope Stability. Int. Sc. Conf. "Complex Geophysical Monitoring in Georgia: History, Modern Problems, Promoting Sustainable Development of the Country", Proceedings, ISBN 978-9941-36-272-9, Publish House of Iv. Javakhishvili Tbilisi State University, Tbilisi, Georgia, October 17-19, 2024, pp. 30 – 33, (in Georgian).

[10] Karimova F.B., Dzhumaniyazov D.I. Small Intrusions and Dikes Associated with Ore Formation (Almalyk-Angren Mining District). Int. Sc. Conf. "Complex Geophysical Monitoring in Georgia: History, Modern Problems, Promoting Sustainable Development of the Country", Proceedings, ISBN 978-9941-36-272-9, Publish House of Iv. Javakhishvili Tbilisi State University, Tbilisi, Georgia, October 17-19, 2024, pp. 34 – 36.

[11] Gorgijandze S., Gorgodze T., Jincharadze G., Kobakhidze N., Gulashvili Z., Silagadze M., Dvalashvili G. Crucial Moment of Topographic Map for Effective Management of Natural Disasters. Int. Sc. Conf. "Complex Geophysical Monitoring in Georgia: History, Modern Problems, Promoting Sustainable Development of the Country", Proceedings, ISBN 978-9941-36-272-9, Publish House of Iv. Javakhishvili Tbilisi State University, Tbilisi, Georgia, October 17-19, 2024, pp. 37 – 39.

[12] Shengelia L., Kordzakhia G., Tvauri G., Guliashvili G., Dzadzamia M. Results of the Study of the Morphology and Exposure of Glaciers in the r. Rioni Basin on Satellite Remote Sensing. Int. Sc. Conf. "Complex Geophysical Monitoring in Georgia: History, Modern Problems, Promoting Sustainable Development of the Country", Proceedings, ISBN 978-9941-36-272-9, Publish House of Iv. Javakhishvili

Tbilisi State University, Tbilisi, Georgia, October 17-19, 2024, pp. 40 – 44, (in Georgian).
[13] Gigiberia M., Kiria J. Results of the Geophysical Survey Conducted in the Vicinity of Lisi Lake. Int. Sc. Conf. "Complex Geophysical Monitoring in Georgia: History, Modern Problems, Promoting Sustainable Development of the Country", Proceedings, ISBN 978-9941-36-272-9, Publish House of Iv. Javakhishvili Tbilisi State University, Tbilisi, Georgia, October 17-19, 2024, pp. 45 – 48, (in Georgian).
[14] Varamashvili N., Gigiberia M. Study of the Reinforced Concrete Construction of Ricoti Bridge by Ultrasonic Method. Int. Sc. Conf. "Complex Geophysical Monitoring in Georgia: History, Modern Problems, Promoting Sustainable Development of the Country", Proceedings, ISBN 978-9941-36-272-9, Publish House of Iv. Javakhishvili Tbilisi State University, Tbilisi, Georgia, October 17-19, 2024, pp. 49 – 52, (in Georgian).
[15] Odilavadze D., Chelidze T., Yavolovskaya O. – Radio Images Investigated by the Method of Physical Modeling of an Archaeogeoradiolocationally Complex Building Object. Int. Sc. Conf. "Complex Geophysical Monitoring in Georgia: History, Modern Problems, Promoting Sustainable Development of the Country", Proceedings, ISBN 978-9941-36-272-9, Publish House of Iv. Javakhishvili Tbilisi State University, Tbilisi, Georgia, October 17-19, 2024, pp. 53 – 56, (in Georgian).
[16] Shavliashvili L., Kuchava G., Shubladze E., Kurtsikidze O., Gavardashvili G., Kordzakhia G. Results of Research of Natural Waters and Soils of Chiatura Municipality. Int. Sc. Conf. "Complex Geophysical Monitoring in Georgia: History, Modern Problems, Promoting Sustainable Development of the Country", Proceedings, ISBN 978-9941-36-272-9, Publish House of Iv. Javakhishvili Tbilisi State University, Tbilisi, Georgia, October 17-19, 2024, pp. 57 – 63, (in Georgian).
[17] Basilashvili Ts. Updated Maximum Flood Discharges for Hydrological Calculations of the Rivers in Western Georgia. Int. Sc. Conf. "Complex Geophysical Monitoring in Georgia: History, Modern Problems, Promoting Sustainable Development of the Country", Proceedings, ISBN 978-9941-36-272-9, Publish House of Iv. Javakhishvili Tbilisi State University, Tbilisi, Georgia, October 17-19, 2024, pp. 64 – 68, (in Georgian).
[18] Kerimov I.A., Bratkov V.V., Bekmurzaeva L.R. Assessment of Modern Agroclimatic Conditions of the North Caucasus in the Context of Climate Change. Int. Sc. Conf. "Complex Geophysical Monitoring in Georgia: History, Modern Problems, Promoting Sustainable Development of the Country", Proceedings, ISBN 978-9941-36-272-9, Publish House of Iv. Javakhishvili Tbilisi State University, Tbilisi, Georgia, October 17-19, 2024, pp. 69 – 71.
[19] Meladze M., Meladze G., Kapanadze N., Pipia M. Impact of Droughts on the Agricultural Sector of the Eastern Georgia Regions. Int. Sc. Conf. "Complex Geophysical Monitoring in Georgia: History, Modern Problems, Promoting Sustainable Development of the Country", Proceedings, ISBN 978-9941-36-272-9, Publish House of Iv. Javakhishvili Tbilisi State University, Tbilisi, Georgia, October 17-19, 2024, pp. 72 – 75, (in Georgian).
[20] Markarashvili E., Papiashvili K., Snesar A., Khakhutaishvili A. Construction Adhesive Cement Based on Household Glass Waste. Int. Sc. Conf. "Complex Geophysical Monitoring in Georgia: History, Modern Problems, Promoting Sustainable Development of the Country", Proceedings, ISBN 978-9941-36-272-9, Publish House of Iv. Javakhishvili Tbilisi State University, Tbilisi, Georgia, October 17-19, 2024, pp. 76 – 78, (in Georgian).
[21] Markarashvili E., Bazgadze Z., G., Chikvaidze I., Sidamonidze N., Snesar A. – Composites Based on Epoxy Resin and Rubber Waste. Int. Sc. Conf. "Complex Geophysical Monitoring in Georgia: History, Modern Problems, Promoting Sustainable Development of the Country", Proceedings, ISBN 978-9941-36-272-9, Publish House of Iv. Javakhishvili Tbilisi State University, Tbilisi, Georgia, October 17-19, 2024, pp. 79 – 81, (in Georgian).
[22] Kiknadze N., Davitadze L., Tavdgiridze G., Kuchava M., Gogitidze T. The Effect of the New Generation Fertilizer "Leonardite" on the Chemical Composition of Red Soil and Mandarin "Unshiu". Int. Sc. Conf. "Complex Geophysical Monitoring in Georgia: History, Modern Problems, Promoting Sustainable Development of the Country", Proceedings, ISBN 978-9941-36-272-9, Publish House of Iv. Javakhishvili Tbilisi State University, Tbilisi, Georgia, October 17-19, 2024, pp. 82 – 87, (in Georgian).
[23] Kvaratskhelia D., Demetrashvili D. Numerical Investigation of Sensitivity of the Temperature Field to Initial Conditions in the Upper Turbulent Layer of the Black Sea Using the Numerical Model of the Sea Dynamics. Int. Sc. Conf. "Complex Geophysical Monitoring in Georgia: History, Modern Problems, Promoting Sustainable Development of the Country", Proceedings, ISBN 978-9941-36-272-9, Publish House of Iv. Javakhishvili Tbilisi State University, Tbilisi, Georgia, October 17-19, 2024, pp. 88 – 91, (in Georgian).
[24] Demetrashvili D. Monitoring and Short-Term Forecasting Systems for European Seas. Int. Sc. Conf.

"Complex Geophysical Monitoring in Georgia: History, Modern Problems, Promoting Sustainable Development of the Country", Proceedings, ISBN 978-9941-36-272-9, Publish House of Iv. Javakhishvili Tbilisi State University, Tbilisi, Georgia, October 17-19, 2024, pp. 92 – 95, (in Georgian).

[25] Tatishvili M., Kapanadze N., Mkurnalidze I., Palavandishvili A. Drought Evaluation in Georgia using SPI and SpEI Indices. Int. Sc. Conf. "Complex Geophysical Monitoring in Georgia: History, Modern Problems, Promoting Sustainable Development of the Country", Proceedings, ISBN 978-9941-36-272-9, Publish House of Iv. Javakhishvili Tbilisi State University, Tbilisi, Georgia, October 17-19, 2024, pp. 96 – 100.

[26] Bliadze T. Statistical Analysis of the Weekly Fire Alerts Count in Georgia and its Regions in 2012-2023. Int. Sc. Conf. "Complex Geophysical Monitoring in Georgia: History, Modern Problems, Promoting Sustainable Development of the Country", Proceedings, ISBN 978-9941-36-272-9, Publish House of Iv. Javakhishvili Tbilisi State University, Tbilisi, Georgia, October 17-19, 2024, pp. 101 – 104.

[27] Bliadze T., Chkhitunidze M., Kirkitadze D. Statistical Characteristics of Mean Monthly and Annual Concentrations of Particulate Matter PM2.5 and PM10 in Tbilisi in 2017-2023. Int. Sc. Conf. "Complex Geophysical Monitoring in Georgia: History, Modern Problems, Promoting Sustainable Development of the Country", Proceedings, ISBN 978-9941-36-272-9, Publish House of Iv. Javakhishvili Tbilisi State University, Tbilisi, Georgia, October 17-19, 2024, pp. 105 – 108.

[28] Surmava A., Kukhalashvili V., Gigauri N., Intskirveli L. Numerical Modeling of Changes in Time and Space of the Concentration of PM10 Dispersed in the Atmosphere of Kutaisi City During Calm. Int. Sc. Conf. "Complex Geophysical Monitoring in Georgia: History, Modern Problems, Promoting Sustainable Development of the Country", Proceedings, ISBN 978-9941-36-272-9, Publish House of Iv. Javakhishvili Tbilisi State University, Tbilisi, Georgia, October 17-19, 2024, pp. 109 – 112, (in Georgian).

[29] Matiashvili S., Chanqseliani Z. Soil Pollution in the Vicinity of Automobile Workshops, Near Populated Areas Across Tbilisi. Int. Sc. Conf. "Complex Geophysical Monitoring in Georgia: History, Modern Problems, Promoting Sustainable Development of the Country", Proceedings, ISBN 978-9941-36-272-9, Publish House of Iv. Javakhishvili Tbilisi State University, Tbilisi, Georgia, October 17-19, 2024, pp. 113 – 116.

[30] Takadze G., Larry D., Wascak J. Harnessing HAVOK and Machine Learning for Cosmic Ray Forecasting. Int. Sc. Conf. "Complex Geophysical Monitoring in Georgia: History, Modern Problems, Promoting Sustainable Development of the Country", Proceedings, ISBN 978-9941-36-272-9, Publish House of Iv. Javakhishvili Tbilisi State University, Tbilisi, Georgia, October 17-19, 2024, pp. 117 – 120.

[31] Uchaneishvili S., Kalmakhelidze S., Avalishvili A., Ivanishvili N., Gogebashvili M. Astrobiological Aspects of Ionizing Radiation-Induced Cognitive Impairments. Int. Sc. Conf. "Complex Geophysical Monitoring in Georgia: History, Modern Problems, Promoting Sustainable Development of the Country", Proceedings, ISBN 978-9941-36-272-9, Publish House of Iv. Javakhishvili Tbilisi State University, Tbilisi, Georgia, October 17-19, 2024, pp. 121 – 123, (in Georgian).

[32] Seperteladze Z., Davitaia E., Aleksidze T., Rukhadze N. The role of Physical-Geographical Factors in the Spatio-Temporal Distribution of Cardiovascular Diseases. Int. Sc. Conf. "Complex Geophysical Monitoring in Georgia: History, Modern Problems, Promoting Sustainable Development of the Country", Proceedings, ISBN 978-9941-36-272-9, Publish House of Iv. Javakhishvili Tbilisi State University, Tbilisi, Georgia, October 17-19, 2024, pp. 124 – 128, (in Georgian).

[33] Japaridze N., Khazaradze K., Chkhitunidze M., Revishvili A. Variability of the Birth, Death and Population Growth Rates in Georgia in 1994-2023. Int. Sc. Conf. "Complex Geophysical Monitoring in Georgia: History, Modern Problems, Promoting Sustainable Development of the Country", Proceedings, ISBN 978-9941-36-272-9, Publish House of Iv. Javakhishvili Tbilisi State University, Tbilisi, Georgia, October 17-19, 2024, pp. 129 – 132.

[34] Japaridze N., Kartvelishvili L., Khazaradze K., Chkhitunidze M., Nikolaishvili M., Revishvili A. Statistical Characteristics of the Daily Values of Air Effective Temperature According to Missenard in Batumi. . Int. Sc. Conf. "Complex Geophysical Monitoring in Georgia: History, Modern Problems, Promoting Sustainable Development of the Country", Proceedings, ISBN 978-9941-36-272-9, Publish House of Iv. Javakhishvili Tbilisi State University, Tbilisi, Georgia, October 17-19, 2024, pp. 133 – 136.

[35] Amiranashvili A., Kartvelishvili L., Matzarakis A. The Interval Forecasting of the Holiday Climate Index in Tsalka (Georgia) to 2026-2035. . Int. Sc. Conf. "Complex Geophysical Monitoring in Georgia: History, Modern Problems, Promoting Sustainable Development of the Country", Proceedings, ISBN 978-9941-36-272-9, Publish House of Iv. Javakhishvili Tbilisi State University, Tbilisi, Georgia, October 17-19, 2024, pp. 137 – 140.

[36] Varamashvili N., Pipia M. A Brief Overview of the Joint Works of the M. Nodia Institute of

Geophysics, TSU and Institute of Hydrometeorology, GTU in the Last Five Years. Int. Sc. Conf. "Complex Geophysical Monitoring in Georgia: History, Modern Problems, Promoting Sustainable Development of the Country", Proceedings, ISBN 978-9941-36-272-9, Publish House of Iv. Javakhishvili Tbilisi State University, Tbilisi, Georgia, October 17-19, 2024, pp. 141 – 144, (in Georgian).

[37] Amiranashvili A. Analysis of Variability of Mean Annual Air Temperature in Tbilisi in 1844-2023 Against the Background of Climate Change. Int. Sc. Conf. "Complex Geophysical Monitoring in Georgia: History, Modern Problems, Promoting Sustainable Development of the Country", Proceedings, ISBN 978-9941-36-272-9, Publish House of Iv. Javakhishvili Tbilisi State University, Tbilisi, Georgia, October 17-19, 2024, pp. 145 – 149.

[38] Bolashvili N., Chikhladze V., Kartvelishvili L., Tatishvili M. Variability of Atmospheric Precipitation in Tbilisi in 1844-2023. Int. Sc. Conf. "Complex Geophysical Monitoring in Georgia: History, Modern Problems, Promoting Sustainable Development of the Country", Proceedings, ISBN 978-9941-36-272-9, Publish House of Iv. Javakhishvili Tbilisi State University, Tbilisi, Georgia, October 17-19, 2024, pp. 150 – 154.

[39] Amiranashvili A., Brocca L., Chelidze T., Svanadze D., Tsamalashvili T., Varamashvili N. Analysis of the Precipitation Regime that Triggered the Landslide in Nergeeti (Imereti, Georgia) on February 7, 2024. Int. Sc. Conf. "Complex Geophysical Monitoring in Georgia: History, Modern Problems, Promoting Sustainable Development of the Country", Proceedings, ISBN 978-9941-36-272-9, Publish House of Iv. Javakhishvili Tbilisi State University, Tbilisi, Georgia, October 17-19, 2024, pp. 155 – 158.

[40] Amiranashvili A., Chelidze T., Svanadze D., Tsamalashvili T., Varamashvili N. Comparison of Satellite and Ground-Based Data on Semi-Annual and Annual Sum of Atmospheric Precipitation for 26 Points in Georgia in 2001-2020. . Int. Sc. Conf. "Complex Geophysical Monitoring in Georgia: History, Modern Problems, Promoting Sustainable Development of the Country", Proceedings, ISBN 978-9941-36-272-9, Publish House of Iv. Javakhishvili Tbilisi State University, Tbilisi, Georgia, October 17-19, 2024, pp. 159 – 163.

[41] Beglarashvili N., Jamrishvili N., Janelidze I., Pipia M., Tavidashvili Kh. Some Results of Analysis of Heavy Precipitation in Tbilisi on July 7, 2024 Based on Ground-Level and Satellite Measurements. . Int. Sc. Conf. "Complex Geophysical Monitoring in Georgia: History, Modern Problems, Promoting Sustainable Development of the Country", Proceedings, ISBN 978-9941-36-272-9, Publish House of Iv. Javakhishvili Tbilisi State University, Tbilisi, Georgia, October 17-19, 2024, pp. 164 – 167.

[42] Amiranashvili A., Chikhladze V., Kekenadze E., Pipia M., Samkharadze I., Telia Sh., Varamashvili N. Meteorological Conditions for the Tornado Formation in Kakheti (Georgia) on June 25, 2024. . Int. Sc. Conf. "Complex Geophysical Monitoring in Georgia: History, Modern Problems, Promoting Sustainable Development of the Country", Proceedings, ISBN 978-9941-36-272-9, Publish House of Iv. Javakhishvili Tbilisi State University, Tbilisi, Georgia, October 17-19, 2024, pp. 168 – 171.

[43] Amiranashvili A., Bliadze T., Chikhladze V. Experimental Modeling of Atmospheric Processes in the Large Cloud Chamber of the M. Nodia Institute of Geophysics, TSU. Past, Present, Development Prospects. Int. Sc. Conf. "Complex Geophysical Monitoring in Georgia: History, Modern Problems, Promoting Sustainable Development of the Country", Proceedings, ISBN 978-9941-36-272-9, Publish House of Iv. Javakhishvili Tbilisi State University, Tbilisi, Georgia, October 17-19, 2024, pp. 172 – 175.

[44] Chikhladze V., Kartvelishvili L. Testing the "Slanting Rain" Recorder in a Thermobaric Chamber. Int. Sc. Conf. "Complex Geophysical Monitoring in Georgia: History, Modern Problems, Promoting Sustainable Development of the Country", Proceedings, ISBN 978-9941-36-272-9, Publish House of Iv. Javakhishvili Tbilisi State University, Tbilisi, Georgia, October 17-19, 2024, pp. 176 – 178, (in Georgian).

[45] Prus B., Bacior S. – Good Practices of Landslide Hazard Monitoring as a Support for Sustainable Space Development – Examples from Poland. Int. Sc. Conf. "Complex Geophysical Monitoring in Georgia: History, Modern Problems, Promoting Sustainable Development of the Country", Proceedings, ISBN 978-9941-36-272-9, Publish House of Iv. Javakhishvili Tbilisi State University, Tbilisi, Georgia, October 17-19, 2024, pp. 179 – 182.

[46] Bakradze T., Glonti N., Erkomaishvili T., Demurishvili Z., Takadze G., Barbakadze P., Gogua R., Alania E. Modulating Effects of Cosmic Rays on Solar Activities. Int. Sc. Conf. "Complex Geophysical Monitoring in Georgia: History, Modern Problems, Promoting Sustainable Development of the Country", Proceedings, ISBN 978-9941-36-272-9, Publish House of Iv. Javakhishvili Tbilisi State University, Tbilisi, Georgia, October 17-19, 2024, pp. 183 – 188, (in Georgian).

საერთაშორისო სამეცნიერო კონფერენცია „კომპლექსური გეოფიზიკური მონიტორინგი საქართველოში: ისტორია, თანამედროვე პრობლემები, ქვეყნის მდგრადი განვითარების ხელშეწყობა“

ნ. ვარამაშვილი, მ. ფიფია

რეზიუმე

წარმოდგენილია ინფორმაცია საერთაშორისო სამეცნიერო კონფერენციაზე „კომპლექსური გეოფიზიკური მონიტორინგი საქართველოში: ისტორია, თანამედროვე პრობლემები, ქვეყნის მდგრადი განვითარების ხელშეწყობა“ მიღვნილი საქართველოში რეგულარული მაგნიტური და მეტეოროლოგიური დაკვირვებების ორგანიზების 180 წლის იუბილეს, რომელიც ჩატარდა 2024 წლის 17-19 ოქტომბერს ივანე ჯავახიშვილის სახელობის თბილისის სახელმწიფო უნივერსიტეტში.

საკვანძო სიტყვები: დედამიწა და მისი გარსები, გეოფიზიკური პროცესები, კომპლექსური გეოფიზიკური მონიტორინგი, ბუნებრივი კატასტროფები, დედამიწის ეკოლოგია, შედეგების შერბილება, მდგრადი განვითარების ხელშეწყობა.

Международная научная конференция “Комплексный геофизический мониторинг в Грузии: история, современные проблемы, содействие устойчивому развитию страны”

Н. Варамашвили, М. Пипия

Резюме

Представлена информация о международной научной конференции „Комплексный геофизический мониторинг в Грузии: история, современные проблемы, содействие устойчивому развитию страны“, посвященной 180-летию организации в Грузии регулярных магнито-метеорологических наблюдений, которая прошла 17-19 октября 2024 года в Тбилисском государственном университете имени Иванэ Джавахишвили.

Ключевые слова: Земля и ее оболочки, геофизические процессы, комплексный геофизический мониторинг, стихийные бедствия, экология Земли, смягчение последствий, содействие устойчивому развитию.

Information for contributors

Papers intended for the Journal should be submitted in two copies to the Editor-in-Chief. Papers from countries that have a member on the Editorial Board should normally be submitted through that member. The address will be found on the inside front cover.

1. Papers should be written in the concise form. Occasionally long papers, particularly those of a review nature (not exceeding 16 printed pages), will be accepted. Short reports should be written in the most concise form not exceeding 6 printed pages. It is desirable to submit a copy of paper on a diskette.
2. A brief, concise abstract in English is required at the beginning of all papers in Russian and in Georgian at the end of them.
3. Line drawings should include all relevant details. All lettering, graph lines and points on graphs should be sufficiently large and bold to permit reproduction when the diagram has been reduced to a size suitable for inclusion in the Journal.
4. Each figure must be provided with an adequate caption.
5. Figure Captions and table headings should be provided on a separate sheet.
6. Page should be 20 x 28 cm. Large or long tables should be typed on continuing sheets.
7. References should be given in the standard form to be found in this Journal.
8. All copy (including tables, references and figure captions) must be double spaced with wide margins, and all pages must be numbered consecutively.
9. Both System of units in GGS and SI are permitted in manuscript
10. Each manuscript should include the components, which should be presented in the order following as follows:
    Title, name, affiliation and complete postal address of each author and dateline.
    The text should be divided into sections, each with a separate heading or numbered consecutively.
    Acknowledgements. Appendix. Reference.
11. The editors will supply the date of receipt of the manuscript.

CONTENTS - სარჩევი

J. Kiria, T. Tsaguria, E. Sakvarelidze, N. Dovgali, L. Davitashvili, G. Kutelia - The Impact of the Earthquake in Racha on the Enguri Arch Dam and the Adjacent Area ჯ. ქირია, თ. ცაგურია, ე. საყვარელიძე, ნ. დოვგალი, ლ. დავითაშვილი, გ. ქუთელია - რაჭის მიწისძვრის გავლენა ენგურჰესის თაღოვან კაშხალსა და მის მიმდებარე ტერიტორიაზე	5 – 7
Z. Zerakidze, J. Kiria, T. Kiria - Confidence Interval of Parameters for Gaussian Statistical Structures Z-Criteria's Application ზ. ზერაკიძე, ჯ. ქირია, თ. ქირია - პარამეტრების ნდობის ინტერვალი გაუსის სტატისტიკური სტრუქტურებისათვის Z - კრიტერიუმის გამოყენებით	8 – 14
D. Odilavadze, T. Chelidze, O. Yavolovskaya - The Radio Image of an Object with an Elongated, Face-Fragmented, Dielectrically Complex Structure was Studied Using the Method of Georadar Physical Modeling დ. ოდილავაძე, თ. ჭელიძე, ო. იავოლოვსკაია - გეორადიოლოკაციაური ფიზიკური მოდელირების მეთოდით გამოკვლეული განგრძობითი, წახნაგოვან-ფრაგმენტული, დიელექტრიკულად რთული აგებულების ობიექტის რადიოსახე	15 – 28
T. Jimsheladze, G. Melikadze, G. Kobzev, A. Tchankvetadze, T. Matiashvili - Reaction of the Geomagnetic Field on the Earthquakes Preparation Process in Georgia თ. ჯიმშელაძე, გ. მელიქაძე, გ. კობზევი, ა. ჭანკვეტაძე, თ. მათიაშვილი - გეომაგნიტური ველის რეაქცია მიწისძვრების მომზადების პროცესზე საქართველოში	29 – 36
N. Kapanadze, G. Melikadze, A. Tchankvetadze, T. Jimsheladze, Z. Magradze, Sh. Gogichaishvili, M. Todadze, E. Chikviladze, L. Chelidze - ^{222}Rn Concentration Levels in Soil Gas and Water in Kvemo Kartli Region, Georgia - ^{222}Rn Mapping ნ. კაპანაძე, გ.მელიქაძე, ა.ჭანკვეტაძე, თ.ჯიმშელაძე, ზ. მაღრაძე, შ. გოგიჩაიშვილი, მ. თოდაძე, ე.ჩიკვილაძე, ლ.ჭელიძე - ^{222}Radon კონცენტრაციის დონეები ნიადაგსა და წყალში ქვემო ქართლის რეგიონში - ^{222}Rn-ის აგეგმვა	37 – 47
Z. Kereselidze, N. Varamashvili - On the Issue of Modelling the Dynamic Picture of the Spread of a Mudflow in the Shovi Gorge due to a Collapse on the Glacier Buba ზ. კერესელიძე, ნ. ვარამაშვილი - ბუბას მყინვარზე ნგრევის გამო შოვის ხეობაში ღვარცოფის ნაკადის გავრცელების დინამიკის მოდელირების საკითხი	48 – 62
Z. Kereselidze, A. Amiranashvili, V. Chikhladze, M. Chkhitunidze, G. Lominadze, E. Tchania - Conical Model of Non-Uniform Rotation and Interaction of Elements of the Atmospheric Rotation Chain in a Linear Approximation ზ.კერესელიძე, ა. ამირანაშვილი, ვ. ჩიხლაძე, მ. ჩხიტუნიძე, გ.ლომინაძე, ე. ჭანია - არაერთგვაროვანი ბრუნვის კონუსისებური მოდელი და ატმოსფერული გრიგალური ჯაჭვის ელემენტების ურთიერთქმედება წრფივ მიახლოებაში	63 – 73
L. Tsulukidze, O. Kharshiladze, A. Ghurchumelia, L. Sorriso-Valvo, Kh. Elbakidze, T. Matiashvili - Coherent Analysis of Intense Geomagnetic Disturbances Using Dusheti Observatory Data and the DST Index ლ. წულუკიძე, ო. ხარშილაძე, ა. ღურჭუმელია, ლ. სორისო-ვალვო, ხ. ელბაქიძე, თ. მათიაშვილი - მძლავრი გეომაგნიტური შეშფოთებების კოჰერენტული ანალიზი დუშეთის ობსერვატორიის მონაცემებისა და DST ინდექსის მაგალითზე	74 – 80
N. Varamashvili, M. Pipia - Some Results of the Joint Research of the M. Nodia Institute of Geophysics, TSU and Institute of Hydrometeorology, GTU from 2019 to 2023 and Prospects for their Further Development ნ. ვარამაშვილი, მ. ფიფია - თსუ, მ. ნოდიას სახ. გეოფიზიკის ინსტიტუტისა და სტუ, ჰიდრომეტეოროლოგიის ინსტიტუტის ერთობლივი კვლევების ზოგიერთი შედეგები 2019-2023 წწ. და მათი შემდგომი განვითარების პერსპექტივები	81 – 95
N. Varamashvili, M. Pipia - International Scientific Conference "Complex Geophysical Monitoring in Georgia: History, Modern Problems, Promoting Sustainable Development of the Country" (Chronicle) ნ. ვარამაშვილი, მ. ფიფია - საერთაშორისო სამეცნიერო კონფერენცია „კომპლექსური გეოფიზიკური მონიტორინგი საქართველოში: ისტორია, თანამედროვე პრობლემები, ქვეყნის მდგრადი განვითარების ხელშეწყობა" (ქრონიკა)	96 – 105
Information for contributors ავტორთა საყურადღებო	106 - 106

საქართველოს გეოფიზიკური საზოგადოების ჟურნალი

მყარი დედამიწის, ატმოსფეროს, ოკეანისა და კოსმოსური პლაზმის ფიზიკა

ტომი 27, № 2

ჟურნალი იბეჭდება საქართველოს გეოფიზიკური საზოგადოების პრეზიდიუმის დადგენილების საფუძველზე

ტირაჟი 20 ცალი

JOURNAL OF THE GEORGIAN GEOPHYSICAL SOCIETY

Physics of Solid Earth, Atmosphere, Ocean and Space Plasma

Vol. 27, № 2

Printed by the decision of the Georgian Geophysical Society Board

Circulation 20 copies

ЖУРНАЛ ГРУЗИНСКОГО ГЕОФИЗИЧЕСКОГО ОБЩЕСТВА

Физика Твердой Земли, Атмосферы, Океана и Космической Плазмы

Том 27, № 2

Журнал печатается по постановлению президиума Грузинского геофизического общества

Тираж 20 экз

Tbilisi-თბილისი-Тбилиси
2024